

**Advanced Formulations of Cyclosporine A and Budesonide for the
Therapy of Inflammatory Bowel Disease**

Dissertation

zur Erlangung des Grades
des Doktors der Naturwissenschaften
der Naturwissenschaftlich-Technischen Fakultät III
Chemie, Pharmazie, Bio- und Werkstoffwissenschaften
der Universität des Saarlandes

von

Christina Draheim

Saarbrücken

2015

Tag des Kolloquiums:	09.07.2015
Dekan:	Prof. Dr.-Ing. Dirk Bähre
Berichterstatter:	Prof. Dr. Claus-Michael Lehr Prof. Dr. Rolf W. Hartmann
Vorsitz:	Prof. Dr. Gerhard Wenz
Akad. Mitarbeiter:	Dr. Jessica Hoppstädter

*Der Fortgang der wissenschaftlichen Entwicklung ist im
Endeffekt eine ständige Flucht vor dem Staunen.*

Albert Einstein

Diese Arbeit wurde im Rahmen des ERA-Net EuroNanoMed Projektes

Delivering Nanopharmaceuticals through Biological Barriers

(Akronym „BIBA“, Grant number: 13N11845) angefertigt.

Abstract

Inflammatory bowel disease, namely Crohn's disease and ulcerative colitis, are chronic diseases, which require a lifelong symptomatic treatment associated with adverse effects and lacking curative approaches.

The present work evaluates the potential of nano- and microparticulate drug delivery systems based on the biodegradable and biocompatible poly (lactic-co-glycolic acid) for oral/rectal administration to improve therapy of inflammatory bowel disease. A design of experiments approach was applied to achieve reproducible and controllable drug delivery system preparation to guarantee consistent quality.

Both nanoparticles and microparticles were loaded with the immunosuppressant cyclosporine A and the corticosteroid budesonide. The formulations were characterized for physico-chemical and biopharmaceutical properties. These properties, cytotoxicity and immunotoxicity were evaluated in different *in vitro* cell culture systems including a three-dimensional cell culture model of the inflamed intestine. *In vivo* animal tests were performed with selected cyclosporine A formulations in a chemically induced colitis model in mice. In particular, cyclosporine A loaded nanoparticles showed, due to reduced systemic bioavailability, a significant improvement of disease characteristic parameters colon length and colon weight/length ratio, and in the histological analysis, compared to a commercially available product (Sandimmun[®] Neoral) and diseased control, respectively.

Zusammenfassung

Chronisch-entzündliche Darmerkrankungen, Morbus Crohn und Colitis ulcerosa, benötigen eine lebenslange, symptomatische, medikamentöse Behandlung, die mit erheblichen Nebenwirkungen assoziiert ist.

Die vorliegende Arbeit evaluiert das Potenzial von aus Polylactid-co-Glycolid hergestellten, für rektale/orale Applikation geeigneten, nano- und mikropartikulären Arzneistoffträgersystemen für eine verbesserte Behandlung. Die Herstellungsmethoden wurden durch statistische Versuchsplanung optimiert, um reproduzierbare, kontrollierbare Prozesse sowie gleichbleibende Qualität zu gewährleisten.

Die Arzneistoffträgersysteme wurden anschließend mit dem Immunsuppressivum Cyclosporin A und dem Kortikosteroid Budesonid beladen, die physikochemischen und biopharmazeutischen Eigenschaften bestimmt sowie diese, die Zytotoxizität und die Immuntoxizität in verschiedenen Zellkulturmodellen, insbesondere auf einen *in vitro* Zellkulturmodell der entzündeten Darmmukosa, charakterisiert. Aufgrund der Resultate wurden die mit Cyclosporin A beladenen Arzneistoffträgersysteme in einem Mausmodell der chemisch induzierten Kolitis getestet. Vor allem die Cyclosporin A beladenen Nanopartikel zeigten, durch eine reduzierte systemische Verfügbarkeit des Arzneistoffes, eine signifikante Verbesserung in den charakteristischen Parametern Kolonlänge, Kolon Gewichts/Längenverhältnis und in der histologischen Analyse im Vergleich zu einem kommerziellen Produkt (Sandimmun®Neoral) und zu erkrankten, unbehandelten Mäusen.

Table of contents

1. Introduction	1
1.1. Inflammatory bowel disease – Clinical manifestation and pathogenesis	1
1.2. Medical therapy of inflammatory bowel disease	3
1.2.1. Cyclosporine A and budesonide as drugs for the treatment of inflammatory bowel disease.....	4
1.3. Dosage forms for the therapy of inflammatory bowel disease.....	7
1.4. State of the art - Polymeric nano- and microparticles for the therapy of inflammatory bowel disease.....	9
1.5. Selected production techniques for the fabrication of PLGA based drug delivery systems	12
1.6. <i>In vitro</i> three-dimensional cell culture model as an advancement in efficacy studies of particulate drug delivery systems	15
1.7. The chemically induced dextran sodium sulfate model of colitis for <i>in vivo</i> studies.....	17
1.8. Aim of this work.....	19
2. A design of experiment study of nanoprecipitation and nano spray drying as processes to prepare PLGA nano- and microparticles with defined sizes and size distributions.....	21
2.1. Introduction	22
2.2. Materials	24
2.3. Methods	25
2.3.1. Preparation of nanoparticles by nanoprecipitation.....	25
2.3.2. Preparation of PLGA particles by nano spray drying	25
2.3.3. Design of experiments.....	26
2.3.4. Factors varied for the nanoprecipitation method in the design of experiments.....	27
2.3.5. Factors varied for the nano spray drying in the design of experiments	27
2.3.6. Determination of particle size and size distribution and yield.....	28
2.3.7. Investigation of morphology by scanning electron microscopy	29
2.3.8. Investigation of robustness for the nanoprecipitation method	30
2.3.9. Investigation of robustness for the nano spray drying	31
2.4. Results.....	32
2.4.1. NPR - Results of the DOE: Influence on size and size distribution	32

2.4.2.	NPR - Optimization based on the DOE	35
2.4.3.	NPR - Investigation of robustness	38
2.4.4.	NSD - Results of the DOE on size and size distribution	39
2.4.5.	NSD - Results of the DOE on yield	43
2.4.6.	NSD – Optimization.....	44
2.4.7.	NSD – Investigation of robustness.....	45
2.5.	Discussion.....	45
2.5.1.	Outcome of the design of experiments for the NPR	46
2.5.2.	Outcome of the design of experiments for the NSD on size and size distribution.....	48
2.5.3.	Design of experiments as tool in the development of nano- and microparticulate drug delivery systems	51
2.6.	Conclusion	51
3.	Advanced formulations of cyclosporine A and budesonide for the therapy of inflammatory bowel disease	53
3.1.	Introduction	54
3.2.	Materials	55
3.3.	Methods	56
3.3.1.	Optimization of the freeze drying process of nanoparticles.....	56
3.3.2.	Preparation of API loaded nanoparticles by nanoprecipitation.....	57
3.3.2.1.	Purification	57
3.3.3.	Preparation of API loaded microparticles by nano spray drying.....	58
3.3.4.	Determination of particles size, size distribution and zeta potential	59
3.3.5.	Investigation of morphology by scanning electron microscopy	59
3.3.6.	Determination of encapsulation efficiency and optimal loading.....	59
3.3.7.	X-ray powder diffraction	61
3.3.8.	<i>In vitro</i> drug release studies	62
3.4.	Results.....	63
3.4.1.	Optimization of freeze drying process of nanoparticles	63
3.4.2.	Determination of encapsulation efficiency and optimal loading.....	65
3.4.3.	Size and size distribution of loaded nanoparticles and microparticles.....	68

3.4.4.	X-ray powder diffraction	71
3.4.5.	<i>In vitro</i> drug release studies	73
3.5.	Discussion.....	74
3.6.	Conclusion	78
4.	Structural analysis and modification of spray dried microparticles	79
4.1.	Introduction	80
4.2.	Materials	80
4.3.	Methods	81
4.3.1.	SAXS analysis	81
4.3.2.	Modification of spray dried microparticles	81
4.3.2.1.	Modification of <i>in vitro</i> release	81
4.3.2.2.	Modification of size by spraying of low molecular weight PLGA.....	82
4.4.	Results.....	83
4.4.1.	SAXS analysis	83
4.4.2.	Modification of spray dried microparticles	83
4.5.	Discussion.....	86
4.6.	Conclusion	88
5.	<i>In vitro</i> efficacy testing of PLGA particles on cell culture model of the inflamed intestinal mucosa	89
5.1.	Introduction	90
5.2.	Materials	90
5.3.	Methods	91
5.3.1.	Preparation and characterization of API loaded nanoparticles and microparticles	91
5.3.2.	Preparation of DID loaded particles	91
5.3.3.	Characterization of DID loaded particles.....	92
5.3.3.1.	Determination of size, size distribution and zeta potential	92
5.3.3.2.	Determination of encapsulation efficiency.....	92
5.3.4.	Cell culture.....	93
5.3.5.	Set-up of triple culture and experimental design of efficacy studies.....	94
5.3.6.	Monitoring of triple culture during efficacy studies.....	95

5.3.7.	Stability of nanoparticles and microparticles in triple culture media	95
5.3.8.	Investigation of cytotoxicity of nano- and microparticles on cells used for the triple culture	96
5.3.9.	Deposition of nano- and microparticles on the triple cell culture model.....	97
5.3.10.	Statistical analysis.....	97
5.4.	Results.....	98
5.4.1.	Characterization of nano- and microparticles	98
5.4.2.	Stability of nanoparticles and microparticles in triple culture media	98
5.4.3.	Investigation of cytotoxicity of nano- and microparticles on cells used for the triple culture	100
5.4.4.	Efficacy studies of budesonide loaded nano- and microparticles on triple culture	101
5.4.5.	Efficacy studies of cyclosporine A loaded nano- and microparticles on triple culture	103
5.4.6.	Deposition of nano- and microparticles on the triple cell culture model.....	105
5.5.	Discussion.....	107
5.6.	Conclusion	108
6.	Investigation of cytotoxicity and immunotoxicity.....	110
6.1.	Introduction	111
6.2.	Methods and Materials	112
6.2.1.	Particle preparation and characterization.....	112
6.2.2.	<i>In vitro</i> cytotoxicity assay.....	113
6.2.3.	Immunotoxicity studies	114
6.2.3.1.	Activation of complement system by nano- and microparticles.....	114
6.2.3.2.	Alteration of cytokine secretions of dendritic cells by nano- and microparticles.....	115
6.3.	Results.....	116
6.3.1.	<i>In vitro</i> cytotoxicity assay.....	116
6.3.2.	Immunotoxicity studies	116
6.3.2.1.	Activation of complement system by nano- and microparticles.....	116
6.3.3.	Alteration of cytokine secretions of dendritic cells by PLGA particles	118
6.4.	Discussion.....	119
6.5.	Conclusion	122
7.	Evaluation of cyclosporine A loaded PLGA based drug delivery systems for inflammatory bowel disease in DSS Balb/C mice model.....	123

7.1.	Introduction	124
7.2.	Materials	125
7.3.	Methods	126
7.3.1.	Preparation and characterization of cyclosporine A loaded nano- and microparticles	126
7.3.2.	Stability of particles in simulated gastrointestinal tract of mice.....	126
7.3.3.	<i>In vitro</i> release profile in simulated gastric fluid	126
7.3.4.	Induction and assessment of DSS-induced colitis and therapeutic efficacy	127
7.3.5.	Histological analysis.....	129
7.3.6.	Cytokine level	130
7.3.7.	Cyclosporine A level in plasma.....	130
7.3.8.	Statistical analysis.....	130
7.4.	Results.....	131
7.4.1.	Characterization of cyclosporine A loaded nano- and microparticles	131
7.4.2.	Stability of particles in simulated gastrointestinal tract of mice.....	131
7.4.3.	<i>In vitro</i> release profile	132
7.4.4.	Clinical parameters - Body weight loss and disease activity index.....	133
7.4.5.	Clinical parameters - Colon length and weight/length ratio	135
7.4.6.	Clinical parameter - Cytokine level	137
7.4.7.	Histological analysis.....	139
7.4.8.	Cyclosporine A level in plasma.....	141
7.5.	Discussion.....	142
7.6.	Conclusion	145
8.	Summary and outlook	146
9.	Zusammenfassung und Ausblick	151
10.	List of abbreviations.....	156
11.	Bibliography	159
12.	Scientific output	175
13.	Acknowledgement/Danksagung	178

1. Introduction

1.1. Inflammatory bowel disease – Clinical manifestation and pathogenesis

Currently around 320.000 patients in Germany suffer from inflammatory bowel disease (IBD) with increasing incidence in Northern Europe, United Kingdom and North America [1], [2]. IBD includes Crohn's disease (CD) and ulcerative colitis (UC). Both forms differ in clinical manifestation, pathogenesis, severity level and progression.

CD is characterized by a chronic transmural inflammation, which affects the entire wall of the bowel down to the serosal layer and can involve all parts of the gastrointestinal tract (GIT) from the mouth to the anus. The often discontinuous inflammation in CD is pre-dominantly situated in the small or/and large intestine, usually with a focus in the distal ileum [3], [4]. CD can be associated with intestinal granulomas, strictures and fistulas. On the other hand, UC affects the innermost mucosa, while the deeper tissue layers of submucosa, muscularis or serosa are not involved. The entire colon is inflamed continuously including a constant involvement of the rectum and a variable involvement of proximal segments of the colon, cecum, ascending and transverse colon. 25%-50% of the patients with UC only show an involvement of the rectum (proctitis) and 25% show an inflammation of the whole extension of the colon [5]. Furthermore, patients suffering from UC have a higher risk of developing colon cancer, because the colonic inflammation plays a key role for colon cancer [6]. A special form of IBD is the indeterminate colitis, which is characterized by an inflammation of the colon and shares clinical characteristics of both UC and CD [5]. Patients with IBD in general have a higher risk of primary sclerosis cholangitis, ankylosing spondylitis and psoriasis [7]. For patients suffering from UC a life time reduction has been observed [5].

IBD patients show common symptoms such as abdominal pain, cramping, bloody stool, diarrhea, fever, fatigue and weight loss [8]. Both IBD forms have an episodic progression of the disease. Diseased phases alternate with phases of remission. Active disease is characterized by an exaggerated immune response with a dominant T-cell activity [3]. CD is dominated by T helper cell 1 (T_H1) and T_H17 immune response, which is triggered by increased synthesis of interleukin (IL)-12 [9]. Therefore, the cytokine profile in CD is dominated by interferon (IFN)- γ , IL-17 and IL-22 [10]. In contrast, UC is mainly T_H2 mediated, resulting in an expansion of natural killer cells producing IL-13 [10]. The difference in the immune response can be associated with the susceptibility of both disease forms to different kinds of treatment.

The hyperactivation of effector immune cells leads to high levels of pro-inflammatory cytokines and mediators including tumor necrosis factor- α (TNF- α), IL-6, IL-8, IFN- γ and cyclooxygenase-2 (COX-2), inducible nitric oxide synthases (iNOS) and metalloproteinase expression, which are involved in the mechanism of tissue damage [11], [12]. The common histological changes associated with IBD occur. They include e.g. villus atrophy, loss of crypts and ulcerations. Moreover, the activation of T-cells and macrophages leads to an uncontrolled inflammation and to inflammatory cycles. The nuclear transcription factor kappaB (NF- κ B) was identified as one key regulator in the pathogenesis. The activation of NF- κ B leads to increased levels of inflammatory mediators (TNF- α , IL-6 and IFN- γ) in both CD and UC.

CD and UC are assumed to be initiated by the interplay of different genetic and environmental factors. These factors deregulate the anti- and pro-inflammatory balance in the gut influencing the intestinal commensal flora and triggering the inappropriate immune response [1], [8], [13]. 99 non-overlapping genetic risk loci, 28 of which are common between CD and UC, were identified in genome wide association studies (GWAS) [14]. These genes are responsible for e.g. the barrier function, epithelial restitution, microbial defence, innate immune regulation, reactive oxygen species generation, autophagy, regulation of adaptive immunity and metabolic pathways associated with cellular homeostasis [14]. A monogenetic mutation in the NOD2 gene was further associated with CD [15]. Homozygous gene carriers have an 11 to 27 times higher probability of developing CD compared to heterozygous gene carriers. Heterozygous gene carriers themselves have a risk factor of 1.75 to 4 compared to non-carriers [15], [16]. NOD2 is a putative intracellular receptor for bacterial peptidoglycan, which is part of the bacterial membrane and induces a protective cascade. The cascade ends in the expression of human α -defensins. α -Defensins are antibiotic effector molecules predominantly expressed in the Paneth cells of the ileum. The mutation of the NOD2 gene leads to a reduced defensin expression. That is why patients carrying a NOD2 mutation show a high inflammation in the ileum [14], [17].

Several environmental risk factors, which contribute to the development of IBD, were proposed and investigated, but due to inconsistent data the role of some of these is still under discussion [13]. Environmental risk factors e.g. excessive childhood hygiene, use of oral contraceptives or diet are associated with an increased risk, whereas appendectomy, breastfeeding and infections/vaccination seem to have a protective effect [1], [13], [17].

Case studies and meta analyses revealed consistent data for the risk factor smoking [18]–[21]. A meta-analysis has demonstrated that smokers have a two times higher risk especially of developing CD [22]. Moreover, CD patients who smoke show more frequent relapses and need more medical treatment and more often surgery to control the disease [22]. For patients suffering from UC smoking seems to have a protective effect supposedly due to an increased mucus and defensin production induced by nicotine [17].

1.2. Medical therapy of inflammatory bowel disease

There is no cure for IBD. Along with that, the patients need a lifelong application of the medical treatment, which is based on mainly corticosteroids, aminosalicylates and immunosuppressants. Currently, the main aims of this symptomatic treatment of IBD are: (a) to reduce the inflammation, (b) to bring the patients into remission, (c) to maintain remission, and (d) to improve the quality of life. Finally, 70%-80% of the patients with CD and 25%-40% of the patients with UC however need surgery to control the disease [3], [8].

Aminosalicylates, e.g. mesalazine, are used in order to treat mild to moderate active CD, UC and to maintain remission in UC [17]. The anti-inflammatory effect of aminosalicylates is based on the reduction of leukotriene production, inhibition of synthesis of pro-inflammatory cytokines and cellular release of IL-1, IL-2 and NF- κ B [23]. Furthermore, aminosalicylates reduce the long-term risk of colon cancer in UC [12]. Several chemical modifications of mesalazine (5-amino-salicylic acid), e.g. olsalazine (5-amino-salicylic acid dimer) and balsalazide (5-amino-salicylic acid linked to 4-aminobenzoyl- β -alanine), are on the market to reduce the resorption in the upper parts of the intestine in comparison to mesalazine. Therefore, the systemic side effects, e.g. nausea, vomiting and headache, can be reduced [4], [23].

Corticosteroids modulate the immune response via the glucocorticoid receptor in the nucleus and inhibit the expression of adhesion molecules and trafficking of immune cells to target tissues [23]. In the last decades they have primarily been used for the treatment of moderate to severe active CD and severe UC, also in combination with aminosalicylates [24]. The therapy induces in 60-92% of cases a remission after 4-6 weeks [17]. The application of corticosteroids is limited due to short-term and long-term adverse effects, e.g. systemic immunosuppression, risk of opportunistic infections, Cushing's syndrome including diabetes mellitus and osteoporosis [25].

Moreover, some patients do not respond to corticosteroids, named as steroid-refractory disease, or the corticosteroids cannot be tapered without relapse, named as steroid-dependent. The significant morbidity under treatment with corticosteroids for CD patients caused a change to newer agents including biologicals [4]. Unfortunately, neither aminosalicylates nor corticosteroids can reduce relapses in CD which is the main goal of the medical treatment in CD.

Azathioprine, methotrexate und biologicals (infliximab, adalimumab, cetrolizumab) are used in order to treat steroid-refractory or steroid-dependent patients and severe disease, in case other therapy options failed to induce remission [4]. As azathioprine, which can cause bone marrow suppression and pancreatitis, needs 2-3 months to reach the full therapeutic efficacy, it is often combined with biologicals (“bridging”) [3], [17]. This combination also reduces the development of antibodies against the biologicals, which is a drawback of a biological therapy [26].

Infliximab, a chimeric monoclonal antibody to TNF- α , was introduced to the medical therapy of CD in 1997 [5], [27]. TNF- α mediates multiple pro-inflammatory processes implemented in the pathogenesis of IBD. Adalimumab and certolizumab pegol are also approved by the American Food and Drug Administration (FDA) and showed efficacy in the treatment of CD [5]. Adalimumab is a recombinant human IgG1 monoclonal antibody that binds with high specificity and affinity to human TNF- α [5]. Certolizumab pegol is a monoclonal humanized anti-TNF- α antibody Fab’ fragment linked chemically to polyethylene glycol (PEG) [5]. All these biologicals have to be applied intravenously or subcutaneously, resulting in a reduced patient compliance. Although these therapies generally demonstrated efficacy in inducing and maintaining remission, they failed in inducing remission in about 50% of the CD patients [4], [23], [26], [28], [29]. Plus, the use of biologicals is further associated with infections and increased risk of neoplasia in combination with immunosuppressive drugs [26].

1.2.1. Cyclosporine A and budesonide as drugs for the treatment of inflammatory bowel disease

The cyclosporine A (CYA) is a cyclic peptide of 11 amino acids (Figure 1.1a), which are partially untypical or rarely encountered in nature, e.g. D-alanine [30]. CYA is a very potent immunosuppressive drug and can be isolated from the fungus *Tolypocladium inflatum* Gams (Beauveria nivea) or chemically synthesised.

In the treatment of IBD CYA is applied to UC patients suffering from fulminant colitis or who being steroid-refractory. The therapy is started intravenously for three to five days (2 mg/kg/day) and is typically continued after reaching remission with oral CYA (5-8 mg/kg/day, in two doses per day), often in co-medication with azathioprine and methotrexate for maintenance therapy [17].

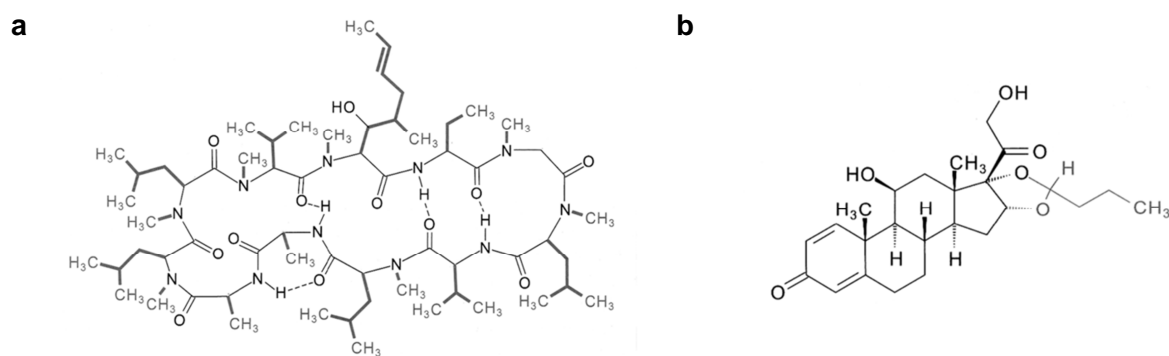


Figure 1.1. Chemical structure of (a) cyclosporine A (M_r 1206.6) as tertiary structure (-- = hydrogen bond) and (b) budesonide (M_r 430.53) (adapted and modified from Steinhilber et al. [31]).

CYA inhibits the production of cytokines secreted by lymphocytes e.g. IL-1 and IL-2 at a high selectivity [30]. Furthermore, CYA inhibits nitric oxide synthesis induced by IL-1 α , lipopolysaccharides and TNF- α . Through the inhibition of IL-2 the expansion of antigen-specific T-cells and the maturation to cytotoxic T-cells is stopped and, therefore, the immune reaction is suppressed [30]. CYA binds on the intracellular receptor cyclophilin, a proline-cis/trans-isomerase [23]. The complex (CYA/cyclophilin) inhibits afterward the calcium/calmodulin depending phosphatase, calcineurin, and blocks the signal transduction. This prevents the activation of transcription factors, e.g. NFAT (nuclear factor of activated T cells) and NF- κ B hindering the synthesis of cytokines in T-cells. NFAT is mostly located in T cells. This explains the high selectivity of CYA and the specific, reversible effect on lymphocytes, especially T_H cells, whereas phagocytic cells of the reticuloendothelial system are not affected [23], [31], [32].

CYA is an inhibitor and substrate of cytochrome P450 3A4 (CYP3A4) and inhibitor of the multidrug efflux transporter p-glycoprotein. Therefore, CYA may increase plasma concentrations of co-medications that are substrates of CYP3A4 or p-glycoprotein or both, e.g. verapamil, carbamazepine resulting in overdosing [17], [31].

The physico-chemical, pharmacokinetic and pharmacodynamic properties of CYA are summarized in Table 1.1. The therapeutic window of CYA is narrow (0.15-0.25 µg/ml [31]) and the plasma levels should be monitored during the therapy to avoid overdosing as well as underdosing and consequently inefficiency. The CYA therapy is associated with adverse effects, e.g. neurological toxicity (tremor), opportunistic infections, renal dysfunction and hypertension, hirsutism and gum hyperplasia [23]. Lifelong application of CYA may lead to hypertension, diabetes mellitus, hyperlipidemia and adiposity [23].

Table 1.1. Physico-chemical, pharmacodynamic and pharmacokinetic properties [23], [33], [34].

substance	cyclosporine A	budesonide
physico-chemical properties		
solubility	soluble in DMSO (25 mg/ml), acetone ethanol, chloroform; practically insoluble in water	freely soluble in methylene chloride; sparingly soluble in ethanol (30 mg/ml); partially soluble in water (saturation concentration 14 µg/ml)
partition coefficient	log P _{octanol/water} 2.92 [35]	log P _{octanol/water} 3.2 [36]
pharmacodynamic and pharmacokinetic properties		
absolute bioavailability	10-90% (depends on the patient population); increased by fatty meals	11%
plasma protein binding	90%	88%
apparent volume of distribution	3.5-13 l/kg	3 l/kg
terminal half-life	5-19 h	2.5 h
maximum plasma concentration after oral application	1.5-2.0 h	5 h
elimination	biliary	renally

Budesonide (BU), a corticosteroid (Figure 1.1b), is a strong antiphlogistic drug with strong local effectiveness. The affinity of BU to the glucocorticoid receptor is 100 fold higher than of hydrocortisone. Like other glucocorticoids BU inhibits the activation of NF-κB. The anti-inflammatory effect results from the inhibition of genes responsible for the synthesis of pro-inflammatory mediators, e.g. IL-1, COX-2 and the activation of the anti-inflammatory IL-1 receptor agonist and IL-10.

The physico-chemical, pharmacokinetic and pharmacodynamic properties of BU are summarized in Table 1.1. BU is metabolized up to 90% during first liver passage to metabolites with less effectiveness (<1% compared to BU), in particular 6-beta-hydroxybudesonide and 16-alpha-hydroxyprednisolon. The metabolites are eliminated renally.

In the therapy of CD BU is a first-line agent for the treatment of affected ileum and/or ascending colon [17], [37], [38]. It can be applied orally (9 mg/day) and locally as foam, suppositories or enema (2 mg/day) in order to target the descending colon and rectum [17]. The extensive first-pass metabolism reduces the systemic bioavailability of BU after oral administration [39], [40]. Therefore, also side effects comparable to other corticosteroids, e.g. weight gain and cushingoid, occur in a reduced pattern. Apart from this, steroid-refractory disease can also not be overcome with BU therapy.

1.3. Dosage forms for the therapy of inflammatory bowel disease

A major issue in the therapy of the local inflammation is the systemic absorption of those highly active drugs which cause adverse effects, especially due to the required lifelong treatment. This effect can be enhanced by the increased permeability of the upper intestinal mucosa during the active state of IBD [41], [42].

IBD differs in its manifestation and the therapy has to be individualized in the applied drug and the drug delivery strategy depending on the location of the inflammation. To achieve an optimal treatment, the drug should ideally be applied locally at the site of inflammation to obtain high concentrations in the affected tissues and to reduce the access to the systemic circulation [43]. Several drugs and a multitude of simple as well as advanced formulations are available on the market for the therapy of IBD. Dosage forms are available to target the inflamed areas via rectal route or which release the encapsulated drugs pH- or time-dependently to target different parts of the GIT via oral route. However, the used galenic strategies are not fully adapted to the pathophysiological changes in IBD.

Proctitis and left-sided colitis, which is characterized by an inflammation of the descending colon, are treated rectally with foams, enemas and suppositories containing either aminosalicylates (mesalazine; Salofalk[®], Claversal[®]) or corticosteroids (betamethasone; Betnesol[®]). In CD, where the inflammation is more distributed and often the ileum involved, the rectal therapy with foams, enemas and suppositories is less suitable.

In general, the oral route is more tolerated by patients, but the solid oral dosage forms require advanced galenic approaches [44]. However, the application of solid oral dosage forms such as capsules, granules, pellets and tablets is often inefficient due to accelerated elimination by diarrhea in IBD. Furthermore, UC patients show a decreased contractility of the colon leading to variable gastrointestinal transit times [45]. Nonetheless, this is the only chance of delivering drugs to the upper parts of the intestine [43].

Coatings of oral dosage forms releasing the encapsulated drug in pH-dependent manner are used in order to target different parts of the intestine [4], [46]. For example mesalazine containing tablets with a stomach resistant coating (Claversal[®], Salofalk[®]) and with colon targeting coating (Asacolitin[®]) have been developed to target the terminal ileum and the colon, respectively [4], [46]. Unfortunately, 20-40% of the released mesalazine is systemically available from these with poly(meth)acrylates (Eudragit[®]) coated tablets and, thus, responsible for observed side effects [4], [46], [47]. Furthermore, several studies revealed a pH change in the GIT depending on the disease state of the patients [48]. In detail, the colonic pH in active and inactive CD was investigated to be ~5.3 in both the proximal and in the distal part. The pH of the small intestine seems not to be affected [49], [50]. For UC proximal colonic pH values ranging individually from 2.3-3.4 have been reported [51]. These pathophysiological changes could influence the drug release resulting either in an incomplete drug release or in an release apart from the targeted part of the GIT [49]. Therefore, these pH-dependent release strategies have been controversially discussed [44], [52].

Moreover, the optimum size range of dosage forms to avoid the accelerated elimination by diarrhea and to increase transit times is so far not finally determined [43]. Hardy et al. investigated options for influencing the residence time in the large intestine even for patients suffering from diarrhea. By reducing the diameter of an oral dosage form (capsule vs. pellet system) an increased residence time in the large intestine could be achieved [53]. Thus, sugar matrix based pellet systems containing BU, which are coated with Eudragit[®]L 100 (Entocort[®]) or a combination of Eudragit[®]S 100 and Eudragit[®]L 100 (Budenofalk[®]), were successfully commercialized for IBD treatment to target the terminal ileum or ascending colon [17], [23], [54], [55]. As they release the BU at pH >5.5 and pH 6.4, respectively, at the moment only patients with inflammation located in the respective parts of the colon benefit from this galenic modification.

Furthermore, efforts have been made to develop controlled release oral dosage forms with a lag phase in the drug release to treat patients with affected parts in the small and large intestine [56]. One of these systems is based on a tablet, which disintegrates in the stomach and releases microgranules (Pentasa[®]). The microgranules coated with ethyl cellulose release the encapsulated mesalazine time-dependently and diffusion controlled [47].

Due to the low solubility of CYA special dosage forms had to be developed in order to deliver CYA orally and intravenously. For example CYA was formulated in a dispersed system, consisting of aqueous phase, lipid phase and surfactant, which forms a microemulsion in contact with water (Sandimmun[®] Neoral) [57]. The small size of the emulsion droplets (<100 nm) supports the fast adsorption and, thus, increases the bioavailability [34]. Nevertheless, the CYA is systemically available from this dosage form causing adverse effects.

CYA and BU were selected as drugs for the presented work, leading to adverse effects when systemically available. Furthermore, with the current dosage forms the drug is also available in healthy parts of the intestine. Therefore, patients would benefit from a dosage form that would deliver the encapsulated CYA and BU directly to the inflamed areas of the intestine. Such a local treatment aimed to reduce the applied dose due to high drug concentrations in the affected tissues. Furthermore, high systemic concentrations would ideally be avoided and, therefore, the side effects of the used drugs could be reduced.

1.4. State of the art - Polymeric nano- and microparticles for the therapy of inflammatory bowel disease

Several well-known properties of particulate formulations in the micro- or nanometer size range (nanoparticles and microparticles) suggest them as a very promising strategy for the therapy of IBD. Preferentially biodegradable and biocompatible polymers, e.g. poly (lactic-co-glycolic acid), (PLGA), and natural compounds such as proteins and lipids are used in order to fabricate nanoparticles (NPs) and microparticles (MPs) in the medical and pharmaceutical context [58]. The selection of material for the formulation of drug delivery systems (DDS) is furthermore a key factor for a (a) successful encapsulation and delivery of drugs, and (b) compatibility in the applied organism.

In the production and development of NPs and MPs as DDS the synthetic, biocompatible and biodegradable polymer PLGA is due to several characteristics the most attractive choice.

PLGA is approved by the FDA in the medical field for the use as implants and surgical sutures [59]. Furthermore, in the human body PLGA will be degraded through hydrolysis of the ester-bonds into its two non-toxic components, lactic acid and glycolic acid, which can be metabolized in the citric cycle [59], [60]. The fastest degradation of PLGA is reached with a 50/50 (wt/wt) ratio of lactic and glycolic acids. In this ratio, PLGA is amorphous and, therefore, optimal for DDS as it decomposes within two months [61], [62]. The degradation proceeds more slowly with higher ratios of lactic acid, which increase the hydrophobic characteristics forcing a reduced water adsorption [61], [62]. Therefore, the faster release rates of encapsulated ingredients were obtained with PLGA at a ratio of 50/50 (lactic/glycolic acid) [63], [64].

The adjustable wide range of degradation times as well as the possibility of modifying the surface by conjugation to the carboxyl groups, offer the ability to encapsulate hydrophobic and hydrophilic drugs (e.g. BU and CYA). Plus, proteins as well as RNA and DNA can be attached on PLGA based DDS [61]. During the past two decades PLGA was extensively studied for the production of nano- and microparticulate DDS for several areas of the human body e.g. blood system, skin [65], lung [66] and intestine [67], [68].

Targeting strategies

With the polymeric NPs and MPs different targeting strategies can be addressed aiming for an improved therapy of IBD by active or passive targeting and pH- or time-dependent release strategies.

For an active targeting with specific targeting moieties on the particle surface a suitable target cell type, which can alter the inflammatory status in IBD alone, has been not identified so far. In addition, a specific and accessible enough surface receptor needs still to be found. Nevertheless, first active targeting strategies have been tested for targeting the epithelial cells and immune-related cells, which are present due to the inflammation and involved in the pathogenesis of IBD [69]–[71].

Passive targeting strategies by oral or rectal application of NPs and MPs were successfully tested and revealed the advantages of the DDS for the therapy of IBD. On the one hand NPs and MPs have been used in order to deliver the encapsulated drugs near to the cells, supporting a faster up-take in the inflamed mucosa and for saving the drug from degradation [72], [73]. A higher expression of p-glycoprotein and CYP3A enzymes in inflamed tissues can increase the degradation of drugs and lead to treatment failure [74].

On the other hand NPs and MPs are able to remain in the ulcerated areas of the colon for prolonged periods of time, due to the destroyed intestinal barrier, whereby they can release the encapsulated drug controlled in situ [67], [75]–[78]. Furthermore, NPs can be entrapped in the mucus layer of the lumen [75]. Due to the inflammation the mucus production increases, which leads to a thicker mucus layer, particularly in the ulcerated areas [72], [79], [80]. By comparing 0.1 μm , 1 μm and 10 μm polystyrene NPs in a model of experimental colitis (trinitrobenzenesulfonic acid (TNBS) Lewis rat model) Lamprecht et al. could show a size depended accumulation in the intestinal mucus and inflamed tissues. The accumulation of 0.1 μm NPs was higher, due to the attachment to the increased mucus layer, the easier penetration into this mucus layer and deposition in ulcerated areas [75], [78].

In order to control the release and avoid high systemic concentrations, mesalazine was covalently bound to poly (ϵ -caprolactone) NPs. After oral administration the particles showed a comparable efficacy to mesalazine solution in a TNBS colitis mice model [81]. These particles were improved by grafting silica NPs with mesalazine, which offer the possibility of a triggered release after 8 h by enzymatic cleavage [81], [82]. The silica NPs accumulated sixfold higher in inflamed tissues in the TNBS colitis model compared to healthy control [82].

Apart from the concept of time-dependent release from particulate formulations, also NPs and MPs with a pH-dependent release were prepared. Both concepts aimed to overcome the issue of the residence time of coated tablets and pellets by size reduction. BU loaded pH-sensitive NPs, consisting of a matrix of PLGA and Eudragit[®]S 100, also showed an accumulation in inflamed tissues in a TNBS rat model [83]. In a recent study BU loaded PLGA NPs were coated with the pH-sensitive Eudragit[®]S 100 and the efficacy was confirmed in different acute and chronic colitis mouse models [67].

Studies with chitosan-calcium-alginate MPs for a colon specific oral delivery of mesalazine revealed in a TNBS colitis model an advantage of negatively charged DDS [84]. This effect was explained with the high concentration of positively charged proteins in inflamed tissues, in particular high amounts of eosinophil cationic protein, which could be determined in the colorectal perfusion fluid of IBD patients [85], [86]. Jubeh et al. underlined these findings by investigating a charge dependent deposition of liposomes after rectal administration. The study revealed a twice as strong adherence of anionic liposomes to the inflamed mucosa in comparison to neutral or cationic liposomes [86], [87].

In summary, these studies substantiate the potential of NPs and MPs for an improved therapy of IBD. A size-dependent accumulation can be proposed and at the moment NPs seems to be favorable in rodent colitis models [75], [81]. However, a recent study revealed a higher accumulation efficiency for MPs in human patients compared to NPs prepared with the same material [76]. This effect has to be further investigated. In addition, a species mechanism was suggested by Leonard et al., which could help to explain this effect, due to the different dimensions. For example the length of small intestine was determined to be <50 cm for mice compared to humans with 3-4 m [88].

Unfortunately, only a few nanoformulations, mainly nanocrystals, have entered the pharmaceutical market until now. It can be presumed that the absence of information concerning production parameters is hindering the scale-up and the more widespread production in particular of matrix based NPs and MPs as DDS in the pharmaceutical industry [89].

1.5. Selected production techniques for the fabrication of PLGA based drug delivery systems

The choice of the appropriate preparation technique for a particulate DDS, NPs or MPs, is based on nature, lipophilicity and stability of the drug, on the nature of polymer and the route of administration, as well as the period of administration [90], [91]. In general, the methods can be divided in three main groups: (a) chemical methods with in situ polymerizations of macromolecules, (b) physico-chemical methods using preformed polymers [91], and (c) mechanical methods using e.g. spray drying for the formation of the particulate DDS [92].

Nanoprecipitation method

The nanoprecipitation method with all their modifications is one of the most used physico-chemical methods for producing DDS [93]–[95]. In general, the nanoprecipitation method is known to be more controllable, reproducible and less time consuming due to fewer preparation steps [89].

For the preparation of DDS by the nanoprecipitation method a polymer is dissolved in a solvent, mostly an organic solution (e.g. acetone), which has to be miscible with a so called non-solvent for the polymer, mostly an aqueous solution [96]. An exemplary set-up is depicted in Figure 1.2.

The drop wise addition of the organic phase into the stirred aqueous phase results in the spontaneous formation of an emulsion. The diffusion of the organic solvent into the outer aqueous phase starts the polymer precipitation [94]. In detail, the formation of particles involves complex interfacial hydrodynamic phenomena and can either be explained by interfacial turbulence [58] or the Gibbs–Marangoni effect [97].

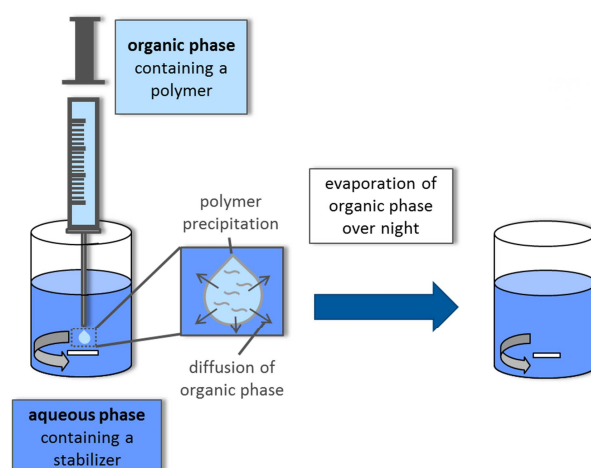


Figure 1.2. Set-up of the nanoprecipitation method.

In general, the aqueous phase is characterized by a high surface tension while the organic phase features a low surface tension. The differences in surface tension cause interfacial turbulences, which form eddies of solvent at the interface and generate interfacial convective flows [94]. Thus, the organic phase diffuses into the aqueous phase taking polymer chains with it. These chains are still in solution and precipitate forming particles due to further diffusion of organic solvent [94]. The nanoprecipitation method is limited to low polymer concentrations, which varies with the used polymer material. As consequence, with the nanoprecipitation method one achieves less DDS per volume in comparison to other physico-chemical methods [98].

Nano spray drying method

The spray drying technique is used routinely as method to convert liquid formulations into a dry powder as storable product. The process works for drug dispersions and dispersed nanoparticulate DDS [99]. Furthermore, the spray drying technique can also be used as mechanical method for formulating DDS in one step without extra washing or drying steps (single step process) for different areas of application [92].

A novel nano spray drying system (Figure 1.3), the Büchi Nano Spray Dryer B-90 (Büchi B-90), was recently developed especially for producing spray dried products in the submicron size range and attaining high formulation yields up to 90%, realized by a vibrating mesh to transport the feeding solution into the drying gas flow [100], [101].

This system (Figure 1.3) differs from a classical spray dryer in three main functions. In contrast to a nozzle for atomization of the feeding solution, the Büchi B-90 uses a stainless steel membrane with defined pores (4 μm , 5.5 μm or 7 μm ; provided by the manufacturer), which vibrates at a fixed ultrasonic frequency by a piezoelectric actuator. This vibrating mesh in the spray head of the Büchi B-90 is responsible for the formation of small droplets of feeding solution and, therefore, the production of particles in the low micron to submicron size range. Secondly, the heating system is formed of an electrically heated porous metal foam. This foam allows an optimal heating and a laminar flow of the drying gas which again provides for a quick evaporation of the sprayed solvents preventing droplet coalescence. The extremely small particles require an alternative mechanism for particle collection other than the classical cyclone collector, which is less suitable and efficient for the collection of particles $<5 \mu\text{m}$, especially for particles smaller than 2 to 3 μm [102]. An electrostatic particle precipitator consisting of a grounded and a collecting electrode allows the particle collection in the Büchi B-90 as third difference to classical spray dryer.

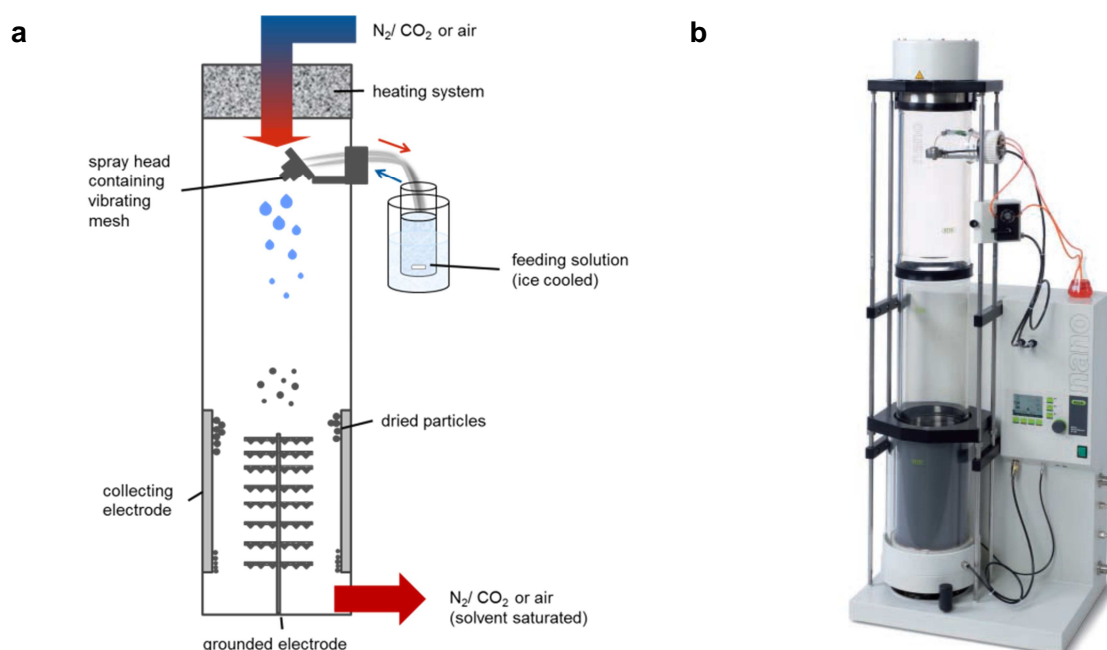


Figure 1.3. (a) Schematic set-up and (b) Photograph of the Büchi B-90 (adapted from Arpagaus et al. [103]).

Compressed air or indoor air is used for spraying of aqueous solutions. Additionally, a mixture of nitrogen and a small amount of carbon dioxide, which is needed for the particle collection, is required for a safety spraying out of organic solutions. The Büchi B-90 can be connected to a cooling unit, the Inert-Loop B-295, which separates the organic solvent from the drying gas.

By today, only a few studies have been published using this system which is available since the year 2009. First studies concentrated on the drying of pharmaceutical excipients (e.g. lactose, chitosan, mannitol, trehalose), proteins [103]–[106] and dry lipid nano-emulsions [92]. Furthermore, the Büchi B-90 has been used for the production of calpain inhibitor nanocrystals [107] and furosemide nanocrystals [92]. Recent studies also focused on the preparation of particles using polymeric wall materials (arabic gum, whey protein, polyvinyl alcohol, modified starch and maltodextrin) and proteins [108], [105] and the encapsulation of model drugs in biodegradable polymers [100], [109]. Spray drying by using the Büchi B-90 was also applied to improve the solubility of pure BU [110]. The solubility was also improved by encapsulating CYA and dexamethasone in PLGA [100]. First studies were carried out focusing on the encapsulation of proteins [105] and model drugs in biodegradable polymers [100], [109], e.g. nimodipine in PLGA MPs for post hemorrhagic cerebral vasospasm [111]. Apart from the pharmaceutical field, the Büchi B-90 was also used in order to produce lithium carbonate hollow spheres for a novel lithium battery approach [112].

1.6. *In vitro* three-dimensional cell culture model as an advancement in efficacy studies of particulate drug delivery systems

For conventional ADME (absorption, distribution, metabolism and excretion) and permeation studies enteric cell lines, in detail Caco-2, HT29 or T84 cell lines, are widely used as *in vitro* models of the healthy intestinal mucosa [113]. These models consist of one cell type only and, therefore, cannot mimic the complex interactions with other cells in the diseased intestine, in particular for IBD of immune cells [114]. As an improvement co- and triple cultures were developed with the major focus on transport studies consisting of enterocytes and immune cells, e.g. macrophages [115], [116]. However, these studies addressed the situation in a healthy intestine. The combination of enteric and immunocompetent cells can be used in order to establish an inflammable intestinal model for IBD as demonstrated by Tanoue et al., who co-cultured Caco-2 and RAW264.7 cells, a macrophage cell line [117].

A recently developed three-dimensional cell culture model (triple culture model) of the inflamed intestinal mucosa by Leonard et al. [88], which was improved by Susewind et al. [118] using cell lines, demonstrated to be an optimal tool for screening of potential nanomedicines, including particulate DDS as well as liposomes, for IBD [119]. This model (Figure 1.4) consists of Caco-2, a human intestinal epithelial cell line, THP-1, which can be stimulated to macrophages, and MUTZ-3, a dendritic-like cell line.

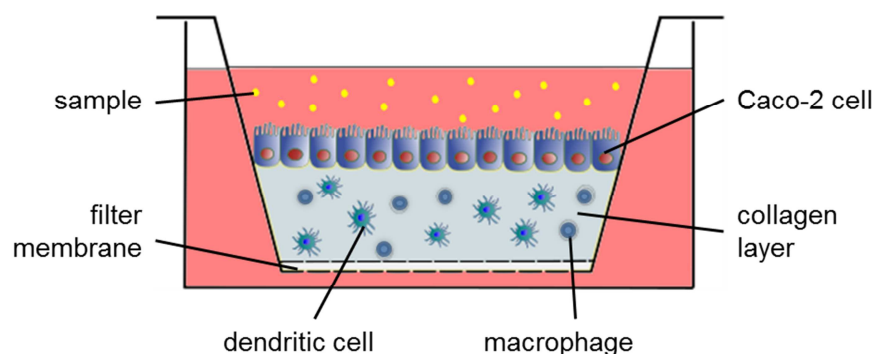


Figure 1.4 Set-up of triple culture on Transwell® inserts (adapted from Draheim and Susewind et al., chapter 12 [120]). The triple culture model consists of macrophages and dendritic cells embedded in collagen. The Caco-2 cells, as intestinal epithelial cell line, are seeded on top of the collagen layer forming a tight monolayer [119]. Image is not drawn to scale.

Through inflammation, the model can mimic the pathophysiological changes of the inflamed intestinal mucosa in chronic IBD patients. They are characterized by reorganization of tight junctions, thus, reduced barrier properties and increased immune cell activity with the release of pro-inflammatory markers [119]. The inflammation of the triple culture model is induced by IL-1 β and afterwards significantly enhanced by the MUTZ-3 and THP-1 cells [119]. The usage of macrophages and dendritic cells integrates the complexity of the pathogenesis in IBD, as both are involved in the inflammatory reactions.

The application of DDS on the apical compartment, which mimics the intestinal lumen, allows testing the anti-inflammatory efficacy via measurement of IL-8 levels and the epithelial barrier integrity by the measurement of the transepithelial electrical resistance (TEER). IL-8 is a pro-inflammatory cytokine that is inducing chemotaxis and activation of granulocytes. Moreover, IL-8 is involved in the initiation and progression of UC and CD in human patients [121]. Additionally, the triple culture model can be used to determine particle deposition within the model [119].

The model shows an improved reproducibility and acts comparable to the before developed model with the primary cell lines. Therefore, it demonstrated its capability of acting as a tool to screen for potential DDS *in vitro* before entering the *in vivo* studies [118], [119].

1.7. The chemically induced dextran sodium sulfate model of colitis for *in vivo* studies

For pre-clinical and efficacy studies of new therapeutic strategies for IBD rats and mice models of colitis are widely used. Although not presenting the complexity of the human disease, the rodent models were validated to study pathophysiological mechanisms and efficacy of new therapeutic strategies, both dosage forms and drugs [122], [123]. According to Wirtz et al. the models can be separated into models, which have (a) defects in epithelial integrity/permeability, (b) defects in innate immune cells, and (c) defects in cells of the adaptive immune system [123]. The defects can be induced chemically, by immune cell transfer or by gene targeting.

Among the chemically induced models of colitis, the dextran sodium sulfate (DSS) model has been extensively characterized. Nowadays, it is widely used to study epithelial repair mechanisms as well as the contribution of innate immune mechanisms [123], [124]. In recent studies, the model has been frequently applied to evaluate the efficacy of novel anti-inflammatory drugs [12], [122], [124]–[127], and drug delivery strategies [67], [71], [72], [77] for an improved therapy of IBD. This model shares many of the macroscopic, histological and immune characteristics of human IBD. In particular, it demonstrates clinical and histological similarity to human UC and is characterized by the following clinical parameters: bloody diarrhea, shortening of the colorectum, gastrointestinal inflammation with histopathological changes like villus atrophy, loss of crypt, ulcerations and infiltrations with granulocytes [123], [125], [128], [129].

DSS is directly toxic to the gut epithelial cells of the basal crypts and affects the integrity of the mucosal barrier [123]. The increased permeability of the intestinal barrier and hyperosmolarity in the lumen due to the DSS cause the bloody diarrhea [130]. Furthermore, an enhanced mucosal production of inflammation related cytokines, from epithelial cells and immune competent cells, leads to an increased immune cell infiltration [130]. The DSS model was evaluated to have an increased production of cytokines in the colonic mucosa: TNF- α , IL-1 β , IL-6, IL-10, IL-12 and IFN- γ [130], [131].

The DSS model can be used to assess an acute or chronic inflammation by adding DSS into the drinking water of the mice or rats. The administration of DSS over a time-period of seven days induces the acute colitis with increased mucosal levels of macrophage-derived cytokines, e.g. TNF- α and IL-6. When the DSS is applied for several cycles, e.g. according to Wirtz et al. for seven days followed by 14 days of water, it results in chronic colitis [128]. The chronic model can be modified by a single initial dose of the genotoxic colon carcinogen azoxymethane. Azoxymethane induces an inflammation-associated colorectal cancer, relevant for UC treatment (chapter 1.1) [6], [132]. The chronic DSS-induced colitis is characterized by focal epithelial regeneration due to the destabilized intestinal repair mechanism and a T_H1 and T_H2 cytokine profile with increased mucosal IFN- γ and IL-4 levels [133].

1.8. Aim of this work

New therapeutic strategies for inflammatory bowel disease are needed as the conventional medical treatment requires a lifelong application and is associated with adverse effects. Passive targeting approaches via nano- and microparticles seem to be favorable due to the ability of the particles to stick to the intestinal mucus and accumulate in the ulcerated areas of the intestinal mucosa. Thereby, the encapsulated drug can be released and applied in a controlled way to the inflamed mucosa may reducing systemic side effects. As of now only a few nanoformulations have entered the pharmaceutical market, because detailed knowledge regarding the formulation processes is lacking.

Therefore, the aims of this work were:

- to develop a small particulate polymeric drug delivery system of the biodegradable and biocompatible PLGA for oral/rectal administration for an improved therapy of inflammatory bowel disease with the perspective of pre-clinical efficacy studies,
- to identify process parameters of two manufacturing processes for preparing nano- and microparticulate PLGA drug delivery systems and to optimize both concerning reproducibility and controllability applying a design of experiments,
- to encapsulate two potential drugs for the treatment of inflammatory bowel disease, cyclosporine A and budesonide, in the nano- and microparticulate PLGA drug delivery systems and to characterize the loaded drug delivery systems,
- to evaluate the safety of the drug delivery systems in cytotoxicity and immunotoxicity studies,
- to evaluate the anti-inflammatory efficacy of the drug delivery systems on an *in vitro* three-dimensional cell culture model of the inflamed intestinal mucosa to select and assess the most suitable particles for *in vivo* studies in a dextran sodium sulfate colitis model.

The work in this thesis was performed in the context of the ERA-Net EuroNanoMed project *Delivering Nanopharmaceuticals through Biological Barriers* (Grant number: 13N11845), acronym 'BIBA', with a focus on the transfer of the preparation of nano- and microparticulate drug delivery systems to larger production scales in a future perspective. Therefore, established excipients and scalable, robust methods for the preparation of the drug delivery systems were selected.

The work in this thesis has been divided into the following chapters exploring the aims of the thesis in detail:

- Chapter 2: A design of experiment study of nanoprecipitation and nano spray drying as processes to prepare PLGA nano- and microparticles with defined sizes and size distributions
- Chapter 3: Advanced formulations of cyclosporine A and budesonide for the therapy of inflammatory bowel disease
- Chapter 4: Structural analysis and modification of spray dried microparticles
- Chapter 5: *In vitro* efficacy testing of PLGA particles on cell culture model of the inflamed intestinal mucosa
- Chapter 6: Investigation of cytotoxicity and immunotoxicity
- Chapter 7: Evaluation of cyclosporine A loaded PLGA based drug delivery systems for inflammatory bowel disease in DSS Balb/C mice model

2. A design of experiment study of nanoprecipitation and nano spray drying as processes to prepare PLGA nano- and microparticles with defined sizes and size distributions

Parts of this chapter have been published in:

Christina Draheim*, Francois de Crécy*, Steffi Hansen, Eva-Maria Collnot, Claus-Michael Lehr, *A Design of Experiment Study of Nanoprecipitation and Nano Spray Drying as Processes to Prepare PLGA Nano- and Microparticles with Defined Sizes and Size Distributions*, Pharmaceutical Research, *in press*. doi: 10.1007/s11095-015-1647-9

Reproduced with permission form Springer. © 2015

*These authors contributed equally to this work.

The author of the thesis made the following contributions to the publication: Conceived, designed and performed experiments concerning preparation and characterization of PLGA particles, selection of factors varied for the design of experiment and optimization and robustness experiments. Analysed and interpreted the data. Wrote the manuscript.

2.1. Introduction

In the production of nano- and microparticulate DDS it is highly important to understand which parameters have an influence on the process and, thus, on the formation of the DDS, or process yield. Size and size distribution are both critical properties, which may affect drug release and bioavailability [59]. With the knowledge of process parameters and limitations, critical quality attributes and sources of variability, reproducibility and controllability of the process and consistent quality of the DDS can be achieved [134]. This knowledge can further be utilized specifically to optimize and adapt the DDS e.g. in size for different application purposes. This is important for research and development of nano- and microscaled DDS and makes the production process more efficient by reducing the number of experiments and material, which is a benefit for expensive active ingredients and excipients.

Furthermore, it facilitates the scale-up process in a future perspective. The complex transfer of nano- and microscaled DDS to a larger production scale is often hindering the advancement of a promising formulation from early development to production stage and can be a bottleneck for entrance of particle-based DDS into the pharmaceutical market [89].

In this context quality by design by applying a design of experiments (DOE) approach to the nanoprecipitation method (NPR) and nano spray drying technique (NSD), both were introduced in chapter 1.5, was pursued in this chapter for the preparation of PLGA based particulate DDS. The NPR represents one of the most frequently used physico-chemical method for producing DDS [93]. In contrast, the NSD is less examined and uses as advantage a vibrating mesh instead of a nozzle in order to atomize the feeding solution (chapter 1.5). PLGA is approved in the medical field, e.g. for surgical sutures (chapter 1.4) [59], [60]. The fastest degradation of PLGA is reached with a 50/50 ratio of lactic and glycolic acids (wt/wt). In this ratio PLGA is amorphous and, therefore, optimal for DDS as it decomposes within two months [61], [62].

Quality by design in the pharmaceutical field means the systematic development of pharmaceutical products on the basis of sound scientific principles to ensure pre-defined product quality [134]–[136]. Quality by design studies have increasingly been used in the field of nano- and microparticulate DDS throughout the last years focusing mainly on the optimization of DDS loaded with active ingredients.

Especially for complex processes, such as processes for production of nanomedicines, DOE methods are excellent quality by design tool for identifying (a) critical process parameters, (b) to understand and (c) to optimize process conditions and, therefore, the final formulation in the field of nano- and microparticulate DDS [105], [135]–[141].

Some recently published studies focused mainly on the optimization of drug loaded DDS. In these studies e.g. the optimization of size [105], [108], [141]–[143] and of drug loading for PLGA NPs [65], [141]–[144], Eudragit®E NPs [135] and liposomes [140] were investigated. Furthermore, DOE studies have been applied to investigate colloidal stability of lipid NPs [145] or the influence of the stabilizer on size and zeta potential of PLGA NPs. Moreover, also the modification of the drug release from established DDS was investigated by a DOE [143], [146]. All these studies describe the optimization in preparation of DDS in a laboratory context. Only Park et al. [135] and Verma et al. [136] underlined the importance to characterize process parameters and limitations, as well as critical quality attributes to achieve high quality products and to facilitate the entrance to further studies [135]. Bürki et al. and Lee et al. were the first to apply a DOE, full factorial design and Taguchi method, respectively, focusing on spray drying of a protein using β -galactosidase [108] and bovine serum albumin [105]. A recent study used a 2^3 factorial design to develop inhalable capreomycin powders [147].

To investigate both methods systematically a fractional factorial design was used based on a response surface approach with an IV (Integrated Variance)-optimal design. A DOE could help to understand in detail the influence of parameters on an investigated process. Compared to classical experiments a DOE has many advantages. For example, a DOE offers the opportunity to vary several factors at the same time and, thus, to evaluate their main effects as well as interactions of factors. In general, interactions of third and fourth order are negligible [148]. Multiple types of factors can be accommodated such as continuous, categorical and discrete factors. Furthermore, experimental limitations, due to safety reasons, can be taken into consideration in the design of the DOE, which is not possible in a classical experimental design [146]. Hence, it appears an adequate tool for the development of DDS. The DOE can also be used in order to characterize new methods without knowing any limitations of the system. Moreover, it can be applied to adapt a method or process for a new application approach [149].

In this chapter for both methods, NPR and NSD, the two major goals of the DOE was to (a) identify parameters controlling the respective process, and (b) identify limitations of the process with regard to fabricable batch sizes for a fixed set of (optimized) process parameters. The different batch sizes should be produced without changing the general apparatus set-up, which is relevant e.g. in the context of early formulation development, characterization and pre-clinical development, in particular in the field of nano- and microscaled DDS. The complexity of the process techniques can cause problems by changing the apparatus [89]. Therefore, a set-up which can be used to produce first test batches up to batches for pre-clinical studies would be a benefit.

Our main focus for the NPR was to prepare PLGA based NPs with a size of 150-200 nm and a narrow size distribution characterized by a polydispersity index (PDI) <0.150. For the NSD the DOE should show controllability, limitations and robustness of the process for the examined variables size, size distribution and yield larger than 50%. The goal for the NSD was to produce PLGA particles as small as possible and with narrow size distributions for creating a novel PLGA based DDS in a single step.

Additionally, after determining the influencing factors for NPR and NSD, limitations of both processes by exploring maximal and minimal batch size were investigated. This is an indicator for the robustness of the process.

2.2. Materials

Poly (lactic-co-glycolic acid) (PLGA; Resomer RG 503 H (lactic/glycolic acid, 50/50, wt/wt; MW 40,300 Da; inherent viscosity 0.41 dl/g) was bought from Evonik Industries AG (Darmstadt, Germany). Poloxamer 407 and polysorbate 80 were purchased from Caesar & Loretz GmbH (Hilden, Germany) and sorbitan monostearate (Span60) was purchased from FAGRON GmbH & Co. KG (Barsbüttel, Germany). Purified water was of Milli-Q quality and prepared by a Millipore Milli-Q Synthesis system (Merck KGaA, Darmstadt, Germany).

All solvents were high-performance liquid chromatography grade and all chemicals met the quality requirements of the European Pharmacopoeia 6.0–7.3.

2.3. Methods

2.3.1. Preparation of nanoparticles by nanoprecipitation

The NPs were produced by NPR as in principle described elsewhere in chapter 1.5. PLGA was weighed accurately and dissolved in the organic phase (acetone; acetone/ethanol, 16/3, v/v). The solution was injected with a Hamilton[®] glass syringe (1005 TTL 5 ml, chromatography service GmbH, Germany) into purified water containing a stabilizer, polysorbate 80 (0.145%, wt/v) or poloxamer 407 (1%, wt/v), forming the aqueous phase. The ratio of organic to aqueous phase was kept constant at 5 ml/10 ml in all experiments. Likewise, in all experiments of the DOE the size of the magnetic stirrer (15 mm x 4.5 mm, VWR, Germany), the inner diameter of the glass beaker (borosilicate glass beaker 3.3, 50 ml, VWR, Germany) and the stirring speed (500 rpm) during the injection were kept constant.

To accurately control the injection speed a high accuracy HARVARD[®] Ultra PHD pump (Hugo Sachs Elektronik, Germany) with a microprocessor controlled, small step angle motor that drives the pusher block was used. The HARVARD[®] Ultra PHD pump operates at constant pressure and constant flow with a flow accuracy of $\pm 0.25\%$ and flow reproducibility of $\pm 0.05\%$. The Hamilton[®] glass syringe was installed in the HARVARD[®] Ultra PHD pump in vertical direction to place the needle into the aqueous phase. After diffusion of organic solvent, which was verified organoleptic and by the measurement of the volume, into the outer phase (aqueous phase), the stirring speed was reduced to 400 rpm and the organic solvent was evaporated by stirring overnight.

2.3.2. Preparation of PLGA particles by nano spray drying

A Büchi Nano Spray Dryer B-90 (Büchi B-90; Büchi Labortechnik GmbH, Essen, Germany) was used for the NSD with a total drying chamber height of 150 cm (long set-up) as provided by the manufacturer (Figure 1.3b). To allow a safe use of organic solvent the spray drying apparatus was operated in the closed mode set-up with inert gas mixture (N_2 and CO_2 at 0.8 bar) (chapter 1.5). The feeding solution was circulated in the spray head and atomized by pushing it through a 4 μm spray mesh, which vibrates at 60 kHz and transports the feeding solution into the drying chamber. As in-process parameter the out-let temperature and the drying gas flow, which was fixed at 115 l/min, were monitored. The out-let temperature was found to be between 29-36°C, which is below glass-transition temperature (T_g) of the PLGA ($\sim 45^\circ C$, determined by differential scanning calorimetry).

The spray dried particles were collected by an electrostatic particle precipitator, generated by a high voltage between a grounded and a collecting electrode.

For preparation of the feeding solution PLGA together with Span60 or poloxamer 407 as stabilizer were accurately weighed and dissolved or suspended in the organic solvent (acetone, ethyl acetate or dichloromethane (DCM)). Afterwards the feeding solution was sprayed under ice-cooling of the supplied dispersion to prevent heating of the circulating solution. The particles were collected by a plastic scratcher and the amount was accurately weighed.

2.3.3. Design of experiments

Design Expert Software[®] (version 08, StatEase Minneapolis, USA) was used to perform a design of experiment study. The design (model) was based on an IV (I = integrated; V = variance)-optimal design for surface response. Response surface designs using optimal designs provide lower average prediction variance over the region of experimentation. The design was chosen to minimize the integral of prediction variance over the region of experimentation, thereby compromising between the minimum number of experiments and maximum information on the investigated effects [148].

The selection of the experimental points for each factor was performed by the software and resulted in a table of experiments. The experiments (runs, R) were organized in a random order to minimize the effect of any drift. The results were evaluated by analysis of variance (ANOVA) and a regression analysis.

The coefficient of determination (R^2) measures the accuracy of the model and is defined as the proportion of the total variance of the experimental points explained by the model. The predicted coefficient of determination (predicted_ R^2) was used to measure the reliability and robustness of the model and is defined in equation 1 (eq. 1).

$$\text{predicted_}R^2 = 1 - \left(\frac{\text{residual cross validated variance}}{\text{total variance}} \right) \quad (\text{eq. 1})$$

In equation 1 the residual cross-validated variance is defined by $\sum_{i=1}^n (y_i - y_{-i})^2$, where y_i equals the experimental response and y_{-i} equals the predicted response using a model based on n-1 other experimental points.

The ANOVA was performed with the Design Expert Software® to reveal the influence of factors on total variance, expressed as effect. The influence between two factors is expressed as interaction. The results were expressed as % of total variance.

2.3.4. Factors varied for the nanoprecipitation method in the design of experiments

The investigated process parameters for the NPR were assigned as factors (Table 2.1). For the NPR two continuous factors (polymer concentration and injection speed), one discrete factor (inner diameter of needle) and two two-level categorical factors (nature of the stabilizer and nature of the solvent) were evaluated. The investigated ranges are summarized in Table 2.1. All factors received a coding for analysing in the DOE. The selection of experimental points leads to the construction of initial 34 experiments including repetitions of five experiments. The investigated responses were size and size distribution. The objective was to produce particles controllable in size, expected to be between 100 and 200 nm, and narrow size distribution (PDI <0.150). The maximum polymer concentration was fixed at 2% (wt/v) based on values commonly reported in the literature [150].

Table 2.1. Factors varied for NPR and the investigated ranges. The factors were separated in continuous, discrete and level categorical factors and coded (A-E) for the DOE.

coding	factor		investigated range
A	continuous	polymer concentration	0.1–2%
B		injection speed	0.25–10 ml/min
C	discrete	inner diameter of needle	0.41/0.60 mm
D	level categorical	stabilizer	polysorbate 80 poloxamer 407
E		organic solvent	acetone acetone/ethanol (16/3, v/v)

2.3.5. Factors varied for the nano spray drying in the design of experiments

The investigated factors for the NSD and ranges are presented in Table 2.2. For the NSD four continuous factors (temperature, polymer concentration, stabilizer concentration and spray rate) and three level categorical factors (nature of organic solvent, pumping rate and nature of stabilizer) were considered. The pumping rate was adjusted to low (level 1) or high (level 2) according to the specification of the manufacturer.

Table 2.2. Factors varied for NSD and the investigated ranges. The factors were separated in continuous and level categorical factors and coded (A-E) for the DOE.

coding	factor	investigated range
A	continuous	temperature
B		50–90°C
C		polymer concentration
D		0.1–5.0%
		stabilizer concentration
		70–100%
E	level categorical	organic solvent
		acetone
		ethyl acetate dichloromethane
F		pumping rate
		low (level 1) high (level 2)
G		stabilizer
		poloxamer 407 Span60

The selection of the experimental points led to the construction of initial 56 experiments including repetitions of four experiments. All factors received a coding for analysing in the DOE.

The examined response variables were size, size distribution and yield with the objectives to produce PLGA particles as small as possible, down to the submicron size range, with narrow size distributions. Furthermore, the yield should be above 50%.

2.3.6. Determination of particle size and size distribution and yield

Particles produced by NPR

Hydrodynamic diameter and polydispersity index (PDI) of NPs were measured by dynamic light scattering (Zetasizer[®] Nano ZS, Malvern Instruments, UK) in purified water at 25°C and a fixed angle of 173°. The measurements were carried out for each batch in triplicate and the mean value and standard deviation (S.D.) was calculated.

Particles produced by NSD

The spray dried particles were characterized by laser diffraction using a Mastersizer[®] 2000 equipped with a Mastersizer[®]2000 µP dispersion module (Malvern Instruments, Herrenberg, Germany) due to their size. The particles were re-dispersed in purified water. Each batch was measured in triplicate and the mean value and standard deviation (S.D.) were calculated.

The volume median size ($d_{0.5}$) as well as the percentile values $d_{0.1}$ and $d_{0.9}$ were calculated by the Mastersizer[®] unit. $d_{0.1}$ and $d_{0.9}$ describe, that 10% or 90% of the particles are smaller than the measured diameter for the corresponding value, respectively. The size distribution (width) is defined in equation 2 (eq. 2). A narrow size distribution is indicated by a small width.

$$width = \frac{d_{0.9}}{d_{0.1}} \quad (\text{eq. 2})$$

In this work an acceptable width ranges was defined from 1, where $d_{0.5}$ is equal to $d_{0.1}$ and $d_{0.9}$, to 50. For example, for a typical particle with $d_{0.5}$ of 1 μm a width of 50 would result by a $d_{0.1}$ of 0.2 μm and a $d_{0.9}$ of 10 μm .

The yield for the NSD is defined in equation 3 (eq. 3). The value for the starting material was corrected for the dead volume of the tubes feeding the spray head (Figure 1.3). Therefore, the supplied dispersion (chapter 2.3.2) was weighed before and after the spray drying process. By subtracting both values the actually spray dried starting material could be determined.

$$yield = \frac{wt_{\text{spray dried product}}}{wt_{\text{starting material}}} * 100\% \quad (\text{eq. 3})$$

2.3.7. Investigation of morphology by scanning electron microscopy

The morphology of spray dried particles and particles produced by NPR were investigated by scanning electron microscopy (SEM). The morphology of the particles can be different due to the preparation technique or selected preparation conditions, in particular for spray drying [109], [151]. For the sample preparation of spray dried particles a small amount of powder was spread on adhesive tape. Surplus of powder was removed by stripping the adhesive tape twice with a second piece of adhesive tape. The remaining powder was deposited onto a double sided adhesive carbon tape, which was afterwards glued onto an aluminium stub.

The particles produced by NPR were re-dispersed in purified water. One drop of the suspension was pipetted onto a silica waver that was glued with double sided adhesive carbon tape onto the aluminium stub.

The samples were sputtered with gold using a Quorum Q150 RES (Quorum Technologies, UK) and examined using a Zeiss Evo HD 15 (Carl Zeiss AG, Germany) at 5 kV.

2.3.8. Investigation of robustness for the nanoprecipitation method

To investigate the practical limitations of the developed process, and therefore the robustness of the used set-up, the minimum possible batch size and the maximum possible batch size for preparing PLGA NPs with a target size of $150 \text{ nm} \pm 10 \text{ nm}$ without changing the experimental set-up was determined. For this purpose the parameter in Table 2.3 were used as revealed in the optimization. The particles were produced in general as described in chapter 2.3.1.

Minimum/maximum batch size is defined for this experiment as the volume of organic solvent used for the NPR. Therefore, the volume was used as starting point for changing experimental parameters. Thus, batches were prepared in triplicate using 5 ml, 2.5 ml, 1.250 ml and 0.625 ml to minimize batch size, 20.0 ml, 40.0 ml and 50.0 ml for the maximum batch size.

The lower limit for the volume was fixed at 0.625 ml as lowest possible volume to allow handling without changing the technical set-up.

Table 2.3. Parameters for the NPR used to determine maximum/minimum possible batch size without changing the set-up and producing NPs with a size of $150 \text{ nm} \pm 10 \text{ nm}$ calculated from the DOE.

factor	coding	parameter
polymer concentration	A	1.3%
inner diameter of needle	B	0.6 mm
injection speed	C	1.531 ml/min
stabilizer	D	poloxamer 407 (1%, wt/v)
organic solvent	E	acetone/ethanol (16/3, v/v)

50.0 ml was set as the maximum (corresponding to 650 mg PLGA weight of polymer used for preparing one batch), which is a reasonably large batch size commonly required during formulation development, batch characterization or pre-clinical development.

2.3.9. Investigation of robustness for the nano spray drying

To investigate the practical limitations of the NSD system the possible minimum batch size and the maximum possible batch size without changing the general experimental set-up were determined. Minimum/maximum batch size is defined for this experiment as the used volume of organic solvent and not related to the polymer concentration or actual yield. For these experiments the volume was again defined as starting point for changing experimental parameter. The total amount (wt) of PLGA and Span60 was hence calculated with respect to the used volume for each individual experiment. Several possible solutions were found which predict the composition of an optimal formulation based on the before defined criteria. The calculation was abridged as 100 solutions had been obtained. From these solutions one formulation was selected for investigating the limitation in batch size giving mean particles size $\sim 2.8 \mu\text{m}$ with a narrow width (0.9). The spray dried particles were produced as described in chapter 2.3.2 using the parameter in Table 2.4.

As the spray dried products always have a wider size distribution compared to particles produced with the NPR the mean particle size should be between 2-5 μm . Based on the dead volume which is defined as the volume remaining in the spray head and in the feeding tubes, which was experimentally determined to be 2.9 ml, 5 ml was fixed as minimum batch size. To find the maximum batch size 10.0 ml, 20.0 ml, 40.0 ml and 50.0 ml batches were sprayed in triplicate. Additionally, also the yield was determined.

Table 2.4. Parameters for the NSD used to determine maximum/minimum possible batch size without changing the set-up.

factor	coding	parameter
temperature	A	71°C
polymer concentration	B	1.1%
stabilizer concentration	C	1.6%
spray rate	D	82%
organic solvent	E	acetone
pumping rate	F	high (level 2)
stabilizer	G	Span60

2.4. Results

2.4.1. NPR - Results of the DOE: Influence on size and size distribution

Using the NPR method NPs in a size range of 50-177 nm were produced with a PDI of 0.013 to 0.294, by combination of the parameters as summarized in Table 2.5. Within the range of investigated factors, only NPs with average sizes above 110 nm met the quality criterion of PDI <0.150. Smaller NPs with average sizes down to 50 nm could be prepared, but only with slightly broader size distributions (PDI up to 0.294).

Table 2.5. Process factors and response for NPR. The investigated process parameters were assigned as factors and coded (A-E) for analysing in the design of experiments. For the NPR two continuous factors: (A) polymer concentration and (C) injection speed; one discrete factor: (B) inner diameter of needle; and further two level categorical factors: (D) nature of the stabilizer and (E) nature of the solvent, were evaluated. The investigated responses were size and size distribution, both measured by dynamic light scattering.

coding	process factors					response	
	A	B	C	D	E	size ^a [nm]	size distribution ^a (PDI)
run	polymer concentration [%]	inner diameter needle [mm]	injection speed [ml/min]	nature of stabilizer	solvent		
1	0.803	0.60	8.341172	poloxamer 407	acetone/ethanol	132.5 ± 1.0	0.041 ± 0.009
2	2.001	0.41	0.250000	poloxamer 407	acetone/ethanol	177.0 ± 0.7	0.013 ± 0.016
3	0.670	0.60	6.587500	polysorbate 80	acetone	119.2 ± 0.4	0.072 ± 0.022
4	0.869	0.41	10.000000	poloxamer 407	acetone/ethanol	131.7 ± 1.8	0.044 ± 0.030
5	1.336	0.41	0.250000	polysorbate 80	acetone/ethanol	148.0 ± 1.2	0.033 ± 0.026
6	1.050	0.41	5.125000	polysorbate 80	acetone	117.9 ± 0.9	0.073 ± 0.015
7	2.010	0.41	0.250000	polysorbate 80	acetone	174.2 ± 0.7	0.057 ± 0.017
8	0.764	0.60	2.200000	poloxamer 407	acetone	161.6 ± 0.8	0.025 ± 0.005
9	2.000	0.60	0.250000	poloxamer 407	acetone	174.2 ± 0.1	0.057 ± 0.014
10	0.102	0.60	10.000000	poloxamer 407	acetone	63.9 ± 0.1	0.132 ± 0.003
11	0.101	0.41	6.062155	poloxamer 407	acetone/ethanol	50.9 ± 0.5	0.168 ± 0.008
12	0.101	0.41	0.250000	polysorbate 80	acetone/ethanol	50.5 ± 0.2	0.220 ± 0.005
13	1.231	0.41	0.250000	poloxamer 407	acetone	155.1 ± 0.8	0.069 ± 0.002
14	0.774	0.60	2.093961	polysorbate 80	acetone/ethanol	116.8 ± 0.7	0.040 ± 0.032
15	2.002	0.41	10.000000	polysorbate 80	acetone/ethanol	124.0 ± 1.1	0.082 ± 0.006
16	2.001	0.60	0.250000	polysorbate 80	acetone/ethanol	151.5 ± 1.8	0.028 ± 0.010
17	0.102	0.41	6.062155	poloxamer 407	acetone/ethanol	48.4 ± 0.8	0.195 ± 0.007
18	2.000	0.41	4.296250	poloxamer 407	acetone	155.3 ± 1.5	0.070 ± 0.017
19	0.100	0.60	0.250000	poloxamer 407	acetone/ethanol	75.1 ± 0.5	0.122 ± 0.007
20	0.100	0.60	10.000000	polysorbate 80	acetone/ethanol	31.6 ± 0.4	0.294 ± 0.294
21	2.004	0.60	10.000000	polysorbate 80	acetone	139.9 ± 0.8	0.060 ± 0.015
22	2.001	0.60	10.000000	poloxamer 407	acetone/ethanol	173.7 ± 3.4	0.024 ± 0.030
23	2.003	0.41	10.000000	polysorbate 80	acetone/ethanol	126.4 ± 0.6	0.062 ± 0.007
24	1.506	0.60	3.175000	poloxamer 407	acetone/ethanol	161.6 ± 0.9	0.022 ± 0.020
25	0.102	0.41	0.250000	poloxamer 407	acetone	73.4 ± 0.4	0.107 ± 0.021
26	1.054	0.41	3.175000	poloxamer 407	acetone/ethanol	132.3 ± 0.3	0.025 ± 0.015
27	1.051	0.41	5.125000	polysorbate 80	acetone	111.9 ± 0.4	0.089 ± 0.006
28	1.544	0.60	6.983995	polysorbate 80	acetone/ethanol	131.4 ± 0.8	0.067 ± 0.009
29	0.621	0.41	7.318750	poloxamer 407	acetone	136.0 ± 1.8	0.054 ± 0.015
30	0.766	0.600	2.200000	poloxamer 407	acetone	157.2 ± 0.7	0.058 ± 0.001
31	2.001	0.41	10.000000	poloxamer 407	acetone	176.6 ± 1.9	0.037 ± 0.009
32	0.103	0.41	10.000000	polysorbate 80	acetone	45.5 ± 0.1	0.231 ± 0.005
33	0.869	0.41	10.000000	poloxamer 407	acetone/ethanol	137.7 ± 0.9	0.067 ± 0.006
34	0.103	0.60	0.250000	polysorbate 80	acetone	70.2 ± 0.8	0.148 ± 0.004

^a mean ± range

None of the experiments failed completely and in none of the experiments aggregates were visible after evaporation of the organic solvent. Depending on the polymer concentration the NP suspensions were opalescent (polymer concentration <0.6%) to milky (polymer concentration >0.6%) in appearance.

SEM images were taken to visualize the NPs and to investigate the morphology. The batches visualized in Figure 2.1 differ in particles density due to the different initial PLGA amounts used for the preparation of different batches for the purpose of a DOE.

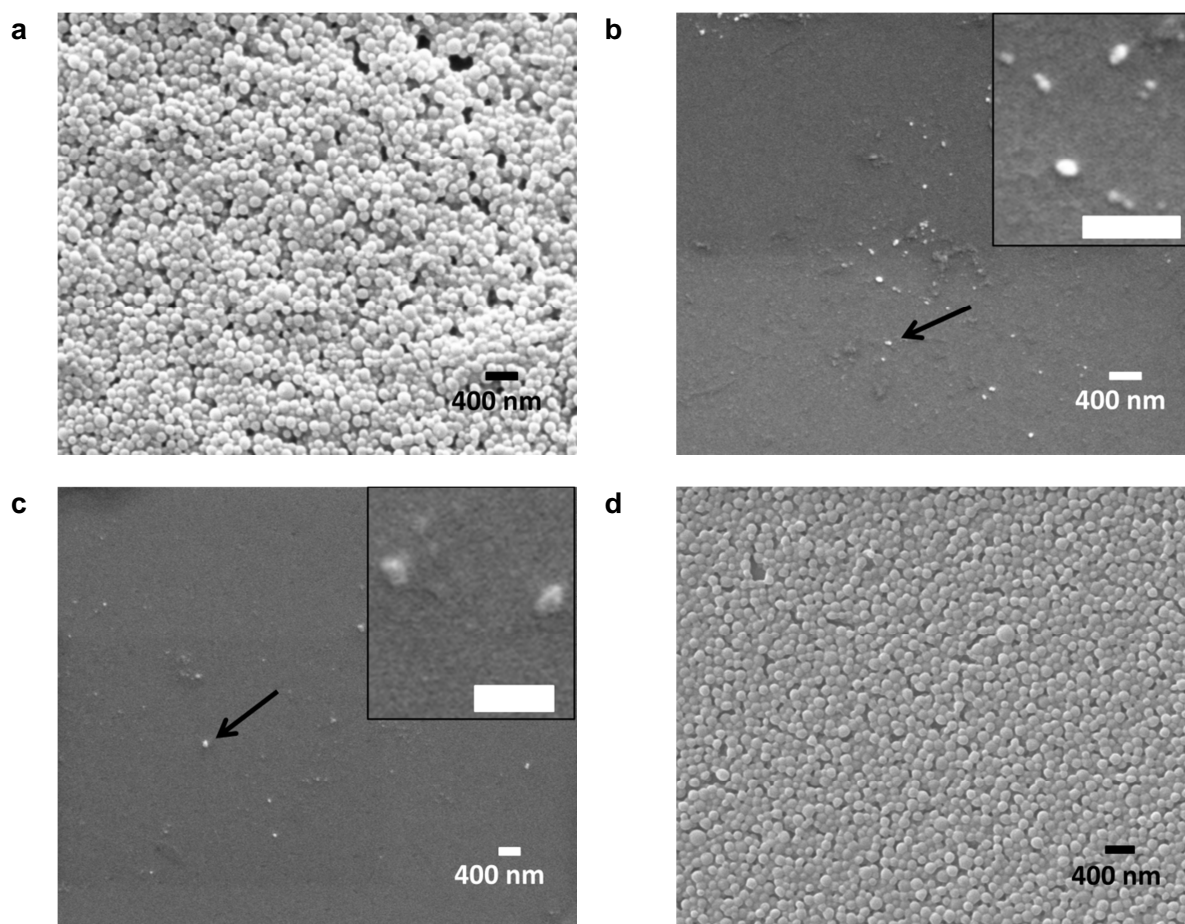


Figure 2.1. Representative SEM images of (a) R 2, (b) R 10, (c) R 20 and (d) particles produced with optimized parameters (chapter 2.4.2) were taken to investigate and to compare the morphology. The SEM images differ in particles density due to the different initial PLGA amounts. (a) NPs are round and spherical in shape with a narrow size distribution. Monodispersity is not further improved prepared compared to a batch prepared with optimal parameters in (d). Runs, which generated smaller particles, show a wider size distribution with irregular shaped NPs (\rightarrow) in (c) and (d).

The SEM image of R 2 (Figure 2.1a) confirms the size measurement and shows that the NPs are round and spherical in shape with a narrow size distribution. The robustness of the NPR with regard to size distribution is also highlighted when comparing R 2 to a batch prepared using calculated optimal parameters (Figure 2.1d), as monodispersity is not further improved. SEM images of R 10 (Figure 2.1b) and R 20 (Figure 2.1c) show that in contrast to R 2 the NPs are smaller with a wider size distribution (arrow points towards small PLGA NPs). Also irregular shaped NPs are visible.

The statistical properties for the whole experiment were calculated: the coefficient of determination is $R^2=0.973$ and $\text{predicted}_R^2=0.950$ for size, $R^2=0.971$ and $\text{predicted}_R^2=0.928$ for size distribution. This demonstrates that the model of the DOE reached high accuracy, good reliability and robustness for both size and size distribution. These values confirm a high controllability of the NPR.

The analysis of variance (ANOVA) of the DOE showed that the polymer concentration is the main factor influencing size and size distribution. The results are summarized in Table 2.6 for size and in Table 2.7 for size distribution. Factors have a significant contribution on the response as the p-value ≤ 0.05 . The ANOVA by partial sum of squares type III demonstrated that 79.5% of total variance was based on the square root of polymer concentration (Table 2.6). The two other noticeable and significant effects were injection speed and nature of stabilizer contributing 2.4% and 7.3% to total variance. Effects equal to or less than 1.5% were contributed by the organic solvent (1.5%), the inner diameter (0.8%) and the interaction between injection speed and organic solvent (0.7%). Other interactions between the factors showed no effect and therefore were not listed in Table 2.6.

Table 2.6. Contribution of process parameters and second order interactions affecting size in the NPR. $p \leq 0.05$ is considered significant.

factor	coding	total variance [%]	p-value
square root of polymer conc.	A	79.48	<0.0001
inner diameter of needle	B	0.83	0.0104
injection speed	C	2.36	<0.0001
stabilizer	D	7.25	<0.0001
organic solvent	E	1.50	0.001
interaction			
injection speed x stabilizer	CxD	0.70	0.0173
polymer concentration	A²	4.2	<0.0001
square of injection speed	C²	0.96	0.0062

Table 2.7. Contribution of process parameters and second order interactions affecting size distribution in the NPR. $p \leq 0.05$ is considered significant.

factor	coding	total variance [%]	p-value
square root of polymer conc.	A	58.00	<0.0001
inner diameter of needle	B	1.04	0.0117
injection speed	C	4.27	<0.0001
stabilizer	D	10.43	<0.0001
organic solvent	E	0.67	0.0369
interaction			
square root polymer conc. x injection speed	AxC	2.24	0.0006
square root polymer conc. x stabilizer	AxD	2.95	0.0001
square root polymer conc. x organic solvent	AxE	4.64	<0.0001
injection speed x stabilizer	CxD	1.37	0.0045
injection speed x organic solvent	CxE	1.28	0.0058
stabilizer x organic solvent	DxE	0.49	0.0713
polymer conc.	A²	9.78	<0.0001

For the size distribution the ANOVA is shown in Table 2.7. All factors showed a significant effect. 58% of total variance was due to the square root of polymer concentration, additional 9.8% due to the polymer concentration. The two other noticeable and significant effects were stabilizer (10.4%) and injection speed (4.3%). An effect <1.5% was determined for organic solvent (0.67%) and the inner diameter (1.04%). All investigated interactions showed an influence with <3.0% of total variance except the interaction between polymer concentration and organic solvent (4.6%). Additionally the other interactions showed no effect and were not listed in Table 2.7.

2.4.2. NPR - Optimization based on the DOE

From the screening data we proposed polynomial models using the Design Expert Software® to fit the experimental data for size and size distribution on factors A-E and combinations thereof. For both size and size distribution all five factors had a statistically significant influence. These fitting should offer the possibility to calculate the respective factors (A-E) for producing NPs with a special size or size distribution.

As the size and size distribution were separate response we get separate equations. Our focus was set on a specific particle size. The results of the fitting are expressed for size and size distribution in equation 4 (eq. 4) and equation 5 (eq. 5), respectively. These equations are significant and reliable, as can be seen from the good values of R^2 and predicted_ R^2 .

$$\begin{aligned} size = & 120.79 + (50.74 * A) + (3.96 * B) - (8.2 * C) - (11.81 * D) - (5.37 * E) - \\ & (4.58 * C * D) - (23.2 * A^2) + (11.73 * C^2) \end{aligned} \quad (\text{eq. 4})$$

$$\begin{aligned} size \ distribution = & 0.066 - (0.068 * A) - (6.98^{-3} * B) + (0.018 * C) + (0.023 * D * 5.76^{-3} * E) - \\ & (0.015 * A * C) - (0.015 * A * D) - (0.019 * A * E) + (0.01 * C * D) + \\ & (9.78^{-3} * C * E) + (4.87^{-3} * D * E) + (0.049 * A^2) \end{aligned} \quad (\text{eq. 5})$$

The equations 4 and 5 are expressed in terms of a coded factor, being a dimensionless number varying between -1 and +1 for continuous or discrete factors, and using the traditional coding for categorical factors.

Based on these equations and as an example two equations were calculated for the different stabilizer using the mixture of ethanol/acetone (3/16, v/v) as organic solvent as expressed in equation 6 (eq.6) for poloxamer 407 and equation 7 (eq. 7) for polysorbate 80.

$$\begin{aligned} size_{poloxamer,acetone:ethanol} = & -14.35 + (224.59 * \sqrt{A}) + (41.73 * B) - (5.80 * C) - (76.41 * A) + \\ & (0.49 * C^2) \end{aligned} \quad (\text{eq. 6})$$

$$\begin{aligned} size_{polysorbate\ 80,acetone:ethanol} = & -28.35 + (224.59 * \sqrt{A}) + (41.73 * B) - (7.68 * C) - \\ & (76.41 * A) + (0.49 * C^2) \end{aligned} \quad (\text{eq. 7})$$

The equations 6 and 7 are expressed in term of (dimensional) actual factors (instead of coded factors). With the equation 6 and 7 process parameters and conditions (factors A, B, C and E) can be proposed in the investigated range of the DOE. The accuracy (trueness and precision) of these equations was therefore tested for the preparation of NPs with a size of 150 nm \pm 10 nm. For calculating the optimal parameters a limitation in injection speed (>1ml/min) was set to allow reduced and feasible production times. The predicted factors were calculated and summarized in Table 2.8.

Table 2.8. Predicted factors for producing NPs with a size of 150 nm ± 10 nm calculated from the results of the DOE for polysorbate 80 and poloxamer 407.

factor	coding	polysorbate 80	poloxamer 407
polymer concentration	A	1.2%	1.1%
inner diameter of needle	B	0.6 mm	0.6 mm
injection speed	C	1.531 ml/min	4.55 ml/min
organic solvent	E	acetone/ethanol (16/3, v/v)	acetone/ethanol (16/3, v/v)

To confirm the predicted factors particles were prepared with the parameter settings shown in Table 2.8 as calculated from equations 6 and 7. Thus, NPs with a size of 133.3 ± 2.7 nm for polysorbate 80 and 135.4 ± 2.2 nm for poloxamer 407 were prepared (n=4). The mean size was smaller than predicted by ca. 17 nm (polysorbate 80), and 15 nm (poloxamer 407), respectively. This was lower than the acceptable lower size limit of 140 nm. For both types of stabilizers we had learned from the DOE that the polymer concentration is the main influencing factor on particle size. Therefore, particles were also prepared with slightly higher polymer concentrations for both stabilizer and the results were presented in Figure 2.2a and Figure 2.2b.

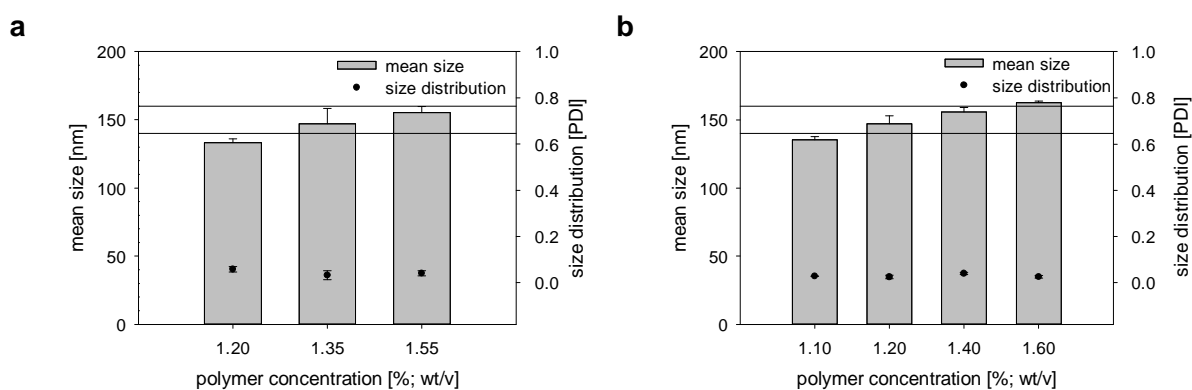


Figure 2.2. Confirmation of predicted factors calculated from the results of the DOE. NPs were produced with different polymer concentrations using (a) polysorbate 80 and (b) poloxamer 407 as stabilizer under conditions summarized Table 2.8. Size and size distribution were measured by dynamic light scattering. The values are presented as the mean ± S.D. (n=4), --- 150 nm ± 10 nm.

Figure 2.2a shows that PLGA concentrations of 1.35-1.55% (compared to 1.2% assigned by the DOE, Table 2.8) generated NPs between 147.2-155.2 nm with a PDI <0.058 using polysorbate 80 as stabilizer, when leaving all other parameters as assigned by the DOE.

PLGA concentrations between 1.20-1.40% (compared to 1.1% assigned by the DOE, Table 2.8) result in particles with sizes between 147.1-155.7 nm and a PDI <0.040 using poloxamer 407 as stabilizer, when leaving all other parameters as assigned by the DOE.

2.4.3. NPR - Investigation of robustness

To investigate the practical limitations of the developed process, and therefore the robustness of the used set-up, the minimum possible batch size and the maximum possible batch size for preparing PLGA NPs with $150 \text{ nm} \pm 10 \text{ nm}$ without changing the experimental set-up was determined.

The measured NP sizes and size distributions were summarized for the minimum and maximum batch size in Figure 2.3. All batches had a size of $150 \pm 10 \text{ nm}$ with a narrow size distribution, PDI <0.042. Therefore, the NPR is very robust and can be used to produce batches with minimum 0.625 ml and at least up to 50.0 ml of organic solvent without changing the experimental set-up.

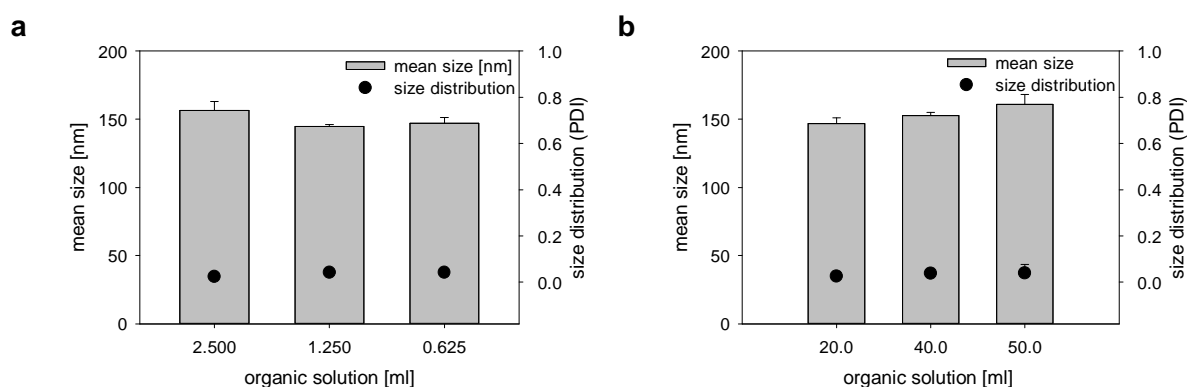


Figure 2.3. Investigation of (a) minimum and (b) maximum batch size (robustness) for the NPR by determining size and size distribution from batches produced with different volumes. The PLGA concentration (1.3%, v/wt) was kept constant for all experiments and poloxamer 407 was selected as stabilizer. Size and size distribution were measured by dynamic light scattering. The values are presented as the mean \pm S.D. (n=3).

2.4.4. NSD - Results of the DOE on size and size distribution

All response values of size, size distribution and yield were presented in Table 2.9. With the spray drying technique stable re-dispersable microparticles (MPs) could be prepared with the lowest mean size ($d_{0.5}$) of 2-163 μm . The smallest mean size was found in R 15 and R 4 with 2.34 μm and 2.38 μm , respectively, both produced with Span60 as stabilizer. The maximum mean size was found in R 21 with 163.3 μm , produced with poloxamer 407 as stabilizer.

With Span60 smaller particle mean sizes ($d_{0.5}$ values), in comparison to particles prepared with poloxamer 407, were prepared, so that particle mean sizes of $<8 \mu\text{m}$ were achieved in 20 runs. For poloxamer 407 only one batch had a mean size of $<8 \mu\text{m}$. Furthermore, particles prepared with poloxamer 407 and a low polymer concentration (0.1% PLGA, wt/v) had a mean size of $<100 \mu\text{m}$. Note that the goal was to produce particles as small in mean size as possible. In the used set-up and with PLGA as polymer we achieved particles in the low micrometer size range.

The evaluation of the DOE shows that the size of the MPs is most affected by the stabilizer (Table 2.10). The ANOVA by partial sum of squares type II demonstrates that 38.91% of total variance is based on the stabilizer. The two other noticeable and significant effects are polymer concentration (4.39%) and stabilizer concentration (6.74%). A very weak influence was determined for the organic solvent with 1.62% of influence, which is not significant. Factors showing no influence were not listed in Table 2.10. The ANOVA also showed that second order interactions have a strong influence on the size of the spray dried particles, but only polymer concentration/stabilizer contributing 21.08% and stabilizer concentration/stabilizer contribution 5.11% were determined to be significant interactions. The remaining second order interactions showed no effect and were therefore not listed in Table 2.10. Nevertheless, the value of the coefficient of determination $R^2=0.899$ and predicted $R^2=0.790$ demonstrated that the model is less accurate, robust and reliable compared to the NPR.

The factors most strongly influencing the size distribution, represented as width, were the polymer concentration (15.33%) and the organic solvent (19.27%) as described in Table 2.11. The other factors are determined to be significant, but had only weak influence $<1\%$. For the interactions between polymer concentration and organic solvent an influence of 6.62% was determined. The remaining second order interactions showed no effect and were not listed in Table 2.11.

Table 2.9. Process factors and response for the NSD.

Run coding	Process factors							Response		
	A T [° C]	B PC [%]	C SC [%]	D spra y rate	E organic solvent	F pumping rate	G stabilizer	^a width	^a d 0.5 [µm]	yield [%]
1	80	0.1	0.67	100	acetone	1x	Span60	124.9 ± 2.0	5.9 ± 0.3	23.49
2	54	2.2	0.92	100	DCM	2x	Span60	10.8 ± 0.3	4.6 ± 0.2	15.32
3	70	5.0	1.51	70	DCM	2x	poloxamer 407	8.2 ± 0.6	41.2 ± 4.2	7.91
4	74	0.7	1.18	72	acetone	2x	Span60	32.3 ± 2.0	2.4 ± 0.1	62.81
5	80	0.1	0.05	90	acetone	2x	poloxamer 407	-*	-*	-*
6	62	0.1	0.05	70	DCM	1x	poloxamer 407	-	-	-
7	90	5.0	2.00	70	ethyl acetate	1x	poloxamer 407	3.9 ± 0.2	26.9 ± 0.5	6.52
8	80	0.1	0.05	100	ethyl acetate	2x	Span60	3.8 ± 0.1	8.6 ± 0.1	41.21
9	70	2.9	0.05	100	DCM	1x	poloxamer 407	9.5 ± 0.6	10.6 ± 0.5	13.17
10	87	0.4	0.76	89	ethyl acetate	2x	Span60	-+	-+	-+
11	85	5.0	1.81	85	ethyl acetate	2x	poloxamer 407	-+	-+	-+
12	86	2.7	0.71	71	ethyl acetate	2x	poloxamer 407	-+	-+	-+
13	70	4.6	0.05	100	acetone	2x	Span60	4.6 ± 0.2	4.0 ± 0.1	25.48
14	70	0.1	2.00	99	acetone	2x	Span60	112.0 ± 7.6	3.7 ± 1.8	58.26
15	58	2.6	0.05	81	DCM	2x	Span60	3.1 ± 0.1	2.3 ± 0.0	17.85
16	90	0.1	2.00	70	ethyl acetate	2x	poloxamer 407	-*	-*	-*
17	70	0.3	2.00	84	DCM	1x	Span60	9.6 ± 0.7	2.8 ± 0.0	31.60
18	70	0.1	0.05	100	acetone	1x	poloxamer 407	-*	-*	-*
19	83	0.1	2.00	70	ethyl acetate	1x	Span60	17.0 ± 2.0	2.4 ± 0.1	13.81
20	80	5.0	2.00	70	acetone	2x	Span60	2.6 ± 0.2	2.8 ± 0.1	43.63
21	50	0.1	2.00	70	DCM	2x	poloxamer 407	95.3 ± 22.8	163.3 ± 23.0	10.10
22	50	0.1	2.00	100	DCM	1x	Span60	22.4 ± 4.0	53.3 ± 4.5	10.73
23	62	0.1	1.24	100	DCM	2x	poloxamer 407	4.6 ± 0.7	111.2 ± 2.1	11.69
24	50	5.0	0.93	70	DCM	1x	Span60	12.1 ± 0.6	10.2 ± 0.7	13.34
25	70	5.0	2.00	100	acetone	1x	Span60	23.2 ± 2.0	4.3 ± 0.6	48.68
26	80	5.0	2.00	100	acetone	2x	poloxamer 407	6.3 ± 1.0	31.2 ± 1.1	12.44
27	70	0.1	0.15	70	acetone	2x	poloxamer 407	-*	-*	-*
28	80	2.7	2.00	100	ethyl acetate	2x	poloxamer 407	-*	-*	-*
29	76	1.8	2.00	100	acetone	1x	Span60	-+	-+	-+
30	74	5.0	0.34	89	acetone	1x	poloxamer 407	7.2 ± 1.1	17.8 ± 0.5	21.98
31	50	5.0	0.05	93	DCM	2x	poloxamer 407	14.7 ± 0.1	10.6 ± 0.7	20.10
32	62	0.1	0.05	70	DCM	1x	poloxamer 407	-*	-*	-*
33	80	0.6	2.00	70	acetone	1x	poloxamer 407	-*	-*	-*
34	70	0.1	0.05	70	acetone	1x	Span60	43.4 ± 4.5	5.9 ± 0.3	46.03
35	85	3.5	1.12	89	ethyl acetate	1x	Span60	113.7 ± 15.4	16.8 ± 6.3	2.82
36	80	3.0	1.69	76	ethyl acetate	2x	Span60	16.2 ± 1.7	2.1 ± 0.1	12.44
37	88	5.0	0.05	100	ethyl acetate	2x	poloxamer 407	10.9 ± 0.1	14.4 ± 0.2	18.07
38	80	5.0	0.05	100	ethyl acetate	1x	Span60	205.3 ± 21.9	15.4 ± 0.6	4.19
39	90	0.1	2.00	100	ethyl acetate	1x	poloxamer 407	-+	-+	-+
40	50	5.0	2.00	100	DCM	2x	Span60	20.3 ± 0.2	36.3 ± 0.7	5.69
41	80	5.0	1.04	100	acetone	1x	Span60	22.6 ± 2.0	3.1 ± 0.1	38.46
42	50	5.0	0.05	93	DCM	2x	poloxamer 407	24.2 ± 6.5	4.9 ± 0.4	12.49
43	80	0.1	1.07	84	ethyl acetate	1x	poloxamer 407	-*	-*	-*
44	70	0.1	0.64	70	DCM	2x	Span60	30.0 ± 0.2	7.6 ± 0.9	29.16
45	74	3.8	2.00	72	acetone	1x	Span60	4.4 ± 0.7	2.8 ± 0.1	54.14
46	70	5.0	2.00	70	acetone	2x	poloxamer 407	15.8 ± 1.1	49.3 ± 5.4	18.00
47	90	2.1	0.05	70	ethyl acetate	1x	Span60	61.3 ± 1.5	2.5 ± 0.3	24.39
48	50	0.1	2.00	70	DCM	2x	poloxamer 407	8.2 ± 2.3	105.4 ± 3.2	13.42
49	80	5.0	0.05	70	acetone	1x	poloxamer 407	50.2 ± 4.0	13.2 ± 8.4	16.71
50	70	5.0	0.05	100	DCM	2x	Span60	8.8 ± 0.4	17.7 ± 0.4	14.18
51	90	3.0	1.71	100	ethyl acetate	2x	Span60	7.9 ± 0.2	5.0 ± 0.0	31.16
52	80	5.0	0.05	70	ethyl acetate	2x	Span60	11.9 ± 1.7	4.5 ± 0.4	4.70
53	55	5.0	2.00	100	DCM	1x	poloxamer 407	-+	-+	-+
54	70	4.6	0.73	80	DCM	1x	Span60	25.0 ± 6.2	10.3 ± 0.2	8.58
55	80	3.4	0.06	70	ethyl acetate	1x	poloxamer 407	-+	-+	-+
56	70	4.6	0.05	100	acetone	2x	Span60	6.2 ± 0.1	4.9 ± 0.1	37.25

(^a mean ± range); T = inlet temperature, PC = polymer concentration, SC = stabilizer concentration;

- experiment failed due to membrane blocking (+) or polymer film (*) formation

Table 2.10. Contribution of process parameters and second order interactions affecting size in the NSD. $p \leq 0.05$ is considered significant.

factor	coding	total variance [%]	p-value
polymer concentration	B	4.39	0.0074
stabilizer concentration	C	6.74	0.0013
organic solvent	E	1.62	0.2335
stabilizer	G	38.91	<0.0001
interaction			
polymer concentration x stabilizer	BxG	21.08	<0.0001
stabilizer concentration x organic solvent	CxE	6.23	0.0071
stabilizer concentration x stabilizer	CxG	5.11	0.0042

Table 2.11. Contribution of process parameters and second order interactions affecting size distribution (width) in the NSD. $p \leq 0.05$ is considered significant.

factor	coding	total variance [%]	p-value
temperature	A	0.11	<0.0001
polymer concentration	B	15.33	<0.0001
stabilizer concentration	C	0.04	<0.0001
spray rate	D	0.20	<0.0001
organic solvent	E	19.27	<0.0001
pumping rate	F	0.45	<0.0001
stabilizer	G	0.30	<0.0001
interaction			
polymer concentration x organic solvent	BxE	6.62	<0.0001

From the ANOVA it is obvious that the formation of particles with NSD is influenced by various factors with the individual factors carrying little weight to the total variance. This is true for the particle size as well as for the width.

The shape of the prepared MPs was investigated by SEM imaging. As the aim was to prepare particles as small as possible one of the batches with the lowest mean sizes (R 4) was investigated, showing that the particles were round and regular shaped (Figure 2.4a).

This batch was produced with a medium amount (1.18%, wt/v; according to the range defined in the DOE) of Span60 as stabilizer and compared to the optimized batch with high stabilizer concentration (1.6%, wt/v) of Span60 in Figure 2.4 d, which was used for determining minimum and maximum batch size (robustness). There was no visible change in the morphology or size distribution.

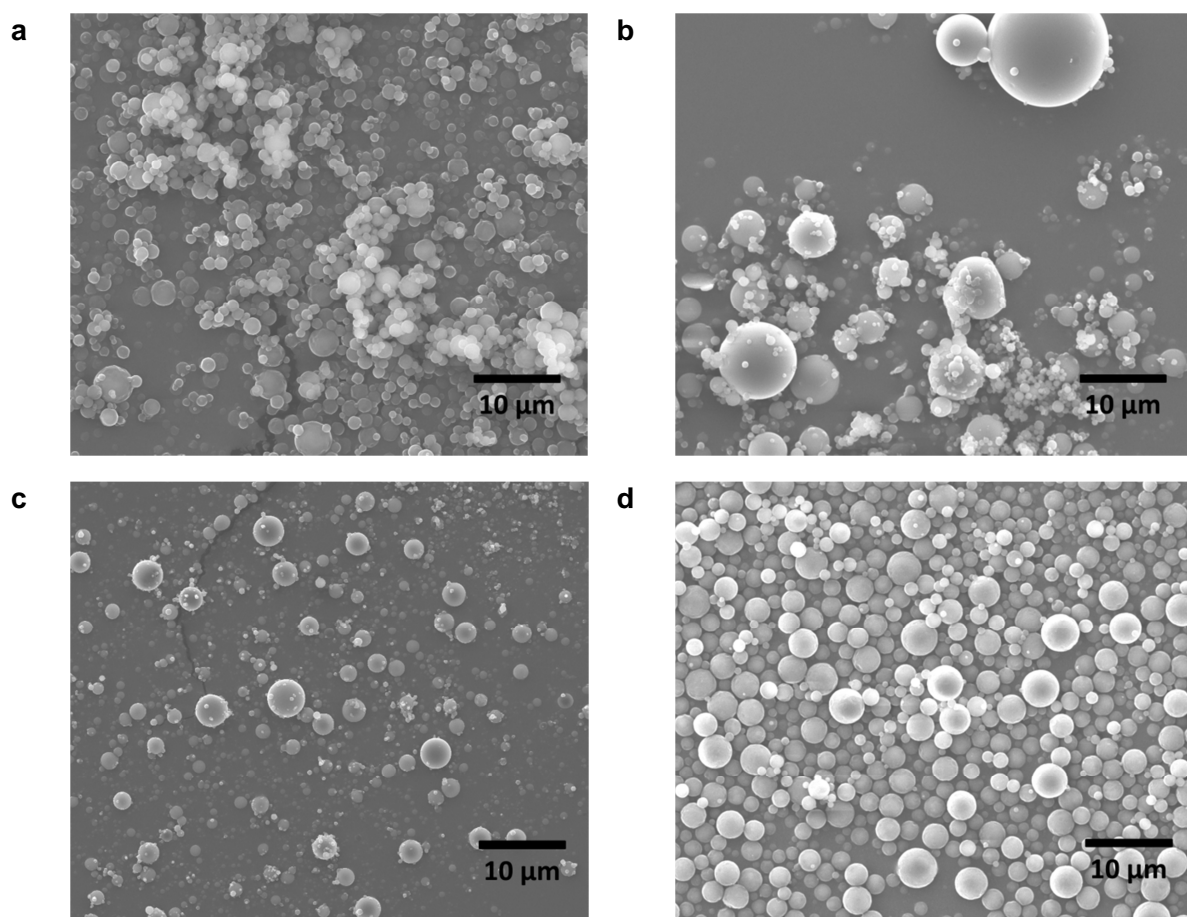


Figure 2.4. Representative SEM images of (a) R 4, (b) R 49, (c) R 56 and (d) optimal formulation used for robustness experiments. (a) Investigation of one of the batches with the lowest mean sizes, which contains medium amount (1.18%, wt/v) of Span60, showing that the particles were round and regular shaped. Compared to the optimal batch with high stabilizer concentration (1.6%, wt/v) of Span60 in (d) no visible change in the morphology or size distribution could be determined. In (b) particles with lower amount (0.05%, wt/v) of poloxamer 407 and in (c) particles produced with a small amount (0.05%, wt/v) of Span60 were visualized showing a fraction of the particles in the submicron range $<1 \mu\text{m}$ and a broad overall size distribution.

In Figure 2.4c particles (R 56) with lower amount (0.05%, wt/v) of Span60 were visualized showing that a fraction of the particles were indeed in the submicron range $<1 \mu\text{m}$, however the overall size distribution was relative broad with an average size of $4.9 \mu\text{m}$. The same effect is also obvious for particles produced with a small amount (0.05%, wt/v) of poloxamer 407 as stabilizer (Figure 2.4b).

2.4.5. NSD - Results of the DOE on yield

Yields were obtained in the range of 1.16% (R 6) to 62.81% (R 4) and listed in Table 2.9. In general the highest yields were achieved with Span60 as stabilizer (R 4=62.81%, R 14=58.26%, R 45=54.14%). For seven out of 56 runs the yield was greater than 40%. Furthermore, a yield greater 30% was determined for runs with mean sizes $<9 \mu\text{m}$ (R 4, R 9, R 14, R 17, R 20, R 25, R 34, R 41, R 45, R 51, R 56).

The evaluation of the DOE showed that the organic solvent is the main factor influencing the yield, being responsible for 30.1% of total variance (Table 2.12). The two other noticeable and significant effects were stabilizer and polymer concentration contributing 13.1% and 8.3% to total variance.

The effect of temperature, stabilizer concentration, spray rate and pumping rate were investigated to be very weak with $<0.1\%$ and not significant. Interestingly, the interactions of temperature/organic solvent and stabilizer/ organic solvent showed an effect of 10.19% and 7.04%, respectively. Also other interactions were tested and had an influence of 3.1-4.2%, which was significant, except the interaction polymer concentration/stabilizer. The remaining second order interactions showed no effect and were not listed in Table 2.12.

The statistical properties for the whole experiment were $R^2=0.899$ and $\text{predicted_}R^2=0.666$. Therefore, the model is less accurate, must be considered with caution for robustness and reliability.

Table 2.12. Contribution of process parameters and second order interactions affecting yield in the NSD. $p \leq 0.05$ is considered significant.

factor	coding	total variance [%]	p-value
temperature	A	0	0.9956
polymer concentration	B	8.33	0.0002
stabilizer concentration	C	0.19	0.5078
spray rate	D	0.44	0.3118
organic solvent	E	30.09	<0.0001
pumping rate	F	0.95	0.1418
stabilizer	G	13.14	<0.0001
interaction			
temperature x stabilizer concentration	AxC	4.02	0.0047
temperature x organic solvent	AxE	10.19	0.0002
polymer concentration x pumping rate	BxF	4.16	0.0041
polymer concentration x stabilizer	BxG	1.65	0.0572
stabilizer concentration x spray rate	CxD	3.25	0.0099
stabilizer concentration x organic solvent	CxE	7.04	0.0017
stabilizer concentration x stabilizer	CxG	4.01	0.0048
organic solvent x pumping rate	ExF	3.11	0.038

2.4.6. NSD – Optimization

As described above by the results of the DOE size and size distribution of particles as well as the yield using NSD is influenced by various factors and therefore more difficult to control. Based on the experimental data we proposed polynomial models using the Design Expert Software® to fit the data for size and size distribution on factors A-G. The goal was to calculate values for the factors (A-G) to reach the smallest possible size and size distribution with maximum yield (optimal formulation). Several possible solutions were found which predict the composition of an optimal formulation based on the before defined criteria.

The calculation was abridged as 100 solutions had been obtained. For determining the robustness (chapter 2.4.6) one formulation of these solutions was selected for investigating the limitation in batch size giving mean particles size $\sim 2.8 \mu\text{m}$ with a narrow width of 0.9.

2.4.7. NSD – Investigation of robustness

All results of size, size distribution and yield were presented in Figure 2.5a and Figure 2.5b. Figure 2.5a shows a slight increase in size from 10.0 to 20.0 ml and in parallel also the width increases. From 40.0 to 50.0 ml the mean size doubles, but the width kept constant. The minimum yield was determined for 5 ml with 60%. For other volumes the yield ranges from 71.1% to 84.8%. From 5.0 ml to 40.0 ml the yield increased, whereas with 50.0 ml the yield decreased slightly. The results show that between 5.0 ml-40.0 ml particles with a mean size of $2.6 \mu\text{m}$ to $4.3 \mu\text{m}$ with a mean width of 0.91 to 2.50 and yield $>60\%$ could be produced.

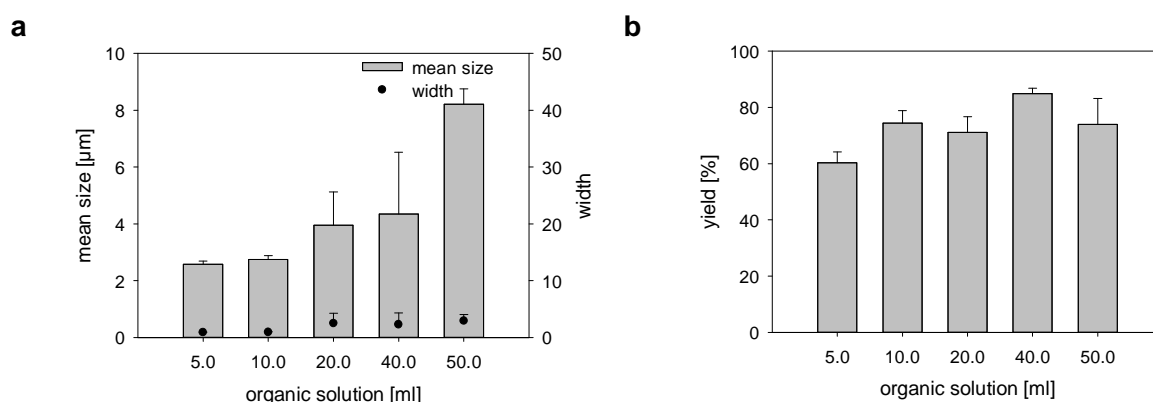


Figure 2.5. Investigation of maximum and minimum batch size (robustness) for the NSD by determining (a) mean size and size distribution (width) and (b) yield from batches produced with different volumes. The concentration of PLGA and Span60 was kept constant. Mean size and size distribution (width) were measured by laser light diffraction. The values are presented as the mean \pm S.D. ($n=3$).

2.5. Discussion

The absence of information regarding the influence of parameters on the production of NP-based DDS is hindering the scale-up and the more widespread production of such systems in the pharmaceutical industry [89]. To enter in the pharmaceutical production and thereafter the pharmaceutical market a transfer from bench top to pharmaceutical production (scale-up) has to be achieved.

It is known that process limitations can become significant in a larger production process, which were not apparent before. At the moment, only one albumin based nanoparticulate DDS (Abraxane[®]) is approved by the FDA and European Medicines Agency (EMA) and a second, which is a polyalkylcyanoacrylate based nanoparticulate DDS (Livatag[®], doxorubicin Transdrug[™]), is currently in phase III clinical trial [152].

To evaluate the influence of process parameters, a DOE was applied on the NPR and NSD. Choosing the optimal design of the DOE a full factorial design requires a large number of experiments. Therefore, fractional factorial designs e.g. response surface designs are appropriate for series varying several factors. Furthermore, a fractional factorial design can reduce costs and material due to the reduced number of experiments [146].

NPR is one of the most frequently used physico-chemical methods [93] for producing NPs as DDS [94], [95]. Compared e.g. to emulsion-diffusion-evaporation methods it is less time consuming, more reproducible and controllable due to less production steps [89] and was, therefore, investigated. Previously performed DOE studies using the NPR studies were mostly focusing on drug loading [65]. So far no study was carried out using a DOE as a tool to screen the production process for parameters influencing size and size distribution. The second method was the spray drying technique selected to formulate DDS in one step without extra washing or drying steps (single step process) [92]. For the NSD a system, the Büchi B-90 was used specially designed to produce and to collect spray dried products with a particle size in the submicron size range [100], which was introduced in chapter 1.5. As of now only a few studies have been done with this spray dryer, mainly investigating the preparation of particles using polymeric wall materials, the drying of pharmaceutical excipients [104] and drying of nano-emulsions [92]. First studies were carried out focusing on the encapsulation of proteins [105] and model drugs in biodegradable polymers [100], [109]. A recent study used a 2³ factorial design to develop inhalable capreomycin powders [147].

2.5.1. Outcome of the design of experiments for the NPR

To use the DOE as a tool in order to understand process parameters was successful for the NPR. The results of the DOE revealed that the size is mostly influenced by the polymer concentration (79.5%), which is thus easy to control. This is in accordance with a meta-analysis performed by Mora-Huertas et al. on published and experimental data showing that the size of submicron particle size can be changed by the polymer concentration, regardless of the nature of polymer, nature of stabilizer or the operating conditions [94].

In the performed experiments in this chapter stable NPs in the range of 110-180 nm were achieved (Table 2.5) with polymer concentrations of 1%-2% (wt/v). None of the experiments failed completely and in none of the experiments aggregates were visible after evaporation of the organic solvent.

Increasing polymer concentrations lead to the formation of larger particles, which is in agreement with the observations of Thioune et al. [153], preparing hydroxypropyl methylcellulose phthalate NPs, and Galindo-Rodriguez et al. [97], preparing polymethacrylic acid copolymer NPs. Moreover, in the present study high polymer concentrations of 2% invariably lead to the largest particle sizes (>170 nm) with narrow size distributions (PDI <0.070) independent of inner needle diameter, injection speed, stabilizer or organic solvent (Table 2.5). At high polymer concentrations the theoretical concentration of polymer chains is higher and a more even distribution of polymer chains among all solvent droplets results in particles with the same size. Low concentrations increase the probability to have less or different concentrations of polymer chains in the droplets. Below a critical polymer concentration hence a wider size distribution results [97]. For the investigated set-up the critical polymer concentration could be proposed to be at ~0.1% (wt/v) (lowest polymer concentrations) or below, which resulted in a dramatic increase in the PDI (0.132–0.294).

In the present study the stirring speed was set to 500 rpm in order to improve distribution of the organic phase into the aqueous phase and largely prevent unstirred layers. Unstirred layers hinder diffusion, which lead to a time-dependent particle growth as the droplets of the organic solvents will not be split evenly at fast injection speeds [94]. A high stirring speed reduces the influence of injection speed, demonstrated in the results of the DOE in Table 2.6, of organic to aqueous phase ratios and of stirring speed, both were fixed in the DOE, on the complex fluid dynamics and, therefore, particle formation [94], [154]. Furthermore, in the present study the stabilizer concentrations were fixed. In the NPR the stabilizer is in general needed to avoid aggregation during particles formation and known to have independent of the concentration an influence on particle mean sizes, which was also demonstrated by the DOE (Table 2.6) with 7.3% of total variance [94]. It was reported that poloxamer 407 generates larger particles in comparison to polysorbate 80 [94]. A tendency could be seen in the optimization of the NPR as both stabilizers need different parameter to generate 150 nm particles.

Indeed, that the influence on size and size distribution was dominated by the polymer concentration might appear relatively obvious. However, the DOE allowed defining a mathematical and statistical reliable correlation, expressed in equations 6 and 7. Using these equations, the process can be easily adapted to generate other particles sizes, between 110-180 nm with narrow size distributions, within the constraints of the dataset used for the development of the equations. We demonstrated furthermore that the used system based on these equations was robust and accurate within a range between some minimally needed and maximally possible volume-based batch size. The maximal batch size using 50 ml of organic solvent allows fabricating particles based on 650 mg PLGA, which is likely suffice for first pre-clinical studies. Very small batch sizes (0.625 ml) allow preparing particles for first physico-chemical characterization studies. Therefore, the used set-up can be adapted in the particle quantity for different experimental purposes.

2.5.2. Outcome of the design of experiments for the NSD on size and size distribution

For the NSD the DOE was designed to investigate controllability, limitations and robustness regarding particle size, size distribution and yield of this so far less characterized system [92]. Therefore, seven factors were screened, which were expected to have an influence on the outcome of the spray drying process. Combining rather a high number of factors is also a limit for a DOE, but necessary to thoroughly screen an unknown system. A reduced number of factors allows investigating more values in the defined ranges, but would not necessarily reduce the number of initial experiments. By reducing the factors of a totally unknown process effects could be missed. Furthermore, the outcome could be so weak, that the other factors had to be investigated in a second DOE, further increasing the number of experiments. The results show clearly that NSD is influenced by various factors and, hence, more difficult to control than the NPR.

The aim was to produce the smallest possible size using PLGA and within the technical constraints of the Büchi B-90 with a spraying tower of 150 cm in length. The results show that the smallest particles, which were prepared, were MPs with an average size of $\sim 2 \mu\text{m}$. This can be explained by the formation of the particles, which is governed in a first step by interplay of polymer concentration in the droplet, pore size of the vibrating membrane used for evaporating the spraying solution and the frequency of vibration. The frequency defines the volume of the droplet, which is injected in the drying gas flow. Further the droplet diameter is mostly influenced by the pore size of the membrane.

The smallest membrane pore size, which is currently available, has a pore size of 4 μm and generates droplets $\sim 8 \mu\text{m}$ [103]. It would be interesting to see the effect on the droplet size using a pore size $\sim 1 \mu\text{m}$, while changing the frequency of vibration (at the moment fixed at 60 kHz by the manufacturer). However, a smaller pore size will increase spraying times. In a second step the droplets are dried in the gas flow forming the particles depending on surface tension and density. Therefore, the feeding material, as well as density and viscosity of the feeding solution, containing in the present study the polymer and the stabilizer, influence the transport through the membrane and the successful particle formation.

In comparison to NPR some experiments failed completely (Table 2.9), in particular if poloxamer 407 was used as stabilizer or if ethyl acetate was used as organic solvent. Especially high viscosity and density of the feeding solution can block the vibrating membrane and droplet coalescence can lead to the formation of a polymer film on the collecting electrode.

Polymer and stabilizer in this study were revealed to have an effect on the particles size (Table 2.10). The identified interaction between polymer concentration/stabilizer underlines this aspect (Table 2.10). This is not unexpected as recent studies had also shown that the polymer concentration influences the particle size [92], [105], [155] or that the particle size is depending on the wall material [92]. Moreover, Beck-Broichsitter et al. determined that the concentration of the feeding solution and also the molecular weight (MW) of PLGA with different lactic/glycolic ratios can influence the size [109]. As in the present study the stabilizer is part of the DDS, the different MW of poloxamer 407 (MW 12,785 g/mol) and Span60 (MW 430 g/mol) could, therefore, influence the particles size as demonstrated by the results in Table 2.9. In general, smaller mean sizes were achieved with Span60 and, furthermore, the mean size increased strongly by increasing the concentration of poloxamer 407 (Table 2.9).

For the size distribution a significant effect of the polymer concentration and of the organic solvent, and of the interaction of these two factors, was determined (Table 2.11). This reflects that intuitively quicker drying of the spray droplets in a gas flow would avoid droplet coalescence. The generated particles had a smooth surfaced as visualized in SEM images in Figure 2.4. More hollow particles were normally obtained with fast drying processes [109], [151].

Due to the complexity interplay of influencing factors on the NSD no single mathematical solution for an optimal formulation could be expressed.

Nevertheless, a selected formulation was robust and accurate to a volume-based evaluation of the minimum (5.0 ml) and the maximally possible (40.0 ml) batch size. Both the maximally possible and the minimum batch size were limited by technical constraints and characterized by a smaller range compared to the NPR.

Yields achieved with the Büchi B-90 ranged between 43-95% as reported in the literature [100], [156], depending e.g. on spray dried material and spray rates [92], [108]. The yields we obtained were in the range of 1.16% to 62.81%. We found in our DOE that yield was mostly influenced by organic solvent, stabilizer and polymer concentration and the interaction between stabilizer/organic solvent (Table 2.12). But in contrast to Bürki et al., no effect of the spray rates were determined [108]. The spray rate in the NSD can only be adjusted indirectly by the relative volume flow, which passes through the membrane. This volume flow is influenced by the viscosity of the feeding solution as well as of the pore size of the spray cap and the inlet temperature of the spray head. Thus, the spray rate can indirectly be influenced by the choice of organic solvent, polymer concentration and stabilizer, which is obvious in the DOE, as the different combinations of organic solvent, polymer concentration and stabilizer resulted in different viscosities of the feeding solution. Therefore, no direct influence on the spray rate could be determined.

In the Büchi B-90 an electrostatic precipitator is used for the particle collection, which has in general an efficacy of 90-99% depending on the sprayed material, mass and the used gas [157]. A low precipitation efficiency of submicron particles in electrostatic particle precipitator is due to the difficulty in charging the spray dried material, which is depending on the electrical resistivity [157]. Low charge results in low particle mobility and low collection efficiency due to fast discharging [158]. In the present study an effect of the interaction temperature/organic solvent on yield was observed, which may indicate that inefficient dried particles have a different ability to be charged than full dried particles. Due to the solvent residues in the sprayed particles a change in the electrical resistivity could be assumed. Electrostatic precipitators are normally constructed with a system to remove the deposited particles from the collector electrode (e.g. a mechanical rapping device), before the saturation is reached. In the Büchi B-90 no such auto-cleaning system is installed and a saturation of the collector electrode was observed, which limits the robustness of the method when spraying large batch sizes. The yield decreased from 84.8% to 74.0%, when using 40 ml and 50 ml initial volume, yielding an effective amount of particles 1080 mg and 1350 mg, respectively (Figure 2.5).

2.5.3. Design of experiments as tool in the development of nano- and microparticulate drug delivery systems

It is obvious that a DOE generates an objective view on an unknown or poorly characterized process. However, the gain of information of a DOE could be little or enormous compared to the investment of practical work. However, the combination of parameters in the DOE can save time and indicate limitations. The main challenge is to precisely ask the questions, which should be answered by the DOE. A DOE is useless/inefficiently answering yes-no questions, such as e.g.: Can my drug be encapsulated in NPs at all? Instead, a DOE will answer the following questions: Do different stabilizers have an effect on the encapsulation efficiency? Does a given stabilizer has a different effect when combined with another solvent?, etc. Depending on the influence of the factors in question, the DOE would reveal a statistical correlation.

Before starting the DOE it is important to perform some preliminary studies to decrease the range of investigated factors and, hence, to increase the accuracy of the DOE model. For example it will not make sense to use an amount of polymer which is insoluble in the organic phase or at so high contents that an injection is impossible due to the increased viscosity. Such limitations can be taken into account in the DOE. A DOE could be a benefit and save time for frequently used processes, e. g. production processes of solid dosage forms, mixing processes, coating processes, improving quality, accuracy and reliability for the respective process in development as well as in research.

2.6. Conclusion

The DOE approach as performed in this study revealed that the particle size and its distribution in the NPR are dominantly controlled by the polymer concentration. Hence, the DOE allowed for the NPR to define a mathematical model and statistically reliable correlation, which can be used for the optimization of the process and prediction of optimal formulation.

It was possible to distinguish between important and unimportant factors based on the unambiguous statistical criteria. Thus, the major advantage of the DOE is to provide a statistically sound basis for discarding unimportant parameters and focusing on the essential ones. The model built by the DOE for the NPR for producing particles with a size of 150 ± 10 nm was accurate, robust and reliable, so that the predicted optimized parameters were in excellent agreement with experimental data.

In case of NSD, the DOE revealed that the formation of particles is more complex as being influenced by various process parameters and, therefore, more difficult to control. The use of the DOE approach allowed discerning the interaction of factors and helped in explaining the indirect influence of factors on the process. We could demonstrate that each of the seven investigated process parameters in the DOE were of significant influence and necessary to be thoroughly addressed. With NSD, the smallest possible particle sizes were in the lower micrometer size range and several possible solutions were found which predict the composition of an optimal formulation based on the DOE. Both NPR and NSD were robust and accurate to a volume-based evaluation of the minimally necessary and the maximally possible batch size using optimized set-ups.

We conclude that DOE can help to optimize well known processes and, furthermore, to understand and optimize innovative manufacturing processes, which is urgently needed for the quality by design preparation of nano- and micronsized DDS.

Parameters used for the following experiments

Based on the results of this chapter the following parameters for the preparation of NPs were selected as listed in Table 2.3. Briefly, 1.3% PLGA, poloxamer 407 and mixture of acetone/ethanol as organic solvent were used. For the NSD parameters were selected as listed in Table 2.4. Briefly, 1.1% PLGA (wt/v), 1.6% Span60 (wt/v) and acetone as organic solvent were selected.

3. Advanced formulations of cyclosporine A and budesonide for the therapy of inflammatory bowel disease

Parts of this chapter will be included in a manuscript for submission to a peer-reviewed journal:

Christina Draheim*, Julia Susewind*, Alexis Guillot, Brigitta Loretz, Steffi Hansen, Eva-Maria Collnot, Markus Limberger, Claus-Michael Lehr, *PLGA based nano- and microsized particles for inflammatory bowel disease therapy: evaluation of size-dependent accumulation and anti-inflammatory effect in an in vitro triple culture model*

*These authors contributed equally to this work.

The author of the thesis made the following contributions to the chapter: Conceived, designed and performed experiments. Analysed and interpreted the data. Wrote the manuscript.

The X-ray powder diffraction (XRD) analysis was kindly performed and designed by Sebastian Slawik at the Material Engineering Center Saarland (MECS). The author thanks the MECS for the support.

3.1. Introduction

The therapy of IBD is at the moment limited to reduce the symptoms and to increase life quality, mainly based on a medical treatment [17]. The daily administration of high doses of immunosuppressive or anti-inflammatory drugs is hence required for the treatment of IBD, leading to severe adverse effects. The application of pellets or tablets, targeting the upper parts of the intestine, is often inefficient in IBD mainly due to enhanced elimination of these dosage forms by diarrhea [43]. Therefore, patients would benefit from a DDS that delivers the used drugs directly to the inflamed areas of the intestine. Such a more local treatment would reduce high systemic concentrations and, furthermore, allow a dose reduction compared to a systemic application reducing side effects.

In IBD a reorganization of the epithelium within ulcerated areas occur due to the inflammation and depending on the level of severity [43], [159]. The ulcerations have been revealed to be an accessible target for particulate DDS in a suitable size range [71], [73], [76]. Particles can accumulate in the inflamed areas of the intestine and remain there for prolonged times, releasing the encapsulated active pharmaceutical ingredient (API) in a controlled manner. Several recent studies show the efficacy of this passive targeting approach and were introduced in chapter 1.4. A size-dependent accumulation was identified: NPs seems to be favorable in rodent colitis models (chapter 1.4) [75], [81]. At the same time a recent study demonstrated a higher accumulation efficiency for MPs, compared to NPs of the same material, in human patient [76]. However, this effect has to be further investigated.

The emergence and more widespread production of particulate DDS in the pharmaceutical industry is hindered by the absence of information regarding the influence of process parameters [89]. The identification of critical process parameters is important in the early stage of DDS development in order to achieve particles of consistent quality. Thus, for the preparation of PLGA particles a DOE was applied on NPR and NSD to understand the control of size and size distribution (chapter 2). The NPR was optimized for producing NPs with a size of 150 ± 10 nm. With the NSD MPs can be fabricated in a single step with a size of ~ 2 - 4 μm . Both methods were robust and accurate across the volume-based batch size range of 0.625-50.0 ml for the NPR and 5-40 ml for the NSD. This is important in the development process, where in the beginning a limited amount of material is available and later the batch size needs to be scalable for larger test series.

In this chapter the immunosuppressive drug CYA and the anti-inflammatory drug BU were encapsulated into the in chapter 2 optimized NPs and MPs.

The two lipophilic drugs were selected due to their potential in IBD therapy and different pharmacological and physico-chemical properties (chapter 1.2), which can influence the encapsulation efficiencies (EE) and the release from the DDS. PLGA can be used to encapsulate hydrophobic drugs, e.g. CYA and BU, and is present in an amorphous state when used at a ratio of 50/50 (lactic/glycolic acids, wt/wt). This leads to a relatively faster decomposition within two month, an optimal degradation time for an orally applied DDS.

CYA, a calcineurin inhibitor, is applied to UC patients suffering from steroid-refractory disease or from fulminant colitis, often also in co-medication with azathioprine and methotrexate for maintenance therapy [17], [29], [160]. BU, a corticosteroid, is a first-line drug for the treatment of inflamed ileum and ascending colon in CD [17], [37]. In contrast to other corticosteroids, BU undergoes an extensive first-pass metabolism, thereby, the systemic bioavailability is reduced to 10-15% after oral administration [39], [40]. Nevertheless, both APIs lead to several serious side effects [161], which should be decreased by using a suitable DDS.

Additionally, in this chapter NPs were transferred to a storable form by freeze drying and this process was further optimized. Afterwards the optimal loading of both drugs was determined by encapsulating increasing amounts of CYA or BU in NPs and MPs. The particles were characterized in size and size distribution. In a second step optimal loaded NPs and MPs were analysed by X-ray powder diffraction, to determine the crystalline content of BU and CYA in NPs and MPs, and *in vitro* release profiles were performed.

The direct comparison of NPs and MPs aimed to improve the understanding of inflammation targeting. The physico-chemical and biopharmaceutical properties (e.g. size, EE and release) were characterized to determine in the following *in vitro* (chapter 5) and *in vivo* experiments (chapter 7) their impact on the success of IBD therapy.

3.2. Materials

Excipients for NP and MP preparation and active ingredients were used as described in chapter 2.2. Budesonide (BU) and tween[®]80 were purchased from Caesar & Loretz GmbH (Hilden, Germany). Cyclosporine A (CYA, Fluka), sucrose and D-(+)-trehalose dehydrate were purchased from Sigma Aldrich (Schnelldorf, Germany). Polyvinyl alcohol (PVA, Mowiol[®]4-88) was purchased from Merck (Merck KGaA, Darmstadt, Germany). Purified water was of Milli-Q quality and prepared by a Millipore Milli-Q Synthesis system (Merck KGaA, Darmstadt, Germany).

All solvents were high-performance liquid chromatography grade and all chemicals met the quality requirements of the European Pharmacopoeia 6.0–7.3.

3.3. Methods

3.3.1. Optimization of the freeze drying process of nanoparticles

Preparation of nanoparticles

The NPs were prepared by nanoprecipitation (NPR) as introduced in chapter 1.5 and described in chapter 2.3.8. Briefly, PLGA (1.3%, wt/v) were weighed accurately and dissolved in a mixture of acetone/ethanol (organic phase, 16/3, v/v). The solution was injected with a Hamilton[®] glass syringe using a 0.6 mm in diameter needle (1005 TTL 5 ml, chromatography service, GmbH, Germany) at 500 rpm and a flow of 4.55 ml/min into purified water containing 1% poloxamer 407 (wt/v) as stabilizer, forming the aqueous phase. The ratio organic phase/aqueous phase was kept at a ratio of 1/2. The poloxamer 407 was separated from the NPs by dialysis (Spectra/Por[®] dialysis membrane, molecular weight cut-off (MWCO) 300 kDa, Carl Roth GmbH & Co. KG, Germany) overnight against purified water. After washing of the NP suspension the volume was readjusted with purified water to the initial volume.

Freeze drying of nanoparticles

The drug free washed NPs were freeze dried separately in the presence of 2.6% trehalose, 1.3% mannitol and 1.3% sucrose in a first step. Hence, the ratio PLGA/sugar is 1/1 (wt/wt) or 1/2 (wt/wt) for trehalose. As the results turned out an unsuccessful re-constitution also mixtures of trehalose at a ratio of 1/1 in combination with polyvinyl alcohol (PVA) were tested. PVA was added as solution (2%, wt/v, pH 7.0) at different concentrations referring to the volume of the NP suspension (0.01%, 0.05%, 0.1%, 0.3%, 0.6%, 1.0%; wt/v). NPs were freeze dried without any cryoprotective agent as a control. Before freeze drying the samples were frozen at -80°C for 12 h. Afterwards the samples were immediately placed into the freeze drying chamber (Christ alpha 2-4 LSC, Germany). The first drying step was performed at 15°C and 0.08 mbar for 72 h. Secondly, the temperature was increased to 20°C and the pressure increased to 0.20 mbar for 2 h. The freeze dried cake was characterized according to following criteria according to Chacón et al. [162]: (a) volume contraction of cake in high, (b) volume contraction of cake in diameter. Sample reconstitution was performed by addition of purified water to restore the starting volume before freeze drying and mild manual shaking.

The particle size and size distribution was measured by dynamic light scattering (chapter 3.3.4). The experiments were performed at least in triplicate. Also the macroscopic appearance of NP suspension after reconstitution was evaluated according to the following criteria: (c) absence of aggregates, (d) few small sized aggregates, and (e) large aggregates [162].

After optimization of both processes freeze drying and drug loading (chapter 3.4.2) stability studies under storage conditions (4°C, in closed vials) were performed. Freeze dried samples of unloaded NPs were analysed for size and size distribution after three and six month. Loaded NPs were analysed only after six month.

3.3.2. Preparation of API loaded nanoparticles by nanoprecipitation

The NPs were prepared by NPR as introduced in chapter 1.5 and described in chapter 3.3.1.

To determine the optimal loading of the NPs, increasing amounts of both APIs were separately encapsulated in the same amount of PLGA (65 mg, equal to 1.3% in 5 ml organic phase). The used ratios API/PLGA (wt/wt) were 0.5/10, 1/10, 2/10, 3/10, 4/10 and 5/10 both dissolved in the organic phase. The ratio of 1/10 was defined as standard loading. The encapsulation of BU was stopped at a ratio of 4/10 due to the resulting EE (chapter 3.4.2.). The volume of organic solvent was kept at 5 ml and the ratio organic phase/aqueous phase was kept at a ratio of 1/2 (5 ml/10 ml). After preparation the particles were washed (chapter 3.3.2.1), freeze dried using trehalose at a ratio of 1/1 (trehalose/PLGA, wt/wt) combined with 0.3% (wt/v) PVA according to the results in chapter 3.4.1 and the EE was determined (chapter 3.3.6). Experiments were performed at least in triplicate.

3.3.2.1. Purification

To separate the free BU content and the stabilizer (poloxamer 407) from the solution the NP suspension was washed four times with purified water by tangential flow filtration using a Minimate™ TFF capsule (MWCO 300 kDa, Pall, Germany). The filtration was carried out by adding four times the initial volume of the aqueous phase.

The free CYA content was separated from the NPs by dialysis (Spectra/Por[®] dialysis membrane, MWCO 300 kDa, Carl Roth GmbH & Co. KG, Germany) over two days against purified water. The dialysis allows also separating the stabilizer.

Different systems were used for the purification as the BU was attaching to the dialysis membrane.

After washing of the NP suspension the volume was readjusted with purified water to the initial volume. This is important to maintain the same concentration for the following freeze drying step.

3.3.3. Preparation of API loaded microparticles by nano spray drying

The MPs were prepared by NSD as introduced in chapter 1.5 and described in chapter 2.3.2 and chapter 2.3.9. Briefly, the Büchi B-90 was operated in the closed mode set-up with inert gas (N₂ and CO₂ at 0.8 bar). As in-process parameters the out-let temperature and the drying gas flow, which was fixed at 115 l/min, were monitored. The out-let temperature was determined to be 28-38°C, which should be below the T_g of the used PLGA (~45°C, determined by differential scanning calorimetry). For preparation of the feeding solution 1.1% PLGA (wt/v), 1.6% Span60 (wt/v) as stabilizer and the API, BU or CYA, were accurately weighted and dissolved in acetone. To determine the optimal loading of the MPs increasing amounts of both APIs were separately encapsulated in the same amount of PLGA (110 mg, equal to 1.1% in 10 ml organic phase). The used ratios API/PLGA (wt/wt) were 0.5/10, 1/10, 1/15, 2/10, 3/10, 4/10 and 5/10. The ratio of 1/10 was defined as standard loading. The encapsulation of BU was stopped at a ratio of 4/10 due to the resulting aggregation of the BU loaded MPs at high ratios (chapter 3.4.2). The volume of acetone was kept for all experiments at 10 ml. The feeding solution was sprayed using the 4 µm mesh under ice-cooling of the supplied dispersion to prevent heating of the circulating solution. The particles were collected by an electrostatic particle precipitator, removed by a plastic scratcher from the collector electrode and the EE was determined (chapter 3.3.6). Experiments were performed at least in triplicate. The MPs are already a dry powder and, thus, do not need an additional washing and freeze drying step.

3.3.4. Determination of particles size, size distribution and zeta potential

Particles produced by NPR

Hydrodynamic diameter and polydispersity index (PDI) of NPs were measured by dynamic light scattering (Zetasizer[®] Nano ZS, Malvern Instruments, UK) as described in chapter 2.3.6. The zeta potential was measured in purified water using the Zetasizer[®] Nano ZS. The measurements were carried out for each batch in triplicate and the mean value and standard deviation (S.D.) were calculated.

Particles produced by NSD

The spray dried MPs were characterized by laser diffraction using a Mastersizer[®] 2000 (Malvern Instruments, Herrenberg, Germany) as described in chapter 2.3.6. The particles were re-dispersed in purified water containing 0.01% PVA under manual shaking for 10 s. All batches were measured each in triplicate and the mean value and standard deviation (S.D.) were calculated. The volume mean diameter ($d_{0.5}$) as well as the percentile values $d_{0.1}$ and $d_{0.9}$ were further calculated by the Mastersizer[®] software. $D_{0.1}$ and $d_{0.9}$ describe, that 10% or 90% of the particles are smaller than the measured diameter for the corresponding value, respectively. The size distribution (width) is defined in equation 8 (eq. 8). A narrow size distribution is indicated by a small width

$$width = \frac{d_{0.9} - d_{0.1}}{d_{0.5}} \quad \text{eq. 8}$$

3.3.5. Investigation of morphology by scanning electron microscopy

The SEM imaging was performed as described in chapter 2.3.8.

3.3.6. Determination of encapsulation efficiency and optimal loading

High-performance liquid chromatography (HPLC) was used for the quantification of both APIs using the following methods. HPLC quantification was performed with a Dionex system (Thermo Fisher GmbH, Idstein, Germany) consisting of a Dionex ISO-3100A pump, a Dionex WPS-3000 TSL autosampler, a Dionex VWD-3400 variable wavelength detector, a Dionex TCC-3000 column compartment and a Dionex SRD-3200 solvent rack. The system ran on Chromeleon software version 6.80 SP2.

A reversed phase column, LiChrosphere® RP18 column (5 µm x 125 mm x4 mm; Merck KGaA, Germany), and an isocratic elution were used. All standards were dissolved in a mixture of acetonitrile/phosphate buffer pH 3.0 (1/1, v/v). The mobile phase consisted for BU of a mixture of acetonitrile/phosphate buffer pH 3.0 (2/3, v/v). The oven temperature was set to 30°C. An injection volume of 80 µl and a flow of 1.9 ml/min were used. The retention time was 4.0 ± 0.1 min detecting BU with UV at 242 nm. The method was linear ($r^2 > 0.999$) between 2.0 µg/ml-100.0 µg/ml with a calculated lower limit of quantification (LOQ) of 2.0 µg/ml. For CYA a mixture of phosphate buffer pH 3.0/methanol (1/9, v/v) was used as mobile phase. The oven temperature was set to 50°C. An injection volume of 30 µl and a flow of 1.0 ml/min were used. The retention time was 2.1 ± 0.1 min detecting CYA with UV at 205 nm. The method was linear ($r^2 > 0.999$) between 10.0 µg/ml-100.0 µg/ml with a calculated LOQ of 6.0 µg/ml.

The EE was determined by a direct method using the final formulation after freeze drying for NPs and after spray drying for MPs. Likewise, a known amount of API loaded NPs or MPs was dissolved in a mixture of acetonitrile/phosphate buffer pH 3 (1/1, v/v) and treated 2x15 min in an ultrasonic bath to disintegrate the PLGA particles. The solution was cooled down to room temperature and filtered through a disposable syringe filter with 0.45 µm pore size (CHROMAFIL GF/PET 45/25). The clear filtrate was collected and analysed by HPLC to determine the API content. Experiments were at least performed in triplicate.

$$EE = \frac{m (API_{encapsulated})}{m (API_{initial})} * 100\% \quad \text{eq. 9}$$

The EE describes the percentage of encapsulated API referring to the initial mass of API and is defined by equation 9 (eq. 9). In this equation $m (API_{initial})$ refers to the weight (m) of API put into the formulation and $m (API_{encapsulated})$ refers to the amount of API measured after re-dispersion and disintegration.

The mass of encapsulated API was used to determine the actual loading. The actual loading is expressed in equation 10 (eq. 10) and describes the actual loading as ratio of weight (m) encapsulated API in mg to 100 mg of PLGA. The actual loading displays the loading capacity.

The theoretical loading can be calculated from the initial amount of API referring to 100 mg of PLGA as expressed in equation 11 (eq. 11).

$$\text{actual loading} = \frac{m(\text{API}_{\text{encapsulated}})}{m(\text{PLGA}_{\text{initial}})} * 100 \quad \text{eq. 10}$$

$$\text{theoretical loading} = \frac{m(\text{API}_{\text{initial}})}{m(\text{PLGA}_{\text{initial}})} * 100 \quad \text{eq. 11}$$

The actual loading and theoretical loading were correlated in one graph for NPs or MPs, and both APIs, respectively (Figure 3.2). This representation can be used to determine the optimal theoretical loading, which is reached, if by increasing initial API mass the actual loading is not increasing proportional.

Optimal loaded NPs and MPs were further analysed by X-ray powder diffraction (chapter 3.3.7) and *in vitro* release profiles (chapter 3.3.8) were performed.

3.3.7. X-ray powder diffraction

The X-ray powder diffraction (XRD) analysis was used to determine the crystalline content of BU and CYA in optimal loaded NPs and MPs (ratio of 1/4, CYA/PLGA, wt/wt, for NPs and MPs; 1/10 and 2/10, BU/PLGA, wt/wt, for NPs and MPs, respectively). First, samples of pure materials (PLGA, Span60 and trehalose) and pure APIs were scanned by XRD to identify the signals from pure material in the formulations as listed in Table 3.1. Further drug free and optimal loaded particles (chapter 3.4.2) both NPs and MPs were investigated as well as physical mixtures of drug free particles mixed with API at concentrations referring to optimal loading. All samples were analysed in dry powder state. A PANalytical X'Pert Pro MPD was used with Cu anode at 40 kV and 40 mA. Samples were scanned across an angular range from 5 to 145 2θ with a step size of 0.013°2θ. The powders were analysed in a nickel or monocrystalline silicon sample holder for small batch sizes, which was used for the APIs. Characteristic high intensity peaks were used in order to determine qualitatively the API contents in the particles.

Table 3.1. Samples analysed by XRD.

sample	nanoparticles	microparticles
API		CYA
API		BU
cryoprotective/ stabilizer	trehalose	Span60
	drug free	drug free
	CYA loaded	CYA loaded
	BU loaded	BU loaded
physical mixture	drug free NPs + CYA	drug free MPs + CYA
physical mixture	drug free NPs + BU	drug free MPs + BU

3.3.8. *In vitro* drug release studies

The release profiles of the optimal loaded NPs and MPs (chapter 3.4.2; ratio of 1/4, CYA/PLGA, wt/wt, for NPs and MPs; 1/10 and 2/10, BU/PLGA, wt/wt, for NPs and MPs, respectively) were investigated in phosphate buffered saline (PBS, 10mM_{NaCl}) pH 6.8, to mimic the conditions in the proximal colon [50], at room temperature in triplicate. To increase the solubility of CYA 0.05% tween[®]80 (wt/v) was added to the PBS.

Sink conditions and determination of saturation concentration

The release was performed under sink conditions, which were defined as 30% of the saturation concentration according to the United States Pharmacopeia (USP, 2003). The saturation concentration was determined to be 42.3 ± 0.8 µg/ml for CYA and 21.7 ± 0.6 µg/ml for BU. The experiments were performed in triplicate. Likewise, BU and CYA as powder were added to 3 ml PBS pH 6.8, containing 0.05% tween[®]80 (wt/v) for CYA, in a snap vial until a visible pellet was formed. The PBS was stirred for 24 h at room temperature. Afterward the supernatant was separated from the pellet by centrifugation for BU (Hettich Rotina 420 R, Hettich Holding GmbH & Co. oHG, Germany; at 15000x g at 20°C for 15 min). For CYA a floating during centrifugation was observed and the separation was performed by filtration through a 450 µm disposable filter (CHROMAFIL GF/PET 45/25). The 1 ml of the clear solution was used to quantify the respective API content using the HPLC methods described in chapter 3.4.2.

In vitro release profiles

Briefly, API loaded NPs or MPs were suspended in 30 ml of the release medium. The release experiments were performed in a stock bottle closed with Parafilm[®]M (BRAND GMBH + CO KG, Germany) to avoid evaporation. The suspension was stirred at 400 rpm. At pre-determined time points 1.5 ml suspension was removed and centrifuged (Hettich Rotina 420 R, Hettich Holding GmbH & Co. oHG, Germany) at 24400x g at 20°C for 15 min. 1 ml of the supernatant was drawn as sample and analysed by HPLC as described in chapter 3.3.6. 1 ml fresh medium was added to the rest of the supernatant to re-disperse the pellet before adding to the release medium. The release was cumulatively calculated and normalized to the actual drug content of the particles, which can be determined from the EE. The following values were defined for classifying the release of the different formulations:

- Fast release: >80% API is released t=4 h,
- Intermediate release: 50-60% API is released t=48 h,
- Slow release: <10% API is released t=4 h and <30% t= 48 h.

3.4. Results

3.4.1. Optimization of freeze drying process of nanoparticles

All results of the macroscopic characterization of the freeze dried samples were summarized in Table 3.2. All freeze dried samples were white and fluffy in appearance. Although no volume contraction was visible for NPs without cryoprotectant (control) an incomplete re-constitution with large aggregates was observed. For trehalose/PVA mixtures and mannitol also no contraction was determined. Mannitol, sucrose and trehalose did not enable a complete reconstitution as macroscopic aggregates were visible. For all these samples, as well as the mixtures of trehalose with 0.05% (wt/v) and 0.01% (wt/v) PVA, although no aggregates were visible, mean sizes >1 µm and size distributions PDI >0.48 were determined. The results for mixtures of trehalose/PVA turned out to be the most promising approach. Moreover, trehalose was described in literature as preferred cryoprotectant agent for DDS due to less hygroscopicity and formation of flexible formation hydrogen bonds between the NPs [163]–[165]. Therefore, trehalose was combined with other concentrations of PVA and compared to NPs before freeze drying in Figure 3.1a.

Table 3.2. Macroscopic characterization of freeze dried samples using mannitol, sucrose or trehalose, also in different combinations with PVA (0.01%, 0.05%, 0.1%, 0.3%, 0.6%, 1.0%; wt/v), as cryoprotective agent. Samples were compared to NPs freeze dried without cryoprotective agent (control).

cryoprotective agent	freeze dried cake		re-constitution
	(a) volume contraction in diameter	(b) volume contraction in height	
without (control)	-	-	large aggregates
mannitol	-	-	large aggregates
sucrose	-	+	few small sized aggregates
trehalose	+	+	large aggregates
trehalose + 1.0% PVA	-	-	absence of aggregates
trehalose + 0.6% PVA	-	-	absence of aggregates
trehalose + 0.3% PVA	-	-	absence of aggregates
trehalose + 0.1% PVA	-	-	absence of aggregates
trehalose + 0.05% PVA	-	-	absence of aggregates
trehalose + 0.01% PVA	-	-	absence of aggregates

+ contraction visible, - no contraction visible

Using 0.1% PVA the size increased dramatically indicating an incomplete re-constitution. For concentrations of 1%, 0.6% and 0.3% PVA, a perfect re-constitution was achieved as the measured particle sizes were slightly higher compared to the particles before freeze drying. It was also obvious, that higher PVA concentrations lead to slightly higher particle sizes. Based on these results, for further experiments trehalose at a ratio of 1/1 (trehalose/PLGA, wt/wt) combined with 0.3% PVA will be used for freeze drying of NPs.

SEM images of the NPs after freeze drying in Figure 3.1b show the stability of the particles during freeze drying. No change of the morphology was observed and the particles were round and spherical as before freeze drying (Figure 3.5). "Bridges" are visible between the particles as well as an embedding of the particles due to the trehalose and PVA between the particles. The bridges consisting of the trehalose and PVA result during the drying.

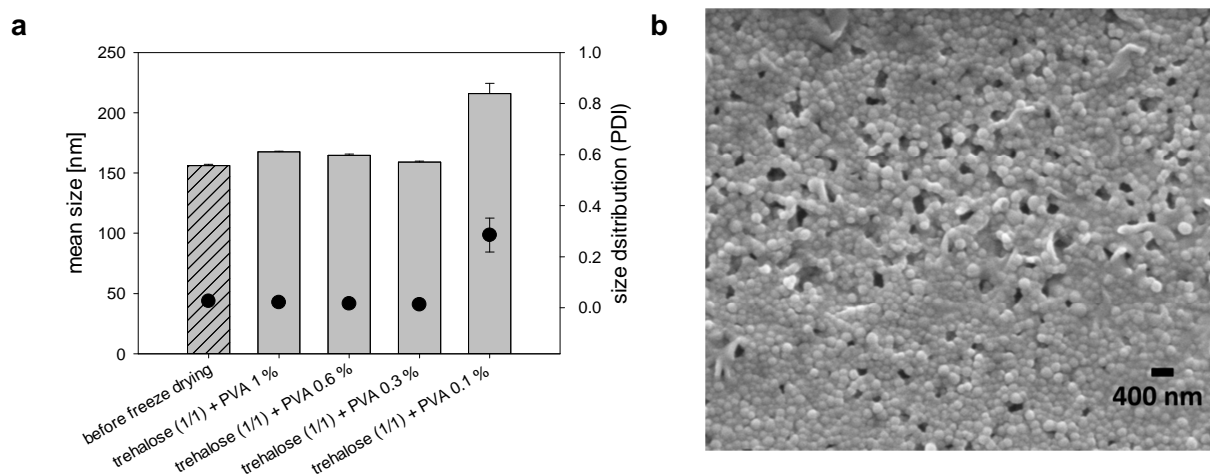


Figure 3.1. (a) Characterization of freeze dried samples in size and size distribution by dynamic light scattering. Different combinations of trehalose and PVA (0.1%, 0.3%, 0.6%, 1.0%, wt/v) were used and compared to NPs before freeze drying. The values are presented as mean \pm S.D. (n=3). (b) SEM image of freeze dried batch using trehalose (1/1, PLGA/trehalose) and 0.3% PVA demonstrating the stability of NPs during freeze drying.

3.4.2. Determination of encapsulation efficiency and optimal loading

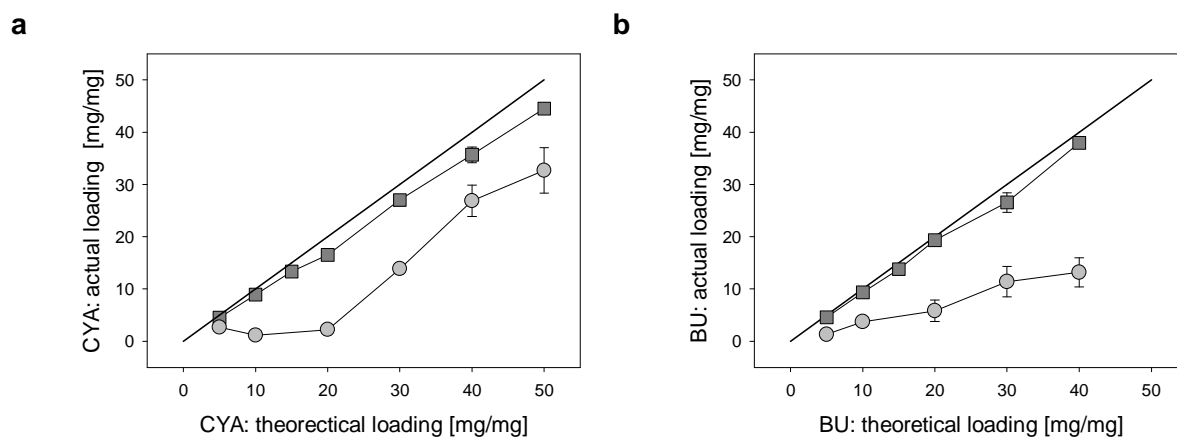
Particulate DDS should be loaded with the highest possible API content as the DDS itself should only act as transporter or reservoir for the respective API. In general, the loading of APIs into DDS is a function of lipophilicity of the API and the polymer used to prepare the DDS [61]. Both API have different physico-chemical properties, therefore, the results have to be considered separately. The EEs were determined and presented in Table 3.3 for CYA and Table 3.4 for BU. The loading values are presented in Figure 3.2a for CYA and in Figure 3.2b for BU. In general, at 100% EE the actual loading would be equal to the theoretical loading (Figure 3.2 line of identity). The optimal theoretical loading is reached if by increasing initial material the actual loading is not increasing proportional.

Table 3.3. EE of CYA loaded NPs and MPs. The values are presented as mean \pm S.D. ($n \geq 3$).

ratio	formulation	
	CYA-NP	CYA-MP
0.5/10	53.3 \pm 3.8	87.9 \pm 3.3
1/10	11.6 \pm 3.6	92.0 \pm 0.8
2/10	11.0 \pm 0.6	90.9 \pm 3.2
3/10	46.2 \pm 9.2	90.1 \pm 1.5
4/10	67.2 \pm 7.5	89.2 \pm 3.8
5/10	65.4 \pm 8.7	89.0 \pm 0.8

Table 3.4. EE of BU loaded NPs and MPs. The values are presented as mean \pm S.D. ($n \geq 3$).

ratio	formulation	
	BU-NP	BU-MP
0.5/10	26.5 \pm 2.5	91.6 \pm 0.2
1/10	36.5 \pm 4.3	91.4 \pm 6.3
2/10	29.7 \pm 9.9	98.3 \pm 5.4
3/10	39.1 \pm 10.3	92.9 \pm 6.6
4/10	34.1 \pm 7.6	94.8 \pm 2.6

Figure 3.2. Actual and theoretical loading of (a) CYA loaded NPs (○) and MPs (■) and of (b) BU loaded NPs (○) and MPs (■). The values are presented as mean \pm S.D. ($n \geq 3$; — line of identity).

EEs between 11% and 67% were determined for encapsulating CYA in NPs (Table 3.3). A high EE (53%) was measured for a ratio of 0.5/10 (CYA/PLGA, wt/wt).

As the spray dried MPs were produced in one step, nearly 100% of the encapsulated CYA was detected for all ratios (Table 3.3), which was to be expected. After spray drying the MPs are available as dry powder, which do not require a washing step. Losses could arise due to adsorption of initial API on equipment surfaces such as beaker, tubes etc. Since a slight decrease in the actual loading and in the EE was observed at ratios $>4/10$ (CYA/PLGA, wt/wt) the optimal loading was fixed at this ratio. The optimal loading results in an actual loading of 26.8 mg CYA/100 mg PLGA and an EE of $67.2 \pm 7.5\%$. Keeping the same ratio of $4/10$ (CYA/PLGA, wt/wt) between NPs and MPs allows a better comparison for following experiments. For the CYA loaded MPs the optimal loading ($4/10$, CYA/PLGA, wt/wt) results in 35.7 mg CYA/100 mg PLGA and an EE of $89.2\% \pm 3.8\%$.

For the BU encapsulation in NPs EE values $<40\%$ (Table 3.4) were determined for all tested ratios. For ratios $>1/10$ (BU/PLGA, wt/wt) a high intra batch variation was observed in the EE (S.D. >9.9 , $n=3$), which was less for the ratio of $4/10$. Hence, the optimal loading was fixed at $1/10$, which was defined as standard loading, resulting in 3.7 mg BU/100 mg PLGA with an EE of $36.5\% \pm 4.3\%$. SEM images of the BU loaded MPs show aggregates at ratios $>2/10$ in (Figure 3.3). Aiming for a loading as high as possible the optimal loading was fixed at $2/10$ resulting in 19.3 mg BU/100 mg PLGA with an EE of $98.3\% \pm 5.4\%$.

For the NPs the final formulation contains also trehalose (100 mg/100 mg PLGA, chapter 3.4.1) as cryoprotective agent and PVA (46 mg/100 mg PLGA) to allow a better re-dispersion. Calculating the final API content based on the EE of the final formulation CYA loaded NPs contain $\sim 94 \mu\text{g}$ CYA per 1 mg of final formulation and BU loaded NPs $\sim 14 \mu\text{g}/\text{mg}$. For the MPs the final formulation contains also the stabilizer Span60 (160 mg/100 mg PLGA, chapter 3.3.3). Therefore, the CYA loaded MPs contain $\sim 144 \mu\text{g}/\text{mg}$ and the BU loaded MPs $\sim 74 \mu\text{g}/\text{mg}$.

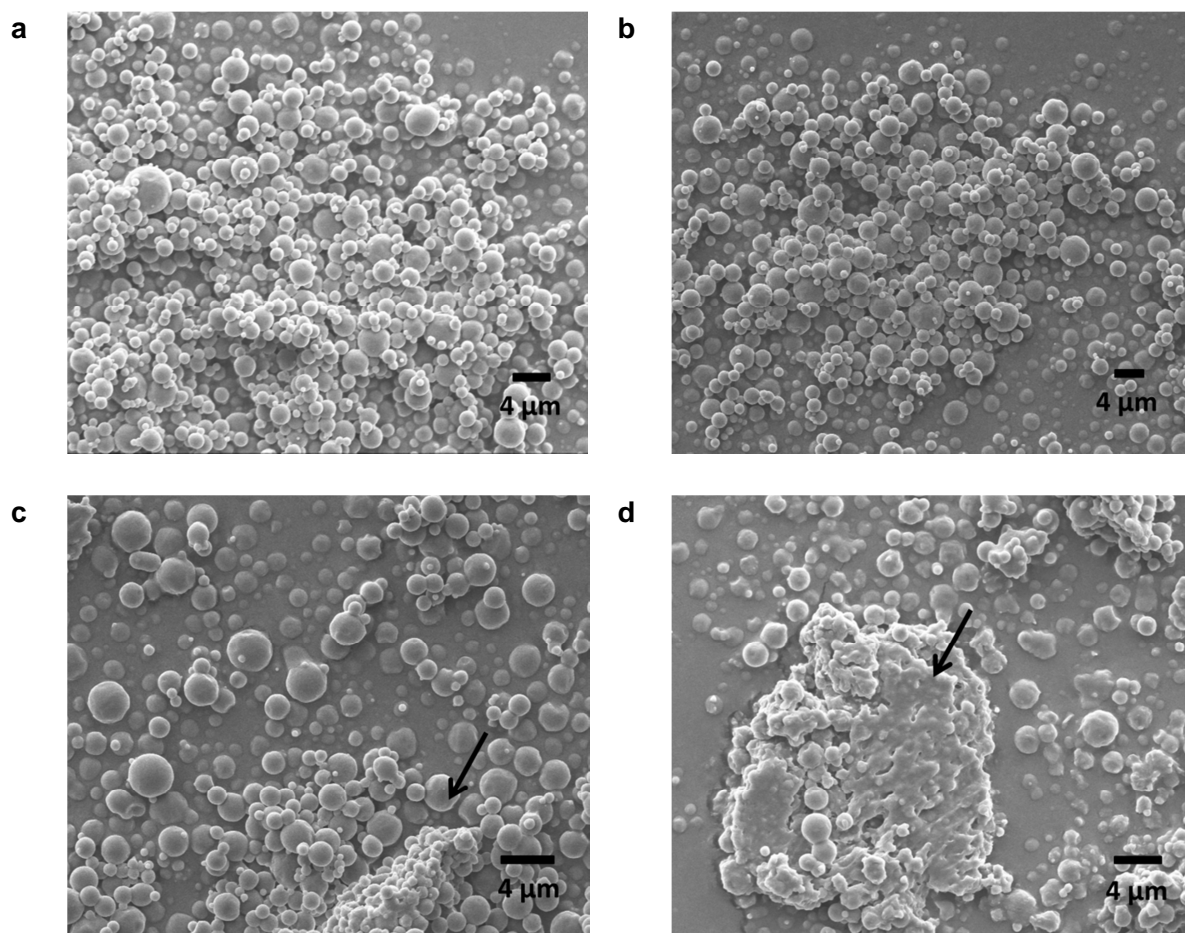


Figure 3.3. Representative SEM images of BU loaded MPs at different ratios: (a) 0.5/10, (b) 2/10, (c) 3/10 and (d) 4/10 (BU/PLGA, wt/wt). Aggregates (marked with an \rightarrow) are significant visible for ratios $>2/10$.

3.4.3. Size and size distribution of loaded nanoparticles and microparticles

The size and size distribution of CYA and BU loaded NPs (CYA-NP, BU-NP) and MPs (CYA-MP, BU-MP) with optimal loading are summarized in Figure 3.4 and compared to drug free NPs (blank). The size and size distribution of loaded particles after storage are, furthermore, presented in Figure 3.4. Batches were visualized by SEM imaging as presented in Figure 3.5.

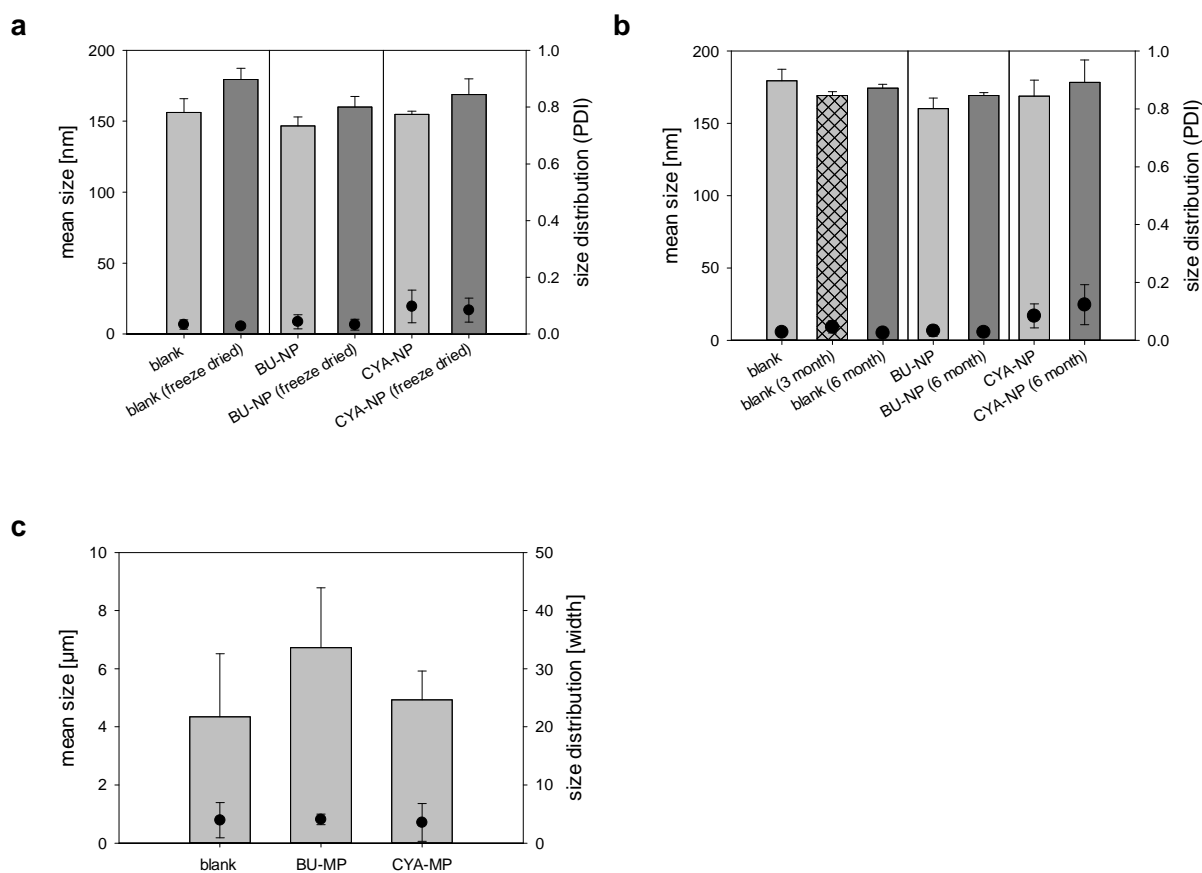


Figure 3.4. (a) Size and size distribution measured by dynamic light scattering of drug free (blank) and loaded NPs (BU-NP, CYA-NP), and (b) characterization in size and size distribution of freeze dried samples after storage. (c) Size and size distribution of drug free (blank) and loaded MPs (BU-MP, CYA-MP), measured by laser light diffraction. The values are presented as mean \pm S.D. (n=3).

By encapsulation of CYA and BU in NPs no significant increase or decrease in size or size distribution was observed (Figure 3.4a). Only for the CYA-NPs a slight increase in the size distribution was determined. Nevertheless, all particles had a size of 150 ± 10 nm with a narrow size distribution (PDI < 0.150). After freeze drying the size increased ~ 23 nm for the drug free NPs, ~ 13 nm for BU loaded and ~ 14 nm for the CYA-NPs for all batches due to the cryoprotective agent PVA. A negative zeta potential was determined, as expected before for PLGA NPs: -27.8 ± 0.61 mV for the drug free, -18.9 ± 0.51 mV for CYA-NPs and -25.0 ± 3.91 mV for BU-NPs. After storage of NPs in Figure 3.4 b no change in size or size distribution was determined for drug free NPs and BU-NPs. Only for CYA-NPs a slight increase in size (~ 10 nm) and size distribution was observed.

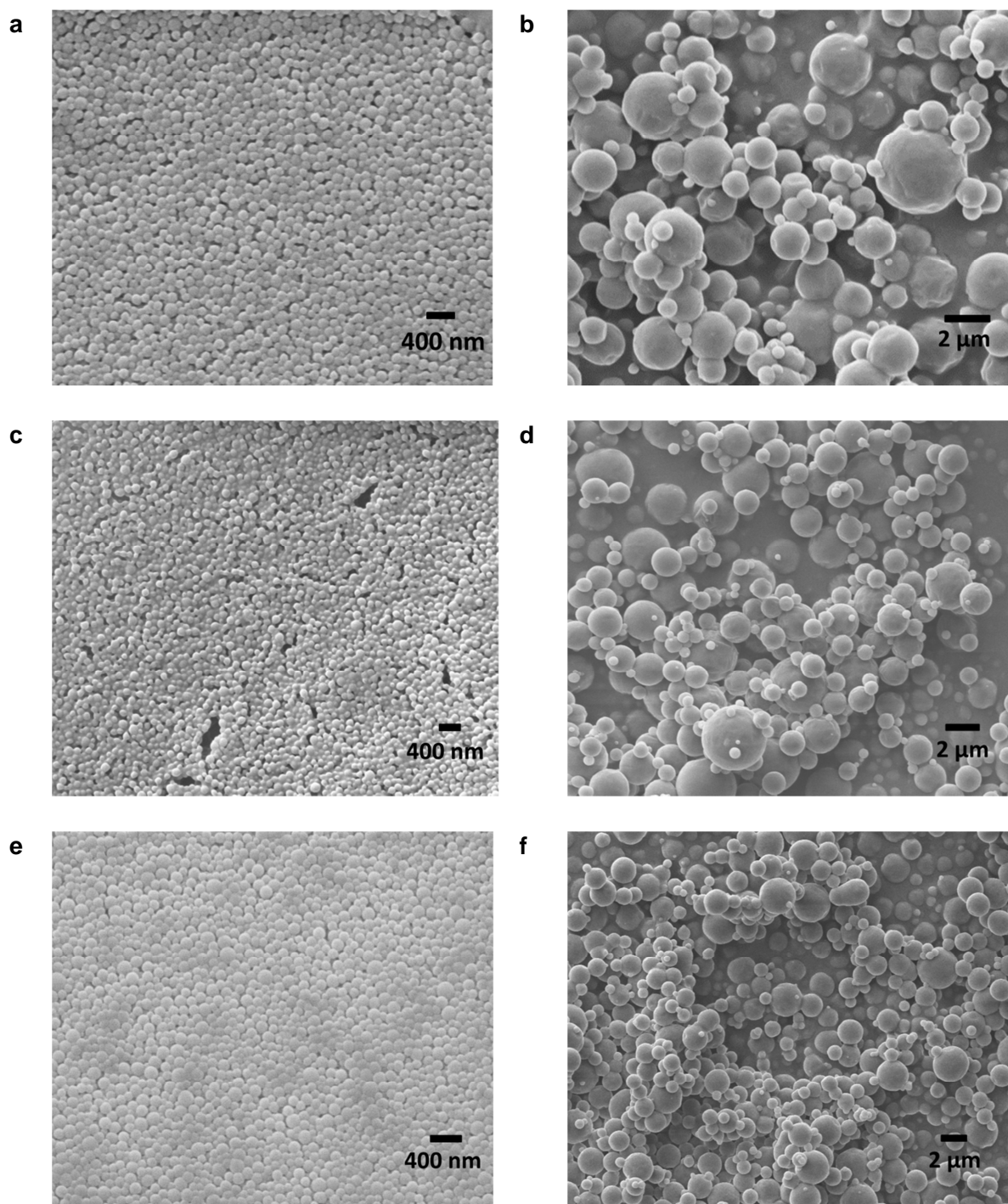


Figure 3.5. Representative SEM images of (a) blank NPs and (b) blank MPs, (c) CYA-NPs and (d) CYA-MPs, and (e) BU-NPs and (f) BU-MPs.

The size of the MPs was in the low micron size range (Figure 3.4c). In comparison to drug free MPs a slight increase in the mean size was determined by encapsulating BU, whereas no change in size was observed by loading the MPs with CYA. Furthermore, no change in size distribution was determined.

The SEM images (Figure 3.5) confirm the narrow size distribution for the NPs. Furthermore, they show that all particles are round and spherical in shape. The surface of the MPs is rough possibly due to the Span60 in the composition.

3.4.4. X-ray powder diffraction

The XRD analysis was used to determine the crystalline content of BU and CYA in the particles. The results are presented in Figure 3.6. Initially, the XRD diffractograms for PLGA, Span60, trehalose and the pure APIs were recorded for identifying characteristic intensity peaks. The used PLGA (50/50, lactic/glycolic acids, wt/wt) is showing a typical signal for amorphous substances (Figure 3.6a/b). Characteristic peaks with high intensity could be identified for trehalose at 23.78° (Figure 3.6a) and for Span60 at 21.38° (Figure 3.6b). For CYA two single peaks at 6.71° and 7.69°, furthermore, a double-peak at 9.05°/9.27° could be used for the identification (Figure 3.6c/d). BU showed two characteristic double peaks at 15.37°/16.00° and 22.76°/23.21° (Figure 3.6e/f). All characteristic peaks were marked with a coloured rectangle (blue=trehalose, yellow=Span60, green=CYA, red=BU). In Figure 3.6c a signal from crystalline CYA was detected at 6.71° and 7.69°. For CYA-MPs in Figure 3.6d no crystalline CYA was detected due to the absence of intensity of characteristic peaks. For both BU-NPs (Figure 3.6e) and BU-MPs (Figure 3.6f) no characteristic peak of BU was detected.

In Figure 3.7 physical mixtures of drug free particles and API were also scanned to verify, if the respective API content could be qualitatively detected, and compared to the scans of pure material, drug free and loaded particles as presented in Figure 3.6. Figure 3.7a and Figure 3.7b show that crystalline CYA could be clearly detected within both NPs and MPs. For physical mixture of BU with drug free particles characteristic peaks of BU could be detected for BU-MPs, but not for BU-NPs (Figure 3.7c/d). In comparison to the BU-MPs, which contain ~74 µg BU/mg in the final formulation, contain the CYA-NPs and CYA-MPs ~94 µg CYA/mg and ~144 µg CYA/mg, respectively. BU-NPs contain ~14 µg BU/mg indicating that the BU content in the NPs is under the lower limit of detection for the XRD method.

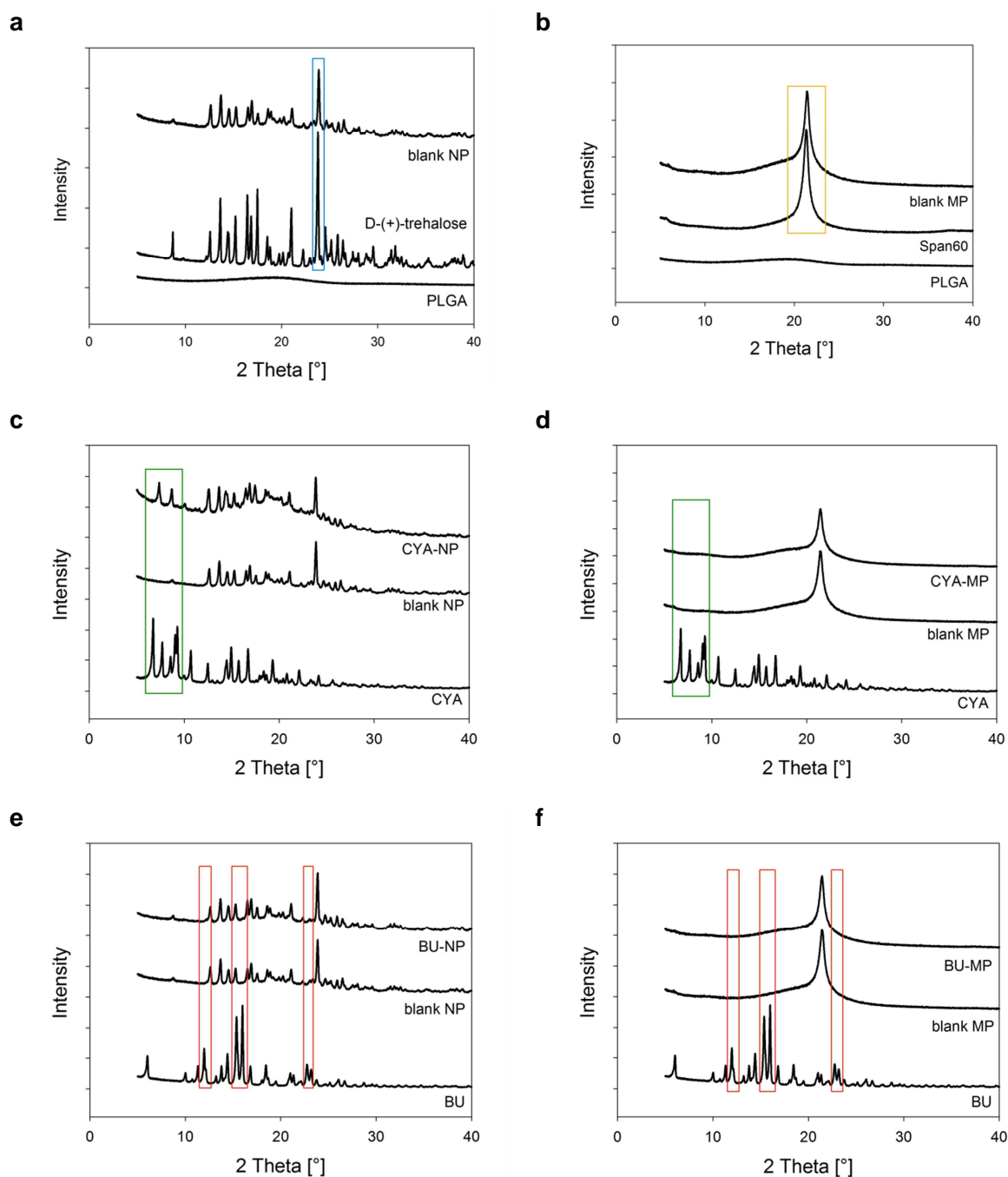


Figure 3.6. XRD scans of (a) pure PLGA, trehalose and drug free NPs (blank NP) and (b) pure PLGA, Span60 and drug free MPs (blank MP), (c) CYA-NPs and (d) CYA-MPs, (e) BU-NPs and (f) BU-MPs. All scans are shown in combination with API and respective drug free particles. Results are presented in 5000 intensity step-size. The coloured rectangles mark the characteristic peaks (blue=trehalose, yellow=Span60, green=CYA, red=BU).

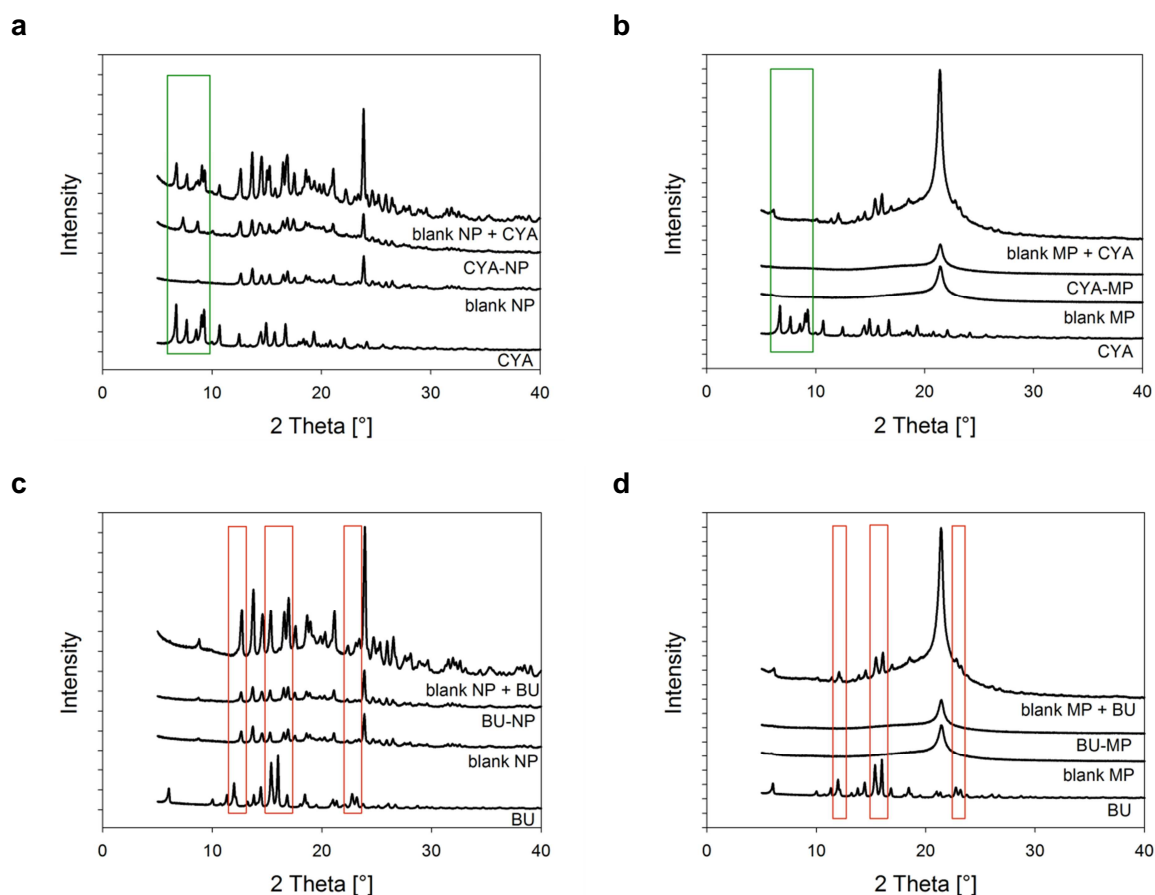


Figure 3.7. XRD scans of physical mixtures (“spiking”) of drug free particles with API. CYA, drug free (blank) particles and CYA loaded particles are presented in comparison with spiked (a) NPs and (b) MPs. BU, drug free (blank) particles and BU loaded particles are presented in comparison with spiked (c) NPs and (d) MPs. Results are presented in 5000 intensity step-size. The coloured rectangles mark the characteristic peaks (green=CYA, red=BU).

3.4.5. *In vitro* drug release studies

The results of the release profile in PBS pH 6.8 are summarized in Figure 3.8. Interestingly, the NPs and MPs show for both API different release behaviours. The CYA-NPs show a low release with a slow burst release with $14.03 \pm 2.4\%$ after 1 h, followed by a very slow sustained release (32.7%, $t=48$ h). The CYA-MP show fast to intermediate release with a high release within 24 h (91.3%; 15.9% after 1 h), that is faster but continuous for the first 6 h and then the release is slowing down and heading to a plateau of approx. 91% ($t=48$ h). In general, a burst release followed by a sustained release is typical for PLGA particles [61].

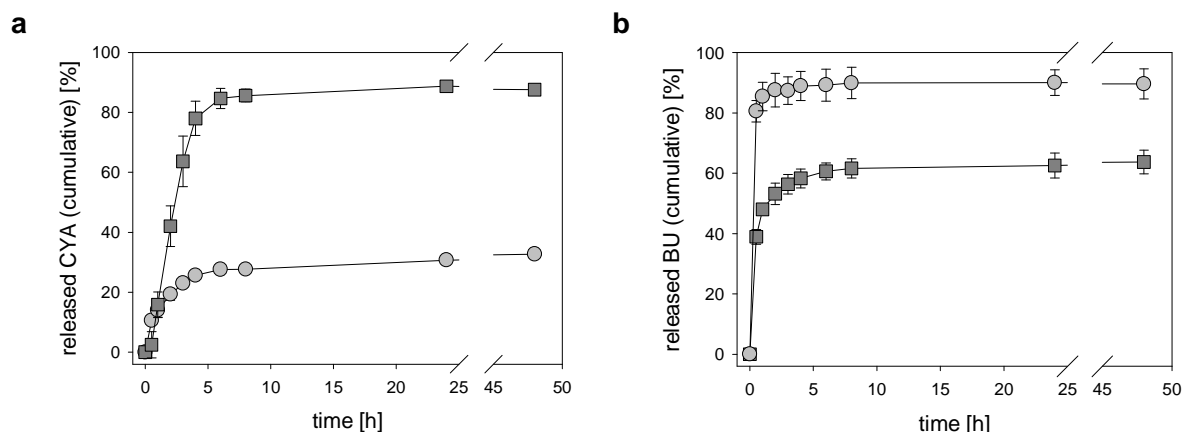


Figure 3.8. *In vitro* release profile of (a) CYA-NPs (○) and CYA-MPs (■) in comparison to (b) BU-NPs (○) and BU-MPs (■). The values are presented as mean \pm S.D. (n=3).

The BU-NPs show a fast, but uncontrolled, strong burst release within 30 min (80.6%; 89.6%, $t=48$ h). This could indicate that, although the particles were washed, BU is attached to the surface of the particles or located at the outer edge of the polymeric particles. In contrast, the BU-MPs show an intermediate release with a slow and sustained release reaching a plateau of after 8-10 h (63.7%, $t=48$ h). 48% of the encapsulated BU is released in 1 h.

3.5. Discussion

Particulate DDS can improve the therapy options in IBD as they can passively accumulate in inflamed intestinal areas of the intestine [75]. Thus, they can form a depot and reduce systemic adverse effects by reduced systemic bioavailability of the encapsulated API. So far NPs seem to be favorable in rodent colitis models [75], [78], whereas MPs show in a recent study a better deposition efficacy in human patients [76]. An enhanced accumulation of MPs in the ulcerated lesions was demonstrated. In contrast NPs were only found in traces of the mucosa in patients with CD and UC [76]. Hence, both NPs prepared by NPR and MPs prepared by NSD were selected to encapsulate the two model drugs CYA and BU. These lipophilic drugs are ideal candidates for the encapsulation in PLGA and both drugs showed efficacy in the treatment of IBD [17], [29], [37], [39], [40], [160].

The NPs are in suspension after the preparation and must be transferred in a storable form. Thus, the freeze drying technique was selected.

For this process the suitable cryoprotectant to prevent particles aggregation and to ensure a maximum stabilization of NPs during freeze drying must be evaluated and its concentration optimized. Sugars are used due to their ability to isolate individual particles (isolation hypothesis) in suspension preventing aggregation during freezing [164]. It has to be taken into account that also the NP concentration influences the freeze drying process. Due to stabilization of the cryoprotectant a complete re-dispersion without change in particle size should be achieved.

In recent publications PLGA based NPs were successfully freeze dried with sucrose and glucose at a concentration of 20% (wt/v) [166]. A complete re-dispersion of poly(lactide acid-co-ethylene oxide) NPs after freeze drying could be obtained when trehalose was added to the NP suspension at a ratio of 1/1 (trehalose/PLGA, wt/wt) [163]. In the present study trehalose was revealed to be the optimal cryoprotectant reaching a complete re-dispersion only in a mixture with PVA. This can be explained by the ability of the PVA to attach on the NPs polymer surface by hydrophobic bonding [167]. This effect can be seen by the slightly increased size after freeze drying (Figure 3.1). Furthermore, it can be proposed that free PVA, which is not attached to the surface of the NPs, can act as stabilizer. The PVA avoids aggregation during freeze drying as it forms a glassy state at low temperatures [167]. Moreover, PVA forms hydrogen bonds from between the polymer and water molecules contributing a better re-dispersion [168].

In this thesis in a first step the DDS were developed (chapter 2) with regard to reproducibility and controllability of the fabrication processes and, therefore, quality of the DDS. Only the polymer was pre-selected due to its biodegradability and biocompatibility and with regard to the used drugs, CYA and BU, which is important for the encapsulation ability apart from the preparation method [90]. In contrast, studies often follow the approach to develop a DDS for a special API. Therefore, it was possible that the encapsulation in NPs or MPs failed for one or both APIs.

After encapsulation of the selected APIs, in our hands for CYA optimized loadings with high EEs could be determined for both carrier NPs (>67%) and MPs (>89%). In general, high EEs for CYA were also reported before, EE>96% for MPs [63] and EE>72% for NPs [64] for particles prepared by emulsion-diffusion-evaporation method.

The emulsion-diffusion-evaporation method contains a meta stable system - the emulsion itself - and was therefore not selected as preparation method.

In this work PLGA based CYA-NPs prepared by NPR for oral delivery by Chacón et al. showed EEs of 47.9% to 84.7% depending on the size (46 nm to 146 nm, respectively) and, hence, on the surface area of particles [162]. Interestingly, in the present study the EE could be increased without changing the size of the particles (Figure 3.2).

Barichello et al. determined with a loading of 0.33/10 an 87.3% EE of for CYA loaded NPs prepared by NPR [169], which was also determined for our lowest loading. This can be explained by the low solubility of CYA in aqueous media (~ 4µg/ml [162]) and distribution in the hydrophobic PLGA matrix due to the lipophilicity of CYA (Table 1.1). Therefore, a smaller amount of CYA could be more easily distributed in the carrier matrix. BU was successfully encapsulated into MPs (EE>91%), but for BU-NPs EE values <40% (Table 3.4) were determined for all tested ratios with a high intra batch variation.

The value of *in vitro* release tests is still under discussion due to limited power to predict the *in vivo* situation. Nevertheless, *in vitro* release tests demonstrate a useful research tool to estimate release kinetics and to compare between various samples and batches. The *in vitro* test might help to unravel the release mechanism, although the test conditions may not reflect the *in vivo* conditions and, thus, the release kinetics cannot directly transferred. In general, the release of APIs from DDS is driven by three main mechanisms: (a) swelling/ erosion, (b) diffusion, and (c) degradation [170]. PLGA based DDS show a biphasic release profile including a burst release followed by a sustained release [61]. Furthermore, the API is released as a function of solubility/lipophilicity and penetration of water into the polymer matrix [61]. In the present study, the release profiles from both carriers for each drug are different. In particular, the diffusion will be influenced by the lipophilicity of the BU and CYA (chapter 1, Table 1.1; BU: $\log P_{\text{octanol/water}}$ 3.2, CYA: $\log P_{\text{octanol/water}}$ 2.92) in the present work.

For CYA-NPs and CYA-MPs an improvement in the release compared to the recent studies in the context of the passive targeting approach was achieved [63], [64]. In addition, the CYA loaded MPs demonstrated the best controlled release profile ($91.3 \pm 4.4\%$ after 24 h), which could be classified as fast to intermediate release. Recently published studies demonstrated that the encapsulation of CYA in PLGA MPs leads to a release of weeks ending in 60% after 50 days [63]. Also for CYA loaded NPs a release over three weeks and more was reported [63].

In the present study the release from the MPs might be supported by the stabilizer and, furthermore, by the crystallization processes during MPs formation by spray drying, which may produce micro voids in the MPs and support water penetration [171]. This would also explain the faster release of CYA from the MPs in comparison to the release from CYA-NPs. Additionally, the results of the XRD studies (Figure 3.6) revealed that the CYA is in an amorphous state in the MPs and, therefore, molecularly dispersed [100], [172].

In contrast, the CYA-NPs (loading 4/10, CYA/PLGA, wt/wt) show a weak crystalline signal indicating that partially crystalline structures of CYA are located in the NPs. At higher drug loading (30%, wt/wt) a crystallization of APIs was reported explaining the crystalline content in the CYA-NPs [173]. Therefore, a reduced burst behaviour and a slow sustained release (Figure 3.8) occur as the release rate is controlled by the solubilisation of crystals.

The *in vitro* release profile of BU-NPs revealed a dramatic burst with 80% in 30 min for NPs in comparison to 40% for MPs, which indicates that the BU is more adsorbed at the surface or encapsulated at the outer edge of the NPs [61]. In previous studies BU loaded PLGA NPs so far showed a strong burst behaviour [67], which can be reduced depending on the method and used stabilizer [174]. A pH-dependent coating or blending of PLGA particles with methacrylate copolymers (Eudragit®S) can trigger the release depending on the pH [67], [83]. Nevertheless, also a relatively fast release (60% in 6 h [67] and 40% in 6 h [83]) was observed after reaching the pH to solubilize the methacrylate copolymer. In the present study ~40% of BU remains in the MPs after 48 h (Figure 3.8). For the BU-MPs it seems that some BU is encapsulated in the inner core of the particle. The rest is released by swelling of the particles and diffusion processes and, furthermore, degradation of the stabilizer, as the Span60 is dispersable in aqueous media [175]. Also the BU encapsulated in MPs was investigated to be in the amorphous state, which was also reported before for spray drying of BU [110], [176].

As the accumulation of particles is size-dependent and NPs are supposed to accumulate at a higher content, building a depot in the inflamed regions [75], a faster release of the encapsulated API in the MPs in comparison to NPs could be a benefit for the application as the MPs could be cleared faster from the lumen by the main symptom of IBD: diarrhea. Moreover, the DDS will stay in the inflamed areas only for a certain time-period due to e.g. the regeneration of epithelium. Alf Lamprecht et al. determined an accumulation of $14.5 \pm 6.3\%$ for 100 nm polystyrene NPs, which decreased after four, six and eight days to $9.1 \pm 2.8\%$, $3.4 \pm 2.2\%$ and $1.9 \pm 1.1\%$, respectively [75].

Therefore, the NPs should ideally have an intermediate to slow release, as presented by the CYA-NPs, to avoid high systemic concentrations and to release the drug in the inflamed areas. A too fast release would result in high systemic concentrations and, thus, side effects of the applied drug.

3.6. Conclusion

CYA had been successfully encapsulated into NPs and MPs leading to different release profiles, both promising for the passive targeting approach. Therefore, both CYA loaded DDS are most promising carrier with regard to the investigated physico-chemical and biopharmaceutical properties in this chapter, in detail higher encapsulation efficiencies and more controlled release.

BU was successfully encapsulated into MPs although ~40% of the BU remains in the DDS after 48 h. BU encapsulated in NPs leads to a high burst release as the BU supposed to be adsorbed at the particle surface. The high burst release could lead to high systemic concentrations when applied *in vivo*.

The difference in release can be explained by the amorphous or crystalline status of the API in the respective particles and the lipophilicity of the drugs.

In a next step the ability of the particles to accumulate size-dependently and their anti-inflammatory efficacy had been tested on a three-dimensional cell culture model in chapter 5.

4. Structural analysis and modification of spray dried microparticles

The author of the thesis made the following contributions to the chapter: Conceived, designed and performed experiments. Analysed and interpreted the data.

The SAXS analysis was kindly performed, designed and analysed by Prof. Dr. Andreas Thünemann at the Bundesanstalt für Materialforschung und -prüfung in Berlin. The author thanks Prof. Dr. Thünemann for his support.

4.1. Introduction

As reported in chapter 2 and chapter 3 a ratio of 1.1/1.6 (PLGA/Span60, wt/wt) is needed for a well dispersable spray dried formulation in the target size range. Thus, Span60 is a quantitative and qualitative significant part of the matrix system and this leads to the question of the location or spatial distribution of the Span60 in the DDS. Therefore, a small angle x-ray scattering (SAXS) study was performed to determine if the Span60 is homogeneously distributed throughout the particles, organized in cluster or only located at the surface of the MPs. In general, SAXS can be used to investigate the morphology, size and internal structure of particulate samples using a suitable set-up and with a limit of particle sizes <100 nm for screening the whole particle [177], [178]. The beam, which can go through the material, interacts with the electrons of the sample and is scattered. The detected scattering pattern is characteristic of the investigated structures. The intensity of the scattered radiation is measured in dependence of the scattering angle [93], [179].

In chapter 2 and chapter 3 the optimization of MPs with regard to size, size distribution and yield, and loading was discussed, respectively. In this part of the work one further attempt was to modulate the release from MPs, in particular for BU, with regard to a depot effect with controlled release (matrix controlled diffusion) over relevant time-period, when particles accumulate at the place of inflammation. According to the structure, the use of polyethylene glycol (PEG) should enable a more controlled and complete release of the encapsulated drug. The proposed mechanism is the swelling of PEG components in aqueous solutions, which create pores [61], [180], [181]. This effect was demonstrated for PEG-PLGA-block co-polymers and, moreover, for PEG blend PLGA particles (PEG-PLGA particles) [180], [181]. Furthermore, PEG can increase the hydrophilicity of DDS improving the swelling properties in aqueous media and supporting, therefore, the release [182].

Additionally, a lower molecular weight PLGA polymer was used to assess the effect of polymer length on the particle size. The aim was to further decrease the size of spray dried particles.

4.2. Materials

Excipients for NP and MP preparation and active ingredients were used as described in chapter 2.2 and chapter 3.2.

Resomer[®] Condensate RG, (lactic/glycolic (50/50, wt/wt); MW 2149 Da) was bought from Evonik (Darmstadt, Germany). Polyethylene glycol 1000 (PEG-1000, MW 1000 Da) was purchased from Sigma Aldrich (Schnelldorf, Germany). Purified water was of Milli-Q quality and prepared by a Millipore Milli-Q Synthesis system (Merck KGaA, Darmstadt, Germany).

All solvents were high-performance liquid chromatography grade and all chemicals met the quality requirements of the European Pharmacopoeia 6.0–7.3.

4.3. Methods

4.3.1. SAXS analysis

SAXS measurements were performed with a Kratky-type instrument (SAXSess from Anton Paar, Austria). The scattered intensities were recorded with a cooled (-40°C) CCD camera (PI-SCX, Princeton Instruments, USA) in the line collimation geometry and integrated into the one-dimensional scattering function $I(q)$ using SAXSQuant 1D software (Anton-Paar, Austria). Drug free MPs, as solid powder and in dispersion, pure PLGA and Span60 were measured to verify the signals. Aqueous solution (purified water) of the drug free MPs (blank MPs) with concentrations in the range of 1.0 to 2.0 g/l were poured into vacuum-tight thin quartz capillaries at room temperature and placed in a TCS 120 temperature-controlled sample holder. The temperature was held constant at 20°C. Background contributions from capillary and solvent scattering were subtracted from the sample scattering. The scattering vector q , defined as $q = 4\pi/\lambda \sin \theta$ where θ is the scattering angle and λ the wavelength of the radiation, varied in the 0.1 to 6.0 nm⁻¹ range. A 100 nm window was, therefore, investigated.

4.3.2. Modification of spray dried microparticles

4.3.2.1. Modification of *in vitro* release

For the modification of spray dried MPs PEG blend PLGA particles [181] were prepared. For this purpose PEG-1000 (MW 1000 Da, Sigma Aldrich, Germany) at a concentration of 5%, 10% and 20% (wt/wt) referring to the used amount of PLGA was used. To prepare the feeding solution 1.1% PLGA (wt/v) and 1.6% Span60 (wt/v) together with BU (loading 1/10, BU/PLGA, wt/wt; standard loading) were dissolved in acetone and stirred at least for 1 h. Afterwards PEG-1000 was added and the solution was stirred until everything was dissolved.

The feeding solution was sprayed as described in chapter 3.3.3. The experiment was performed at least in triplicate. The particles were compared to particles without PEG using the standard loading (1/10, BU/PLGA, wt/wt; standard loading). The morphology was investigated before and after incubation for 24 h in purified water at room temperature as described before by Cleek et al. by SEM imaging as described in chapter 2.3.7 [181].

All spray dried MPs, non-modified and modified, were characterized as described in chapter 3. All release studies were performed as described in chapter 3.3.8. The release was performed at least in triplicate and stopped after 24 h due to the resulting profile (Figure 4.2). The size and size distribution was measured by laser light diffraction as described in chapter 3.3.4. The EE of loaded MPs was determined as described in chapter 3.3.6.

4.3.2.2. Modification of size by spraying of low molecular weight PLGA

Particles were prepared with low molecular weight PLGA (Resomer[®] Condensate RG, MW 2149 Da) as described before in chapter 3.3.3 and compared to MPs produced with PLGA with a MW of 40,300 Da.

The size and size distribution were measured by laser light diffraction as described in chapter 3.3.4. The morphology was investigated by SEM imaging as described in chapter 2.3.7.

4.4. Results

4.4.1. SAXS analysis

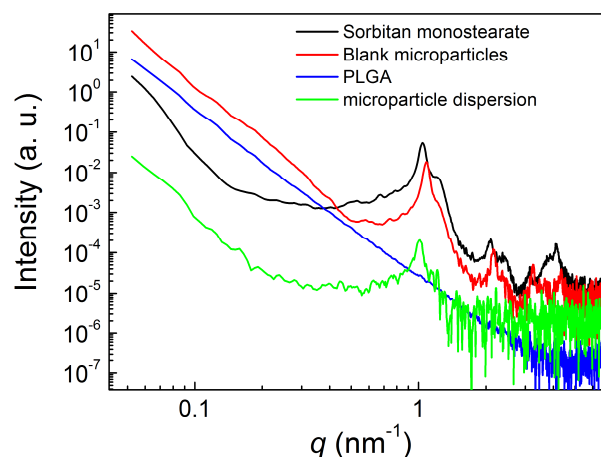


Figure 4.1. SAXS analysis of PLGA (blue line), Span60 (sorbitan monostearate, black line), drug free (blank) MPs as powder (red line) and blank MPs in dispersion (green line). The graph shows the scattered intensities referring to scattering vector q in nm^{-1} .

The SAXS intensities of sorbitan monostearate (Span60), PLGA and drug free MPs (size: $2.58 \pm 0.13 \mu\text{m}$, width: 0.92 ± 0.06), in dispersion and as powder are presented in Figure 4.1 as a function of the scattering vector. Both ingredients of the MPs give a representative signal. The signal of PLGA (blue line) shows a pattern which is typical for an amorphous substance [183]. That is the expected result for a spray dried polymer, as no crystalline signal was detected, and is in agreement with the XRD studies (chapter 3, Figure 3.6). The Span60 (black line) shows a typical peak at $1 \text{ q} (\text{nm}^{-1})$ [183]. The MPs measured in solid state (red line) show a shift of the Span60 signal towards higher $q (\text{nm}^{-1})$ values. No shift could be detected when particles were measured in dispersion (green line). The shift of the signal indicates that the Span60 is under tensions in the particles. The contact with the aqueous solution leads to a relaxation and, therefore, the peak of Span60 (green line) shows the same scattering vector as the pure Span60.

4.4.2. Modification of spray dried microparticles

Spray drying of PLGA particles with 5-20 % (w/w) of PEG-1000 for blending leads to PEG-PLGA particles with a size $3.1\text{-}3.5 \mu\text{m}$ for 5% and 10% of PEG, which is increased to $6.4 \mu\text{m}$ for 20% PEG. The spray dried MPs form a white, free flowing powder.

All results for size, size distribution, EE and yield were summarized in Table 4.1. High yields ranging between 72.1% and 78.5%, and also an expected high EE >95% could be achieved for a loading of 1/10 (BU/PLGA, wt/wt). The *in vitro* release profile of modified MPs is presented in Figure 4.2 and leads for all concentrations of PEG to a strong burst effect ranging from 67.9% (20% PEG) to 74.8% (5% PEG) released BU after 1 h. Overall, the cumulative amount of released BU within 24 h remains in the same range than for PLGA MPs without PEG modification at the loading of BU (1/10, BU/PLGA, wt/wt). Furthermore, ~25-32% remain in the PEG-PLGA MPs after 24 h, which is the same amount as for MPs without PEG. No improvement could be achieved with the modification.

Table 4.1. Size, size distribution, EE and yield of PEG-PLGA particles (n=4). Different PEG concentrations were used in the particles ranging from 5-20% referring to the used amount of PLGA. Data are presented as mean \pm S.D. (n=3).

formulation	PEG content	size [μm]	size distribution [width]	EE [%]	yield [%]
I	5%	3.1 \pm 0.15	3.6 \pm 0.80	96.84 \pm 0.10	75.6 \pm 4.5
II	10%	3.5 \pm 0.59	5.3 \pm 6.05	97.24 \pm 0.16	72.1 \pm 8.4
III	20%	6.4 \pm 5.33	3.6 \pm 2.21	95.57 \pm 0.54	78.5 \pm 6.7

PEG-PLGA particles were incubated 24 h in purified water to investigate a swelling behaviour according to Cleek et al. and visualized by SEM imaging [181]. SEM images of PEG-PLGA particles before incubation (Figure 4.3a) are spherical in shape, and have an uneven and rough surface. All other PEG concentrations show equal morphology in the SEM images. The surface seems to be wax like due to the PEG and Span60 (chapter 3, Figure 3.5). SEM images of PEG-PLGA particles incubated 24 h with purified water (Figure 4.3b) show no pore development. This might be due to the size of the particles with ~3-6 μm compared to the particles produced by Cleek et al. with ~64-92 μm . Due to the dispersibility of Span60 in water and the solubility of PEG punctual erosions (Figure 4.3b, marked with an \rightarrow) on the surface could be assumed. These erosions were only visible after incubation.

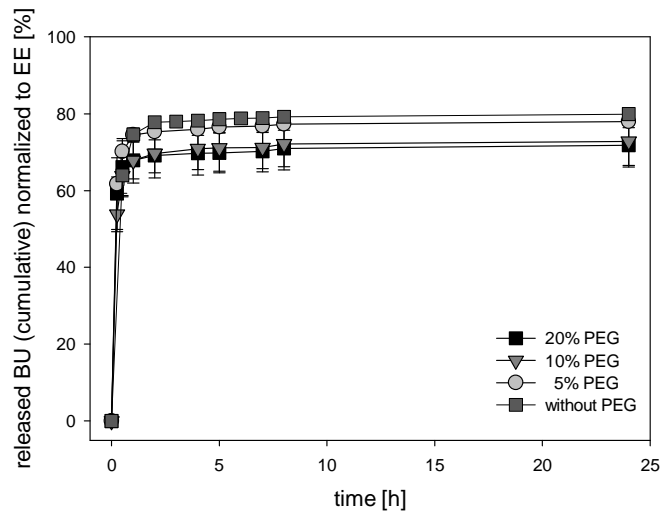


Figure 4.2. *In vitro* release profile of BU-MPs containing PEG at different concentrations (n=4) in comparison to BU-MPs without PEG (n=3). The loading was for all formulations 1/10 (BU/PLGA, wt/wt, standard loading). The values are presented as mean \pm S.D.

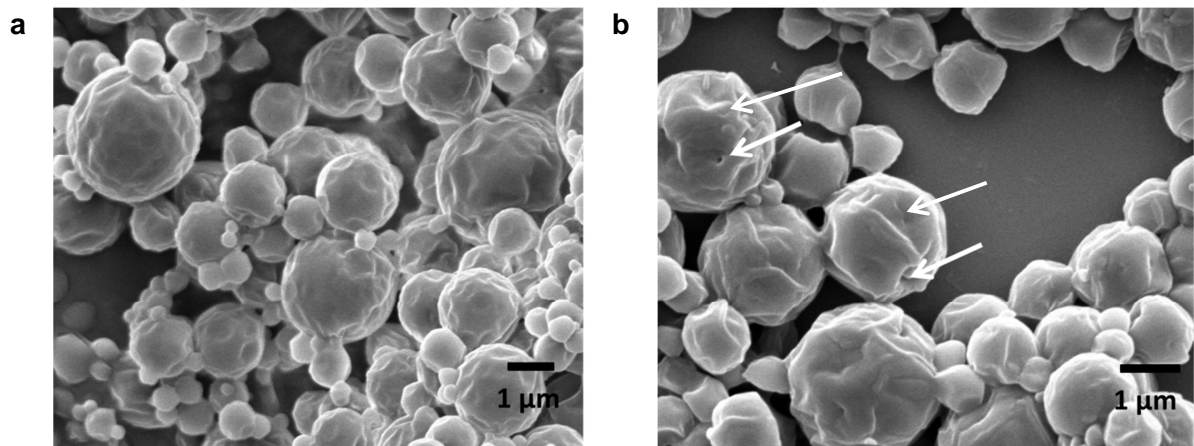


Figure 4.3. Representative SEM images of PEG-PLGA particles (containing 10% PEG). (a) PEG-PLGA MPs before incubation in purified water and (b) after incubation over 24 h in purified water according to Cleek et al. [181]. In (b) punctual erosions are visible and marked with a white arrow (\rightarrow).

To modify the size of the MPs with the aim to reach a reduction in size, the used PLGA (MW 40,300 Da) was exchanged to low molecular weight PLGA (MW 2149 Da). The spray drying process was successful and a white and free flowable powder could be collected. The results of size and size distribution as well as a visualization of particles are presented in Figure 4.4. No change in size was determined compared to the in chapter 2 optimized particles (Figure 4.4a). The particles are smooth and spherical in shape (Figure 4.4b).

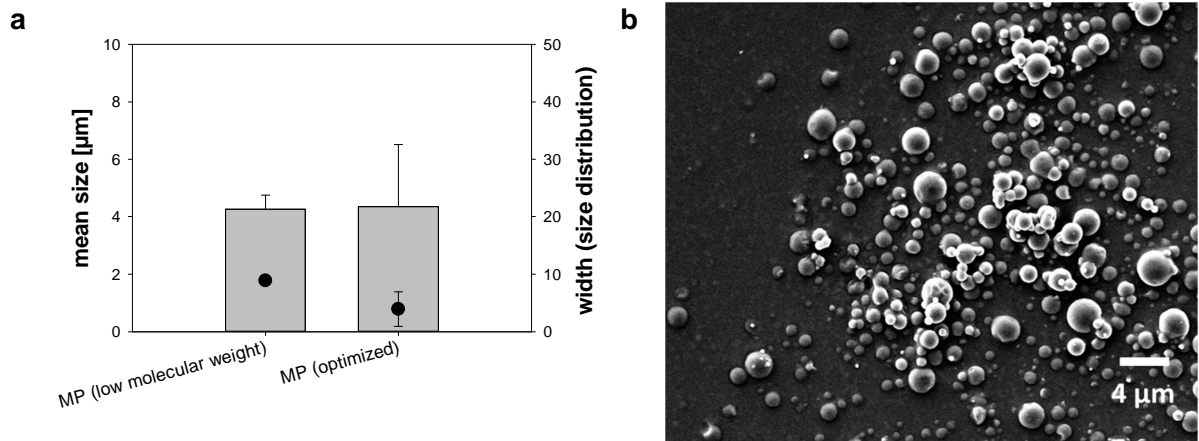


Figure 4.4. (a) Size (\Rightarrow) and size distribution (\bullet) of MPs produced with low molecular weight ($n=2$, mean \pm range) and optimized MPs ($n=3$, mean \pm S.D.). (b) Representative SEM image of MPs prepared with low molecular weight PLGA.

4.5. Discussion

The results from the SAXS measurement revealed a peak shift for the Span60 and, therefore, a tension in the particles could be concluded (Figure 4.1). With used SAXS method only a 100 nm window could be screened. To screen the complete particle a particle accelerator would be necessary, which makes the analysis of the whole particles very costly. However, the measurement supports the structural analysis. In an aqueous dispersion the MPs swell, due to the PLGA matrix (chapter 3.5) [170] or/and Span60 disperses [175] leading to a relaxation of the particles. From the results of the SAXS analysis it could be proposed that the Span60 is organized in clusters and not homogeneously distributed all over the particle due to the investigated tension and, therefore, peak shift. A homogeneous distribution would not lead to tensions in the MPs.

Spraying PLGA in combination with PEG and Span60 leads to no improvement of the total released amount of BU within 24 h as the profiles are comparable to the profile from MPs prepared without PEG. Furthermore, a strong burst release could be determined and ~25-32% remained in the particles after 24 h. A strong burst release was observed before for PEG blended PLGA MPs [181]. In general, the three basic mechanisms (a) swelling/ erosion, (b) diffusion, and (c) degradation are responsible for releasing the encapsulated API in polymeric DDS (chapter 3) [170]. PLGA based DDS show in general a biphasic release profile including a burst release followed by a sustained release [61].

The burst release is driven by API which is attached on the surface and, therefore, relatively fast in contact with the medium. Moreover, DDS prepared by spray drying have a more porous quality, compared to DDS prepared by classical physico-chemical methods (e.g. NPR) [182]. By modifying the MPs with PEG a matrix system based on PLGA, Span60 and PEG was fabricated. Due to the hydrophilicity of the PEG it can be suggested that in the fabricated MPs the PEG is not homogeneously distributed, but more clustered in the PEG-PLGA particles as also reported by Mu et al. [182]. This would also explain the punctual erosions in Figure 4.3. Furthermore, Cleek et al. explained that in a blending the release might be influenced by polymer chain entanglements between PLGA and PEG [181]. In the present study it can be assumed that the strong burst release of the encapsulated BU is also supported by the PEG. PEG is water soluble and will be re-dispersed in the release medium, forcing surface and bulk erosion/swelling. The supposed porous structure promote the release due to enhanced water penetration [181]. As the degradation of the used PLGA takes two to three month, the release of BU from the particles is due to drug diffusion and solubility/dispersibility of PEG and, furthermore, Span60 as discussed in chapter 3 [175]. Cleek et al. demonstrated that the initial burst effect could dependent on the PLGA/PEG blend ratio, which was not observed in the present study [181].

Additionally, the interaction between API and DDS, and the loading could influence the release [184]. Polakovic et al. demonstrated by mathematically modelled release profiles, that a slower release from high loaded PLGA particles (30%, wt/wt) is supported by API crystals [173]. At low loading the release rate is diffusion controlled [173]. The XRD studies (chapter 3, Figure 3.6) revealed that the BU in the MPs is in an amorphous state and, therefore, the release rate diffusion controlled.

The distribution of PEG in a block-co-polymer is more homogeneously compared to a blending. In a recent study a successful modification in release was demonstrated compared to particles produced only by PLGA, although the release was faster using the block-co-polymer [180].

MPs prepared with PLGA with a molecular weight of 2149 Da show no reduction in mean size (mean size ~ 4 μm) compared to MPs sprayed with PLGA of 40,300 Da. Reported before by Schafroth et al. a slight size reduction could be detected from 2.23 μm to 0.95 μm for spray dried CYA loaded PLGA MPs by using PLGA with 15,000 Da instead of 40,000 Da [100].

In chapter 2 the DOE revealed that the size is mostly affected by the stabilizer (for nature of stabilizer 38.91% of total variance, for concentration 6.74%) and depending on the interaction between polymer concentration/stabilizer (21.08%) shown in Table 2.10 in the present work. In the present experiments the polymer concentration was not changed. Therefore, it could be assumed that spraying low molecular weight PLGA will not influence the particle size, but may change the particle matrix. Hence, the influence of the Span60 (stabilizer) as component of the particles was also visible in these experiments.

4.6. Conclusion

SAXS analysis underlined the hypothesis that the stabilizer Span60 is organized not only at the particle surface but also in clusters in the MPs.

By blending the PLGA MPs with PEG no improvement in the release could be achieved for the present application approach. The use of PEG did not help to reduce the burst effect or to achieve a higher percentage in release of the encapsulated BU. 25-32% of the encapsulated BU remained in the particles.

No change in size was determined by spraying PLGA with lower molecular weight due to the strong influence of the used stabilizer on size in this study.

5. *In vitro* efficacy testing of PLGA particles on cell culture model of the inflamed intestinal mucosa

Parts of this chapter will be included in a manuscript for submission to a peer-reviewed journal:

Christina Draheim*, Julia Susewind*, Alexis Guillot, Brigitta Loretz, Steffi Hansen, Eva-Maria Collnot, Markus Limberger, Claus-Michael Lehr, *PLGA based nano- and microsized particles for inflammatory bowel disease therapy: evaluation of size-dependent accumulation and anti-inflammatory effect in an in vitro triple culture model*

*These authors contributed equally to this work.

The author of the thesis made the following contributions to the chapter: prepared nano- and microparticles, performed stability and characterization studies and contributed to the deposition studies by confocal laser scanning microscopy. Wrote the manuscript.

The three-dimensional cell culture model was established by Julia Susewind [118]. Julia Susewind further performed all cell culture experiments, measured TEER and IL-8 data, made confocal images, analysed all data from these experiments.

5.1. Introduction

Enteric cell lines, e.g. Caco-2, HT29 or T84, are accepted models of the normal, healthy intestinal mucosa [113], but cannot mimic the complex interactions with immune cells in the diseased intestine of IBD patients [114]. To test the anti-inflammatory efficacy and size-dependent accumulation of the nano- and microparticulate DDS, which development was reported in chapter 2 and optimization in loading in chapter 3, a three-dimensional cell culture model (triple culture model) of the inflamed intestinal mucosa was used. The triple culture model consists of three cell lines: Caco-2, THP-1, which can be stimulated via phorbol myristate acetate to macrophages, and MUTZ-3 a dendritic-like cells [118]. The usage of macrophages and dendritic cells as key players in inflammatory reactions is crucial for the inflammation stimulation and address the complexity of the pathogenesis in IBD.

The inflammation of the model is induced by addition of the pro-inflammatory cytokine IL-1 β . This cytokine was shown to lead to pathophysiological changes, which are in accordance with observed inflammation in the intestinal barrier in IBD patients e.g. IL-8 release, reorganization of tight junctions, and reduced epithelial barrier integrity [88]. These changes were also observed in the triple culture model using cell lines [118]. Therefore, the model can be used to evaluate effects of particulate DDS by monitoring decreasing TEER values, indicating reduced epithelial barrier integrity, and increased IL-8 release.

In this chapter CYA-NPs and CYA-MPs and, furthermore, BU-NPs and BU-MPs, all optimal loaded (chapter 3), were applied in the apical compartment of the triple culture model to simulate the application from the luminal side (oral/rectal administration). By loading the NPs and MPs with the far-red fluorescent dye DID, the size-dependent accumulation at the site of inflammation was investigated by confocal laser scanning microscopy (CLSM).

5.2. Materials

Excipients for NP and MP preparation and active ingredients were used as described in chapter 2.2 and chapter 3.2.

DMEM, RPMI1640 and α MEM cell culture medium were purchased from Gibco (Carlsbad, CA, USA). Fetal bovine serum (FBS), phosphate buffered saline (PBS), Penicillin/Streptomycin (Pen/Strep), non-essential amino acids (NEAA) and sodium pyruvate were obtained from PAA (Pasching, Austria).

Trypsin, ethylenediaminetetraacetic acid (EDTA) and phorbol myristate acetate (PMA) were purchased by Sigma (Steinheim, Germany). T75 flasks and 6 well cell culture plates were obtained from Corning Incorporated (Acton, MA, USA). IL-1 β was obtained from Promokine (Heidelberg, Germany). Purified water was of Milli-Q quality and prepared by a Millipore Milli-Q Synthesis system (Merck KGaA, Darmstadt, Germany).

All solvents were high-performance liquid chromatography grade and all chemicals met the quality requirements of the European Pharmacopoeia 6.0–7.3.

5.3. Methods

5.3.1. Preparation and characterization of API loaded nanoparticles and microparticles

The BU and CYA loaded NPs and MPs were prepared with an optimal loading as described in chapter 3.3.2 and chapter 3.3.3, respectively. Hence, for CYA a loading of 4/10 (CYA/PLGA, wt/wt) for both NPs (CYA-NP) and MPs (CYA-MP) was used. For BU a loading of 1/10 (BU/PLGA, wt/wt) was used for the NPs (BU-NP) and of 2/10 for the MPs (BU-MP).

Hydrodynamic diameter, polydispersity index (PDI) and zeta potential (ZP) of NPs were measured by laser light scattering as described in chapter 2.3.6 and chapter 3.3.4. The size and size distribution (width) of MPs were measured by laser light diffraction as described in chapter 3.3.4. The encapsulation efficiency (EE) was determined as described in chapter 3.3.6.

5.3.2. Preparation of DID loaded particles

The DID (1,1'-dioctadecyl-3,3,3',3'-tetramethylindodicarbocyanine perchlorate, Invitrogen, Life Technologies GmbH, Darmstadt, Germany; excitation maximum: 644 nm, emission maximum: 665 nm) loaded NPs (DID-NPs) and MPs (DID-MPs) were prepared as described in chapter 3.3.2 and chapter 3.3.3, respectively, for imaging the particles on the triple culture.

Nanoparticles

Briefly, for the DID-NPs the lipophilic DID was encapsulated following the described protocol in chapter 3.3.2. A DID stock solution (25 mg/ml, in ethanol) was directly added (10 μ l stock solution per 10 mg of PLGA) in the mixture of acetone/ethanol (16/3, v/v).

The DID-NPs could be separated from the stabilizer poloxamer 407 by a fast dialysis overnight (Spectra/Por[®] dialysis membrane, MWCO 300 kDa, Carl Roth GmbH & Co. KG, Germany) against purified water.

Microparticles

For imaging the particles on the triple culture model the lipophilic DID was encapsulated in the MPs following the described protocol in chapter 3.3.3. A DID stock solution (25 mg/ml, in ethanol) was directly added (10 µl stock solution per 10 mg of PLGA) to the feeding solution.

5.3.3. Characterization of DID loaded particles

5.3.3.1. Determination of size, size distribution and zeta potential

The DID-NPs were characterized in size and size distribution re-dispersed in purified water by NP tracking analysis using a NanoSight[®] LM10 HS system (NTA, NanoSight Limited, UK). The measurements were carried out for each batch in triplicate. The mean diameter (d 0.5) as well as the percentile values d 0.1 and d 0.9 were further calculated by the NanoSight[®] software. The size distribution (width) is defined in eq. 8. A narrow size distribution is indicated by a small width. A different system had to be used for the DID loaded particles as the 633 nm laser in the Zetasizer[®] could excite the DID. The emission would interfere with the laser light scattering measurement and falsify the measurement. The used NTA system was equipped with a 532 nm laser allowing the measurement without interference.

The ZP was measured in purified water using a Zetasizer[®] Nano ZS (Malvern Instruments, UK).

5.3.3.2. Determination of encapsulation efficiency

For determining the EE, the DID-NPs (~2-3 mg) were accurately weight and disintegrated in 5 ml acetonitrile for 1 h at 400 rpm. Afterwards, 5 ml of purified water was added and the solution stirred for 10 min to get a clear solution. The solution was placed for 15 min in an ultrasonic bath and then cool down to room temperature.

The spray dried DID-MPs (~3-5 mg) were disintegrated in 200 µl acetone. Afterwards, first 5 ml of acetonitrile were added dropwise followed by 5 ml purified water.

The fluorescence intensity of 100 µl of each solution was measured by plate reader (Tecan Infinite M 200, Tecan Deutschland GmbH, Crailsheim, Germany; excitation: 630 nm, emission: 674 nm) in triplicate. For the standards a stock solution (25 mg DID in 2.4 ml ethanol) was diluted with a mixture of acetonitrile/purified water (1/1, v/v) to standards with a concentration between 0.16 µg/ml - 5.2 µg/ml. The method was linear ($r^2 > 0.99$) between 0.16 µg/ml - 5.2 µg/ml with a calculated lower limit of detection (LOD) of 0.090 µg/ml and a LOQ of 0.091 µg/ml. All experiments were performed in triplicate.

5.3.4. Cell culture

For the set-up of the triple culture Caco-2 (a human adenocarcinoma cell line), THP-1 (a human monocytic cell line) and MUTZ-3 (a human monocytic cell line) cells were used.

Caco-2 clone HTB37, passage 30-50, was obtained from ATCC (American Type Culture Collection, Rockville, MD). Cells were cultured in DMEM supplemented with 20% FBS, 1% NEAA and 1% sodium pyruvate in a T75 flask and maintained at 37°C and 5% CO₂. This cell culture medium will be designed as Caco-2 medium. Medium was changed every second day and cells were sub-cultured once a week with 0.1% trypsin and 0.02% EDTA and 0.5x10⁶ cells were seeded in a new T75 flask.

THP-1 cells were purchased from DSMZ (Deutsche Sammlung von Mikroorganismen und Zellkulturen, Braunschweig, Germany) and cultured in RPMI1640 supplemented with 10% FBS under similar conditions as Caco-2 cells. The cell culture medium will be designed as THP-1 medium. To differentiate THP-1 to macrophage-like cells, THP-1 cells are incubated with cell culture medium that contains 5 ng/ml PMA. After 48 h cells are attached at the bottom of the T75 flask and can be harvested.

MUTZ-3 cells were purchased from DSMZ. Cells were cultured in a 6-well plate with αMEM supplemented with 20% FBS and 20% conditioned medium from 5637 cells. The cultivation of MUTZ-3 cells in conditioned medium differentiates them to dendritic-like cells. 5637 cells are human blastoma carcinoma cells, obtained from DSMZ. 5637 cells were cultured in RPMI1640 supplemented with 10% FBS in a T75 flask. Medium was collected every second day, filtrated and used as supplement for MUTZ-3 medium.

5.3.5. Set-up of triple culture and experimental design of efficacy studies

Caco-2, THP-1 and MUTZ-3 cells were used to set up a triple culture of the inflamed intestinal mucosa as previously developed [118], [119]. MUTZ-3 cells and differentiated THP-1 cells were collected and embedded in a bovine collagen type I (Advanced Biomatrix, Tucson, Arizona, USA) layer with human AB serum (Invitrogen, Wisconsin, USA). 150 μ l were pipetted in transwell filter inserts (Corning Incorporated, Acton, MA, USA, 0.4 μ m pore size, 1.12 cm² area). 10⁴ cells were seeded per cell type per well. The cells were incubated for 1 h at 37°C and 5% CO₂ until the collagen was solid. The Caco-2 cells were trypsinated, collected and 6x10⁴ cells were seeded on top of the collagen layer.

The experimental set-up is depicted in Figure 5.1. Triple culture was grown for 11 days with 500 μ l Caco-2 medium containing 1% Pen/Strep in the apical and THP-1 medium containing 1% Pen/Strep in the basolateral compartment. Medium was changed every second day. On day 11 cells were inflamed by adding 10 ng/ml of IL-1 β into the apical compartment for 48 h. After two days (day 13) IL-1 β was removed and cells were treated with CYA loaded DDS for 8 h at a concentration of 1.2 μ g CYA/ml, and with BU loaded DDS for 4 h at a concentration of 0.4 μ g BU/ml [119]. Therefore, the particles were re-suspended and diluted to the respective concentrations in Caco-2 medium.

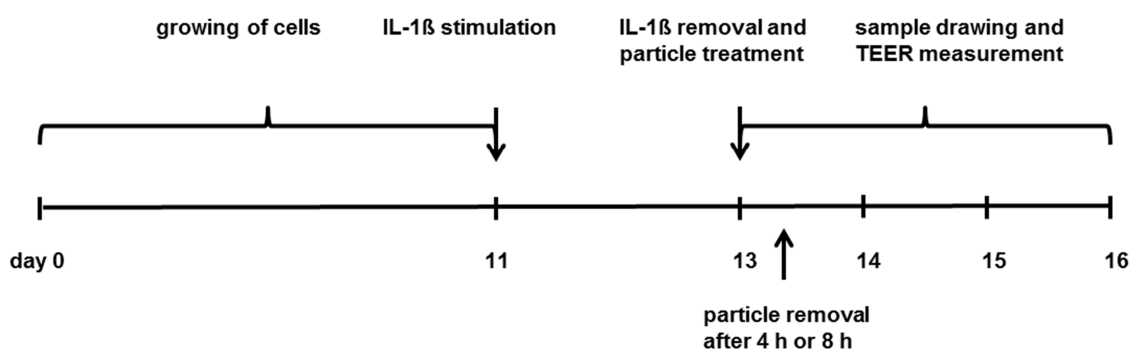


Figure 5.1. Experimental set-up of efficacy studies on triple culture model.

The concentrations were evaluated in tolerability and effectiveness before. Due to the different pharmacological mechanism of CYA, CYA was expected to act slower anti-inflammatory as BU. For that reason a longer time-period was chosen which was still physiologically relevant [23]. Both incubation times refer to transition times of oral formulations through the human intestine [23].

Based on the loading, DDS were applied on the following concentrations: CYA-NPs at ~13.5 µg/ml, CYA-MPs at ~7.6 µg/ml, BU-NPs at ~24.0 µg/ml and BU-MPs at ~5.2 µg/ml. All formulations were compared to a drug solution (stock solution: 1.2 µg CYA/ml, 0.4 µg BU/ml) and to drug free NPs or MPs at a concentration referring to the loaded particles. The drug solutions were prepared by dilution with Caco-2 medium from a stock solution in ethanol (CYA: 12 mg/ml, BU: 100 mg/ml). Afterwards, the formulations were removed, cells were washed with PBS and fresh cell culture medium was added. TEER values and IL-8 release were measured before, and 24 h, 48 h and 72 h after treatment with the drug loaded particles as can be seen in Figure 5.1. Each test group was performed with n=6.

5.3.6. Monitoring of triple culture during efficacy studies

To control the confluence of epithelial monolayer the TEER was measured with an electric voltohmmeter (EVOM, World Precision Instruments, Sarasota, USA) and chop stick electrodes. After inflammation TEER values decrease [185]. Recovery is indicated by an increase in TEER. For the experiments only triple cultures with TEER values $>400 \Omega \cdot \text{cm}^2$ at day 11 were used in order to show high enough barriers properties before the inflammation.

For the measurement of IL-8 level to determine the efficacy of the anti-inflammatory API [88], 50 µl supernatant from apical compartment were collected before applying the particles, and 24 h, 48 h and 72 h after application. The IL-8 amount was measured in the supernatant by CBA Flex set for IL-8 (BD Biosciences, Heidelberg, Germany) following protocol provided by the manufacturer. Measurement was performed via bead array analysis using a flow cytometer (FACS Calibur, BD Biosciences, Heidelberg, Germany) and the data were analysed by FCAP array v3.0.1 cytometric bead array analysis software.

5.3.7. Stability of nanoparticles and microparticles in triple culture media

Approximately 2 mg of drug free, CYA and BU loaded particles, NPs and MPs, were accurately weight and re-dispersed in 2.0 ml of Caco-2 or THP-1 medium. The particles were incubated for 24 h at 37°C shaking at 100 rpm in an incubator (GLF 3031, Germany). At pre-defined time points (0, 4, 8 and 24 h) 100 µl of the Caco-2 or THP-1 medium-particle suspension were diluted with purified water to 2 ml. The experiments were performed in triplicate. Hydrodynamic diameter and polydispersity index (PDI) of NPs were measured by laser light scattering as described in chapter 2.3.6.

The size and size distribution (width) of MPs were measured by laser light diffraction as described in chapter 3.3.4. An increase in size and size distribution would indicate the formation of aggregates and, therefore, instability.

The dilution in purified water is necessary to avoid light scattering of medium components e.g. proteins. The amount of particles was chosen according to the respective size characterization technique.

5.3.8. Investigation of cytotoxicity of nano- and microparticles on cells used for the triple culture

NPs and MPs should not show any toxic effects on the triple culture, hence, a cytotoxicity assay (LDH assay) was performed with the three different cell types (Caco-2, THP-1, Mutz-3), which were used in the triple culture model. The cells were seeded separately and incubated with different concentrations of NPs and MPs without any API for 24 h. For NPs concentrations between 6 mg/ml and 0.006 mg/ml were used and for MPs concentrations between 1.43 mg/ml and 0.00143 mg/ml. Different concentrations were due to the different loading of NPs and MPs. The highest concentration is e.g. equal to a concentration of 100 µg BU/ml applying loaded particles.

Different cell types were seeded separately in 96 well plates and grown for seven days. For Caco-2 cells 6×10^4 cells were seeded per well, for THP-1 and MUTZ-3 1×10^4 cells per well according to the triple culture set-up. Cells were incubated with different concentrations of NPs and MPs at 37°C and 5% CO₂. After 24 h 100 µl of the supernatants were collected and LDH reagents were prepared after manufacturer protocol (Roche, Mannheim, Germany). Cells were incubated with the reagent for 3 min at room temperature and the excitation was measured at 492 nm. Cell culture medium and 1% Triton X (v/v) were used as negative and positive control, respectively.

5.3.9. Deposition of nano- and microparticles on the triple cell culture model

To investigate the deposition of NPs and MPs on the inflamed triple culture model DID loaded particles were applied at the following concentrations referring to the concentrations of the loaded particles: NPs at ~13.5 µg/ml and MPs at ~7.6 µg/ml incubated for 8 h (CYA), and NPs at ~24.0 µg/ml and MPs at ~5.2 µg/ml incubated for 4 h (BU). The set-up of triple culture model and incubation of particles on the triple culture model were performed as described in chapter 5.3.5. The experiment was performed in triplicate

For the investigation of particle deposition the triple cultures were stained using anti-occludin antibody for the tight junctions and DAPI for the nucleus. Cells were fixed with 3% paraformaldehyde for 30 min at room temperature and incubated with 50 mM NH₄Cl for 10 min. After removal of NH₄Cl, cells were incubated at room temperature for 30 min with 1% BSA and 0.05% Saponin in PBS. The primary antibody (monoclonal mouse anti-occludin, Zymed, San Francisco, CA, USA) was diluted 1:200 in PBS and incubated with the cells at 4°C overnight. The cells were washed with PBS and incubated with the secondary antibody (Alexa488 anti-mouse, LifeTechnologies, Darmstadt, Germany) for 1 h at room temperature. After washing with PBS, cells were incubated with DAPI (100 ng/ml) for 15 min and mounted with fluorescence mounting medium (DAKO Glostrup, Denmark) on object slides.

Images were taken with a confocal laser scanning microscope (CLSM, LSM 150, Zeiss, Göttingen, Germany) and processed with Zen 2012 software (Zeiss, Göttingen, Germany). DID was detected in the red spectral region (laser excitation: 633 nm, emission: 647-695 nm), Alexa488 was detected in the green spectral region (laser excitation: 488 nm, emission: 506-544 nm) and DAPI was detected in the blue spectral region (laser excitation: 405 nm, emission: 434-487 nm).

5.3.10. Statistical analysis

The statistical analysis was performed by one way ANOVA followed by Holm-Sidak multiple comparison using Sigma Plot 12.5 software (Systat Software GmbH, Erkrath, Germany).

5.4. Results

5.4.1. Characterization of nano- and microparticles

The physico-chemical characterization of NPs and MPs used for studies on the triple culture model were summarized in Table 5.1 for NPs and in for MPs Table 5.2, and confirmed the characterization in chapter 3.

Table 5.1. Physico-chemical characterization (size, size distribution, zeta potential, EE and API content in final formulation) of NPs used for studies on triple culture model. The values are presented as mean \pm S.D. (n=3).

formulation	size [nm]	PDI	zeta potential [mV]	EE [%]	API in final formulation [μ g/mg]
drug free NP	149.8 \pm 2.2	0.020 \pm 0.010	-29.2 \pm 1.3	-	-
CYA-NP	142.1 \pm 0.7	0.050 \pm 0.037	-20.1 \pm 0.7	62.4 \pm 4.3	96.36
BU-NP	137.3 \pm 0.4	0.009 \pm 0.010	-26.7 \pm 1.5	36.0 \pm 2.1	16.67
formulation	size [nm]	width	zeta potential [mV]	EE [%]	API in final formulation [μ g/mg]
DID-NP	144.7 \pm 7.8	0.81 \pm 0.14	-21.8 \pm 1.1	68.3 \pm 11.9	2.57

Table 5.2. Physico-chemical characterization (size, size distribution, EE and API content in final formulation) of MPs used for studies on triple culture model. The values are presented as mean \pm S.D. (n=3).

formulation	size [μ m]	width	EE	API in final formulation [μ g/mg]
drug free MP	3.45 \pm 0.03	1.45 \pm 0.06	-	-
CYA-MP	4.14 \pm 0.63	2.35 \pm 0.86	96.2 \pm 4.6	132.90
BU-MP	6.45 \pm 0.26	1.71 \pm 0.03	101.5 \pm 1.2	76.34
DID-MP	3.95 \pm 0.13	2.78 \pm 0.10	103.3 \pm 0.6	3.00

5.4.2. Stability of nanoparticles and microparticles in triple culture media

The anti-inflammatory efficacy of the drug free (blank) and API loaded NPs and MPs with optimal loading were tested in a triple culture model of the inflamed intestine. Therefore, the stability according to size and size distribution was tested by incubating the particles in the two culture media (Caco-2- and THP-1-medium), which were previously defined (chapter 5.3.4 and 5.3.5) and are used in the triple culture model. The results for size and size distribution were summarized in Figure 5.2 for NPs and in Figure 5.3 for MPs.

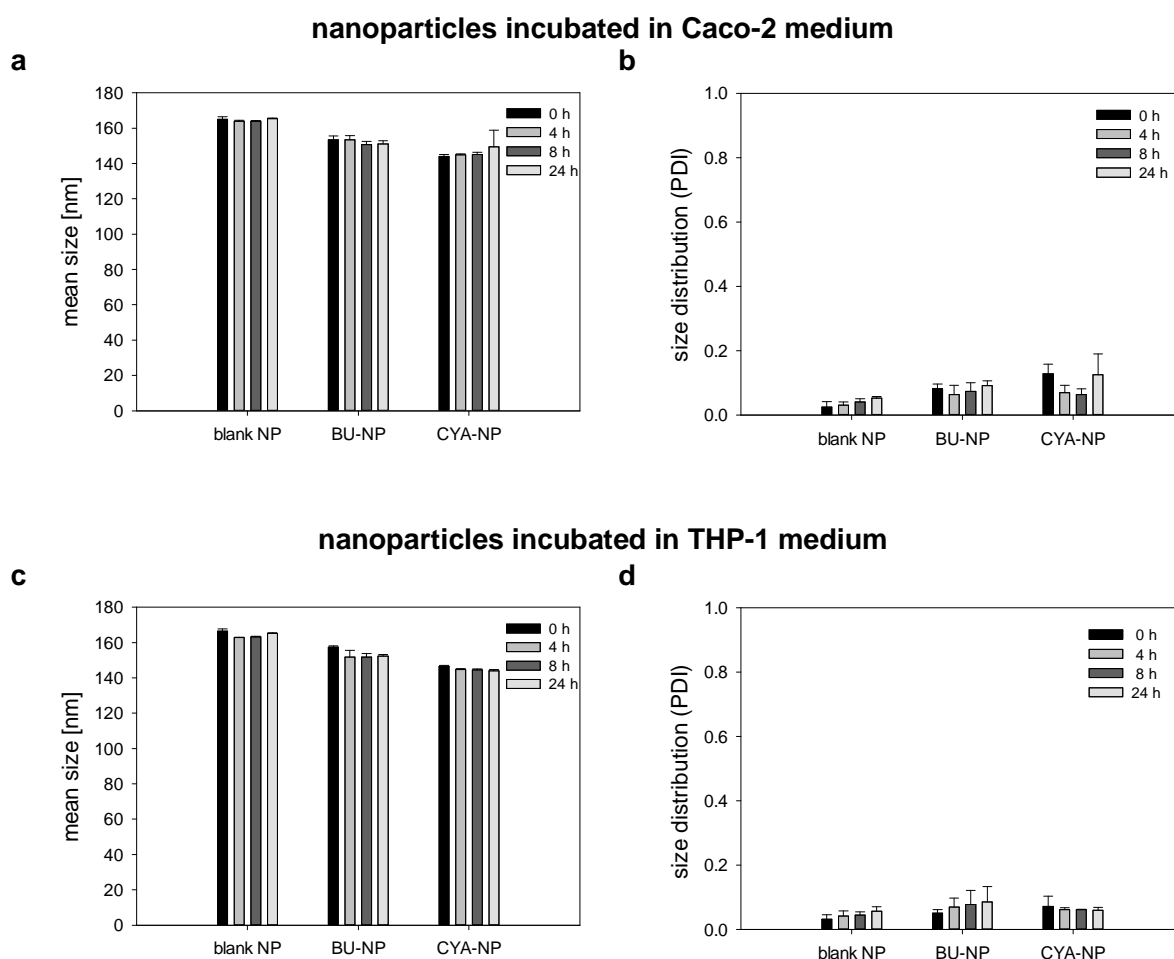


Figure 5.2. Stability (according to size and size distribution) of drug free (blank) NPs, CYA-NPs and BU-NPs in triple culture media at different time points: (a) size and (b) size distribution of NPs incubated in Caco-2 medium and (c) size and (d) size distribution of NPs incubated in THP-1 medium. The size and size distribution were measured by dynamic light scattering. The results were presented as mean \pm S.D. (n=3).

All NPs were stable over 24 h. No significant changes in size or size distribution were determined in both cell culture media. In Caco-2 medium also no aggregation of the MPs was determined by increasing size or size distribution. In the THP-1 medium the size and size distribution increased for all MPs, drug free and loaded after 24 h. From t_{0h} to t_{4h} the size of the MPs decreased in different values, in particular in the Caco-2 medium, possibly due to the Span60 in the composition, which may disperses [175].

All formulations are stable enough for evaluation in the triple culture model as the incubation times are set to 4 h for BU loaded and 8 h for CYA loaded particles (chapter 5.3.5).

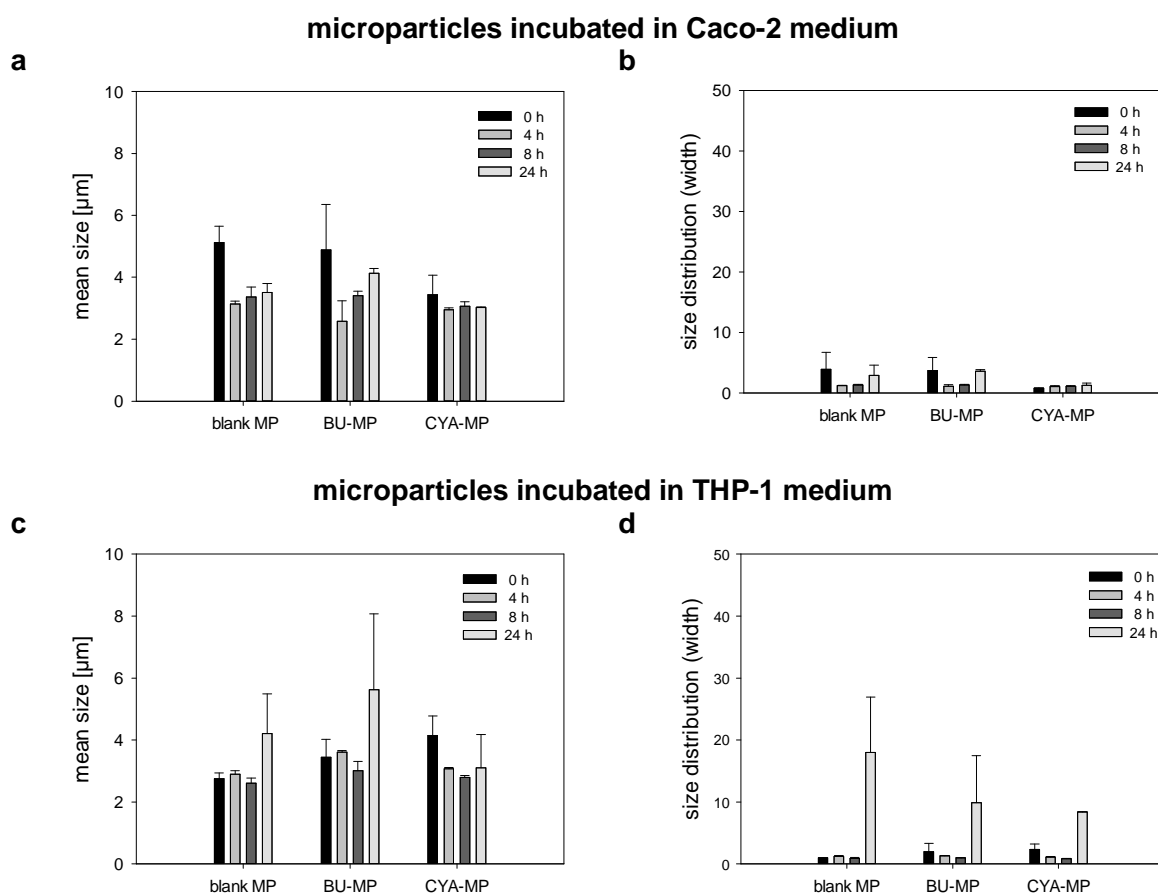


Figure 5.3. Stability (size, size distribution, zeta potential, EE and API content in final formulation) of drug free (blank) MPs, CYA-MPs and BU-MPs in triple culture media at different time points: (a) size and (b) size distribution of MPs incubated in Caco-2 medium and (c) size and (d) size distribution of MPs incubated in THP-1 medium. The size and size distribution were measured by laser light diffraction. The results were presented as mean \pm S.D. (n=3).

5.4.3. Investigation of cytotoxicity of nano- and microparticles on cells used for the triple culture

The results of the cytotoxicity assay on Caco-2, THP-1 and MUTZ-3 cells are summarized in Figure 5.4. For further experiments it was important that the tested concentrations of the DDS were in a non-toxic range. NPs show 40% toxicity at the highest tested concentration (~6 mg/ml) for THP-1 and MUTZ-3 cells (Figure 5.4a). MPs do not show any toxic effect on the three cell types in the tested concentrations (Figure 5.4b). In general, Caco-2 cells are more robust than the monocytic cell lines.

For both NPs and MPs no toxicity in the used concentrations for the triple culture experiments was determined. On the triple culture model, depending on the loading, CYA-MPs were applied at concentrations of $\sim 7.6 \mu\text{g/ml}$, CYA-NPs at $\sim 13.5 \mu\text{g/ml}$, BU-NPs at $\sim 24.0 \mu\text{g/ml}$ and BU-MPs at $\sim 5.2 \mu\text{g/ml}$.

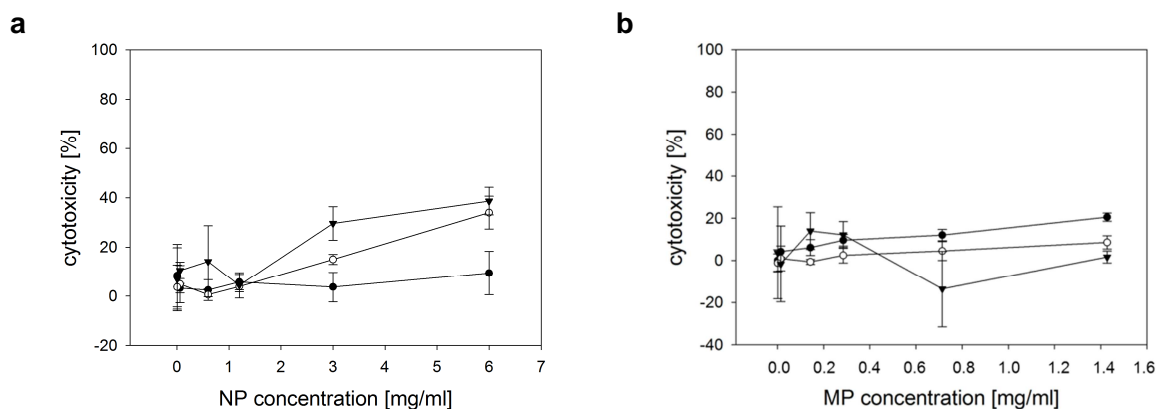


Figure 5.4. Results of cytotoxicity assay (LDH assay) for (a) NPs and (b) MPs incubated with Caco-2 (●), THP-1 (○) and MUTZ-3 (▲) cells at different concentrations. The results were presented as mean \pm S.D. (n=3).

5.4.4. Efficacy studies of budesonide loaded nano- and microparticles on triple culture

The results of the TEER measurement following BU-NPs and BU-MPs incubation were summarized in Figure 5.5 and results for determined IL-8 values in Figure 5.6. The results were compared to an uninfamed and an inflamed triple culture as controls, furthermore, to free BU solution and drug free (blank) NPs and MPs.

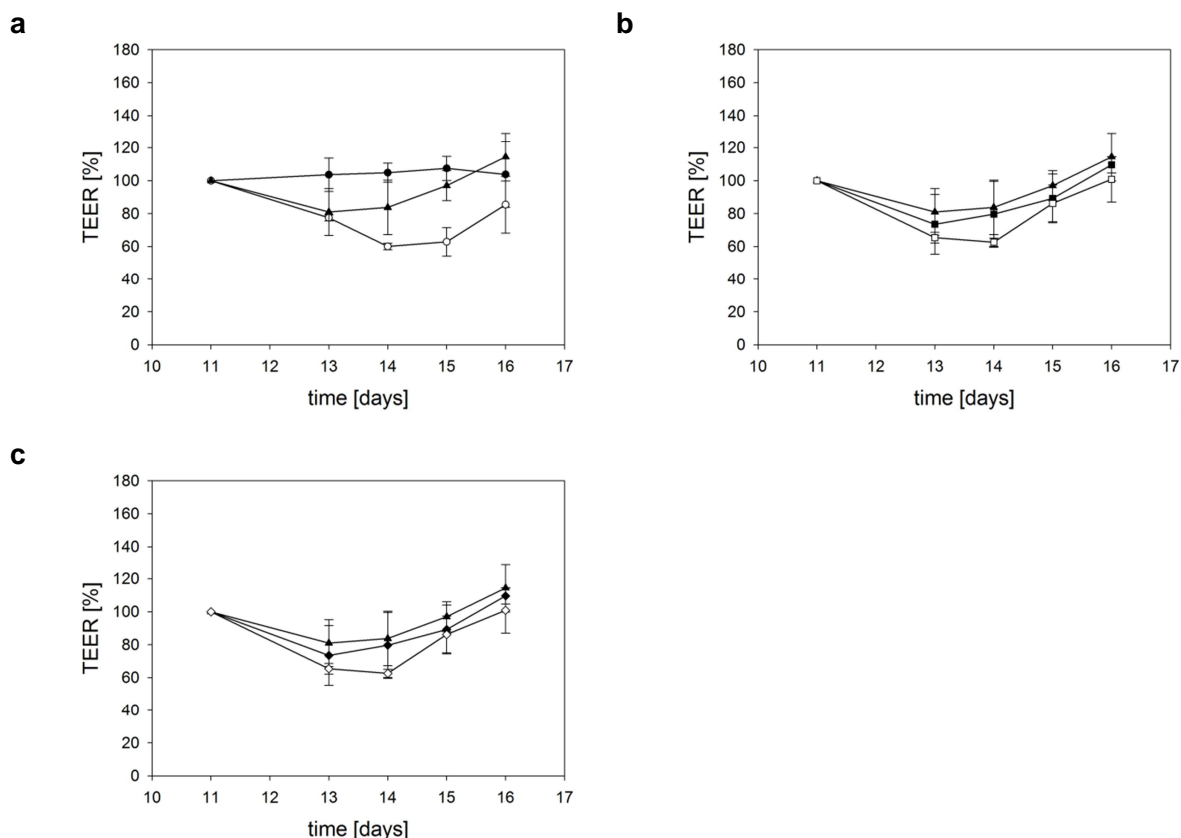


Figure 5.5. TEER measurement during triple culture experiments: (a) inflamed control (○), uninflamed control (●) and free BU solution (▲); (b) blank NP (■), BU-NP (□) and free BU solution (▲); (c) blank MP (◆), BU-MP (◇) and free BU solution (▲). Treatment according to Figure 5.1: Inflammation started at day 11 by addition of IL-1 β , which was removed at day 13. Treatment was started on day 13. The results were presented as mean \pm S.D. (n=6).

The treatment with BU solution and BU loaded DDS leads to an increase in TEER values back to the level before the inflammation (Figure 5.5b and Figure 5.5c). That indicates a closing of the tight junctions between the Caco-2 cells, which were opened through inflammation. In comparison to Figure 5.5a, the uninflamed control show also an increase in TEER, which is more slowly than the treated samples and need more than three days to fully recovered. Surprisingly, drug free NPs and MPs show also increasing TEER values (Figure 5.5b and Figure 5.5c).

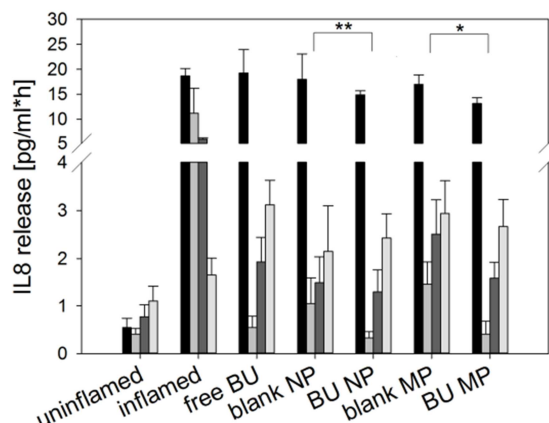


Figure 5.6. IL-8 release after treatment of the triple culture model with drug free (blank) NPs and MPs and BU-NPs and BU-MPs in comparison to BU solution in the apical compartment at different time points. (■ 0 h, ▒ 24 h, ▓ 48 h, ◻ 72 h after treatment). The results were presented as mean \pm S.D. (n=6; ** = $p < 0.001$, * = $p < 0.05$ are considered to be significant).

The IL-8 levels decreased after treatment with BU-NPs and BU-MPs (Figure 5.6) in comparison to inflamed control. The level of uninflamed control is reached after 24 h. Also the application of the drug free particles decreased the IL-8 levels. A significant difference in the IL-8 release was determined for the BU-NPs ($p < 0.001$) and BU-MPs ($p < 0.05$) compared to drug free NPs and MPs, respectively, at 24 h after treatment. In comparison, the inflamed control shows that IL-8 is decreasing more slowly when cells remain untreated (Figure 5.6). For all treated groups IL-8 levels increasing slowly at 48 h and 72 h after treatment.

5.4.5. Efficacy studies of cyclosporine A loaded nano- and microparticles on triple culture

The results of efficacy experiments with the CYA-NPs and CYA-MPs were summarized in Figure 5.7 for TEER values and in Figure 5.8 for determined IL-8 level. The results were compared to an uninflamed and an inflamed triple culture as controls, furthermore, to free CYA solution and drug free (blank) NPs and MPs.

The TEER values determined for the CYA loaded particles are in accordance with the results revealed for the BU loaded particles. CYA solution as well as CYA-NPs and CYA-MPs lead to a recovery of the TEER values (Figure 5.7b and Figure 5.7c). Drug free (blank) NPs and MPs show also increasing TEER values (Figure 5.7b and Figure 5.7 c).

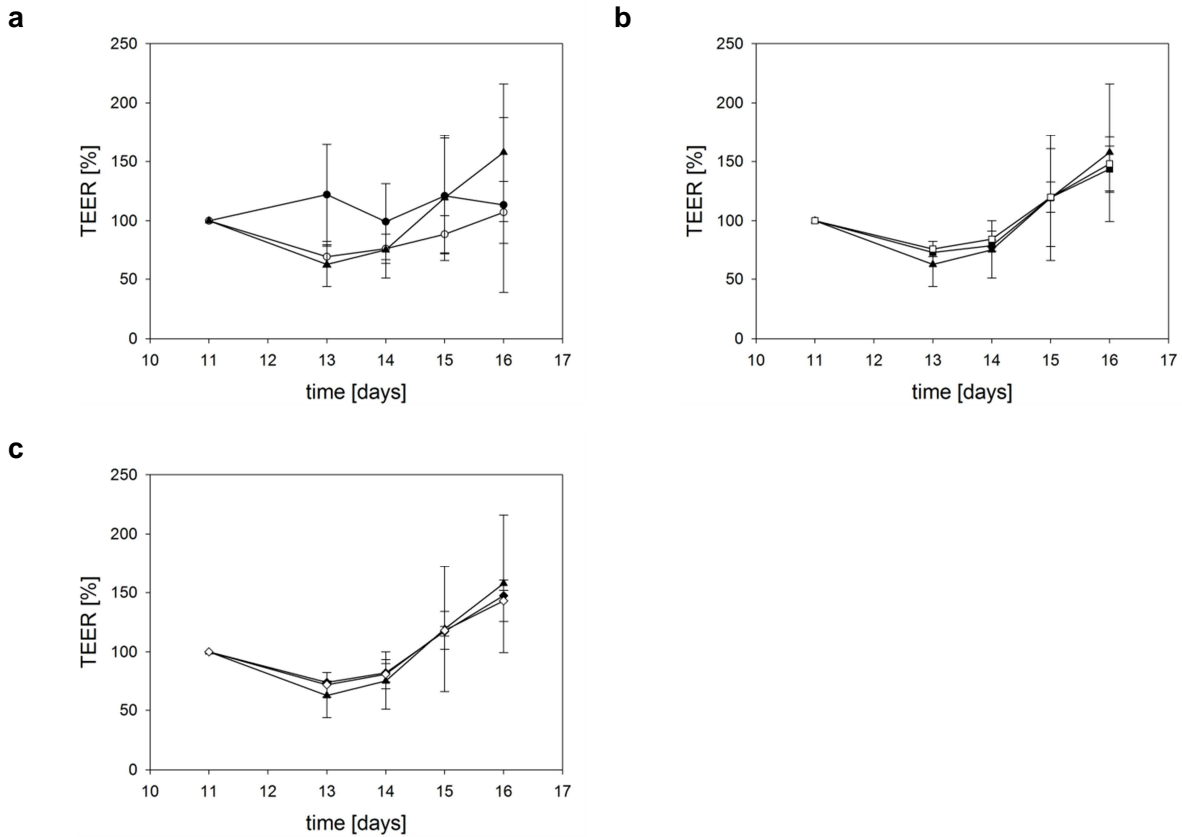


Figure 5.7. TEER measurement during experiments: (a) inflamed control (○), uninflamed control (●) and free CYA solution (▲); (b) blank NPs (■), CYA-NPs (□) and free CYA solution (▲); (c) blank MPs (◆), CYA-MPs (◇) and free CYA solution (▲). Treatment according to Figure 5.1: Inflammation started at day 11 by addition of IL-1 β , which was removed at day 13. Treatment was started on day 13. The results were presented as mean \pm S.D. (n=6).

The results of IL-8 measurement (Figure 5.8) reveal an anti-inflammatory effect with CYA-NPs and CYA-MPs. The IL-8 release decreased after treatment with the different formulations. A significant difference in the IL-8 release was determined for the CYA-NPs ($p < 0.001$) and CYA-MPs ($p < 0.05$) compared to drug free NPs and MPs at 24 h after treatment. Furthermore, a significant difference between pure CYA solution and CYA-NPs was determined. The increase of IL-8 after 48 h and 72 h was equal to the uninflamed control.

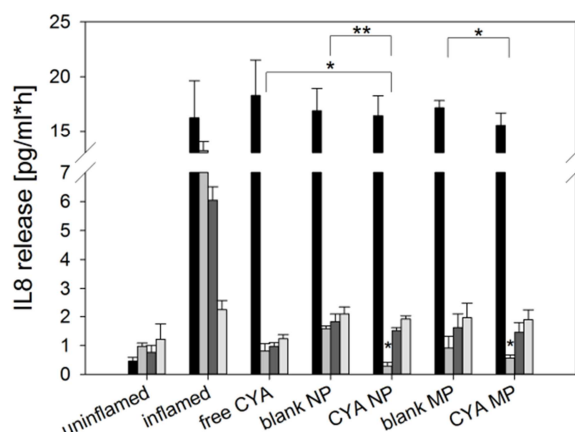


Figure 5.8. IL-8 release after treatment of the triple culture model with drug free (blank) NPs and MPs and CYA-NPs and CYA-MPs in comparison to CYA solution in the apical compartment at different time points (■ 0 h, ▒ 24 h, ■ 48 h, □ 72 h after treatment). The results were presented as mean \pm S.D. (n=6; ** = $p < 0.001$, * = $p < 0.05$ are considered to be significant).

5.4.6. Deposition of nano- and microparticles on the triple cell culture model

The inflamed triple culture model was treated with DID-NPs and DID-MPs to investigate the accumulation of particles. Confocal images in Figure 5.9 showed that NPs as well as MPs were located and stick on top of the triple culture on the Caco-2 cells, although the cells were washed several times after incubation with the particles. In Figure 5.9a and Figure 5.9c the z-stack demonstrated that the signal from the NPs is located in the Caco-2 monolayer. Therefore, it could be assumed NPs were up-taken by Caco-2 cells. Examples were marked with an arrow (\rightarrow). Moreover, NPs were detected at the intercellular space.

The MPs in Figure 5.9b and Figure 5.9 d were distributed over the cell borders (tight junctions staining in green) and stick on top of the Caco-2 cells, which was expected due to their bigger size.

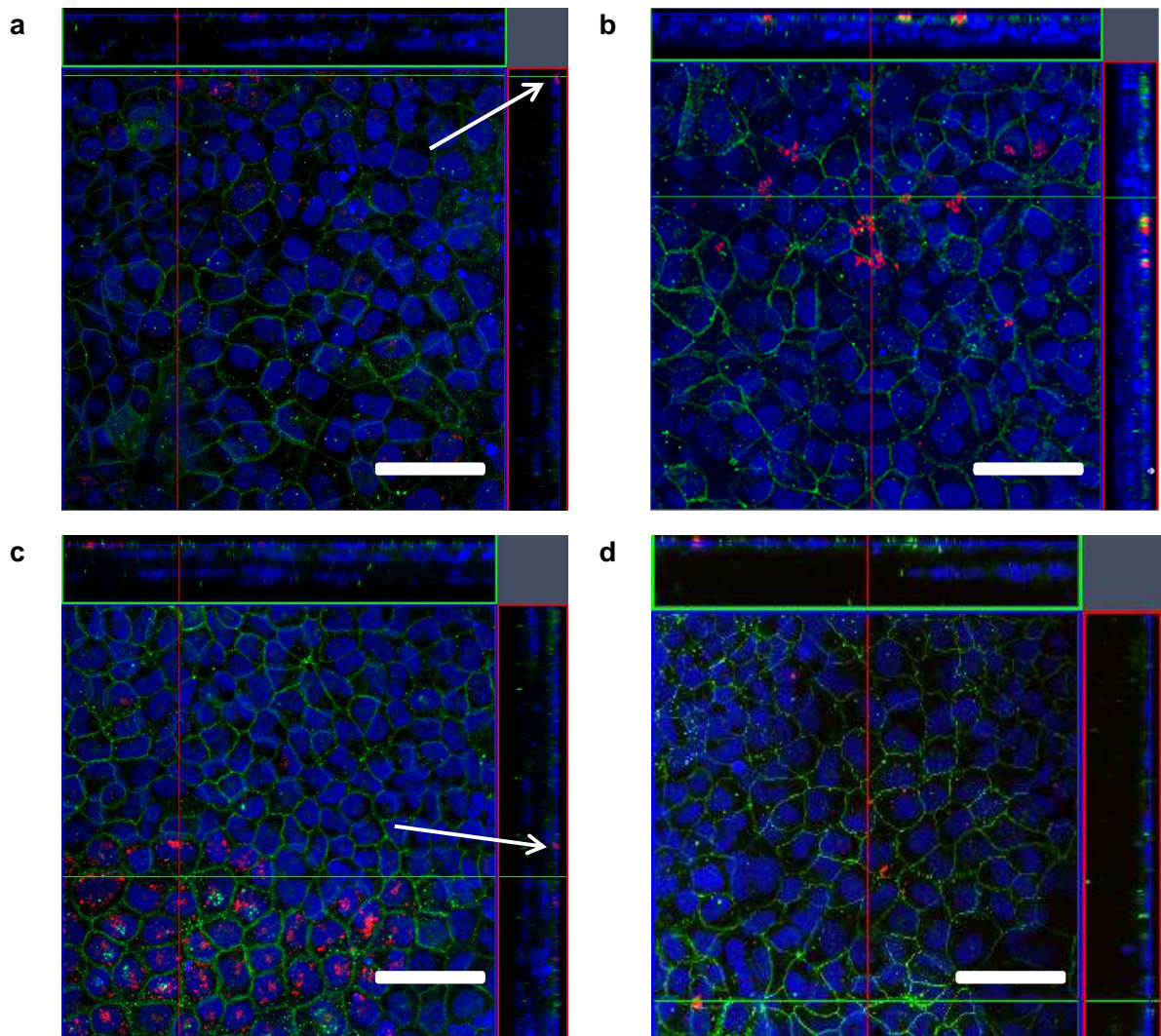


Figure 5.9. Deposition of particles on triple culture model: Representative CLSM images of the inflamed triple culture model incubated with DID-NPs and DID-MPs in the apical compartment. On top and at the right side z-stacks are shown (position marked by red and green line). (a) Shows DID-NPs and (b) DID-MPs referring to the used CYA concentration, (c) DID-NPs and (d) DID-MPs referring to the used BU concentration. Images were randomly selected. (scale bar=50 μ m; \rightarrow NPs assumed to be up-taken in Caco-2 cells; blue: DAPI stained nuclei, green: tight junctions stained with anti-occludin antibody, red: DID loaded particles).

5.5. Discussion

A triple culture model consisting of intestinal epithelial cells and immune competent cells was used to evaluate the anti-inflammatory effect as well as the size-dependent accumulation of the developed DDS. Two independent read outs, the TEER values and the IL-8 level, allowed to determine the anti-inflammatory efficacy of the particulate DDS. Nevertheless, the TEER measurement showed fluctuations and was demonstrated to be a less robust parameter of the used model. The triple culture model shows a self-healing process after removal of IL-1 β , which can be monitored by a recovery of the TEER in the inflamed control compared to the uninflamed control (Figure 5.5 and Figure 5.7) [119]. Therefore, the self-healing process limits the timeframe for testing the particles on the triple culture model.

All loaded DDS showed anti-inflammatory effects, detectable via both markers, with a faster recovery of the TEER values compared to the uninflamed control. Interestingly, also for the drug free DDS an anti-inflammatory effect measured by TEER values and IL-8 level was determined, which was already observed in earlier studies with the triple culture model [119]. Additionally, Beloqui et al. determined an anti-inflammatory effect of drug free pH-sensitive PLGA/Eudragit[®]S 100 NPs in a murine DSS-induced colitis model [77]. It can be assumed, according to Leonhard et al., that soluble signaling parameters in the inflammatory cascade of IL-8 could be adsorbed on the particle surface [119]. Furthermore, it was hypothesized that drug free particles could interact with immune cells and lead to a pre-occupation of the immune system [119]. A theory which has yet to be confirmed [119]. In addition, a recent study could demonstrate that lactate released from PLGA accelerates wound healing, including an anti-inflammatory effect, applied as subcutaneous implant or as NPs in different mice wound models [186], [187].

BU-NPs and BU-MPs both showed similar effects in comparison to BU solution on the IL-8 level. The BU-NPs release nearly 100% of the encapsulated BU in 4 h of incubation time and, hence, a similar effect could be expected. In contrast, the BU-MPs release 58% in 4 h in PBS (chapter 3, Figure 3.8).

The CYA loaded NPs and MPs reduce the IL-8 level slightly more after 24 h in comparison to the BU loaded DDS with less increased values after 72 h. For the CYA-NPs a significant effect, in comparison to CYA solution, could be determined. The release from the CYA-NPs is characterized by a low burst release with ~14.0% after 1 h, followed by a very slow sustained release with ~28% after 8 h (chapter 3, Figure 3.8). The CYA-MPs, which release 86% in 8 h, also showed a reduced IL-8 level, which was not significant compared to drug solution.

Therefore, in particular for the BU-MPs, CYA-NPs and CYA-MPs, an additive effect of API and carrier can be assumed for improving the anti-inflammatory efficacy. Additive effects were reported before and can be material dependent [187] or due to the accumulation on the triple culture model in combination with a controlled sustained release [119].

After the incubation of the different formulations the medium was changed and, hence, free drug also released from the DDS was removed.

The main advantage of the particulate formulations in comparison to the drug solution is that they remain on the triple culture as revealed by the CLSM images (Figure 5.9). According to the loading the triple culture model was incubated with different concentrations of NPs and MPs. Unfortunately, a quantitative analysis of the amount of remaining particles was not possible within the used technique, but could be interesting for further investigations. Nevertheless, it can be proposed that the remaining particles release the residual encapsulated drug leading to the prolonged anti-inflammatory effect. Additionally, from the CLSM images an up-take of the NPs in Caco-2 cells could be noted. Recent studies confirm this effect demonstrated with 15 nm gold NPs [118] and 183 nm PLGA NPs [71]. Furthermore, MPs were detected at the cell walls and NPs, independently of the loading, at the intercellular space indicating a size-dependent accumulation/deposition. Trough inflammation with IL-1 β the tight junctions between the Caco-2 cells open due to lower expression of tight junction proteins ZO-1 and occluding [188]. The pores of the open tight junctions, which are between 58-104 nm, are too small to be passed by the used DDS [189]. However, the inflammation leads to intercellular spaces in which particles can accumulate [119].

5.6. Conclusion

The anti-inflammatory effect and, furthermore, the deposition of the optimized NPs and MPs could be successfully tested on the triple culture model consisting of three cell lines (enterocytes, macrophages and dendritic-like cells) using TEER and IL-8 measurement as meaningful markers for inflammation. Therefore, the method offers an easier selection of the most suitable formulations for progression to *in vivo* efficacy studies (chapter 7).

All carrier, interestingly also the drug free DDS, lead to an anti-inflammatory effect with regard to investigated parameters, which were improved compared to the inflamed control. Furthermore, an improvement in the parameters was determined for the loaded DDS

compared to drug free DDS, and to the free drug solution. In particular, for the CYA-NPs significantly reduced IL-8 level could be determined in comparison to CYA solution.

NPs were deposited at the intercellular space and up-taken in Caco-2, whereas MPs were detected at the cell walls indicating a size-dependent accumulation/deposition. It can be concluded that the deposited particles release the residual encapsulated drug leading to the prolonged anti-inflammatory effect.

Based on tested parameters, CYA-NPs seem to be the most effective formulation on the triple culture. The model revealed the effects less time-consuming and less expensively compared to *in vivo* studies in rodent models and, especially without using animals.

6. Investigation of cytotoxicity and immunotoxicity

The following authors contributed to this chapter:

Anne-Claude Couffin, Frédérique Mittler and Fabrice Navarro (CEA Grenoble, LETI, MINATEC Campus, Grenoble, France) designed, performed and analysed the cell viability assay posed under chapter 6.2.2.

Christian Villiers and Patrice Marché (Centre Recherche U823 INSERM-University Grenoble, France) designed, performed and analysed the activation of complement system and the activation or suppression of cytokine secretion of dendritic cells as posed under chapter 6.2.3, chapter 6.2.3.1 and chapter 6.2.3.2.

The author of the thesis contributed to the design of the experiments, interpreted and discussed the data. Wrote the manuscript.

6.1. Introduction

The developed DDS should offer a new therapeutical opportunity for IBD and were fabricated as carrier to transport the encapsulated API to the inflamed areas of the intestine via the oral or the rectal route. As a new therapy opportunity the developed carriers have to be non-cytotoxic at relevant concentrations e.g. for testing on the triple culture model (chapter 5). Although PLGA is a well investigated and established excipient in biomedical applications, particles with a size <1000 nm have different physico-chemical properties compared to the bulk material [190]. The combination with further excipients and the fabrication process can be also of impact for the biocompatibility. Moreover, NPs and MPs can be up-taken by cells and facilitate intracellular effects. Of further importance, the particles should not be recognized as exogenous material by the innate immune system and antigen presenting cells, since an activation of the immune system can decrease the drug effect and lead long-term medication.

The WST-1 assay was performed to assess the cytotoxicity of drug free NPs and MPs on 3T3 mouse fibroblasts and on J774A.1 murine macrophages [23]. The WST-1 assay uses the mitochondrial succinate tetrazolium reductase system in metabolic active cells to cleave a carbon to carbon bond in the slightly red tetrazolium salt WST-1 and turn it to the dark red formazan. The assay was also performed with a macrophage cell line due to their phagocytic activity, therefore, their ability to take up and accumulate particles [43], [191]. Additionally, macrophages are also involved in the pathogenesis of IBD [69], [117].

Furthermore, the potential of NPs and MPs to interfere with reactions of the innate immune system were assessed. As crucial parts of the innate immunity, the complement system activation and the alteration, activation and suppression, of cytokine secretion of dendritic cells were investigated in appropriate *in vitro* assays. The complement system consists of a group of liver synthesized plasma proteins and cell membrane receptors expressed by several types of immune cells including macrophages and dendritic cells [191]. Some components of the complement system can bind to foreign molecules or particles leading to their opsonisation. Such complexes are better phagocytosed by macrophages and dendritic cells after interaction with their complement receptors. The complement system is also involved in chemotaxis, cell lysis of foreign cells or microorganisms, and agglutination of pathogens [23]. The complement system can be activated on three pathways, classical, alternative and lectin initiating a cascade.

The cascade results in massive amplification of response and the formation of the membrane attack complex, which causes terminal cell lysis [23]. CH₅₀ (classical pathway) and APH₅₀ assays (alternative pathway) are diagnostic tests to determine the ability of serum for complement activation by measurement of the haemolytic activity. The results of both assays (CH₅₀ and APH₅₀) refer to the reciprocal dilution of a serum required to produce 50% haemolysis of a standard preparation of erythrocytes. For the classical pathway sheep erythrocytes are used, which were sensitized by anti-(red cell) IgG. The classical pathway, which requires calcium and magnesium ions, is then initiated by IgM on the surface of the antibody sensitized sheep erythrocytes. For the alternative pathway rabbit erythrocytes are used as sheep erythrocytes are inefficient at activating this pathway [192].

The complement system and dendritic cells in tissues are the first line of defense of the innate immune system [191]. Dendritic cells activate cells of the innate immune response, e.g. natural killer cells, via secretion of cytokines. Furthermore, dendritic cells are antigen presenting cells to T-lymphocytes, thus, allowing the initiation of the specific immune response [193]. Therefore, dendritic cells were revealed to be an optimal tool to study the impact of DDS on the immune system as demonstrated by Villiers et al. [193]. Drug free NPs and MPs were hence incubated with lipopolysaccharides (LPS) activated dendritic and non-activated dendritic cells to measure the modulation of the cytokine release to test the interference with the development of an immune response.

6.2. Methods and Materials

6.2.1. Particle preparation and characterization

In the following studies of this chapter drug free NPs and MPs were investigated. Excipients for NP and MP preparation and active ingredients were used as described in chapter 2.2 and chapter 3.2. The particles were fabricated as described in chapter 3.3.2 for NPs and in chapter 3.3.3 for MPs. The size and size distribution of both NPs and MPs were measured as described in chapter 3.3.4.

6.2.2. *In vitro* cytotoxicity assay

In accordance to the International Organization for Standardization recommendation n_10993, NIH-3T3 murine fibroblast cells (H-3T3 cell line, adherent cells, American Type Culture Collection (ATCC) N^oCRL-1658TM) and additionally J774A.1 murine macrophages were chosen according to the application to perform classical WST-1 cytotoxic assay. The cell lines were purchased from the ATCC. The cell viability was determined using a WST-1 assay (Roche Diagnostics, Germany). The cells were maintained according to routine cell culture procedures and seeded at a density of ($\sim 5 \cdot 10^4/\text{cm}^2$) in 96 well plates (Nunc, Sigma Aldrich, Schnelldorf, Germany). After 24 h incubation at 37°C, different concentrations of NPs and MPs, ranging from 100 to 1500 $\mu\text{g}/\text{ml}$, were added for 24 h to the culture medium. Each test group was performed with $n=6$.

Cytotoxicity was assessed for 24 h following the particle removal using the WST-1 assay and expressed as cell viability. WST-1 reagent (soluble formazan derivative reagent) was added (10%, v/v) to the culture medium and kept in the incubator for 3 h. Cells without particles and cells incubated with a solution of H_2O_2 (10 mM) were used as negative and positive controls, respectively. Absorbance was afterwards recorded at 450 nm (soluble formazan titration) and 690 nm (background subtraction) using a microplate reader (Tecan Infinite M 1000, Tecan Deutschland GmbH, Crailsheim, Germany). The absorbance difference (450 nm–690 nm) is directly proportional to the number of viable cells. The percentage cell viability is determined using the following equation 12 (eq. 12). In this equation AS, APC and ANC represent the absorbance of the sample, the positive control (cells treated with H_2O_2 10 mM) and the negative control (only cells), respectively. Furthermore, concentrations of particles showing 50% reduction in cell viability (IC_{50} value) were calculated by Sigma Plot 12.5 software (Systat Software GmbH, Erkrath, Germany).

$$viability = \frac{(AS - APC)}{(ANC - APC)} * 100 \quad \text{eq. 12}$$

6.2.3. Immunotoxicity studies

6.2.3.1. Activation of complement system by nano- and microparticles

In order to determine the effect of drug free NPs and MPs on complement system, human serum was incubated at 37°C for a maximum of 24 h in the presence of NPs and MPs at 250 µg/ml, then serum samples were kept frozen before complement pathways activity measurement. The human serum contains all components of the complement system.

The activity was measured using sheep erythrocytes in a medium containing 2.5% glucose, 5 mM diethylmalonylurea, 142 mM NaCl, 0.05% gelatine, 0.5 mM MgCl₂ and 0.15 mM CaCl₂ (pH 7.5). Sheep erythrocytes were previously sensitized with rabbit antiserum to sheep red cells, cell suspension was adjusted to 3.7×10⁶ cells/ml (absorbance (A) recorded at 660 nm, A₆₆₀=0.3). Complement alternative pathway was measured in the same medium using rabbit erythrocyte at the concentration of 6×10⁶ cells/ml (A₆₆₀=0.48). Sheep red cells are inefficient at activating the alternative pathway, so rabbit erythrocytes are used. In both cases, 1 ml of erythrocytes was pre-incubated at 37°C for 5 min before addition of 50 µl of the human serum previously incubated in the presence of NPs. After a rapid mixing, the absorbance was monitored at 660 nm for classical and alternative pathways, respectively. All the experiments were performed at 37°C. Through mixing of the red blood cells an activation of the complement system takes place ending in the leakage of haemoglobin. The leakage is measured by the absorbance of the haemoglobin in the cell supernatant. Subsequently, the modification of the complement activation in the presence of particles is determined.

Haemolytic activity, CH₅₀ and APH₅₀ for classical and alternative pathway, respectively, was determined by measuring the time required for the reduction of absorbance to 50% of its initial value (50% lysis). The determination of percentage of complement activity was obtained by comparison of the result with those obtained with serum composed of a mixture of fully active (positive control) and of fully inactive serum (negative control) to assure the functionality of the assay (incubated 30 min at 56°C) mixed with various ratios. An activation of the complement system by particles would lead to modification of reduction of absorbance.

6.2.3.2. Alteration of cytokine secretions of dendritic cells by nano- and microparticles

Dendritic cells were generated from bone marrow extracted cells from C57BL/6 mice (Charles River, l'Arbresle, France) as previously described by Faure et al. [194]. The bone marrow cells were isolated by flushing from the femurs. Erythrocytes and GR1 positives cells were removed by magnetic cell sorting, and the remaining negatively sorted cells were re-suspended at 5×10^5 cells/ml in complete Iscove's modified Dubelcco's medium (IMDM, Gibco, Invitrogen, Grand Island, NY, USA) supplemented with factors GM-CSF, FLT-3L and IL-6 (Peprotech, Rocky Hill, NJ, USA) and cultured at 37°C in the presence of 5% CO₂. GM-CSF is produced by the GM-CSF-transfected J558 cell line (provided by D. Gray, University of Edinburg, UK) and FLT-3 ligand (FLT-3L) is produced by the FLT-3 L-transfected BL16-F10 cell line (provided by G. DranoV, Boston, USA). The transformation of the progenitors into fully active dendritic cells occurs during a 10 days culture.

Determination of activation of cytokine secretion by particle treatment with unstimulated dendritic cells

After washing, dendritic cells (10^6 cells/ml) were seeded in 24 well plates. After 24 h drug free NPs and MPs were added at concentrations of 0.01-0.5 mg/ml, and the cells were further incubated at 37°C for 24 h or 48 h.

Determination of interference of particles with cytokine secretions of pre-stimulated dendritic cells

After washing, dendritic cells (10^6 cells/ml) were seeded in 24 well plates and incubated in culture medium containing LPS (LPS 2 µg/ml, from *Escherichia coli* 026:B6, Sigma, St. Louis, MI, USA) for 24 h. LPS is a ligand for toll like receptor 4 (TLR 4) expressed by dendritic cells, thus, inducing their activation. Afterwards, drug free NPs and MPs were added at concentrations of 0.01-0.5 mg/ml, and the cells were further incubated at 37°C for 24 h and 48 h.

Cytokines, IL-6 and IL-12, were measured in the supernatant of cell cultures by immunoassays using BD OptEIA™ for murine cytokines (BD Bioscience Pharmingen, France) according to the procedures recommended by the manufacturer. Each experiment was performed at least three times with cells issued from different cultures and each measurement is performed in duplicate. The supernatants are harvested after 24 h incubation at 37°C.

6.3. Results

6.3.1. *In vitro* cytotoxicity assay

The WST-1 assay was performed to assess the cytotoxicity, expressed in Figure 6.1 as cell viability, of drug free NPs and MPs on 3T3 mouse fibroblasts and on J774A.1 murine macrophages. The NPs in this experiment had a size of 149.8 ± 2.2 nm (PDI: 0.02 ± 0.01 , ZP: -21.3 ± 1.37 mV) and the MPs a size of 8.4 ± 0.95 μ m (width: 4.4 ± 0.17). The results for the NPs in Figure 6.1a exhibit at least 80% of cell viability after 24 h incubation, even for relatively high concentrations (1500 μ g/ml). For both cell lines 3T3 and J774A.1 the IC_{50} values are >1500 μ g/ml. For MPs in Figure 6.1b a strong decrease in the cell viability was observed for concentration >250 μ g/ml for the 3T3 ($IC_{50} \sim 250$ μ g/ml) and >100 μ g/ml for the J774A.1 cells ($IC_{50} < 100$ μ g/ml).

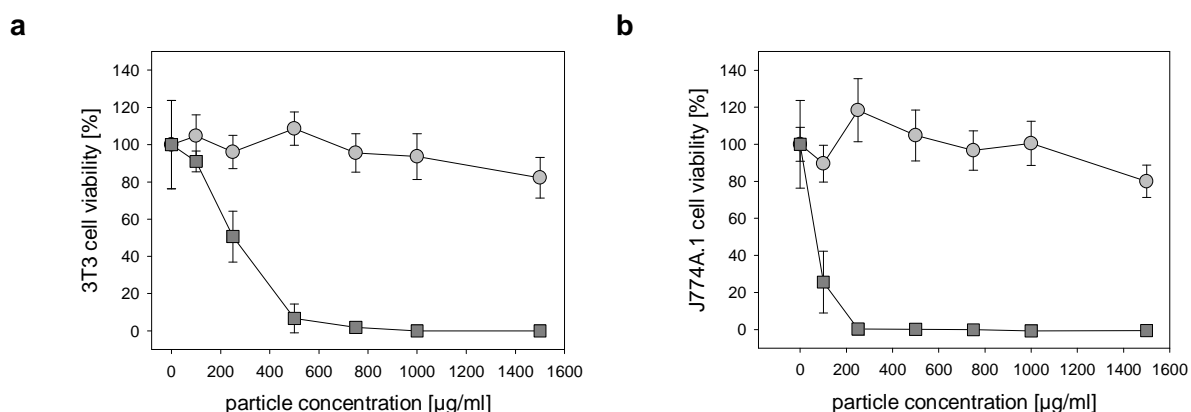


Figure 6.1. Cell viability (WST-1 assay) after 24 h incubation of drug free NPs (○) and MPs (■) for (a) 3T3 cells and (b) J774A.1 cells. Results were presented as mean \pm S.D. (n=6).

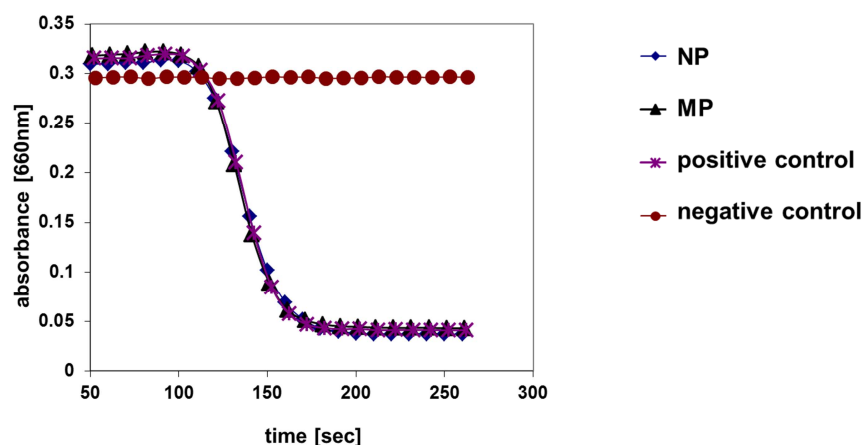
6.3.2. Immunotoxicity studies

6.3.2.1. Activation of complement system by nano- and microparticles

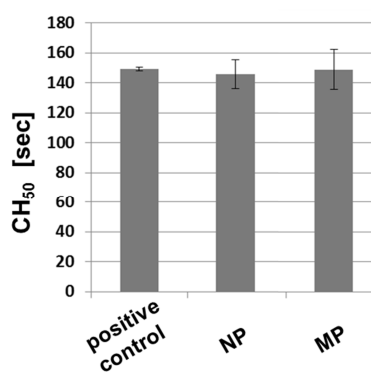
Complement activation via classical or alternative pathway was measured by erythrocyte cells lysis. The NPs in this experiment had a size of 141.2 ± 1.6 nm (PDI: 0.05 ± 0.02 , ZP: -34.6 ± 1.15 mV) and the MPs a size of 7.2 ± 0.35 μ m (width: 5.0 ± 0.17). In Figure 6.2a as example the absorbance measurement is demonstrated for the classical pathway. The negative control shows no change in the absorbance as the components in the human serum were inactivated for this control.

The positive control demonstrates the activation of the complement system with reduced absorption based on the cell lysis. In addition to Figure 6.2a, in Figure 6.2b no modification of the CH_{50} could be determined for NPs and MPs in comparison to positive control. The same result was obtained for the alternative pathway demonstrated in Figure 6.2c. Therefore, no activation by drug free NPs and MPs was observed, on both pathways, indicating that the formulations were not recognized as exogenous material based on this assay.

a



b



c

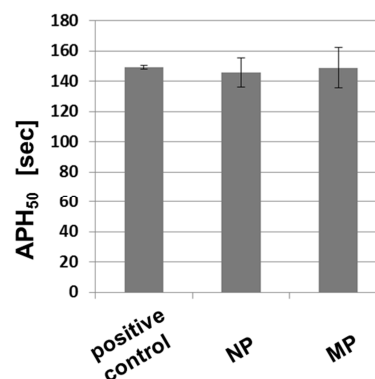


Figure 6.2. Determination of activation of complement system. (a) Measurement of the time required for the reduction of absorbance to 50% of its initial value, which is equal to 50% lysis, for classical pathway. (b) CH_{50} and (c) APH_{50} for drug free NPs and MPs in comparison to positive control. Results were presented as mean \pm S.D. (n=6).

6.3.3. Alteration of cytokine secretions of dendritic cells by PLGA particles

The incubation of NPs and MPs with dendritic cells, investigating the activation of immune system by these DDS, did not induce secretion of IL-6 or of IL-12, therefore, no graph could be shown. Hence, the dendritic cells were not activated by drug free NPs or MPs at the different concentrations demonstrating that these DDS do not display pro-inflammatory activity themselves.

Investigating the suppression of immune system (Figure 6.3) by incubating the particles with LPS pre-activated dendritic cells, a slight and concentration dependent effect was determined on IL-6 secretion in presence of NPs (Figure 6.3a). Therefore, a slight effect can be investigated in relevant concentrations e.g. for *in vitro* efficacy studies on triple culture model (chapter 5) as NPs were applied at ~0.0135 mg/ml and ~0.024 mg/ml.

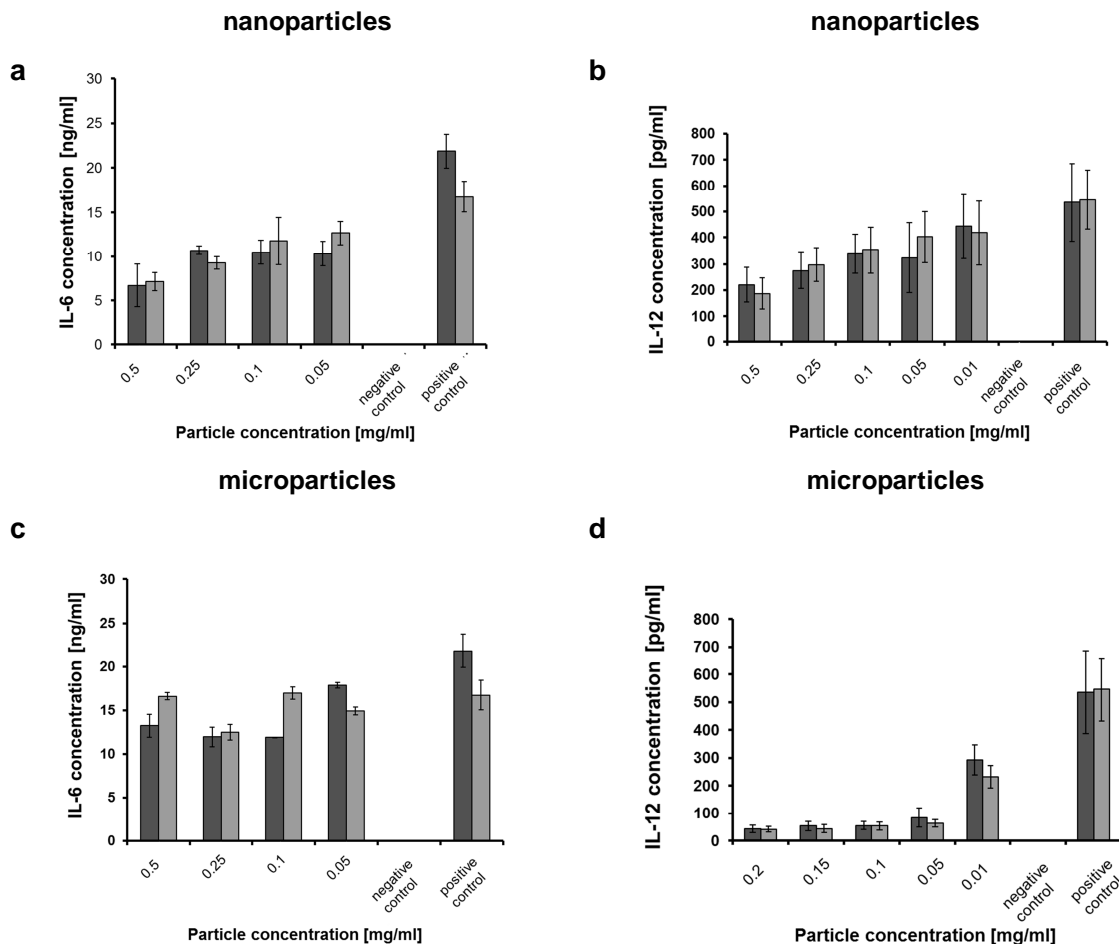


Figure 6.3. IL-6 and IL-12 concentrations after exposure of different concentrations of NPs and MPs to LPS activated dendritic cells. (a) IL-6 and (b) IL-12 level after incubation with NPs. (c) IL-6 and (d) IL-12 level after incubation with MPs. Results were expressed as mean \pm S.D. (n=3; ■ 24 h and ▒ 48 h incubation time).

No effect on the IL-6 secretion was determined for MPs (Figure 6.3c) and, consequently, no effect was investigated in used concentrations (<0.01 mg/ml) for *in vitro* efficacy studies on triple culture model (chapter 5). Depending on the loading MPs were applied at concentrations of ~0.0076 mg/ml and ~0.0052 mg/ml.

The IL-12 secretion in presence of NPs was concentration dependent slightly suppressed (Figure 6.3b), but no effect was determined in the used concentrations which are <0.05 mg/ml for *in vitro* efficacy studies. A strong concentration dependent suppression of IL-12 secretion by MPs was detected (Figure 6.3 d) also for the lowest concentration with 0.01 mg/ml. No differences in results were obtained by prolongation of the incubation time from 24 h to 48 h.

6.4. Discussion

PLGA was used over decades in the medical field e.g. as suture [195] and has been shown to be extremely safe as a material for macroscopic DDS, e.g. implants and also microparticulate DDS [61]. Furthermore, it can be suggested that the chemical composition of PLGA does not rise toxicity [196]. However, unique effects may occur through preparation of novel nano- and microparticulate formulations. Several studies revealed that biodistribution and toxicological effects of materials change upon formulating it as NPs [197]. Effects can originate due to size, also preparation techniques as well as due to excipients, which differ e.g. according to the freeze and spray drying techniques used in this study. NPs were freeze dried using the sugar trehalose as cryoprotective agent, while MPs contained Span60 to enable re-dispersion after spray drying. The MPs consists to a high value of Span60 (0.592 mg per mg final formulation) which forms together with the PLGA the matrix system. Span60 is widely used in cosmetics, food products, and oral as well as topical pharmaceutical formulations [175]. The LD₅₀ value was determined in rats after oral application to be 31 g/kg, indicating no toxicity, and the World Health Organization (WHO) assessed in 1974 Span60 as safe food additive [198]. The acceptable daily intake of 25 mg/kg bodyweight was evaluated as it is metabolized to sorbitol and stearic acid [198]. During the last decades Span60 was widely used for the formulation of DDS, in particular niosomes [199] and nanocapsules [200], [201]. The disaccharide trehalose is approved for the use as cryoprotective agent for proteins, particularly for parenteral administration and liposomes [175]. It is rapidly metabolized to glucose by the specific enzyme trehalase and evaluated as nontoxic and non-irritant excipient (LD₅₀ in rats after oral administration >5g/kg).

The NPs demonstrate marginal to low toxicity with IC_{50} values $>1500 \mu\text{g/ml}$. For MPs a strong decrease in the cell viability was observed for concentration $>250 \mu\text{g/ml}$ for the 3T3 ($IC_{50} \sim 250 \mu\text{g/ml}$) and $>100 \mu\text{g/ml}$ for the J774A.1 ($IC_{50} < 100 \mu\text{g/ml}$). Nevertheless, macrophages show a higher sensitivity and they have the possibility to phagocyte size-dependent materials [191], [202]. One other explanation for the enhanced toxicity could be the high sedimentation rates that occur during 24 h incubation and, therefore, mechanical stress for the cells, which has to further investigated. Additionally, the effect could be cell line dependent. To underline this, Semete et al. investigated the toxicity of spray dried PLGA particles (300 nm-1 μm) in Caco-2 and HeLa cells, a cervical cancer cell line, in concentrations of 0.001-0.1 mg/ml and determined no toxic effect. Furthermore, in the present work the cytotoxicity was also determined on the cell lines used for set-up of the triple culture model (chapter 5.4.3). The experiments were performed via LDH assay at concentrations between 0.006-6.0 mg/ml for NPs and 0.0014-1.4 mg/ml MPs on monocultures of Caco-2, THP-1 and Mutz-3 cells. The different concentrations were selected according to the different tested concentrations and loading. The cell lines were robust to MPs, even at the highest concentration (chapter 5.4.3, Figure 5.4). The NPs show no toxicity except for the highest concentration with 40% toxicity for THP-1 and MUTZ-3 cells. In general, Caco-2 cells are known to be more resistant to toxic effects, especially when they are differentiated to a confluent monolayer.

Apart from cellular toxicity the particles should stay for a period of time in the living individual, e.g. in rodent colitis models for *in vivo* studies as well as in a future perspective in the human patient. Therefore, the particles should not be recognized as exogenous and cause an immune reaction including inflammation [190]. The assay used in this immunology study represents the investigations of the innate immune response. The innate immune system is non-specific, has an immediate response, e.g. for binding compounds of the complement system in seconds, and consists of cell-mediated and humoral components (complement system). The first line of defense of the innate immune system consists of the complement system and dendritic cells in tissues secreting IL-6 and IL-12 [23]. IL-6 is both a pro-inflammatory and anti-inflammatory cytokine, furthermore it may promote B-cell stimulation. IL-6 is secreted in the first phase of the immune response as pro-inflammatory cytokine and can cross the blood brain barrier inducing fever. The cytokine IL-12 is the T-cell stimulating factor linking innate and adaptive immune responses via the induction and differentiation of the T_H cells [23].

In this study, no activation of the complement system could be measured for NPs as well as for MPs and, therefore, both were not recognized as exogenous material. The absence of detectable levels of IL-6 and IL-12 is an indicator of safety for these particles as they are not activating immune responses by themselves. Interestingly, the particles had concentration dependent an effect of the IL-12 secretion of with LPS stimulated dendritic cells. Does a modulation of the IL-12 secretion have consequences? IL-12 is a regulator of T_H cells and important for the cellular defense and adaptive immune system. In the first phase of the immune response IL-12 is a key factor for T_H1 responses characterized by IFN- γ secretion [203]. Suppression of IL-12 secretion of dendritic cells may reduces the crosstalk between innate and adaptive immune system, but only in the early stage of T_H1 immune response. In the following immune response IL-23 plays a more important role and supports the inflammatory process [203]. Moreover, in the second phase of the immune response IL-12 can also be secreted by phagocytes e.g. macrophages. IL-12 is further associated with food allergy or autoimmune diseases including psoriasis, multiple sclerosis, rheumatoid arthritis, and CD [9], [204]. Several studies aimed to reduce IL-12 levels for these allergies and diseases [205]. In a study in human patients Mannon et al. applied successfully an anti-IL-12 antibody (3 mg/kg, weekly) as co-medication for active CD [206]. In mouse models IL-12 p35 (IL-12 subunit) deficiency and IL-12Rb1 (part of the IL-12 receptor) deficiency ameliorates the induced colitis. Furthermore, IL-12 p40 (IL-12 subunit) deficiency significantly protects the rodent models from developing colitis [207]. Other studies in rodent colitis models demonstrated that antibodies directed against IL-12 p40 can prevent and/or reverse colitis [9], [208].

In conclusion, the decrease of IL-12 production by dendritic cells may reduce their potential to promote T_H1 response, therefore damper further inappropriate response such as those observed in autoimmune diseases.

In the present study the effect of IL-12 suppression was obvious at a concentration of 0.01 mg/ml for MPs and 0.05 mg/ml for NPs (Figure 6.3). Hence, this effect would not influence the dendritic cells in the triple culture model of the *in vitro* studies in chapter 4, as MPs were applied at ~0.0076 mg/ml and ~0.0052 mg/ml and NPs at ~0.0135 mg/ml and of ~0.024 mg/ml. In a future perspective the question is if it would be possible to reach such (high) concentrations *in vivo* at the side of inflammation influencing the local dendritic cells. Therefore, the effective concentration *in vivo* had to be confirmed first. In the study of Mannon et al. the patients received 3 mg of the antibody IL-12 per kg of body weight weekly per subcutaneous injection to achieve a significant effect [206].

As one of the major goals in the present work was to reduce the applied drug doses by accumulation of the DDS in the inflamed areas of the intestine, in a first step this hypothesis should be confirmed to reveal the effective concentrations of the loaded DDS. A step towards in this direction is the evaluation of efficacy of the formulations in a rodent colitis model as followed in chapter 7. However, if a local effect on the immune system could be reached it would rather assist the drug effect.

6.5. Conclusion

The NPs and MPs showed no toxicity in relevant concentration for *in vitro* testing e.g. on the triple culture model of the inflamed intestinal mucosa. No activation of the complement system was determined for NPs as well as for MPs, therefore the particles were not recognized as exogenous material via the investigated mechanism.

The absence of detectable levels of cytokines (IL-6 and IL-12) by incubation of dendritic cells in presence of the particles underlines the safety of the particles as they are not activating immune responses by themselves. Interestingly, the particles suppress concentration dependent the IL-12 secretion of stimulated dendritic cells and the effect should be considered in further investigations.

As far as such *in vitro* results can predict the *in vivo* effects, there is no result within the cytotoxicity and immunotoxicity testing performed here that would raise concerns about the safety of NPs as well as of MPs.

7. Evaluation of cyclosporine A loaded PLGA based drug delivery systems for inflammatory bowel disease in DSS Balb/C mice model

Parts of this chapter will be included in a manuscript for submission to a peer-reviewed journal:

Ana Melero*, Christina Draheim*, Elisa Giner, Raquel Talens, Teresa María Garrigues, José Esteban Peris, M^a Carmen Recio, Rosa Giner, Steffi Hansen, Claus-Michael Lehr, *Evaluation of cyclosporine A loaded PLGA based drug delivery systems for inflammatory bowel disease in DSS Balb/C mice model*

*These authors contributed equally to this work.

The author of the thesis made the following contributions to this chapter: Performed experiments concerning preparation and characterization of PLGA particles and cytokine production. Conceived, designed the experiments and analysed and interpreted the data. Wrote the manuscript.

7.1. Introduction

The medical treatment of IBD is mostly based on the daily administration of corticosteroids and immunosuppressants to induce remission and prevent relapses [17], [37]. The required doses of corticosteroid and immunosuppressant drugs can induce severe side effects. Novel therapy strategies using nano- and microparticulate DDS aim to improve the treatment by local application of the used drugs. Therefore, high drug concentrations in the affected tissues could be obtained avoiding their access to the systemic circulation in sufficient amount and rate to reduce systemic side effects [4], [43]. In previous studies NPs and MPs had shown to be able to remain in the ulcerated areas of the colon for prolonged periods of time, where they can control a sustained release of the drug *in situ*. This accumulation of particles can be used for a passive targeting approach [67], [75]–[77]. Furthermore, the particles can be entrapped in the mucus layer of the lumen [75]. Through the inflammation an increased mucus production is observed, which leads to a thicker mucus layer, in particular in the ulcerated areas [72], [79], [80].

However, following this passive targeting approach the appropriate or optimal size of such DDS is not fully clear at the moment. NPs had shown their efficacy in rodent models [67], [75], whereas the literature suggests that MPs seem to be more favorable in human patients compared to NPs [76]. Therefore, two formulations, PLGA based NPs and MPs, which differ in size and in manufacturing technology were compared in the same *in vivo* model using dextran sodium sulfate (DSS) to induce colitis in Balb/C mice [124]. On both processes for producing the particles a DOE was before applied in chapter 2 to identify process parameters influencing size and size distribution to address reproducibility and controllability of the manufacturing processes and, therefore, to achieve consistent quality of the DDS at the early state of development. Furthermore, both carriers demonstrated their safety with regard to cytotoxicity and immunotoxicity in chapter 5 and chapter 6 with comparable results in different *in vitro* cell culture systems. In this chapter NPs and MPs loaded with CYA were selected according to their physico-chemical and biopharmaceutical properties (chapter 3) and in *in vitro* testing on the triple culture model (chapter 5). CYA loaded NPs and MPs demonstrated higher encapsulation efficiencies, a more controlled release and significantly better anti-inflammatory efficacy compared to BU loaded DDS. In general, CYA demonstrated to be successful in the treatment of IBD, but also causes several serious side effects through its systemic bioavailability [17], [160], [161], which should be decreased by using a suitable DDS.

Among the chemically induced models of colitis, the DSS model has been extensively characterized and is widely used to study epithelial repair mechanisms as well as the contribution of innate immune mechanisms [123]. This model shares many of the macroscopic, histological and immune characteristics of human IBD and is characterized by bloody diarrhoea, ulcerations and infiltrations with granulocytes. The DSS-induced colitis in Balb/C mice is further characterized by an inflammation only located in caecum and colon, which reflects characteristics of UC [125], [133], [209]. Pathophysiological changes of the DSS model can be recorded by clinical parameters: body weight loss, stool consistency, blood in stool, colon length, colon weight/length ratio as well as colon histology. In this study an acute DSS model was used, which shows an increased mucosal production of macrophage-derived cytokines, in particular TNF- α and IL-6 [131]. Hence, inflammation markers (IL-1 β , IL-6, TNF- α) and anti-inflammatory cytokines (IL-4, IL-10) in the colon were measured. Due to the toxicity to the gut epithelial cells of the basal crypts, DSS affects the integrity of the mucosal barrier [123] and allows, therefore, to investigate the passive targeting approach by deposition of particles in ulcerated regions of the intestine.

Before starting the *in vivo* study the stability with regard to the size of the NPs and MPs was investigated and release profiles were performed at pH 3, as the pH in the GIT of mice differs from humans [210]. For the *in vivo* efficacy studies an oral dose of 50 mg/kg referring to the weight of the mice was administered, following by a dose response with 25 mg/kg and 12.5 mg/kg for the NPs [125]. The formulations were compared to the commercially available oral CYA formulation (Sandimmun[®] Neoral) and drug free NPs and MPs in both healthy animals and DSS colitis mice.

7.2. Materials

Excipients for NP and MP preparation and active ingredients were used as described in chapter 2.2 and chapter 3.2. Sandimmun[®] Neoral capsules (Sandimmun) were donated by a local pharmacy.

All solvents were of high-performance liquid chromatography grade and all chemicals met the quality requirements of the European Pharmacopoeia 6.0–7.3.

7.3. Methods

7.3.1. Preparation and characterization of cyclosporine A loaded nano- and microparticles

The CYA-NPs and CYA-MPs were prepared with an optimal loading as described in chapter 3.3.2 and chapter 3.3.3, respectively. Hence, for CYA a loading of 4/10 (CYA/PLGA, wt/wt) for both, NPs (CYA-NP) and MPs (CYA-MP), was used.

Hydrodynamic diameter and polydispersity index (PDI) were measured by laser light scattering and zeta potential (ZP) of NPs were measured by laser light scattering as described in chapter 2.3.6. The size and size distribution (width) of MPs were measured by laser light diffraction as described in chapter 3.3.4. The encapsulation efficiency (EE) was determined as described in chapter 3.3.6.

7.3.2. Stability of particles in simulated gastrointestinal tract of mice

The stability of particles in the GIT was investigated according to the findings of McConnell et al. [210]. Hence, the particles were incubated in simulated gastric fluid (SGF) without pepsin according to the United States Pharmacopeia (USP, 2003), and adjusted with 0.1 N NaOH to pH 3.0. The experiments were performed in triplicate at room temperature. Drug free NPs (freeze dried) or MPs were weighted and incubated in 10.0 ml SGF pH 3.0. The particles were shaken at 100 rpm in an incubator (GLF 3031, Germany) and at pre-defined time points (0 h, 1 h, 2 h, 4 h, 8 h and 24 h). Size and size distribution were measured as described in chapter 2.3.6 for NPs and in chapter 3.3.6 for MPs. An increase in size or size distribution indicates an agglomeration of particles and, therefore, instability. The results of size were expressed in % referring to the initial size at 0 h (100%).

7.3.3. *In vitro* release profile in simulated gastric fluid

According to the pH values in the GIT of mice published by McConnell et al. [210], the release of CYA-NPs and CYA-MPs was investigated in SGF (USP, 2003) without pepsin adjusted to pH 3.0 with 0.1 N NaOH at room temperature. As SGF does not include a buffering system the pH was monitored during the experiment and determined to be pH 3.0 for the whole experimental time. To increase the solubility of CYA, 0.05% tween[®]80 (wt/v) was added to the SGF.

The sink conditions were defined as 30% of the saturation concentration according to the USP (USP, 2003). The *in vitro* release profiles and determination of saturation concentration were performed as described in chapter 3.3.8. The saturation concentration was determined to be $41.7 \pm 0.23 \mu\text{g/ml}$ ($n=3$) for CYA. The results were calculated cumulative and expressed as percent normalized to the EE. The release was compared to a release in PBS at pH 6.8. The experiments were performed in triplicate.

7.3.4. Induction and assessment of DSS-induced colitis and therapeutic efficacy

Female Balb/C mice (Harlan Interfauna Iberica, Barcelona, Spain), 6-8 weeks old, with weights ranging from 18 to 20 g, were acclimatized under a 12 h light/dark cycle at 22 °C and 60% humidity, fed with a standard laboratory rodent diet and water ad libitum for seven days before starting the experiments. All animal care and experimental protocols were approved by the Institutional Ethics Committee of the University of Valencia (No. 108), in accordance with current Spanish legislation (RD1201/2005) and Helsinki declaration under the procedure number of: A1360059439693.

Animals were randomly assigned to groups (six mice per group, seven mice for blank and 11 mice for control) distributed as in Table 7.1. Acute colitis was induced by adding 3% (wt/v) DSS to the drinking water of Balb/C mice for seven days (Figure 7.1). Blank mice received water at libitum. DSS was removed at day seven.

Table 7.1. Control and treatment groups in **DSS colitis mice** and in **healthy mice**. Drug free NPs and MPs were applied at a dose referring to 50 mg/kg of loaded particles.

groups	treatment	nomenclature	experiment in DSS colitis mice/in healthy mice
1	blank (healthy mice)	blank	healthy animals
2	DSS (colitis mice)	control	DSS colitis mice
3	Sandimmun (25 mg/kg)	Sandimmun (25 mg/kg) + DSS	DSS colitis mice
4	Sandimmun (50 mg/kg)	Sandimmun (50 mg/kg) + DSS	
5	drug free NP	NP (50 mg/kg) + DSS	
6	CYA loaded NP (50 mg/kg)	CYA-NP (50 mg/kg) + DSS	
7	CYA loaded NP (25 mg/kg)	CYA-NP (25 mg/kg) + DSS	
8	CYA loaded NP (12.5 mg/kg)	CYA-NP (12.5 mg/kg) + DSS	
9	drug free MP	MP (50 mg/kg) + DSS	
10	CYA loaded MP (50 mg/kg)	CYA-MP (50 mg/kg) + DSS	
11	Sandimmun (50 mg/kg)	Sandimmun (50 mg/kg)	healthy mice
12	drug free NP	NP (50 mg/kg)	
13	CYA loaded NP (50 mg/kg)	CYA-NP (50 mg/kg)	
14	drug free MP	MP(50 mg/kg)	
15	CYA loaded MP (50 mg/kg)	CYA-MP (50 mg/kg)	

Concentrations of 50 mg/kg, 25 mg/kg and 12.5 mg/kg CYA-NPs and 50 mg/kg CYA-MPs were administered daily, starting with 50 mg/kg and compared to Sandimmun administered at 50 mg/kg and 25 mg/kg, respectively. Drug free NPs and MPs were administered at a dose referring to 50 mg/kg of loaded particles (Table 7.1). Therefore, NPs and MPs were suspended and diluted in drinking water, and administered by oral gavage (200 μ l/day). Sandimmun solution was extracted from Sandimmun[®] Neoral capsules by washing the capsules three times with ethanol. The respective dose was diluted from this stock solution directly before administration with PBS pH 7.4. Blank and control mice received daily drinking water by oral gavage mimicking the administration stress. The last dose of formulations was given at day eight (1.5 h before sacrifice) to measure the CYA levels in blood.

All groups were also tested at the highest concentration (50 mg/kg) in healthy mice (five to six mice per group) to evaluate toxic or side effects of the particles, which can be detected by the appearance of the fur and the body weight (indicator for quality of life).

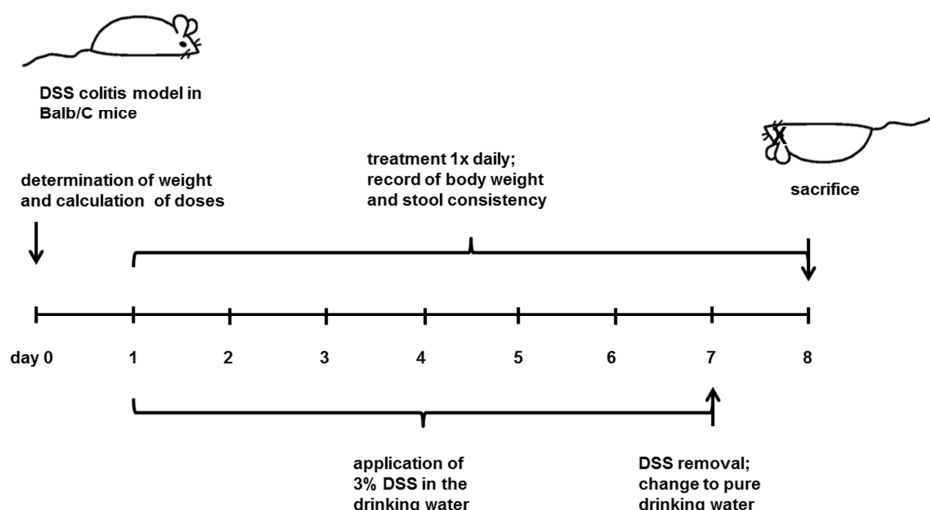


Figure 7.1. Experimental set-up *in vivo* studies.

Animals were sacrificed at day eight by heart blood puncture after anaesthesia of the mice with isofluran (CP-Pharma, Germany), and the entire colon (from the caecum to anus) was resected. Resected colon tissue samples were rinsed with ice-cooled phosphate buffer to remove luminal content. Tissue wet weight and colon length were determined and expressed as a colon weight/length quotient. Colon length is shortened under inflammation and colon weight is increased due to development of edema in the inflamed areas. The colons of each test group were blinded and randomly separated for histological analysis (chapter 7.3.5) and measurement of cytokine levels (chapter 7.3.6). The samples for the cytokine measurement were frozen immediately and stored at -80 °C until use.

Animal body weights (being an indicator for quality of life), stool consistency, rectal bleeding, appearance of fur and consumed DSS solution volume, were recorded daily throughout all the experiments.

The disease activity index (DAI) was determined according to Mladenovska et al. [84] assessing weight loss, stool consistency and rectal bleeding. No weight loss was counted as 0 points, 1–5% as 1 point, 5–10% as 2 points, 10–20% as 3 points and >20% as 4 points. For stool consistency, 0 points were given for well-formed pellets, 2 points for pasty and semi-formed stools that did not stick to the anus and 4 points were given for liquid stools that stick to the anus. Bleeding was scored as 0 point for no blood, 2 points for positive finding and 4 points for gross bleeding. The mean of these scores was forming the clinical score ranging from 0 (healthy) to 4 (maximal activity of colitis).

7.3.5. Histological analysis

Colon samples used for histopathology (n=3) were opened longitudinally along the main axis, rolled up in a spiral starting from distal to proximal margin (“swiss role”), fixed in 4% formaldehyde, paraffin embedded, sectioned and stained with hematoxylin and eosin. The “swiss role” allows to the observation of the whole colon, distal and proximal part. The slides were analysed by light microscopy and scored as described previously [211] according to the criteria listed in Table 7.2.

Table 7.2. Histopathological scores for DSS-induced colitis. Results were expressed as means of scores [211].

Grade	Severity of inflammation (amount of cell infiltration)	Extend of inflammation (cell infiltration location)	Extent of crypt damage
0	none	none	no damage
1	mild	mucosa	basal one third
2	moderate	mucosa + submucosa	basal two third
3	severe	transmural	crypt loss/ epithelium conserved
4	n. a.	n. a.	crypt and epithelium loss

n. a. = not applicable

7.3.6. Cytokine level

The colons ($n \geq 3$) were cut in small pieces and then suspended (20%, w/v) in ice-cold PBS containing 0.1% Igepal CA-630, homogenized, sonicated for 30 s and centrifuged at 20000x g for 10 min at 4°C. Supernatants were collected and protein concentrations were determined by Bradford colorimetric method [212].

Then, IL-1 β , IL-4, IL-6, IL-10 and TNF- α concentration in the supernatants were measured by ELISA kit for each IL (eBioscience, San Diego, USA) according to the manufacturer's instructions and expressed as pg/ml per mg protein.

7.3.7. Cyclosporine A level in plasma

Plasma samples were analysed by means of an HPLC device (Agilent, Barcelona Spain). The analytical conditions were as follows: Column, Kromasil C18 25x4mm; flow: 1.2 ml/min; detection wavelength: 210 nm; injection volume: 50 μ l; retention time: 3.2 min; temperature of analysis: 65°C. The mobile phase consisted of a mixture of acetonitrile/methanol/purified water (7/2/1, v/v/v). Three calibration curves were prepared for inter and intraday validation of the method in the concentration range: 5-100 μ g/ml. Therefore, 100 μ l of plasma samples were spiked with different volumes of a CYA standard solution in ethanol at a concentration of 500 μ g/ml, and then mixed (vortex mixer) for 5 min. 500 μ l acetonitrile were added and samples were mixed (vortex mixer) for 5 min. Samples were then centrifuged again at 20000x g for 11 min. After sacrifice of the mice by heart puncture, heparinized blood samples were centrifuged under the conditions noted above and further prepared following the protocol for the standards, except for the addition of CYA standard solution.

7.3.8. Statistical analysis

The results are expressed as the mean \pm standard deviation (S.D.). Statistical significance was performed by means of one-way analysis of variance (ANOVA) and Holm-Sidak test for multiple comparisons. Sigma Plot 12.5 software (Systat Software GmbH, Erkrath, Germany) was used for all calculations.

7.4. Results

7.4.1. Characterization of cyclosporine A loaded nano- and microparticles

The physico-chemical properties were determined for NPs and MPs and summarized in Table 7.3 and Table 7.4, respectively. NPs have a size of 160 nm and CYA-NPs of 158 nm with a narrow size distribution and a negative zeta potential, which is typical for PLGA particles.

The MPs have a size of 2.8 μm and the CYA-MPs of 2.7 μm with a wider size distribution, which is typical for spray dried products.

Table 7.3. Physico-chemical characteristics of NPs used for *in vivo* studies.

formulation	size [nm]	PDI	zeta potential [mV]	EE [%]	loading [$\mu\text{g}/\text{mg}$]
drug free NP	160.5 \pm 2.1	0.03 \pm 0.02	-27.8 \pm 0.5		-
CYA-NP	158.1 \pm 2.0	0.04 \pm 0.04	-31.0 \pm 6.1	61.4 \pm 2.8	85.3

Table 7.4. Physico-chemical characteristics of MPs used for *in vivo* studies.

formulation	size [μm]	width	EE [%]	loading [$\mu\text{g}/\text{mg}$]
drug free MP	2.8 \pm 0.06	1.8 \pm 0.06	-	-
CYA-MP	2.7 \pm 0.02	1.2 \pm 0.02	100.5 \pm 2.2	142.4

7.4.2. Stability of particles in simulated gastrointestinal tract of mice

The colloidal stability according to size and size distribution after incubation in SGF at pH 3 is summarized in Figure 7.2. During 24 h of incubation no change in size and size distribution was determined for the NPs (Figure 7.2a). For the MPs (Figure 7.2b) a reduction of 18.5% after 1 h incubation time was observed. A re-dispersibility of the particle aggregates and dispersion of Span60 could be assumed.

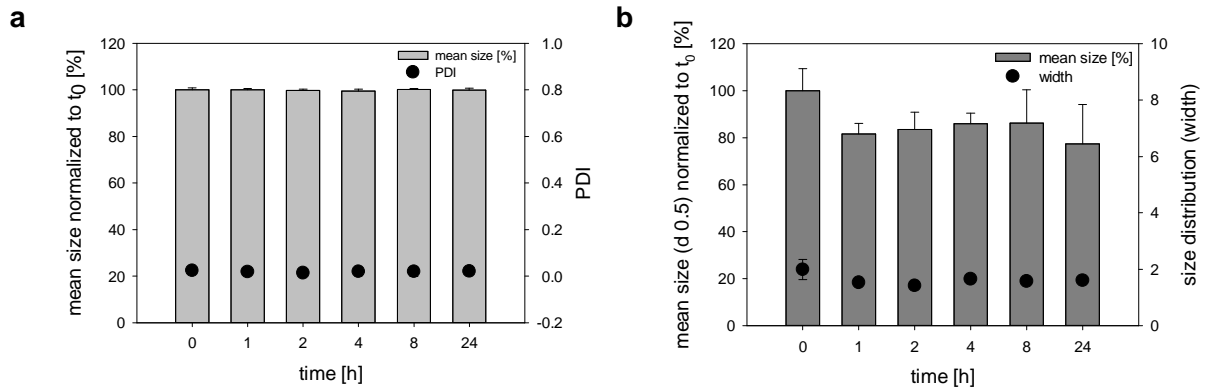


Figure 7.2. Stability measured as size and size distribution of (a) NPs and (b) MPs in SGF at pH 3.0. The data were presented as mean \pm S.D. (n=3).

7.4.3. *In vitro* release profile

The administered particles should be stable following their administration by oral gavage. According to the work of Mc Connell et al. [210] the stability can be also assessed by release studies at pH 3.0 in SGF (Figure 7.3). The CYA-NPs release the encapsulated CYA slower (67.1 ± 8.8 % released CYA after 24 h) compared to the CYA-MPs with 89.0 ± 9.3 % in 24 h. Compared to release studies in PBS pH 6.8 showed a minimal change in the release of CYA from CYA-MPs, whereas the burst release is reduced for the CYA-NPs at pH 6.8.

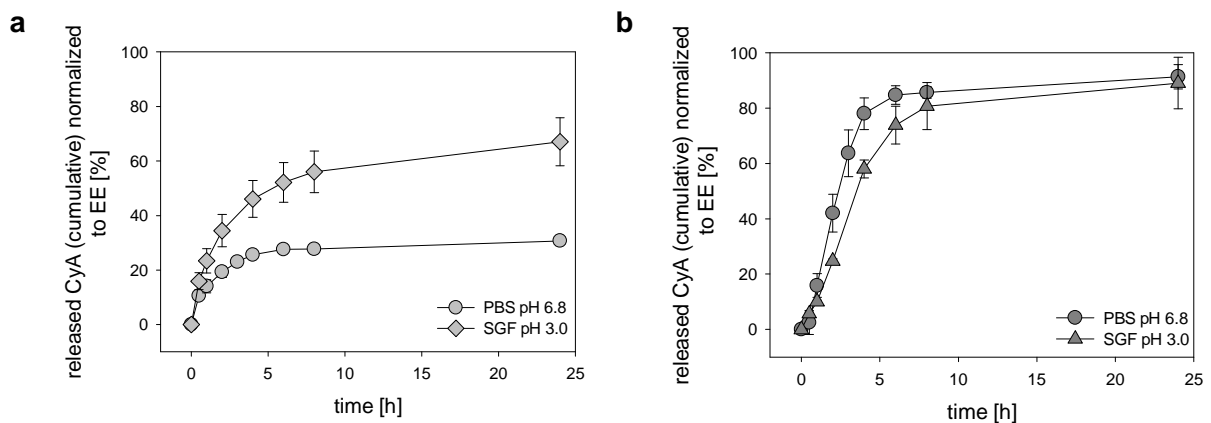


Figure 7.3. *In vitro* release profile over 24 h. (a) CYA-NPs and (b) CYA-MPs in SGF at pH 3.0 in comparison to a release in PBS at pH 6.8. The data were presented as mean \pm S.D. (n=3).

7.4.4. Clinical parameters - Body weight loss and disease activity index

The monitored body weight loss as indicator for the quality of life is presented in (Figure 7.4). Due to the assessed mild colitis a light reduction in the body weight of the control group starting at day 6 was determined. For a drastic weight reduction a dose of 5% DSS solution should be applied, but often animals die at this concentration. Based on a benefit-risk balance and ethical reasons 3% was used as other parameters, in particular, colon length, colon weight/ratio, reveal significant results at this concentration. DSS intake was measured and ranged between 3.5-4.7 ml/day per mouse, except for CYA-MPs with 2.0 ml/day.

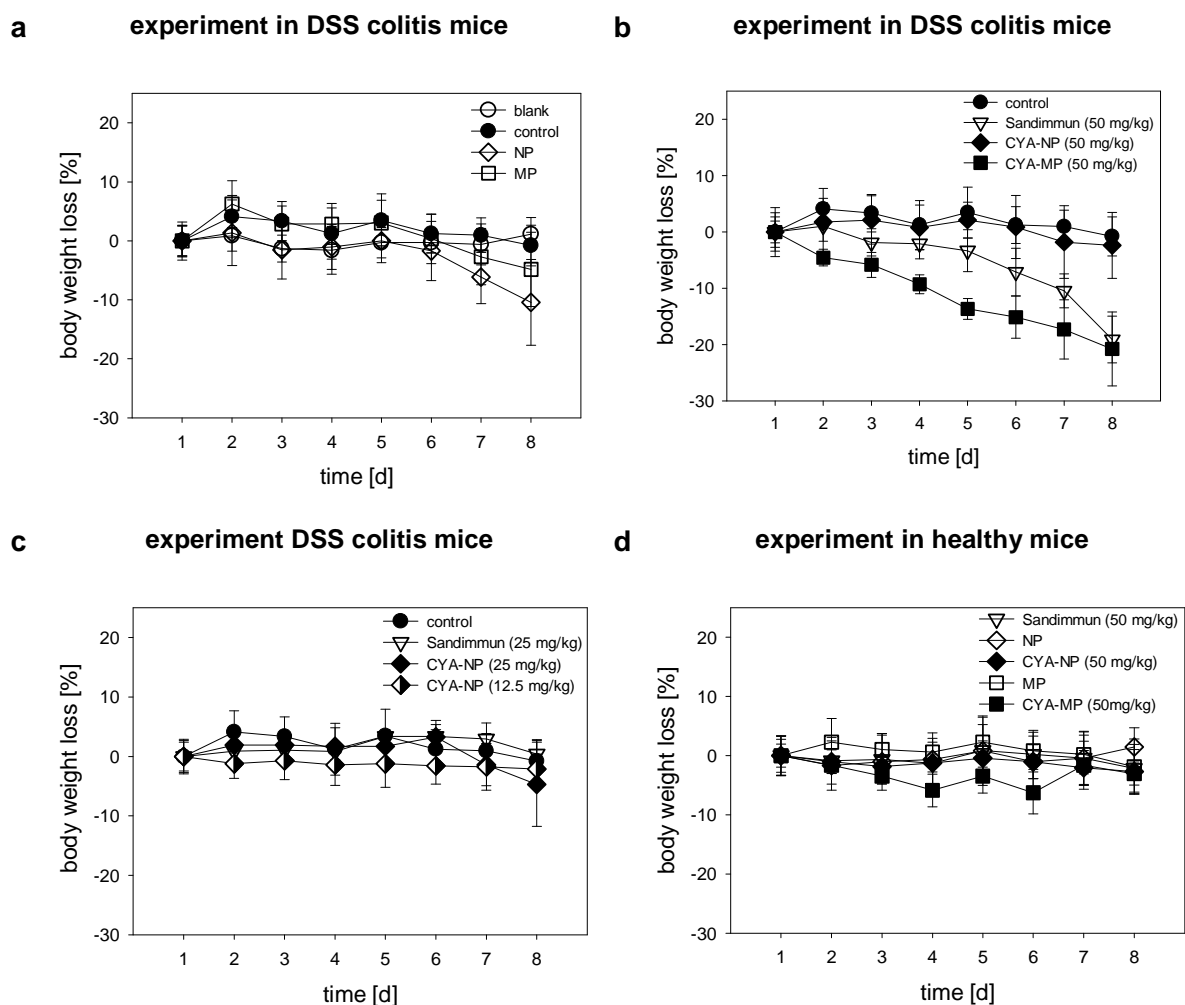


Figure 7.4. Body weight loss of (a) control mice, blank mice and DSS colitis mice receiving drug free NPs and MPs, (b) DSS colitis mice receiving Sandimmun, CYA-NPs and CYA-MPs at 50 mg/kg, (c) DSS colitis mice receiving Sandimmun (25 mg/kg) and NPs at 25 mg/kg and at 12.5 mg/kg, (d) healthy mice receiving Sandimmun, CYA-NPs, CYA-MPs and drug free NPs and MPs at 50 mg/kg. The data were presented as mean \pm S.D. ($n \geq 6$).

Drug free MPs (Figure 7.4a) showed a slight body weight reduction in DSS colitis mice compared to the administration in the healthy mice (Figure 7.4d). For the drug free NPs a stronger weight reduction starting at day 6 to day 7 was observed. Sandimmun at 50 mg/kg (Figure 7.4b) induced body weight reduction starting at day 2 and reduced dramatically the body weight after day 5, whereas no change in the body weight was determined for administration of 25 mg/kg Sandimmun (Figure 7.4c). The Sandimmun (50 mg/kg) group was silent in behaviour and the fur was shaggy. One mouse died at day 3. All groups that received Sandimmun were more active than the blank mice.

For the mice receiving CYA-NPs (50 mg/kg), only a slight reduction, less than for Sandimmun, from day 5 to day 8 was determined comparable to control mice (Figure 7.4b). One mouse died at day 7, although all mice had a normal behaviour and fur. Unfortunately, CYA-MPs administered in DSS colitis mice decreased the body weight dramatically up to 20% loss of the initial weight starting at day 2 (Figure 7.4b). The group was silent in behaviour and the fur was shaggy. Furthermore, a reduced water intake was determined. Also CYA-NPs administered at a dose of 25 mg/kg reduced the body weight in a slightly higher value starting at day 5 than the control mice and Sandimmun at 25 mg/kg (Figure 7.4c). The body weight of DSS colitis mice receiving CYA-NPs at a dose of 12.5 mg/kg was positively constant over the whole experiment, but the fur of the mice was light shaggy.

All healthy mice treated with Sandimmun or particles, both drug free and loaded, showed no effect on body weight, except the CYA-MPs, which showed a light fluctuation between day 4 and day 6 (Figure 7.4d). The administration to healthy mice intended to assess the safety of the particles as drug vehicle.

Disease activity index

The stool consistency and rectal bleeding were recorded daily and scored with the body weight as DAI. The mean of these scores was forming the clinical score ranging from 0 (healthy) to 4 (maximal activity of colitis) as presented in Figure 7.5. No statistical significance could be determined. The control mice developed diarrhea starting at day 2, which is typical for the colitis model. All other groups receiving DSS started to develop semi-formed stools between day three and day four.

Sandimmun administered at 25 mg/kg and 50 mg/kg, as well as drug free NPs and MPs and CYA-NPs at 12.5 mg/kg, showed no improvement in the DAI compared to control mice (Figure 7.5).

All other groups receiving CYA-NPs showed a reduced DAI, in particular the 25 mg/kg dosing regime. CYA-MPs at 50 mg/kg showed a worsening in the DAI compared to the control mice.

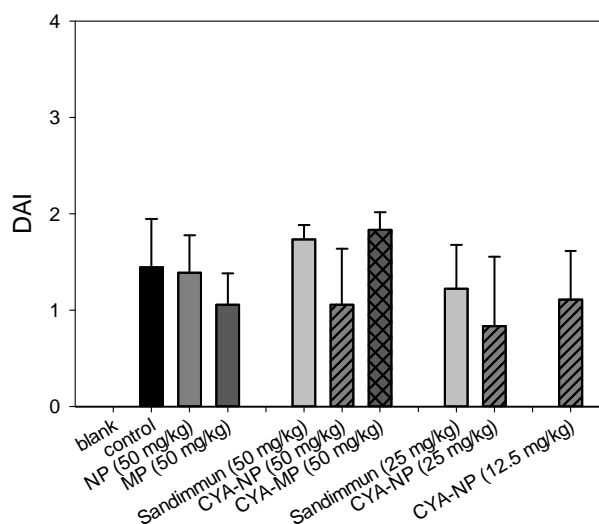


Figure 7.5. Effect of treatment presented as disease activity index (DAI). DAI is expressed as means of score (mean \pm S.D.) of body weight loss, stool consistency and rectal bleeding, ranging from 0 (healthy) to 4 (maximal activity of colitis) according to Mladenovska et al. [84]. No weight loss was counted as 0 points, 1–5% as 1 point, 5–10% as 2 points, 10–20% as 3 points and >20% as 4 points. For stool consistency 0 point was given for well-formed pellets, 2 points for pasty and semi-formed stools that did not stick to the anus and 4 points were given for liquid stools that stick to the anus. Bleeding was scored as 0 point for no blood, 2 points for positive finding and 4 points for gross bleeding.

7.4.5. Clinical parameters - Colon length and weight/length ratio

For this model, the colon length is the main marker for indicating an efficient developed colitis. A shortening of the colon indicates a progression of disease. To test a possible negative effect of the particles in the mice, all healthy mice were treated with Sandimmun and particles, both drug free and CYA loaded, showing no significant change in colon length (Figure 7.6a).

All results of the colon length for the diseased mice are summarized in Figure 7.6b. Sandimmun does not influence the colon length at a dose of 50 mg/kg, whereas an increase in colon length was observed for 25 mg/kg. The drug free NPs also showed a slight increase, which is not significantly different from the control mice. The CYA-NPs at all concentrations increased significantly ($p < 0.001$) the colon length >8.4 cm, compared to Sandimmun at 50 mg/kg, but no dose dependency was observed.

CYA-NPs at 25 mg/kg showed a slight increase, which is not significant ($p=0.161$), in colon length compared to the same dose of Sandimmun.

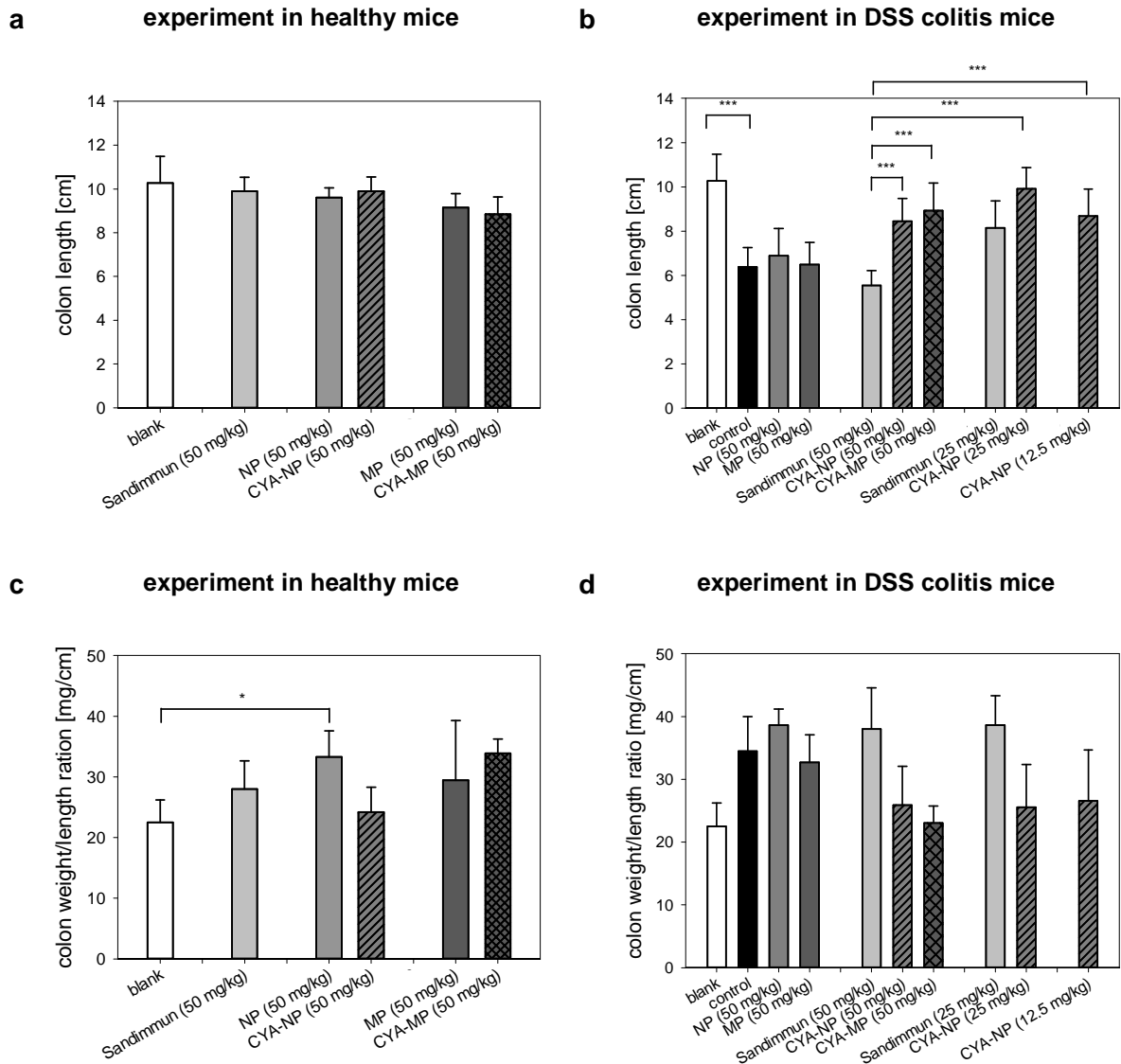


Figure 7.6. Colon length [cm] and colon weight/length ratio [mg/cm] of mice. (a) Colon length [cm] of healthy mice treated with NPs and MPs at different doses in comparison to blank mice and treatment with Sandimmun ($n \geq 6$). (b) Colon length [cm] of diseased mice treated with NPs and MPs at different doses in comparison to blank mice, control mice and administration of Sandimmun ($n \geq 6$). (c) Colon weight/length ratio [mg/cm] of healthy mice treated NPs and MPs in comparison to blank mice and administration of Sandimmun ($n \geq 3$). (d) Colon weight/length ratio [mg/cm] of diseased mice treated with NPs and MPs at different doses in comparison to blank mice, control mice and treatment with Sandimmun. The data were presented as mean \pm S.D. Statistical significance was assessed by ANOVA using Holm-Sidak for multiple comparison ($***p < 0.001$, $p^{**} < 0.01$, $p^* < 0.05$).

The drug free MPs had no effect on the colon length. The CYA-MPs showed a significant effect compared to Sandimmun (50 mg/kg, $p < 0.001$) and drug free MPs ($p = 0.012$) with an increased colon length of 8.8 ± 0.8 cm. CYA-NPs administered at 25 mg/kg showed an increase up to 9.9 ± 1.0 cm, which is comparable to the colon length of blank mice (10.2 ± 1.1 cm). CYA-NPs at 50 mg/kg increased the colon length to 8.1 ± 1.0 cm and CYA-NPs at 12.5 mg/kg to 8.7 ± 1.2 cm. All with CYA loaded particles treated mice show a significant recovery in colon length, CYA-NPs (50 mg/kg $p = 0.001$, 25mg/kg and 12.5 mg/kg $p < 0.001$) and CYA-MPs ($p = 0.001$), compared to Sandimmun (50 mg/kg).

The results for the colon weight/length ratio are summarized in Figure 7.6c for healthy mice and Figure 7.6d for DSS colitis mice. The marker combines the two effects, which occur under inflammation: shortening of colon length and increasing of colon weight due to development of edema. Healthy mice (Figure 7.6c) treated with Sandimmun, CYA-NPs, drug free and CYA-MPs show a slight increase, in colon weight/length ratio, which was not significant. Only drug free NPs show an increase in the ratio in healthy mice.

In Figure 7.6d diseased mice treated with Sandimmun, in both concentrations, further drug free NPs and MPs, show no significant difference in the weight/length ratio compared to the control mice. All CYA-NPs demonstrate values ~ 25 mg/cm for the colon weight/length ratio, which is near to the value of the blank mice (22.5 ± 3.7 mg/cm). Also the CYA-MPs had a colon weight/length ratio (23.0 ± 3.7 mg/cm), which is comparable to the blank mice.

7.4.6. Clinical parameter - Cytokine level

The results of the cytokine level in colon for the different cytokines are presented in Figure 7.7. For the pro-inflammatory cytokines no reduction could be reached for both concentrations of Sandimmun compared to control mice. CYA-NPs (25 mg/kg) show a reduction in IL-6 and TNF- α levels, but not in the IL-1 β level. IL-6 is also reduced by drug free and CYA-MPs compared to control. IL-4 is upregulated for Sandimmun at 50 mg/kg, drug free NPs and MPs and, furthermore, for CYA-MPs. For all concentrations of CYA-NPs IL-4 is significant downregulated compared to control mice and Sandimmun at 50 mg/kg. IL-10 is upregulated for Sandimmun at 25 mg/kg and CYA-NPs at 12.5 mg/kg compared to control mice.

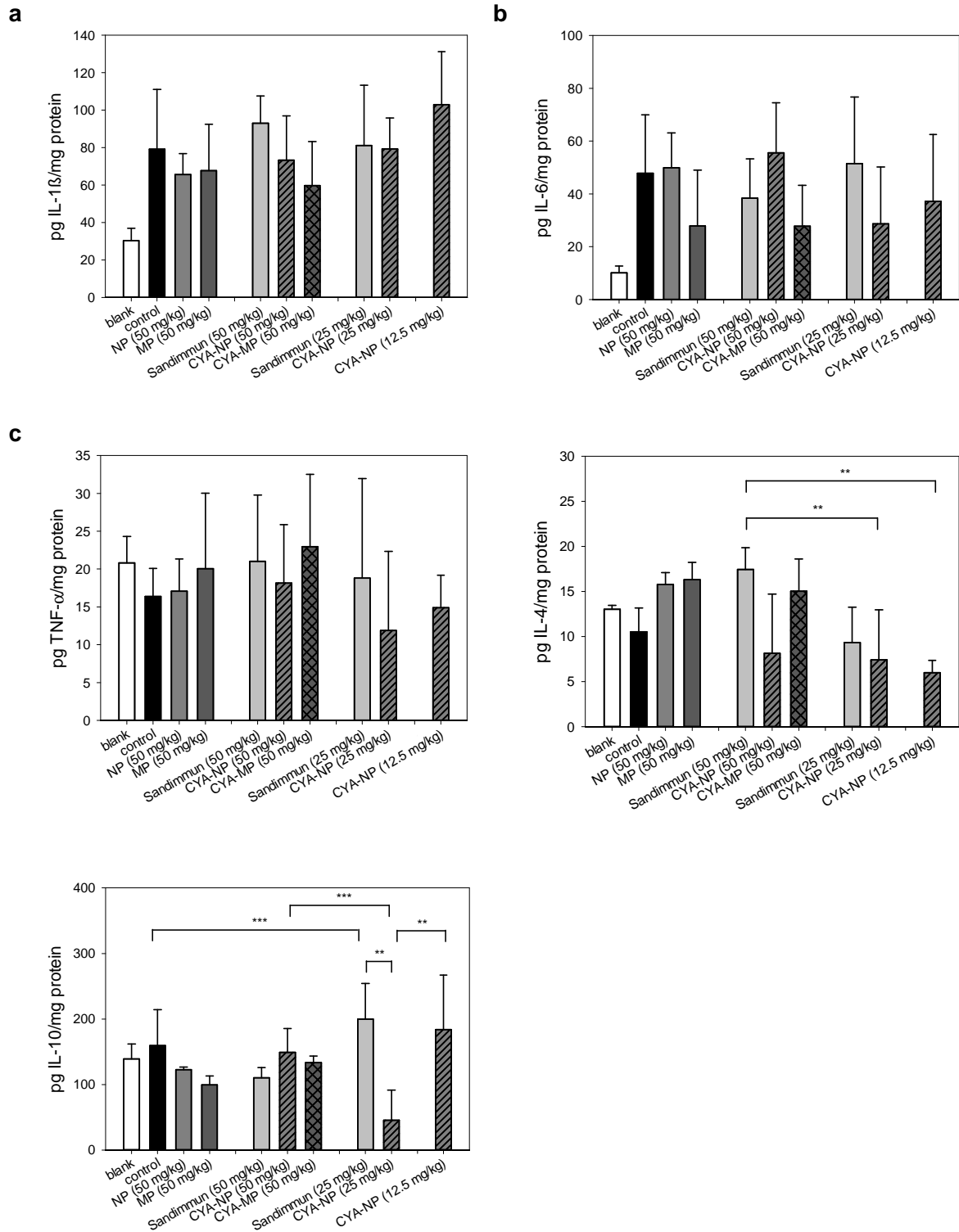


Figure 7.7. Cytokine levels in colon: IL-1 β , IL-6, TNF- α , IL-4 and IL-10. For the drug free particles an equal amount referring to the loaded particles at a dose of 50 mg/kg was used. The data were presented as mean \pm S.D. (n \geq 3). Statistical significance was assessed by ANOVA using Holm-Sidak for multiple comparison (***p<0.001, p**<0.01, p*<0.05).

7.4.7. Histological analysis

For the histopathological analysis colon samples were randomly investigated and representative microscopic images are presented in Figure 7.8 for all treatment groups in DSS colitis mice compared to blank mice and control mice. The histopathological score was also calculated and is summarized in Figure 7.9. The control mice (Figure 7.8b) show typical changes with a total loss of the colon architecture including mucosal ulcerations, crypt damage, and complete loss of villis, edema, and cell infiltration into mucosal tissue. Furthermore, the major affected part is the distal colon, which is typical for the DSS model. These changes resulted in a high histopathological score and reveal the functionality of the used DSS model. As expected before drug free NPs and MPs show a high score, which is higher in comparison to control mice (Figure 7.9).

The results demonstrate that all with CYA treated mice, except the CYA-MPs, have therapeutic and protective efficacy according to the histological analysis. For Sandimmun (50mg/kg) in Figure 7.8c the images reveal a medium destroyed *lamina propria* with signs of lost colon architecture and ulcerations, but some crypts are conserved. Cell infiltration can be seen only in the *lamina propria* and not in the submucosa.

The results are also comparable for Sandimmun at 25 mg/kg (Figure 7.8d). For CYA-NPs at 50 mg/kg and 25 mg/kg (Figure 7.8e and Figure 7.8g) only a slight inflammation with highly conserved crypts and slightly elongated villis, low cell infiltration and a conserved *lamina propria* could be determined. Both CYA-NP at 50 mg/kg and 25 mg/kg show a significant reduction in the histopathological score compared to control mice ($p=0.003$, $p=0.004$, respectively) and drug free NPs ($p<0.001$) (Figure 7.9). CYA-NPs (50 mg/kg) further reduce significantly (by ~25%) the score compared to Sandimmun (50 mg/kg). The results for CYA-NP administered at a dose of 25 mg/kg are comparable to a dose of 50 mg/kg, whereas for 12.5 mg the score increases (Figure 7.9).

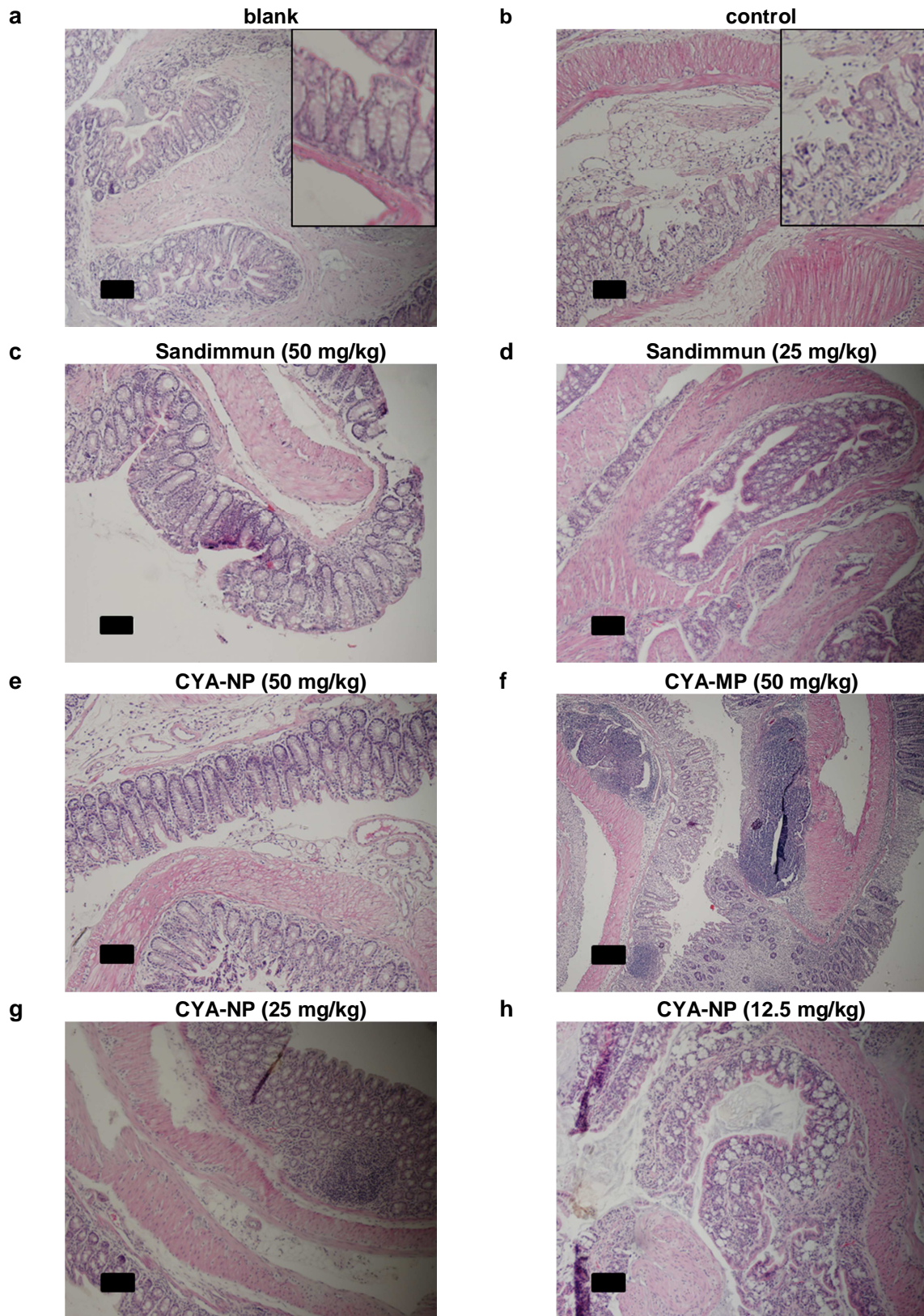


Figure 7.8. Histological manifestation in DSS colitis mice. Hematoxylin and eosin stained images of representative colons are shown at the same magnification (10x, scale bar=100 μ m).

The CYA-NPs at 12.5 mg/kg (Figure 7.8h) showed less anti-inflammatory effectiveness with severe inflammation including mild to moderate cell infiltration and mild crypt loss, but conserved colon architecture. The results for the CYA-MPs (Figure 7.8f) show a completely destroyed mucosa, elongated and destroyed villis and, furthermore, with immune related cells highly infiltrated lymph nodes. The CYA-MPs show a histopathological score equal to control.

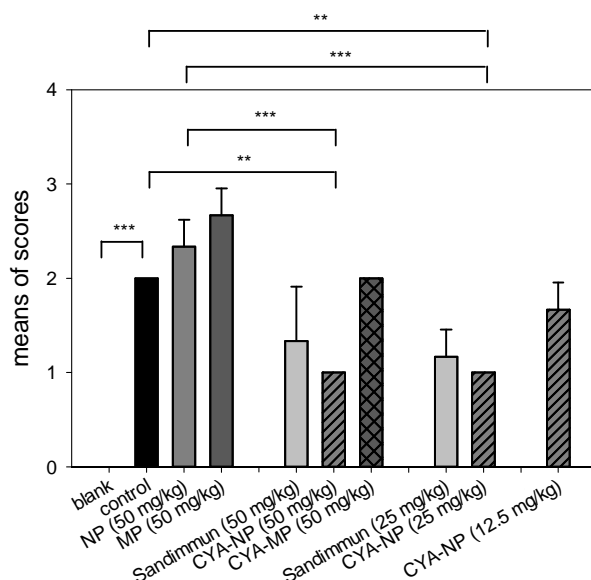


Figure 7.9. Histopathological score. The data were presented as mean ± S.D. (n=3). Statistical significance was assessed by ANOVA using Holm-Sidak for multiple comparison (***p<0.001, **p<0.10, *p<0.05).

7.4.8. Cyclosporine A level in plasma

The method was validated for mouse plasma samples with interday and intraday variation coefficient <3% for the concentration range of 5-100 µg/ml ($R^2=0.9989$) with a detection limit of 0.31 µg/ml, and a quantification limit of 1.05 µg/ml. For the samples from blank mice and control mice, as well as mice treated with drug free NPs and MPs, no CYA peak was detected, as it was expected. In the case of the mice treated with the different CYA formulations and doses, some differences could be observed. None of the NPs formulations provided any detectable CYA peak. Sandimmun at the dose of 25 mg/kg, provided detectable, but non-quantifiable concentrations of CYA. For the CYA-MPs and Sandimmun at the dose of 50 mg/kg, administered in DSS colitis mice, quantifiable CYA amounts were determined, 45.77 ± 0.83 µg/ml and 58.45 ± 0.17 µg/ml, respectively. The plasma concentrations were slightly lower in healthy mice with the intact mucosa, 42.57 ± 0.82 µg/ml for CYA-MPs and 53.71 ± 1.27 µg/ml for Sandimmun, both at 50 mg/kg.

7.5. Discussion

The DSS-induced acute colitis model in rodents is frequently used as a pre-clinical model to test drugs for IBD and had also been used to evaluate the efficacy of novel drug delivery strategies in recent studies [67], [125]. Among the chemically induced models of colitis, it has been extensively characterized and demonstrated to establish a robust colitis within four to eight days [123], [213]. Due to the toxicity to the gut epithelial cells of the basal crypts, DSS affects the integrity of the mucosal barrier with main features of the macroscopic and histological characteristics of human IBD, and is widely used to study epithelial repair mechanisms as well as the contribution of innate immune mechanisms [123]. One limitation of this model is the lack of involvement of the adaptive immune system in the pathogenesis of the inflammation [123], [125], [130]. The model shows inflammation only in caecum and colon and resembles to UC [125], [209]. Therefore, the model is the most adequate model among the chemically induced models to evaluate the efficacy of CYA loaded particles in this work.

In general, concentrations from 2-5% [128] of DSS in the drinking water can be applied to induce an acute colitis in rodents of different severity, which depends either on the used mice strain/breeder, molecular weight of DSS, or the different environmental factors in the laboratories [129], [209], [213], [214]. 2% enables to see clear differences, whereas 5% can induce colitis of high severity. For our ethical considerations high concentrations of DSS induces a too severe disease which is not needed to see the differences, therefore, 3% DSS were applied in this study.

CYA, a immunosuppressive calcineurin inhibitor, is applied to UC patients suffering from fulminant colitis and do not respond to intravenous corticosteroids [29]. The therapy is started intravenously (i.v.) for three to five days and typically continued with oral CYA often in co-medication with corticosteroids and azathioprine, or methotrexate for maintenance therapy [17]. The CYA therapy is associated with adverse effects when CYA is systemically available e.g. neurological toxicity, infections, renal dysfunction, nephrotoxicity and hypertension [17]. Therefore, patients would benefit from a drug delivery system that would deliver the encapsulated CYA directly to the inflamed areas of the intestine. Such a local treatment would ideally allow a dose reduction compared to a systemic application. Furthermore, high systemic concentrations would be avoided and, therefore, the side effects of the used drugs could be reduced. CYA is at the moment available as oral dosage form and also for i.v. injection. Therefore, the NPs and MPs were tested by oral gavage.

With the CYA-NPs at all concentrations a significant improvement in the marker colon length and colon weight/length ratio could be demonstrated, compared to Sandimmun (50 mg/kg and 25 mg/kg, Figure 7.6). The results from the histological analysis reveal that the histopathological changes such as total loss of the colon architecture including mucosal ulcerations, damage crypts and villis, edema, and cell infiltration are significantly reduced applying CYA-NPs compared to control and are overall better compared to Sandimmun. Interestingly, no dose dependency could be observed for the CYA-NPs, which was also reported in previous studies using a CYA solution [215]. Banić et al. demonstrated in a 2, 4-dinitrofluorobenzene colitis mouse model that CYA administered intraperitoneally had a concentration-dependent anti-inflammatory effect in contrast to an intracolonic administration. The latter should be addressed with the particles in this study. The CYA-NPs does not influence the body weight neither in healthy nor in DSS colitis mice and were, therefore, revealed as safe. Drug free NPs reduce the body weight in DSS animals. An effect which was not observed applying drug free MPs. Drug free NPs seem to have a negative effect on the inflammation, which is compensated by CYA encapsulated in NPs. The toxicity and immunotoxicity were tested before (chapter 6) and the performed tests would not raise concerns about the safety of the particles. Therefore, a physical effect of the particles could be assumed triggering the destruction of the mucosa as also the histopathological score was 15% higher compared to control. The body weight reduction might be due to the increased permeability of the upper intestinal mucosa of the mice based on the inflammation [41], [42]. In previous studies of our group, testing BU loaded NPs, such effect was not obvious [67]. Depending on the effective dose of CYA ranging in mg/kg, which is much higher as the applied BU 0.168 mg/kg, ~36.5 mg of particles had to be applied per day for the highest dose.

The CYA-MPs decreased strongly the body weight, indicating an intoxication of the animals by CYA as also the DSS-water intake was decreased in DSS colitis mice. The applied high dose of CYA (50 mg/kg) could lead to toxic effects as reported in previous studies applying 50 mg/kg [125], [215], and as could be seen in the body weight reduction of Sandimmun at 50 mg/kg compared to the CYA-MPs. By encapsulating the CYA in MPs and NPs achieving a controlled release, the toxicity of CYA should be reduced in this study due to the reduced systemic bioavailability of CYA. The CYA-NPs applied at 50 mg/kg show no intoxication and seems to have a protective effect, which can be associated with the release. The CYA-MPs release the encapsulated drug much faster (89.0 ± 9.3 % in 24 h, Figure 7.3) as compared to the CYA-NPs (67.1 ± 8.8 % in 24 h). The slower release demonstrates, therefore, a protective effect.

Apart from the reduction in body weight the CYA-MPs as well as the drug free MPs show a complete destroyed mucosa in the histopathological analysis (Figure 7.8 and Figure 7.9) equal to control mice and, therefore, further doses were not tested in this study. Nevertheless, the results revealed that both markers, colon weight and colon weight/length ratio, were significantly improved compared to control mice and Sandimmun, demonstrating, thus, absolute values which were comparable to CYA-NPs. In a future perspective the efficacy of MPs should be further investigated with a more slow and controlled release as a recent study revealed a high accumulation efficiency for MPs in human patients compared to NPs from the same material [76]. The negative effect of the MPs could be dependent on the animal species used for the experimental set-up, as suggested by Leonard et al., due to the different dimensions (e.g. the length of small intestine was determined to be <50 cm for mice compared to humans with 3-4 m) [88]. The MPs might damage the mucosa in the GIT of the mice during their transit time due to the inflexible PLGA matrix. Furthermore, particles prepared with different preparation processes should be evaluated to have an effect on the used model, as the change in the preparation method is often associated with a change in the used stabilizer. However, the MPs seems to be a promising approach and a change to a rat model with other dimensions would offer the possibility to test the particles with a modified release at lower concentrations [216].

The administration of DSS to the mice leads to an increased immune cell infiltration and, therefore, enhanced mucosal production of pro-inflammatory cytokines, IL-1 β and IL-6, from epithelial cells and immune competent cells, typical for the acute DSS model [130], [131]. IL-6 presents the intestinal inflammation, and IL-1 β and TNF- α are associated with a generic inflammation. For the pro-inflammatory TNF- α also an enhanced mucosal production was determined, which was also high for the blank mice and, therefore, an effect of the treatment groups could not be determined. Furthermore, the anti-inflammatory IL-4 was measured, which was equal for control mice and blank mice in this study [133]. CYA can have a paradoxical pro-inflammatory effect, which was described by Rafiee et al. and could influence the measured cytokine levels [217].

The model also allowed determining plasma levels to evaluate the systemic bioavailability of CYA. Sandimmun showed plasma concentrations only with the highest dose (50 mg/kg), being higher in diseased mice in comparison to healthy mice. The CYA-MPs showed quantifiable plasma concentrations, which were lower than those obtained for the Sandimmun. This is probably due to the controlled release, which was faster than the one provided by the NPs.

The plasma concentrations obtained from CYA-MPs (50 mg/kg) were also lower in healthy mice compared to diseased mice. None of the NPs showed any plasma profile of drug, confirming the hypothesis that the slow controlled release formulations reduce the access of drug to systemic circulation preventing severe side effects.

In summary, the DSS-induced colitis could be successfully treated with the CYA-NPs according to the data obtained for the investigated markers. Nevertheless, this model allows also measuring the CYA plasma levels. Therefore, the systemic bioavailability could be investigated, which was significantly reduced by encapsulation of CYA in NPs.

As Koboziev et al. resumed, a lot of potential drugs for an improved therapy of IBD were identified and only a few studies have been able to translate the results demonstrated in acute chemically induced models to chronic colitis mouse models [213]. However, testing the most promising particles, based on this study the CYA-NPs, in a chronic rodent colitis model should be addressed in a future perspective to underline the efficacy. In contrast to acute colitis, the chronic DSS-induced colitis is characterized by focal epithelial regeneration due to the destabilized intestinal repair mechanism and, moreover, by a T_H1 and T_H2 cytokine profile with increased mucosal IFN- γ and IL-4 levels [133].

7.6. Conclusion

CYA-NPs showed efficacy in the investigated parameters, colon length, colon weight/length ratio, and in the histological analysis and, moreover, reduced systemic bioavailability. Furthermore, they demonstrated a significant improvement compared to control and Sandimmun.

The CYA-MPs demonstrated effectiveness in colon length, colon weight/length ratio, but led to increased pathological changes of the mucosa. Furthermore, CYA-MPs led to an intoxication of CYA determined by a strong body weight reduction and shaggy fur, whereas the CYA-NPs had a protective effect by the encapsulation of the CYA.

Especially, the CYA-NPs, offer a promising therapeutic alternative for an improved treatment of IBD. Further *in vivo* studies should be performed based on the results of the systemic bioavailability (CYA plasma level). These studies should address the determination of the lowest effective dose and the evaluation of the CYA-NPs in a chronic model of the DSS-induced colitis, which is characterized by focal epithelial regeneration, and a T_H1 and T_H2 cytokine profile.

8. Summary and outlook

Inflammatory bowel disease (IBD) including Crohn's disease and ulcerative colitis are chronic, episodic, inflammatory disorders of the gastrointestinal tract. The classical medical therapy applying corticosteroids or immunosuppressant drugs via tablets or pellet systems is often inefficient mainly due to enhanced elimination of the dosage forms by diarrhea and, therefore, limited time for drug release. The reduction of dosage form size may help to minimize the fast clearance from the gastrointestinal tract increasing local drug concentrations in the inflamed tissues [53].

Nanoparticles (NPs) and microparticles (MPs) had shown to be able to remain in the ulcerated areas of the inflamed tissues for prolonged periods of time offering the possibility of a passive targeting approach [67], [75]–[77]. Furthermore, they can be entrapped in the mucus layer of the lumen [75]. A size-dependent accumulation of particulate drug delivery systems (DDS) in inflamed areas of the colonic mucosa in rats was previously demonstrated [75]. In contrast, a recent study revealed a higher accumulation efficacy of MPs in comparison to NPs in human patients [76]. The mechanism is not yet fully understood and has to be further investigated. However, it seems to be supported by an increased permeability of the inflamed epithelium and up-take of NPs into invading intestinal macrophages [41], [42], [76].

The major motivation of this work was to develop a small particulate polymeric DDS for oral/rectal administration for an improved therapy of IBD using reproducible and controllable preparation techniques. To improve the understanding of inflammation targeting by passive targeting as well as physico-chemical and biopharmaceutical properties of the DDS on the success of IBD therapy, a nanoparticulate and a microparticulate DDS were developed and both were compared. In both DDS the immunosuppressive drug cyclosporine A (CYA) and the anti-inflammatory drug budesonide (BU) were encapsulated. Both drugs were selected due to differences in their pharmacological and physico-chemical properties, and their effectiveness in the therapy of IBD.

This work was performed in the context of the ERA-Net EuroNanoMed project *Delivering Nanopharmaceuticals through Biological Barriers*, acronym 'BIBA', with a focus on the transfer of the preparation of particulate DDS to larger production scales in a future perspective. Therefore, established excipients and scaleable, robust methods for the preparation of the DDS were selected.

In the first part of this work a design of experiments (DOE) approach was applied to a nanoprecipitation method (NPR) and a nano spray drying technique (NSD) as processes for preparing poly (lactic-co-glycolic acid) (PLGA) NPs and MPs. In particular, the determination of the feasible size range, critical factors influencing particle size, size distribution or yield, and the robustness towards variations of the batch size were investigated. A fractional factorial design for response surface was applied to study the influence on continuous, categorical and discrete factors. The NPR yielded NPs (150-200 nm) with narrow size distributions (PDI <0.15). The polymer concentration was the main factor in this process, which was found to be very robust towards varying the batch size (0.625-50.0 ml). In contrast, the NSD, which yielded MPs (2-163 μm), is influenced by various factors and, therefore, more difficult to control and less robust towards varying the batch size (5-40 ml). By a factorial design approach to NPR, an equation could be derived, which allowed the prediction of several optimal formulations with defined particle sizes and distributions. It could be demonstrated that a DOE can be an optimal quality tool to optimize well known systems and to understand unknown processes as well as to achieve consistent quality of the DDS.

In size and size distribution optimized DDS were further improved for drug load for the selected lipophilic drugs CYA and BU. The loaded DDS were characterized in size and size distribution and *in vitro* release tests were performed. With the NSD high encapsulation efficiencies of ~90% were yielded for both drugs. For the NPR the encapsulation of CYA (67%) is more efficient than for BU (37%). From NPs and MPs different release profiles were obtained, which can be explained by the amorphous or crystalline status, determined by X-ray powder diffraction, as well as the lipophilicity of the drugs in the respective particles. In particular, both CYA loaded NPs and MPs demonstrated promising release profiles for the passive targeting approach. In addition, the CYA loaded MPs demonstrated the best controlled release profile. Moreover, a protocol for freeze-drying the nanoparticulate formulations was developed to obtain a storable product.

As the matrix of the spray dried MPs consists of PLGA and the stabilizer Span60, the question of the location or spatial distribution of the Span60 was addressed by a small angle X-ray scattering study. MPs measured in solid state showed a tension inside the particles, whereas in aqueous solution no tension could be detected leading to the conclusion of a clustered organisation of Span60 within the particles.

Furthermore, the ability to modify the MPs in release by blending the MPs with poly (ethylene glycol), using BU as model drug, was investigated. Additionally to modify the MPs in size, low molecular weight PLGA (2149 Da in comparison to 40,300 Da) was spray dried for the fabrication of MPs. By blending the MPs no improvement in the release could be achieved for the application approach. A strong burst release was determined already at small amounts of poly (ethylene glycol) and, furthermore, 25-32% of the encapsulated BU remained in the MPs. No change in size was determined by spraying PLGA with lower molecular weight due to the strong influence of the used stabilizer on size as revealed previously by the DOE.

The anti-inflammatory efficacy as well as the size-dependent accumulation of all optimal loaded NPs and MPs were evaluated on an *in vitro* three-dimensional cell culture model of the inflamed intestinal mucosa (triple culture model), consisting of Caco-2, THP-1 and MUTZ-3 cell lines. The transepithelial electrical resistance (TEER) and IL-8 levels were measured to monitor the anti-inflammatory effect of the particles. Furthermore, particles, which incorporated a far-red fluorescent dye (DID), were added to the triple culture model and visualized by confocal laser scanning microscopy to investigate the deposition of the particles. The anti-inflammatory effect was more significant after treatment with CYA loaded NPs and MPs compared to a CYA solution. However, the treatment with BU loaded NPs and MPs as well as drug free particles showed also an anti-inflammatory effect. NPs were deposited at the intercellular spaces and up-taken in Caco-2 cells, while MPs were detected at the cell walls indicating a size-dependent accumulation/deposition. It can be concluded that the deposited particles release the residual encapsulated drug leading to the improved anti-inflammatory effect.

Cytotoxicity and immunotoxicity studies were further applied on the drug free particles since an activation of the immune system by the particles could decrease the drug effect and lead to long-term medication. Hence, a WST-1 assay was performed to assess the cytotoxicity of particles on 3T3 mouse fibroblasts and on J774A.1 murine macrophages. Additionally, the complement system activation and the alteration, activation and suppression, of cytokine secretion (IL-6 and IL-12) of dendritic cells were investigated in appropriate *in vitro* assays to test the interference with the development of an immune response. The NPs and MPs show no toxicity in relevant concentrations for *in vitro* testing and no activation of the complement system was determined. The absence of detectable levels of IL-6 and IL-12 by incubation of dendritic cells in presence of the particles underlines the safety of the particles as they are not activating immune responses by themselves.

A concentration dependent suppression (NP: <0.05 mg/ml, MP: 0.01-0.5 µg/ml) of the IL-12 secretion was investigated and should be considered in further investigations. No result within the performed cytotoxicity and immunotoxicity testing would raise concerns about the safety of NPs and MPs.

Finally, both CYA loaded DDS were selected as most promising particles with regard to the investigated physico-chemical and biopharmaceutical properties, and *in vitro* parameters to enter *in vivo* studies in a chemically induced dextran sodium sulfate mouse model of acute colitis. NPs and MPs both loaded and drug free were orally applied by gavage at different concentrations to diseased and healthy mice, and compared to a commercially available product (Sandimmun[®] Neoral, Sandimmun). All particles were tested in healthy mice to evaluate the safety of the particles. Pathophysiological changes were recorded by clinical parameters: body weight, stool consistency, blood in stool, colon length, and colon weight/length ratio as well as colon histology. The CYA levels in plasma after sacrifice at day 8 were measured to determine the systemic bioavailability of the CYA from the particles. Furthermore, cytokine levels in colon of pro-inflammatory (IL-1 β , IL-6, TNF- α) and anti-inflammatory cytokines (IL-4, IL-10) were determined as indicators of inflammation status. The CYA loaded NPs showed efficacy in the investigated parameters, colon length, and colon weight/length ratio, and in the histological analysis, plus a reduced systemic bioavailability of the CYA. Furthermore, they showed a significant improvement compared to control and Sandimmun. The CYA loaded MPs demonstrated effectiveness in colon length, colon weight/length ratio, but led to increased pathological changes of the mucosa. Furthermore, the CYA loaded MPs led to intoxication with CYA determined by a strong body weight reduction and shaggy fur, whereas the CYA-NPs had a protective effect by the encapsulation of the CYA due to the reduced bioavailability.

Suggestions for future work

The present work revealed the potential of nano- and microparticulate DDS for an improved therapy for IBD demonstrating the need of the characterization of the used preparation techniques as well as *in vivo* and *in vitro* methods for the evaluation of the efficacy of the drug delivery systems.

Future work should focus on a novel, promising strategy for the encapsulation of BU to reduce the high burst release and to facilitate, therefore, the entrance of the BU loaded DDS to *in vivo* efficacy studies.

This could be achieved, e.g. (a) using swellable methacrylate copolymers for the encapsulation, or (b) by encapsulation in PLGA based nanocapsules consisting of an oily core surrounded by the PLGA. With the evaluated knowledge of the used NPR the particulate formulations could be easily transferred to the preparation with this method.

In an *in vitro* model of the inflamed intestinal mucosa and *in vivo* model of chemically induced colitis, in particular the CYA loaded DDS showed anti-inflammatory efficacy. However, the size-dependency could not be fully clarified in the present work. The *in vitro* triple culture model cannot be used to determine a deposition of particles in a mucus layer. In the *in vivo* model the MPs were less tolerated and no accumulation studies with fluorescent particles were performed.

Future work should focus on further *in vivo* studies in rodent models based on the results of the systemic bioavailability (CYA plasma level). These studies should address the determination of the lowest effective dose and evaluation of particles deposition using fluorescent particles. Furthermore, the DDS should be evaluated in a chronic model of chemically induced colitis, which is characterized by focal epithelial regeneration, and a T_H1 and T_H2 cytokine profile.

9. Zusammenfassung und Ausblick

Chronisch-entzündliche Darmerkrankungen (IBD) - Morbus Crohn und Colitis ulcerosa - sind chronische, episodisch auftretende, entzündliche Veränderungen des Darms. Die klassische medikamentöse Therapie mit Tabletten oder Pellet-Systemen, die Kortikosteroide oder Immunsuppressiva enthalten, ist oft ineffizient. In Folge des mit den Erkrankungen einhergehenden Durchfalls, wird die Transitzeit der Arzneiformen und damit auch der zur Verfügung stehende Zeitraum für die Arzneistofffreisetzung reduziert. Mit einer Verkleinerung der Arzneiformen könnte eine Verlängerung der Verweildauer im Darm erreicht werden [53].

Nano- und mikropartikuläre Arzneistoffträgersysteme (NP und MP) können in ulzerierten Regionen des entzündeten Darmgewebes akkumulieren und ermöglichen damit ein passives Targeting. Zudem können sich die NP und MP an der Mukusschicht des Darms anlagern [67], [75]–[77]. Eine optimale Zielgröße der partikulären Arzneistoffträgersysteme konnte bislang noch nicht klar definiert werden. Während NP sich in einem chemisch induzierten Rattenmodell der Kolitis verstärkt im ulzerierten Gewebe anreicherten, zeigten MP bei an IBD leidenden Patienten eine verstärkte Anreicherung in ulzerierten Gewebläsionen im Vergleich zu NP [76]. Der zugrunde liegende Mechanismus ist noch nicht vollständig geklärt. Vermutet wird ein Zusammenhang mit der erhöhten Permeabilität des entzündeten Epithels und eine damit verbundene Aufnahme der NP in Epithelzellen und Makrophagen, die in das entzündete Gewebe einwandern [41], [42], [76].

Zielsetzung dieser Arbeit war die Entwicklung von partikulären Arzneistoffträgersystemen, für eine verbesserte Therapie von entzündlichen Darmerkrankungen, unter der Verwendung von reproduzierbaren und kontrollierbaren Herstellungstechniken. Die partikulären Arzneistoffträgersysteme sollten sich vor allem für die orale/rektale Applikation eignen. Um ein besseres Verständnis für das Targeting-Prinzip mit NP und MP zu bekommen sowie den Einfluss von physikochemischen und biopharmazeutischen Eigenschaften der Arzneistoffträgersysteme auf den Erfolg der Therapie von IBD zu untersuchen, wurden jeweils ein nano- und ein mikropartikuläres Arzneistoffträgersystem entwickelt und miteinander verglichen.

Die Arzneistoffträgersysteme wurden, aufgrund ihrer bisherigen Effizienz in der Therapie von IBD, mit dem Immunsuppressivum Cyclosporin A (CYA) und dem Kortikosteroid Budesonid (BU) beladen.

Diese Arbeit wurde im Rahmen des ERA-Net EuroNanoMed Projektes *Delivering Nanopharmaceuticals through Biological Barriers* (Akronym „BIBA“) angefertigt, welches den Fokus auf eine spätere, potenzielle Übertragbarkeit der Formulierung auf einen industriellen Maßstab legte. Daher wurden etablierte Ausgangssubstanzen für die Herstellung der Arzneistoffträgersysteme, wie das Poly(lactid-co-Glycolid) (PLGA) ausgewählt sowie skalierbare, robuste Herstellungsmethoden angewandt.

Für die Herstellung der, auf PLGA basierenden, partikulären Arzneistoffträgersysteme wurden eine Nanopräzipitationsmethode (NPR) und die Nano-Sprühtrocknung (NSD) ausgewählt. Durch Anwendung statistischer Versuchsplanung (DOE) konnte für beide Methoden der mögliche Größenbereich, kritische Prozessfaktoren, die Partikelgröße, die Partikelgrößenverteilung und Partikelausbeute sowie die Robustheit bei der Variation der Chargengröße untersucht werden. Ein fraktioniertes Design (Response Surface) ermöglichte es zudem, den Einfluss von kontinuierlichen, kategorischen und diskreten Faktoren zu bestimmen. Mittels NPR konnten NP (150-200 nm) mit einer engen Größenverteilung ($PDI < 0.15$) hergestellt werden, wobei die Polymerkonzentration den Haupteinflussfaktor für die Partikelgröße und Partikelgrößenverteilung darstellt. Die NPR zeigte eine große Robustheit in der Variation der Chargengröße (0.625-50.0 ml) bei gleichbleibender Partikelgröße und Partikelgrößenverteilung. Mit der NSD konnten MP (2-163 μm) hergestellt werden, wobei der Prozess durch mehrere der untersuchten Faktoren beeinflusst wurde. In der Folge war dieser schwerer zu kontrollieren und zeigte sich zudem weniger robust in der Variation der Chargengröße (5-40 ml). Basierend auf den Ergebnissen der statistischen Versuchsplanung, konnte für die NPR eine Gleichung erstellt werden, mit deren Hilfe definierte Partikelgrößen und Partikelgrößenverteilungen vorausberechnet werden können. Somit erwies sich die statistische Versuchsplanung als erfolgreiche Methode zur Verbesserung bekannter Herstellungsprozesse wie der NPR und ermöglichte darüber hinaus ein besseres Verständnis für neuere und komplexere Methoden wie der NSD.

Die in Partikelgröße und Partikelgrößenverteilung optimierten partikulären Arzneistoffträgersysteme wurden anschließend mit CYA und BU beladen, und in ihrer Größe sowie Größenverteilung charakterisiert. Zudem wurden *in vitro* Freisetzungsprofile der NP und MP ermittelt. Um die, sich nach der Herstellung in Suspension befindlichen, NP in eine lagerbare Form zu bringen, wurde ergänzend eine Gefriertrocknungsmethode entwickelt. Für beide Arzneistoffe konnte bei der Beladung von MP eine hohe Einkapselungseffizienz erreicht werden (>90%). Für die NP wurde für die Beladung mit CYA (67%) eine höhere Einkapselungseffizienz im Vergleich zu BU (37%) erhalten.

Die Arzneistoffträgersysteme weisen für jeden Arzneistoff ein anderes Freisetzungsverhalten auf. Die mit CYA beladenen NP zeigen eine langsame Freisetzung des CYA. Die mit CYA beladenen MP setzen das CYA am besten kontrolliert frei. Dies beruht zum einen auf den kristallinen oder amorphen Anteilen des Arzneistoffes in den Arzneistoffträgersystemen, welche mit Röntgendiffraktometrie (XRD) bestimmt wurden, und zum anderen auf der Lipophilie der verwendeten Arzneistoffe.

Die Untersuchung der sprühgetrockneten MP mit Röntgenkleinwinkelstreuung (SAXS) sollte Aufschluss geben über die Lokalisation des Stabilisator Span 60 in der Matrix der PLGA MP. Beim Vergleich der Vermessung der MP in Lösung und in Pulverform ergab sich eine Spannung in den Partikeln in Pulverform, die auf eine nicht-homogene Verteilung des Span60 zurückzuführen ist. Zudem wurde versucht, die Freisetzung aus den MP am Beispiel von BU durch das Verblenden der Partikel mit Polyethylenglykol zu erreichen. Hier konnte keine Verbesserung erzielt werden, da eine sehr schnelle Freisetzung des BU innerhalb der ersten Stunde erfolgte, und zudem 25-32% des BU nach 24 h in den Partikeln verbleibt. Auch eine Verringerung der Größe der MP, unter Verwendung von PLGA eines geringeren Molekulargewichtes, führte nicht zum angestrebten Erfolg.

Die anti-entzündlichen Eigenschaften der Arzneistoffträgersysteme sowie die größenabhängige Deposition, wurden *in vitro* in einem drei-dimensionalen Zellkulturmodell der entzündeten Darmmukosa, bestehend aus Caco-2, THP-1 und MUTZ-3 Zelllinien, untersucht. Der transendotheliale elektrische Widerstand (TEER) und die IL-8 Level im Zellkulturmedium dienten dabei als Marker für anti-entzündliche Effizienz. Die Deposition von mit dem Fluoreszenzfarbstoff DID beladenen NP und MP wurde mittels konfokaler Laser-Scanning-Mikroskopie bestimmt. Beladene und unbeladene Arzneistoffträgersysteme zeigten einen anti-entzündlichen Effekt. Dieser war für mit CYA beladene NP und MP signifikant besser. Ergänzend konnte gezeigt werden, dass NP in Caco-2 Zellen aufgenommen wurden und sich in den Zellzwischenräumen ablagern, wohingegen MP auf den Caco-2 Zellen akkumulieren, was auf einen größenabhängigen Effekt hindeutet.

In einem weiteren Schritt wurde die Zytotoxizität und Immunotoxizität unbeladener NP und MP untersucht, da eine Aktivierung des Immunsystems mit Therapieversagen assoziiert sein kann. Für die Zytotoxizitätsstudien mittels WST-1 Assay erfolgte die Testung auf murinen Makrophagen- (J774A.1) und Fibroblasten-Zelllinien (3T3). Zur Bestimmung der Immunotoxizität wurden die Komplementaktivierung sowie die Beeinflussung der Zytokinsekretion (IL-6 und IL-12) dendritischer Zellen untersucht.

Die NP und MP zeigten weder zytotoxische Effekte auf den getesteten Zelllinien in relevanten Konzentrationen, noch eine Aktivierung des Komplementsystems. Die Abwesenheit von nicht-detektierbaren Zytokinleveln unterstreicht zudem die Sicherheit der Arzneistoffträgersysteme, da sie selbst keine Immunantwort auslösen. Eine konzentrationsabhängige Unterdrückung (NP: <0.05 mg/ml, MP: 0.01-0.5 µg/ml) der IL-12 Ausschüttung konnte festgestellt werden und sollte für weitere Untersuchungen berücksichtigt werden.

In Kombination mit den physikochemischen und biopharmazeutischen Eigenschaften, zeigten sich insbesondere die mit CYA beladenen MP und NP am besten geeignet für die *in vivo* Testung in einem Mausmodell der Dextran-Natriumsulfat-induzierten, akuten Kolitis. In diesem wurden die CYA beladenen NP und MP im Vergleich zu unbeladenen Arzneistoffträgersystemen sowie einem kommerziell erhältlichen Produkt (Sandimmun® Neoral, Sandimmun) getestet. Die pathophysiologischen Veränderungen des Modells wurden anhand der Parameter Körpergewicht, Stuhlkonsistenz, Auftreten von rektalen Blutungen, Kolonlänge, Kolon Gewichts/Längenverhältnis und Kolonhistologie untersucht. Zudem wurden die CYA Plasmalevel nach der letzten Verabreichung der Formulierungen gemessen. Um den Entzündungsstatus zu bestimmen, wurden die Level an pro-inflammatorischen (IL-1β, IL-6, TNF-α) und anti-inflammatorischen (IL-4, IL-10) Zytokinen im Kolon gemessen. Insbesondere die mit CYA beladenen NP zeigten, durch eine reduzierte systemische Verfügbarkeit des Arzneistoffes, eine signifikante Verbesserung in den charakteristischen Parametern Kolonlänge, Kolon Gewichts/Längenverhältnis sowie in der histologischen Analyse, im Vergleich zu Sandimmun und erkrankten, unbehandelten Mäusen. Die mit CYA beladenen MP zeigten eine Verbesserung in den Parametern Kolonlänge, Kolon Gewichts/Längenverhältnis, aber auch verstärkte pathophysiologische Veränderungen in der histologischen Analyse. Zudem wird bei der Verabreichung der MP durch die schnelle systemische Verfügbarkeit von CYA, eine Intoxikation mit CYA vermutet. Dies äußerte sich in einer starken Gewichtsveränderung sowie einer Veränderung des Fells der Mäuse. Ein protektiver Effekt hingegen zeigte sich, bei den mit CYA beladenen NP, durch die reduzierte systemische Verfügbarkeit.

Ausblick

Die vorliegende Arbeit zeigt das Potenzial von nano- und mikropartikulären Arzneistoffträgersystemen für eine verbesserte Therapie von IBD. Zudem wird die Notwendigkeit der Charakterisierung der verwendeten Herstellungsmethoden sowie die Verwendung von *in vivo* und *in vitro* Modellen für die Bewertung der Effizienz der Arzneistoffträgersysteme verdeutlicht.

Zukünftige Forschungsanstrengungen sollten sich auf eine verbesserte Strategie der Verkapslung von BU z. B. unter der Verwendung von quellbaren Methacrylsäure-Copolymeren oder durch die Herstellung von Nanokapseln konzentrieren, um eine kontrollierte Freisetzung zu erhalten und damit die Testung dieser Formulierungen in *in vivo* Studien zu ermöglichen. Mit dem Wissen über die Kontrollierbarkeit der NPR könnte dieses für den Transfer z. B. der Nanokapseln auf eine bestimmte Größe angewendet werden.

In den verwendeten *in vitro* und *in vivo* Modellen zeigten speziell die mit CYA beladenen Arzneistoffträgersysteme eine anti-entzündliche Effizienz. Jedoch konnte der größenabhängige Effekt nicht weiter bestätigt werden. Daher sollten zukünftige Studien in weiteren Nagermodellen durchgeführt werden sowie die niedrigste effektive Dosierung und die Deposition der NP und MP im Kolon evaluiert werden. Zudem sollte die Effizienz der Arzneistoffträgersysteme in einem chronisch entzündlichen Modell der Kolitis getestet werden, welches durch eine Regeneration des Epithels und durch ein T_H1 und T_H2 Zytokinprofil charakterisiert ist.

10. List of abbreviations

A	absorbance
ADME	absorption, distribution, metabolism and excretion
ANOVA	analysis of variance
API	active pharmaceutical ingredient
ATCC	American Type Culture Collection
BU	budesonide
Büchi B-90	Büchi Nano Spray Dryer B-90
CD	Crohn's disease
CLSM	confocal laser scanning microscopy
COX-2	cyclooxygenase-2
CYA	cyclosporine A
CYP	cytochrome P450
Da	Dalton
DAI	disease activity index
DCM	dichloromethane
DDS	drug delivery systems
DID	1,1'-dioctadecyl-3,3',3'-tetramethylindodicarbocyanine perchlorate
DOE	design of experiments
DSMZ	Deutsche Sammlung von Mikroorganismen und Zellkulturen
DSS	dextran sodium sulfate
EDTA	ethylenediaminetetraacetic acid
EE	encapsulation efficiency
EMA	European Medicines Agency
FBS	fetal bovine serum
FDA	Food and Drug Administration
GIT	gastrointestinal tract
GWAS	genome wide association studies
IBD	inflammatory bowel disease
IL	interleukin
IFN	interferon
iNOS	inducible nitric oxide synthases
i.v.	intravenous
HPLC	high-performance liquid chromatography

LOD	lower limit of detection
LOQ	lower limit of quantification
LPS	lipopolysaccharides LPS
NEAA	non-essential amino acids
NFAT	nuclear factor of activated T cells
NF- κ B	nuclear transcription factor kappaB
NP	nanoparticle
NPR	nanoprecipitation method
NSD	nano spray drying technique
MECS	Material Engineering Center Saarland
MP	microparticle
MW	molecular weight
MWCO	molecular weight cut-off
PEG	polyethylene glycol
PBS	phosphate buffered saline
Ph. Eur.	European Pharmacopeia
PDI	polydispersity index
Pen/Strep	Penicillin/Streptomycin
PLGA	poly (lactic-co-glycolic acid)
PMA	phorbol myristate acetate
PVA	polyvinyl alcohol
R	run
SAXS	small angle x-ray scattering
S.D.	standard deviation
SEM	scanning electron microscopy
SGF	simulated gastric fluid
Span60	sorbitan monostearate
TEER	transepithelial electrical resistance
T _g	glass-transition temperature
T _H	T helper cell
TNBS	trinitrobenzenesulfonic acid
TNF- α	tumor necrosis factor- α
UC	ulcerative colitis
USP	United States Pharmacopeia
WHO	World Health Organization

XRD	X-ray powder diffraction
ZP	zeta potential

11. Bibliography

- [1] E. Loftusjr, "Clinical epidemiology of inflammatory bowel disease: incidence, prevalence, and environmental influences," *Gastroenterology*, vol. 126, no. 6, pp. 1504–1517, May 2004.
- [2] Kompetenznetz chronisch entzündliche Darmerkrankungen e.V., "Darmerkrankungen: Chronisch oder temporär?," 2014. [Online]. Available: <http://www.kompetenznetz-ced.de/darmerkrankungen.html>.
- [3] J. C. Preiß and R. Duchmann, "Neue Therapieverfahren bei chronisch-entzündlichen Darmerkrankungen," *Der Gastroenterologe*, vol. 2, no. 6, pp. 423–429, Oct-2007.
- [4] F. Grimpén and P. Pavli, "Advances in the management of inflammatory bowel disease.," *Intern. Med. J.*, vol. 40, no. 4, pp. 258–64, Apr. 2010.
- [5] D. C. Baumgart and W. J. Sandborn, "Inflammatory bowel disease: clinical aspects and established and evolving therapies," *Lancet*, vol. 369, pp. 1641–1657, 2007.
- [6] T. Jess, E. V Loftus, F. S. Velayos, W. S. Harmsen, A. R. Zinsmeister, T. C. Smyrk, C. D. Schleck, W. J. Tremaine, L. J. Melton, P. Munkholm, and W. J. Sandborn, "Risk of intestinal cancer in inflammatory bowel disease: a population-based study from olmsted county, Minnesota.," *Gastroenterology*, vol. 130, no. 4, pp. 1039–46, Apr. 2006.
- [7] C. N. Bernstein, A. Wajda, and J. F. Blanchard, "The clustering of other chronic inflammatory diseases in inflammatory bowel disease: a population-based study.," *Gastroenterology*, vol. 129, no. 3, pp. 827–36, Sep. 2005.
- [8] DCCV e.V. Deutsche Morbus Crohn/ Colitis ulcerosa Vereinigung, "Morbus Crohn und Colitis ulcerosa," *Medizinische Grundlagen*, 2011. [Online]. Available: <https://www.dccv.de/betroffene-angehoerige/medizinische-grundlagen/>.
- [9] A. M. Barrie and S. E. Plevy, "The interleukin-12 family of cytokines: Therapeutic targets for inflammatory disease mediation," *Clin. Appl. Immunol. Rev.*, vol. 5, no. 4, pp. 225–240, Jul. 2005.
- [10] W. Strober and I. J. Fuss, "Proinflammatory cytokines in the pathogenesis of inflammatory bowel diseases.," *Gastroenterology*, vol. 140, no. 6, pp. 1756–67, May 2011.
- [11] I. Atreya, R. Atreya, and M. F. Neurath, "NF-kappaB in inflammatory bowel disease.," *J. Intern. Med.*, vol. 263, no. 6, pp. 591–6, Jun. 2008.
- [12] E. Giner, I. Andújar, M. C. Recio, J. L. Ríos, J. M. Cerdá-Nicolás, and R. M. Giner, "Oleuropein ameliorates acute colitis in mice.," *J. Agric. Food Chem.*, vol. 59, no. 24, pp. 12882–92, Dec. 2011.
- [13] N. A. Molodecky and G. G. Kaplan, "Environmental Risk Factors for Inflammatory Bowel Disease," *Gastroenterol. Hepatol. (N. Y.)*, vol. 6, no. 5, pp. 339–346, 2010.
- [14] B. Khor, A. Gardet, and R. J. Xavier, "Genetics and pathogenesis of inflammatory bowel disease.," *Nature*, vol. 474, no. 7351, pp. 307–17, Jun. 2011.

-
- [15] J. Wehkamp, J. Harder, M. Weichenthal, M. Schwab, E. Schäffeler, M. Schlee, K. R. Herrlinger, a Stallmach, F. Noack, P. Fritz, J. M. Schröder, C. L. Bevins, K. Fellermann, and E. F. Stange, "NOD2 (CARD15) mutations in Crohn's disease are associated with diminished mucosal alpha-defensin expression.," *Gut*, vol. 53, no. 11, pp. 1658–64, Nov. 2004.
- [16] C. Abraham and J. H. Cho, "Mechanisms of disease: Inflammatory bowel disease," *N. Engl. J. Med.*, vol. 361, pp. 2066–2078, 2009.
- [17] K. Herrlinger, B. Wittig, and E. F. Stange, "Chronic inflammatory intestinal diseases. Pathophysiology and therapy," *Internist (Berl.)*, vol. 50, no. 10, pp. 1229–46, Oct. 2009.
- [18] E. Lindberg, C. Tysk, K. Andersson, and G. Jarnerot, "Smoking and inflammatory bowel disease. A case control study," *Gut*, no. 29, pp. 352–357, 1988.
- [19] P. G. Persson, A. Ahlbom, and G. Hellers, "Inflammatory bowel disease and tobacco smoke - a case-control study," *Gut*, vol. 31, no. 12, pp. 1377–1381, 1990.
- [20] D. T. Rubin and S. B. Hanauer, "Smoking and inflammatory bowel disease," *European Journal of Gastroenterology and Hepatology*, vol. 12, no. 8. pp. 855–862, 2000.
- [21] E. V Loftus, "Clinical epidemiology of inflammatory bowel disease: incidence, prevalence, and environmental influences," *Gastroenterology*, vol. 126, no. 6, pp. 1504–1517, May 2004.
- [22] B. M. Calkins, "A Meta-Analysis of the Role of Smoking in Inflammatory Bowel Disease," *Dig. Dis. Sci.*, vol. 34, no. 12, pp. 1841–1854, 1989.
- [23] K. Aktories, U. Förstermann, F. Hofmann, and K. Starke, *Allgemeine und spezielle Pharmakologie und Toxikologie*, 5th ed. Elsevier GmbH, Urban & Fischer Verlag, 2005.
- [24] A. C. Ford, C. N. Bernstein, K. J. Khan, M. T. Abreu, J. K. Marshall, N. J. Talley, and P. Moayyedi, "Glucocorticosteroid therapy in inflammatory bowel disease: systematic review and meta-analysis.," *Am. J. Gastroenterol.*, vol. 106, no. 4, pp. 590–9; quiz 600, Apr. 2011.
- [25] G. R. Lichtenstein, "Current Research in Crohn ' s Disease and Ulcerative Colitis : Highlights from the 2010 ACG Meeting," vol. 6, no. 12, p. Supplement 17, 2010.
- [26] S. B. Hanauer, B. G. Feagan, G. R. Lichtenstein, L. F. Mayer, S. Schreiber, J. F. Colombel, D. Rachmilewitz, D. C. Wolf, A. Olson, W. Bao, P. Rutgeerts, and I. S. Group, "Maintenance infliximab for Crohn' s disease : the ACCENT I randomised trial," *Lancet*, vol. 359, pp. 1541–1549, 2002.
- [27] K. L. Isaacs, J. D. Lewis, W. J. Sandborn, B. E. Sands, and S. R. Targan, "State of the art: IBD therapy and clinical trials in IBD.," *Inflamm. Bowel Dis.*, vol. 11 Suppl 1, no. November, pp. S3–12, Nov. 2005.
- [28] S. Targan, S. Hanauer, S. J. H. van Deventer, L. Mayer, H. D. Present, T. Braakman, K. de Woody, T. Schaible, and P. J. Rutgeerts, "A short-term study of chimeric monoclonal antibody cA2 to tumor necrosis factor a for crohn's disease," *N. Engl. J. Med.*, vol. 337, pp. 1029–1035, 1997.
- [29] A. C. Ford, W. J. Sandborn, K. J. Khan, S. B. Hanauer, N. J. Talley, and P. Moayyedi, "Efficacy of biological therapies in inflammatory bowel disease: systematic review and meta-analysis.," *Am. J. Gastroenterol.*, vol. 106, no. 4, pp. 644–59, quiz 660, Apr. 2011.

-
- [30] H. Lüllmann, K. Mohr, and L. Hein, *Taschenatlas Pharmakologie*, 4th ed. Stuttgart: Georg Thieme Verlag, 2004, pp. 306–308.
- [31] D. Steinhilber, M. Schubert-Zsilavec, and H. J. Roth, *Medizinische Chemie*. Stuttgart: Deutscher Apotheker Verlag Stuttgart, 2005.
- [32] S. Lichtiger, H. D. Present, A. Kornbluth, I. Gelernt, J. Bauer, G. Galler, F. Michelassi, and S. Hanauer, “Cyclosporine in severe ulcerative colitis refractory to steroid therapy,” *N. Engl. J. Med.*, vol. 330, no. 26, pp. 1841–1845, 1994.
- [33] Novartis Pharmaceuticals Corporation, “Fachinformation: Sandimmune ® Soft Gelatin Capsules.” p. 20, 2013.
- [34] B. D. Kahan, J. Dunn, C. Fitts, D. Van Buren, D. Wombolt, R. Pollak, R. Carson, J. W. Alexander, M. Choc, R. Wong, and D. S. Hwang, “Reduced inter- and intrasubject variability in cyclosporine pharmacokinetics in renal transplant recipients treated with a microemulsion formulation in conjunction with fasting, low-fat meals, or high-fat meals,” in *Transplantation*, 1995, vol. 59, no. 4, pp. 505–511.
- [35] L. B. Lopes, J. H. Collett, and M. V. L. B. Bentley, “Topical delivery of cyclosporin A: An in vitro study using monoolein as a penetration enhancer,” *Eur. J. Pharm. Biopharm.*, vol. 60, pp. 25–30, 2005.
- [36] U. B. Kompella, N. Bandi, and S. P. Ayalasomayajula, “Subconjunctival nano- and microparticles sustain retinal delivery of budesonide, a corticosteroid capable of inhibiting VEGF expression,” *Investig. Ophthalmol. Vis. Sci.*, vol. 44, pp. 1192–1201, 2003.
- [37] P. L. Kozuch and S. B. Hanauer, “Treatment of inflammatory bowel disease: a review of medical therapy,” *World J. Gastroenterol.*, vol. 14, no. 3, pp. 354–77, Jan. 2008.
- [38] G. Greenberg, B. G. Feagan, F. Martin, L. R. Sutherland, A. B. R. Thomson, C. N. Williams, L.-G. Nilsson, and T. Persson, “Oral Budesonide for active Crohn’s disease,” *N. Engl. J. Med.*, 1994.
- [39] H. Ali, E.-M. Collnot, M. Windbergs, and C.-M. Lehr, “Nanomedicines for the treatment of inflammatory bowel diseases,” *Eur. J. Nanomedicine*, vol. 5, no. 1, pp. 23–38, Jan. 2013.
- [40] N. J. Talley, M. T. Abreu, J.-P. Achkar, C. N. Bernstein, M. C. Dubinsky, S. B. Hanauer, S. V Kane, W. J. Sandborn, T. A. Ullman, and P. Moayyedi, “An evidence-based systematic review on medical therapies for inflammatory bowel disease,” *Am. J. Gastroenterol.*, vol. 106 Suppl, no. S1, pp. S2–25; quiz S26, Apr. 2011.
- [41] W. Fries, E. Mazzon, S. Squarzone, A. Martin, D. Martines, A. Micali, G. C. Sturniolo, S. Citi, and G. Longo, “Experimental colitis increases small intestine permeability in the rat,” *Lab. Invest.*, vol. 79, no. 1, pp. 49–57, 1999.
- [42] K. Teahon, S. Somasundaram, T. Smith, I. Menzies, and I. Bjarnason, “Assessing the site of increased intestinal permeability in coeliac and inflammatory bowel disease,” *Gut*, vol. 38, no. 6, pp. 864–869, Jun. 1996.
- [43] E.-M. Collnot, H. Ali, and C.-M. Lehr, “Nano- and microparticulate drug carriers for targeting of the inflamed intestinal mucosa,” *J. Control. Release*, vol. 161, no. 2, pp. 235–46, Jul. 2012.

- [44] Y. Meissner and A. L. F. Lamprecht, "Alternative Drug Delivery Approaches for the Therapy of Inflammatory Bowel Disease," *J. Pharm. Sci.*, vol. 97, no. 8, pp. 2878–2891, 2008.
- [45] S. N. Reddy, G. Bazzocchi, S. Chan, K. Akashi, J. Villanueva-Meyer, G. Yanni, I. Mena, and W. J. Snape, "Colonic motility and transit in health and ulcerative colitis," *Gastroenterology*, vol. 101, no. 5, pp. 1289–1297, 1991.
- [46] W. Ulbrich and A. Lamprecht, "Targeted drug-delivery approaches by nanoparticulate carriers in the therapy of inflammatory diseases Targeted drug-delivery approaches by nanoparticulate carriers in the therapy of inflammatory diseases," *J. R. Soc. Interface*, no. November, 2009.
- [47] Röhm GmbH, "NEWS - Colon Targeting: Röhm Pharma Polymers Develops Two New Colon Delivery Systems," *Pharma Polymers/ No. 7*, pp. 1–6, 2000.
- [48] E. L. McConnell, H. M. Fadda, and A. W. Basit, "Gut instincts: explorations in intestinal physiology and drug delivery.," *Int. J. Pharm.*, vol. 364, no. 2, pp. 213–26, Dec. 2008.
- [49] S. G. Nugent, "Intestinal luminal pH in inflammatory bowel disease: possible determinants and implications for therapy with aminosalicylates and other drugs," *Gut*, vol. 48, no. 4, pp. 571–577, Apr. 2001.
- [50] Y. Sasaki, R. Hada, H. Nakajima, S. Fukuda, and A. Munakata, "Improved localizing method of radiopill in measurement of entire gastrointestinal pH profiles: Colonic luminal pH in normal subjects and patients with Crohn's disease," *Am. J. Gastroenterol.*, vol. 92, no. 1, pp. 114–118, 1997.
- [51] J. Fallingborg, L. A. Christensen, B. A. Jacobsen, and S. N. Rasmussen, "Very low intraluminal colonic pH in patients with active ulcerative colitis," *Dig. Dis. Sci.*, vol. 38, no. 11, pp. 1989–1993, Nov. 1993.
- [52] A. G. Press, I. A. H. Tmann, L. H. Mann, B. Fuchs, M. F. U. C. Hs, M. Clinic, and I. Medical, "Gastrointestinal pH profiles in patients with inflammatory bowel disease," *Aliment Pharmacol Ther*, no. 12, pp. 673–678, 1998.
- [53] J. G. Hardy, C. G. Wilson, and E. Wood, "Drug delivery to the proximal colon," *J. Pharm. Pharmacol.*, vol. 37, no. 12, pp. 874–877, 1985.
- [54] Dr. Falk GmbH, "Budenofalk 3mg - Update 2006," 2006.
- [55] P. Lundin, P. Larson, P. Wollmer, and S. Edsbäcker, "Intestinal Delivery of Budesonide Given Orally as Plain versus Modified-Release (Entocort) Capsules." p. 1, 2001.
- [56] A. Gazzaniga, A. Maroni, M. E. Sangalli, and L. Zema, "Time-controlled oral delivery systems for colon targeting.," *Expert Opin. Drug Deliv.*, vol. 3, no. 5, pp. 583–97, Sep. 2006.
- [57] S. Friman and L. Bäckman, "A New Microemulsion Formulation of Cyclosporin: Pharmacokinetic and Clinical Features," *Clin. Pharmacokinet.*, vol. 30, no. 3, pp. 181–193, 1996.
- [58] D. Quintanar-Guerrero, E. Allémann, H. Fessi, and E. Doelker, "Preparation techniques and mechanisms of formation of biodegradable nanoparticles from preformed polymers.," *Drug Dev. Ind. Pharm.*, vol. 24, no. 12, pp. 1113–28, Dec. 1998.

- [59] F. Danhier, E. Ansorena, J. M. Silva, R. Coco, A. Le Breton, and V. Préat, "PLGA-based nanoparticles: an overview of biomedical applications.," *J. Control. Release*, vol. 161, no. 2, pp. 505–22, Jul. 2012.
- [60] M. L. Hans and A. M. Lowman, "Biodegradable nanoparticles for drug delivery and targeting," *Curr. Opin. Solid State Mater. Sci.*, vol. 6, no. September, pp. 319–327, 2002.
- [61] H. K. Makadia and S. J. Siegel, "Poly Lactic-co-Glycolic Acid (PLGA) as Biodegradable Controlled Drug Delivery Carrier," *Polymers (Basel)*, vol. 3, no. 3, pp. 1377–1397, Aug. 2011.
- [62] N. Wang and X. S. Wu, "Synthesis, characterization, biodegradation, and drug delivery application of biodegradable lactic/glycolic acid oligomers: Part II. Biodegradation and drug delivery application," *J. Biomater. Sci. Polym. Ed.*, vol. 9, no. 1, pp. 75–87, Jan. 1998.
- [63] Y. Li, K. J. Zhu, J. X. Zhang, H. L. Jiang, J. H. Liu, Y. L. Hao, H. Yasuda, A. Ichimaru, and K. Yamamoto, "In vitro and in vivo studies of cyclosporin A-loaded microspheres based on copolymers of lactide and epsilon-caprolactone: comparison with conventional PLGA microspheres.," *Int. J. Pharm.*, vol. 295, no. 1–2, pp. 67–76, May 2005.
- [64] J. L. Italia, D. K. Bhatt, V. Bhardwaj, K. Tikoo, and M. N. V. R. Kumar, "PLGA nanoparticles for oral delivery of cyclosporine: nephrotoxicity and pharmacokinetic studies in comparison to Sandimmune Neoral.," *J. Control. Release*, vol. 119, no. 2, pp. 197–206, Jun. 2007.
- [65] C. M. Moraes, A. P. de Matos, E. de Paula, A. H. Rosa, and L. F. Fraceto, "Benzocaine loaded biodegradable poly-(d,l-lactide-co-glycolide) nanocapsules: factorial design and characterization," *Mater. Sci. Eng. B*, vol. 165, no. 3, pp. 243–246, Dec. 2009.
- [66] N. Pirooznia, S. Hasannia, A. S. Lotfi, and M. Ghanei, "Encapsulation of alpha-1 antitrypsin in PLGA nanoparticles: in vitro characterization as an effective aerosol formulation in pulmonary diseases.," *J. Nanobiotechnology*, vol. 10, p. 20, Jan. 2012.
- [67] H. Ali, B. Weigmann, M. F. Neurath, E. M. Collnot, M. Windbergs, and C.-M. Lehr, "Budesonide loaded nanoparticles with pH-sensitive coating for improved mucosal targeting in mouse models of inflammatory bowel diseases.," *J. Control. Release*, vol. 183, pp. 167–77, Jun. 2014.
- [68] J.-S. Choi, K. Seo, and J.-W. Yoo, "Recent advances in PLGA particulate systems for drug delivery," *J. Pharm. Investig.*, vol. 43, no. 3, pp. 155–163, Jun. 2012.
- [69] Y. Tabata, Y. Inoue, and Y. Ikada, "Size effect on systemic and mucosal immune responses induced by oral administration of biodegradable microspheres.," *Vaccine*, vol. 14, no. 17–18, pp. 1677–85, Dec. 1996.
- [70] B. Xiao, H. Laroui, E. Viennois, S. Ayyadurai, M. A. Charania, Y. Zhang, Z. Zhang, M. T. Baker, B. Zhang, A. T. Gewirtz, and D. Merlin, "Nanoparticles with surface antibody against CD98 and carrying CD98 small interfering RNA reduce colitis in mice.," *Gastroenterology*, vol. 146, no. 5, pp. 1289–300.e1–19, May 2014.
- [71] R. Coco, L. Plapied, V. Pourcelle, C. Jérôme, D. J. Brayden, Y.-J. Schneider, and V. Préat, "Drug delivery to inflamed colon by nanoparticles: comparison of different strategies.," *Int. J. Pharm.*, vol. 440, no. 1, pp. 3–12, Jan. 2013.
- [72] H. Laroui, G. Dalmasso, H. T. T. Nguyen, Y. Yan, S. V. Sitaraman, and D. Merlin, "Drug-loaded nanoparticles targeted to the colon with polysaccharide hydrogel reduce colitis in a mouse model.," *Gastroenterology*, vol. 138, no. 3, pp. 843–53.e1–2, Mar. 2010.

- [73] A. Lamprecht, H. Yamamoto, H. Takeuchi, and Y. Kawashima, "Nanoparticles enhance therapeutic efficiency by selectively increased local drug dose in experimental colitis in rats.," *J. Pharmacol. Exp. Ther.*, vol. 315, no. 1, pp. 196–202, Oct. 2005.
- [74] D. Sriram, P. Yogeewari, N. Srichakravarthy, and T. R. Bal, "Synthesis of stavudine amino acid ester prodrugs with broad-spectrum chemotherapeutic properties for the effective treatment of HIV/AIDS.," *Bioorg. Med. Chem. Lett.*, vol. 14, no. 5, pp. 1085–7, Mar. 2004.
- [75] A. Lamprecht, U. Schäfer, and C. M. Lehr, "Size-dependent bioadhesion of micro- and nanoparticulate carriers to the inflamed colonic mucosa.," *Pharm. Res.*, vol. 18, no. 6, pp. 788–93, Jun. 2001.
- [76] C. Schmidt, C. Lautenschlaeger, E.-M. Collnot, M. Schumann, C. Bojarski, J.-D. Schulzke, C.-M. Lehr, and A. Stallmach, "Nano- and microscaled particles for drug targeting to inflamed intestinal mucosa – a first in vivo study in human patients," *J. Control. Release*, pp. 1–7, Nov. 2012.
- [77] A. Beloqui, R. Coco, P. B. Memvanga, B. Ucar, A. des Rieux, and V. Pr eat, "pH-sensitive nanoparticles for colonic delivery of curcumin in inflammatory bowel disease.," *Int. J. Pharm.*, vol. 473, no. 1–2, pp. 203–12, Oct. 2014.
- [78] A. Lamprecht, N. Ubrich, H. Yamamoto, U. Schäfer, H. Takeuchi, P. Maincent, Y. Kawashima, and C. M. Lehr, "Biodegradable nanoparticles for targeted drug delivery in treatment of inflammatory bowel disease.," *J. Pharmacol. Exp. Ther.*, vol. 299, no. 2, pp. 775–81, Nov. 2001.
- [79] A. Dvorak and G. Dickersin, "Crohn's disease: transmission electron microscopic studies. I. Barrier function. Possible changes related to alterations of cell coat, mucous coat, epithelial cells, and Paneth cells.," *Hum. Pathol.*, vol. 11, pp. 561–71, 1980.
- [80] A. Swidsinski, V. Loening-Baucke, F. Theissig, H. Engelhardt, S. Bengmark, S. Koch, H. Lochs, and Y. D orffel, "Comparative study of the intestinal mucus barrier in normal and inflamed colon.," *Gut*, vol. 56, no. 3, pp. 343–50, Mar. 2007.
- [81] D. Pertuit, B. Moulari, T. Betz, A. Nadaradjane, D. Neumann, L. Ismaïli, B. Refouvelet, Y. Pellequer, and A. Lamprecht, "5-Amino Salicylic Acid Bound Nanoparticles for the Therapy of Inflammatory Bowel Disease.," *J. Control. Release*, vol. 123, no. 3, pp. 211–8, Nov. 2007.
- [82] B. Moulari, D. Pertuit, Y. Pellequer, and A. Lamprecht, "The targeting of surface modified silica nanoparticles to inflamed tissue in experimental colitis.," *Biomaterials*, vol. 29, no. 34, pp. 4554–60, Dec. 2008.
- [83] A. Makhlof, Y. Tozuka, and H. Takeuchi, "pH-Sensitive nanospheres for colon-specific drug delivery in experimentally induced colitis rat model," *Eur. J. Pharm. Biopharm.*, vol. 72, no. 1, pp. 1–8, May 2009.
- [84] K. Mladenovska, R. S. Raicki, E. I. Janevik, T. Ristoski, M. J. Pavlova, Z. Kavrovski, M. G. Dodov, and K. Goracinova, "Colon-specific delivery of 5-aminosalicylic acid from chitosan-Calginate microparticles.," *Int. J. Pharm.*, vol. 342, no. 1–2, pp. 124–36, Sep. 2007.
- [85] T. T. Jubeh, S. Antler, S. Haupt, Y. Barenholz, and A. Rubinstein, "Local prevention of oxidative stress in the intestinal epithelium of the rat by adhesive liposomes of superoxide dismutase and tempamine.," *Mol. Pharm.*, vol. 2, no. 1, pp. 2–11, 2005.

- [86] T. T. Jubeh, M. Nadler-Milbauer, Y. Barenholz, and A. Rubinstein, "Local treatment of experimental colitis in the rat by negatively charged liposomes of catalase, TMN and SOD.," *J. Drug Target.*, vol. 14, no. 3, pp. 155–63, Apr. 2006.
- [87] T. T. Jubeh, Y. Barenholz, and A. Rubinstein, "Differential adhesion of normal and inflamed rat colonic mucosa by charged liposomes.," *Pharm. Res.*, vol. 21, no. 3, pp. 447–53, Mar. 2004.
- [88] F. Leonard, E. Collnot, and C. Lehr, "A Three-Dimensional Coculture of Enterocytes, Monocytes and Dendritic Cells To Model Inflamed Intestinal Mucosa in Vitro," *Mol. Pharm.*, vol. 7, no. 6, pp. 2103–2119, 2010.
- [89] S. Galindo-Rodríguez, F. Puel, S. Briançon, E. Allémann, E. Doelker, and H. Fessi, "Comparative scale-up of three methods for producing ibuprofen-loaded nanoparticles.," *Eur. J. Pharm. Sci.*, vol. 25, no. 4–5, pp. 357–67, 2005.
- [90] J. Kreuter, "Nanoparticles--a historical perspective.," *Int. J. Pharm.*, vol. 331, no. 1, pp. 1–10, Feb. 2007.
- [91] K. S. Soppimath, T. M. Aminabhavi, a R. Kulkarni, and W. E. Rudzinski, "Biodegradable polymeric nanoparticles as drug delivery devices.," *J. Control. Release*, vol. 70, no. 1–2, pp. 1–20, Jan. 2001.
- [92] X. Li, N. Anton, C. Arpagaus, F. Belleteix, and T. F. Vandamme, "Nanoparticles by spray drying using innovative new technology: The Büchi Nano Spray Dryer B-90.," *J. Control. Release*, vol. 147, no. 2, pp. 304–310, Jul. 2010.
- [93] N. Anton, J.-P. Benoit, and P. Saulnier, "Design and production of nanoparticles formulated from nano-emulsion templates-a review.," *J. Control. Release*, vol. 128, no. 3, pp. 185–99, Jun. 2008.
- [94] C. E. Mora-Huertas, H. Fessi, and A. Elaissari, "Influence of process and formulation parameters on the formation of submicron particles by solvent displacement and emulsification-diffusion methods critical comparison.," *Adv. Colloid Interface Sci.*, vol. 163, no. 2, pp. 90–122, Apr. 2011.
- [95] A. N. and B. S. Fessi H, Puisieux F, Devissaguet J Ph, "Nanocapsule formation by interfacial polymer deposition following solvent displacement," *Int. J. Pharm.*, vol. 55, pp. 1–4, 1989.
- [96] C. E. Mora-Huertas, H. Fessi, and a Elaissari, "Polymer-based nanocapsules for drug delivery.," *Int. J. Pharm.*, vol. 385, no. 1–2, pp. 113–42, Jan. 2010.
- [97] S. Galindo-Rodríguez, E. Allémann, H. Fessi, and E. Doelker, "Physicochemical Parameters Associated with Nanoparticle Formation in the Salting-out, Emulsification-Diffusion, and Nanoprecipitation Methods," *Pharm. Res.*, vol. 21, no. 8, pp. 1428–1439, 2004.
- [98] H. Fessi, "Process for the preparation of dispersible colloidal systems of a substance in the form of nanoparticles," 1992.
- [99] S. S. Guterres, "Spray-drying technique to prepare innovative nanoparticulated formulations for drug administration : a brief overview," *Brazilian J. Phys.*, vol. 39, no. 1, 2009.
- [100] N. Schafroth, C. Arpagaus, U. Y. Jadhav, S. Makne, and D. Douroumis, "Nano and microparticle engineering of water insoluble drugs using a novel spray-drying process.," *Colloids Surf. B. Biointerfaces*, vol. 90, pp. 8–15, Feb. 2012.

- [101] M. Beck-Broichsitter, C. Schweiger, T. Schmehl, T. Gessler, W. Seeger, and T. Kissel, "Characterization of novel spray-dried polymeric particles for controlled pulmonary drug delivery," *J. Control. Release*, Oct. 2011.
- [102] Y. F. Maa, P. A. Nguyen, K. Sit, and C. C. Hsu, "Spray-drying performance of a bench-top spray dryer for protein aerosol powder preparation.," *Biotechnol. Bioeng.*, vol. 60, no. 3, pp. 301–9, Nov. 1998.
- [103] C. Arpagaus, "Nano Spray Dryer B-90: Literature review and applications," *Büchi Inf. Bull.*, no. 63, p. 8, 2011.
- [104] N. Schafroth and M. Meuri, "Laboratory scale spray-drying of lactose: A review," *Eur. Ind. Pharm.*, no. 15, pp. 4–8, 2012.
- [105] S. H. Lee, D. Heng, W. K. Ng, H.-K. Chan, and R. B. H. Tan, "Nano spray drying: a novel method for preparing protein nanoparticles for protein therapy.," *Int. J. Pharm.*, vol. 403, no. 1–2, pp. 192–200, Jan. 2011.
- [106] K. Schmid, C. Arpagaus, and W. Friess, "Evaluation of the Nano Spray Dryer B-90 for pharmaceutical applications.," *Pharm. Dev. Technol.*, vol. 16, no. 4, pp. 287–94, Aug. 2011.
- [107] K. Baba and K. Nishida, "Calpain inhibitor nanocrystals prepared using Nano Spray Dryer B-90.," *Nanoscale Res. Lett.*, vol. 7, no. 1, p. 436, Aug. 2012.
- [108] K. Bürki, I. Jeon, C. Arpagaus, and G. Betz, "New insights into respirable protein powder preparation using a nano spray dryer.," *Int. J. Pharm.*, vol. 408, no. 1–2, pp. 248–56, Apr. 2011.
- [109] M. Beck-Broichsitter, C. Schweiger, T. Schmehl, T. Gessler, W. Seeger, and T. Kissel, "Characterization of novel spray-dried polymeric particles for controlled pulmonary drug delivery.," *J. Control. Release*, vol. 158, no. 2, pp. 329–35, Mar. 2012.
- [110] M. A. Boraey, S. Hoe, H. Sharif, D. P. Miller, D. Lechuga-Ballesteros, and R. Vehring, "Improvement of the dispersibility of spray-dried budesonide powders using leucine in an ethanol–water cosolvent system," *Powder Technol.*, Feb. 2012.
- [111] N. Bege, T. Renette, T. Endres, M. Beck-Broichsitter, D. Hänggi, and T. Kissel, "In situ forming nimodipine depot system based on microparticles for the treatment of posthemorrhagic cerebral vasospasm.," *Eur. J. Pharm. Biopharm.*, no. January, Jan. 2013.
- [112] Y. Sun, X. Song, J. Wang, and J. Yu, "Preparation of lithium carbonate hollow spheres by spray pyrolysis," *Cryst. Res. Technol.*, vol. 46, no. 2, pp. 173–177, Feb. 2011.
- [113] J. M. Mullin, N. Agostino, E. Rendon-huerta, and J. J. Thornton, "Keynote review : Epithelial and endothelial barriers in human disease," *Drug Discov. Today*, vol. 10, no. 6, pp. 395–408, 2005.
- [114] S. J. H. van Deventer, "Taming the mucosal immune response in Crohn's disease," *Best Pract. Res. Clin. Gastroenterol.*, vol. 16, no. 6, pp. 1035–1043, Dec. 2002.
- [115] A. Béduneau, C. Tempesta, S. Fimbel, Y. Pellequer, V. Jannin, F. Demarne, and A. Lamprecht, "A tunable Caco-2/HT29-MTX co-culture model mimicking variable permeabilities of the human intestine obtained by an original seeding procedure.," *Eur. J. Pharm. Biopharm.*, vol. 87, no. 2, pp. 290–8, Jul. 2014.

- [116] C. Schimpel, B. Teubl, M. Absenger, C. Meindl, E. Fröhlich, G. Leitinger, A. Zimmer, and E. Roblegg, "Development of an Advanced Intestinal in Vitro Triple Culture Permeability Model To Study Transport of Nanoparticles.," *Mol. Pharm.*, vol. 11, pp. 808–818, Feb. 2014.
- [117] T. Tanoue, Y. Nishitani, K. Kanazawa, T. Hashimoto, and M. Mizuno, "In vitro model to estimate gut inflammation using co-cultured Caco-2 and RAW264.7 cells.," *Biochem. Biophys. Res. Commun.*, vol. 374, no. 3, pp. 565–9, Sep. 2008.
- [118] J. Susewind, C. de S. Carvalho-Wodarz, U. Repnik, E.-M. Collnot, N. Schneider-Daum, G. W. Griffiths, and C.-M. Lehr, "A 3D co-culture of three human cell lines to model the inflamed intestinal mucosa for safety testing of nanomaterials," *Nanotoxicology*, p. in press, 2015.
- [119] F. Leonard, H. Ali, E. Collnot, B. J. Crielaard, T. Lammers, G. Storm, and C.-M. Lehr, "Screening of Budesonide Nanoformulations for Treatment of Inflammatory Bowel Disease in an Inflamed 3D Cell-Culture Model," *ALTEX*, vol. 3, no. 29, pp. 275–285, 2012.
- [120] C. Draheim, J. Susewind, A. Guillot, B. Loretz, S. Hansen, E.-M. Collnot, M. Limberger, and C.-M. Lehr, "PLGA based nano- and microsized particles for inflammatory bowel disease therapy: evaluation of size-dependent accumulation and anti-inflammatory effect in an in vitro triple culture model (manuscript to be submitted)."
- [121] G. Múzes, B. Molnár, Z. Tulassay, and F. Sipos, "Changes of the cytokine profile in inflammatory bowel diseases," *World J. Gastroenterol.*, vol. 18, no. 41, pp. 5848–5861, 2012.
- [122] E. Giner, M.-C. Recio, J.-L. Ríos, and R.-M. Giner, "Oleuropein protects against dextran sodium sulfate-induced chronic colitis in mice.," *J. Nat. Prod.*, vol. 76, no. 6, pp. 1113–20, Jun. 2013.
- [123] S. Wirtz and M. F. Neurath, "Mouse models of inflammatory bowel disease.," *Adv. Drug Deliv. Rev.*, vol. 59, no. 11, pp. 1073–83, Sep. 2007.
- [124] M. Marín, R. María Giner, J.-L. Ríos, and M. C. Recio, "Intestinal anti-inflammatory activity of ellagic acid in the acute and chronic dextrane sulfate sodium models of mice colitis.," *J. Ethnopharmacol.*, vol. 150, no. 3, pp. 925–34, Dec. 2013.
- [125] H. Sann, J. Von Erichsen, M. Hessmann, A. Pahl, and A. Hoffmeyer, "Efficacy of drugs used in the treatment of IBD and combinations thereof in acute DSS-induced colitis in mice.," *Life Sci.*, vol. 92, no. 12, pp. 708–18, Apr. 2013.
- [126] S. Murthy, N. S. Murthy, D. Coppola, and D. L. Wood, "The efficacy of BAY y 1015 in dextran sulfate model of mouse colitis.," *Inflamm. Res.*, vol. 46, no. 6, pp. 224–33, Jun. 1997.
- [127] G. Hartmann, C. Bidlingmaier, B. Siegmund, S. Albrich, J. Schulze, K. Tschoep, a Eigler, H. a Lehr, and S. Endres, "Specific type IV phosphodiesterase inhibitor rolipram mitigates experimental colitis in mice.," *J. Pharmacol. Exp. Ther.*, vol. 292, no. 1, pp. 22–30, Jan. 2000.
- [128] S. Wirtz, C. Neufert, B. Weigmann, and M. F. Neurath, "Chemically induced mouse models of intestinal inflammation.," *Nat. Protoc.*, vol. 2, no. 3, pp. 541–6, Jan. 2007.
- [129] M. Mähler, I. J. Bristol, E. H. Leiter, A. E. Workman, E. H. Birkenmeier, C. O. Elson, and J. P. Sundberg, "Differential susceptibility of inbred mouse strains to dextran sulfate sodium-induced colitis.," *Am. J. Physiol.*, vol. 274, no. 3 Pt 1, pp. G544–51, Mar. 1998.

- [130] Y. Yan, V. Kolachala, G. Dalmaso, H. Nguyen, H. Laroui, S. V Sitaraman, and D. Merlin, "Temporal and spatial analysis of clinical and molecular parameters in dextran sodium sulfate induced colitis.," *PLoS One*, vol. 4, no. 6, p. e6073, Jan. 2009.
- [131] I. Okayasu, S. Hatakeyama, M. Yamada, T. Ohkusa, Y. Inagaki, and R. Nakaya, "A novel method in the induction of reliable experimental acute and chronic ulcerative colitis in mice," *Gastroenterology*, no. 98, pp. 694–702, 1990.
- [132] T. Tanaka, H. Kohno, R. Suzuki, Y. Yamada, S. Sugie, and H. Mori, "A novel inflammation-related mouse colon carcinogenesis model induced by azoxymethane and dextran sodium sulfate.," *Cancer Sci.*, vol. 94, no. 11, pp. 965–73, Nov. 2003.
- [133] L. A. Dieleman, M. J. Palmen, H. Akol, E. Bloemena, A. S. Peña, S. G. Meuwissen, and E. P. Van Rees, "Chronic experimental colitis induced by dextran sulphate sodium (DSS) is characterized by Th1 and Th2 cytokines.," *Clin. Exp. Immunol.*, vol. 114, no. 3, pp. 385–91, Dec. 1998.
- [134] L. X. Yu, "Pharmaceutical quality by design: product and process development, understanding, and control.," *Pharm. Res.*, vol. 25, no. 4, pp. 781–91, Apr. 2008.
- [135] S.-J. Park, G.-H. Choo, S.-J. Hwang, and M.-S. Kim, "Quality by design: screening of critical variables and formulation optimization of Eudragit E nanoparticles containing dutasteride.," *Arch. Pharm. Res.*, vol. 36, no. 5, pp. 593–601, May 2013.
- [136] S. Verma, Y. Lan, R. Gokhale, and D. J. Burgess, "Quality by design approach to understand the process of nanosuspension preparation.," *Int. J. Pharm.*, vol. 377, no. 1–2, pp. 185–98, Jul. 2009.
- [137] S. Belotti, A. Rossi, P. Colombo, R. Bettini, D. Rekkas, S. Politis, G. Colombo, A. Giulia, and F. Buttini, "Spray dried amikacin powder for inhalation in cystic fibrosis patients: A quality by design approach for product construction," *Int. J. Pharm.*, p. <http://dx.doi.org/10.1016/j.ijpharm.2014.05.055>, 2014.
- [138] X. Xu, M. A. Khan, and D. J. Burgess, "A quality by design (QbD) case study on liposomes containing hydrophilic API: II. Screening of critical variables, and establishment of design space at laboratory scale.," *Int. J. Pharm.*, vol. 423, no. 2, pp. 543–53, Feb. 2012.
- [139] P. Lebrun, F. Krier, J. Mantanus, H. Grohgan, M. Yang, E. Rozet, B. Boulanger, B. Evrard, J. Rantanen, and P. Hubert, "Design space approach in the optimization of the spray-drying process.," *Eur. J. Pharm. Biopharm.*, vol. 80, no. 1, pp. 226–34, Jan. 2012.
- [140] X. Xu, A. P. Costa, M. A. Khan, and D. J. Burgess, "Application of quality by design to formulation and processing of protein liposomes.," *Int. J. Pharm.*, vol. 434, no. 1–2, pp. 349–59, Sep. 2012.
- [141] D. Cun, D. K. Jensen, M. J. Maltesen, M. Bunker, P. Whiteside, D. Scurr, C. Foged, and H. M. Nielsen, "High loading efficiency and sustained release of siRNA encapsulated in PLGA nanoparticles: quality by design optimization and characterization.," *Eur. J. Pharm. Biopharm.*, vol. 77, no. 1, pp. 26–35, Jan. 2011.
- [142] A. Bozkir and O. M. Saka, "Formulation and investigation of 5-FU nanoparticles with factorial design-based studies.," *Farmaco*, vol. 60, no. 10, pp. 840–6, Oct. 2005.

- [143] K. Dillen, J. Vandervoort, G. Van den Mooter, L. Verheyden, and A. Ludwig, "Factorial design, physicochemical characterisation and activity of ciprofloxacin-PLGA nanoparticles," *Int. J. Pharm.*, vol. 275, no. 1–2, pp. 171–187, May 2004.
- [144] K. Derakhshandeh, M. Erfan, and S. Dadashzadeh, "Encapsulation of 9-nitrocamptothecin, a novel anticancer drug, in biodegradable nanoparticles: factorial design, characterization and release kinetics.," *Eur. J. Pharm. Biopharm.*, vol. 66, no. 1, pp. 34–41, Apr. 2007.
- [145] T. Delmas, A.-C. Couffin, P. A. Bayle, F. de Crécy, E. Neumann, F. Vinet, M. Bardet, J. Bibette, and I. Texier, "Preparation and characterization of highly stable lipid nanoparticles with amorphous core of tuneable viscosity.," *J. Colloid Interface Sci.*, vol. 360, no. 2, pp. 471–81, Aug. 2011.
- [146] M. C. Gohel and a F. Amin, "Formulation optimization of controlled release diclofenac sodium microspheres using factorial design.," *J. Control. Release*, vol. 51, no. 2–3, pp. 115–22, Mar. 1998.
- [147] A. Schoubben, S. Giovagnoli, M. C. Tiralti, P. Blasi, and M. Ricci, "Capreomycin inhalable powders prepared with an innovative spray-drying technique.," *Int. J. Pharm.*, p. <http://dx.doi.org/10.1016/j.ijpharm.2014.04.042>, Apr. 2014.
- [148] P. J. W. Mark J. Anderson, *DOE simplified*, Second edi. Productivity Press, 2007.
- [149] J. A. Jacquez, "Design of Experiments," *Pergamon, J. Franklin Inst.*, vol. 335B, no. 2, pp. 259–279, 1998.
- [150] P. Legrand, S. Lesieur, A. Bochot, R. Gref, W. Raatjes, G. Barratt, and C. Vauthier, "Influence of polymer behaviour in organic solution on the production of polylactide nanoparticles by nanoprecipitation.," *Int. J. Pharm.*, vol. 344, no. 1–2, pp. 33–43, Nov. 2007.
- [151] R. Vehring, W. Foss, and D. Lechugaballesteros, "Particle formation in spray drying," *J. Aerosol Sci.*, vol. 38, no. 7, pp. 728–746, Jul. 2007.
- [152] P. Couvreur, "Nanoparticles in drug delivery: past, present and future.," *Adv. Drug Deliv. Rev.*, vol. 65, no. 1, pp. 21–3, Jan. 2013.
- [153] O. Thioune, H. Fessi, J. P. Devissaguet, and F. Puisieux, "Preparation of pseudolatex by nanoprecipitation: Influence of the solvent nature on intrinsic viscosity and interaction constant," *Int. J. Pharm.*, vol. 146, no. 2, pp. 233–238, Jan. 1997.
- [154] F. Lince, D. L. Marchisio, and A. A. Barresi, "Strategies to control the particle size distribution of poly-epsilon-caprolactone nanoparticles for pharmaceutical applications.," *J. Colloid Interface Sci.*, vol. 322, no. 2, pp. 505–15, Jun. 2008.
- [155] R. Vehring, "Pharmaceutical particle engineering via spray drying.," *Pharm. Res.*, vol. 25, no. 5, pp. 999–1022, May 2008.
- [156] C. Arpagaus and N. Schafroth, "Spray Drying of biodegradable polymers in Laboratory Scale," *Respir. Drug Deliv. Eur.*, pp. 269–274, 2009.
- [157] A. A. Varonos, J. S. Anagnostopoulos, and G. C. Bergeles, "Prediction of the cleaning efficiency of an electrostatic precipitator," *J. Electrostat.*, vol. 55, no. 2, pp. 111–133, Jun. 2002.

- [158] A. Jaworek, A. Krupa, and T. Czech, "Modern electrostatic devices and methods for exhaust gas cleaning: A brief review," *J. Electrostat.*, vol. 65, no. 3, pp. 133–155, Mar. 2007.
- [159] S. B. Hanauer, "Inflammatory bowel disease: epidemiology, pathogenesis, and therapeutic opportunities.," *Inflamm. Bowel Dis.*, vol. 12 Suppl 1, no. January, pp. S3–9, Jan. 2006.
- [160] A. Kornbluth, "Cyclosporine in inflammatory bowel disease.," *Curr. Gastroenterol. Rep.*, vol. 1, no. 6, pp. 486–90, Dec. 1999.
- [161] M. Clark, J.-F. Colombel, B. C. Feagan, R. N. Fedorak, S. B. Hanauer, M. a Kamm, L. Mayer, C. Regueiro, P. Rutgeerts, W. J. Sandborn, B. E. Sands, S. Schreiber, S. Targan, S. Travis, and S. Vermeire, "American gastroenterological association consensus development conference on the use of biologics in the treatment of inflammatory bowel disease, June 21-23, 2006.," *Gastroenterology*, vol. 133, no. 1, pp. 312–39, Jul. 2007.
- [162] M. Chacón, J. Molpeceres, L. Berges, M. Guzmán, and M. R. Aberturas, "Stability and freeze-drying of cyclosporine loaded poly(D,L lactide-glycolide) carriers.," *Eur. J. Pharm. Sci.*, vol. 8, no. 2, pp. 99–107, May 1999.
- [163] F. Jaeghere, E. Allémann, J.-C. Leroux, W. Stevels, J. Feijen, E. Doelker, and R. Gurny, "Formulation and Lyoprotection of Poly(Lactide Acid-Co-Ethylene Oxide) Nanoparticles: Influence on Physical Stability and In Vitro Cell Uptake," *Pharm. Res.*, vol. 6, pp. 859–867, 1999.
- [164] W. Abdelwahed, G. Degobert, S. Stainmesse, and H. Fessi, "Freeze-drying of nanoparticles: formulation, process and storage considerations.," *Adv. Drug Deliv. Rev.*, vol. 58, no. 15, pp. 1688–713, Dec. 2006.
- [165] L. M. Crowe, D. S. Reid, and J. H. Crowe, "Is trehalose special for preserving dry biomaterials?," *Biophys. J.*, vol. 71, no. 4, pp. 2087–93, Oct. 1996.
- [166] A. Saez, M. Guzmán, J. Molpeceres, and M. R. Aberturas, "Freeze-drying of polycaprolactone and poly(D,L-lactide-glycolic) nanoparticles induce minor particle size changes affecting the oral pharmacokinetics of loaded drugs.," *Eur. J. Pharm. Biopharm.*, vol. 50, no. 3, pp. 379–87, Nov. 2000.
- [167] W. Abdelwahed, G. Degobert, and H. Fessi, "A pilot study of freeze drying of poly(epsilon-caprolactone) nanocapsules stabilized by poly(vinyl alcohol): formulation and process optimization.," *Int. J. Pharm.*, vol. 309, no. 1–2, pp. 178–88, Feb. 2006.
- [168] H. Takeuchi, H. Yamamoto, T. Toyoda, H. Toyobuku, T. Hino, and Y. Kawashima, "Physical stability of size controlled small unilamellar liposomes coated with a modified polyvinyl alcohol," *Int. J. Pharm.*, vol. 164, no. 1–2, pp. 103–111, Apr. 1998.
- [169] J. M. Barichello, M. Morishita, K. Takayama, and T. Nagai, "Encapsulation of hydrophilic and lipophilic drugs in PLGA nanoparticles by the nanoprecipitation method.," *Drug Dev. Ind. Pharm.*, vol. 25, no. 4, pp. 471–6, Apr. 1999.
- [170] J. Cheng, B. A. Teply, I. Sherifi, J. Sung, G. Luther, F. X. Gu, E. Levy-Nissenbaum, A. F. Radovic-Moreno, R. Langer, and O. C. Farokhzad, "Formulation of functionalized PLGA-PEG nanoparticles for in vivo targeted drug delivery.," *Biomaterials*, vol. 28, no. 5, pp. 869–76, Feb. 2007.

- [171] T. Urata, K. Arimori, and H. Nakano, "Modification of release rates of cyclosporin A from poly(L-lactic acid) microspheres by fatty acid esters and in-vivo evaluation of the microspheres.," *J. Control. Release*, vol. 58, no. 2, pp. 133–41, Mar. 1999.
- [172] C. Gómez-Gaete, N. Tsapis, M. Besnard, A. Bochot, and E. Fattal, "Encapsulation of dexamethasone into biodegradable polymeric nanoparticles.," *Int. J. Pharm.*, vol. 331, no. 2, pp. 153–9, Mar. 2007.
- [173] M. Polakovic, T. Görner, R. Gref, and E. Dellacherie, "Lidocaine loaded biodegradable nanospheres. II. Modelling of drug release.," *J. Control. Release*, vol. 60, no. 2–3, pp. 169–77, Aug. 1999.
- [174] A. Dinda, I. Biswal, D. Das, S. Si, S. Kumar, B. B. Barik, and M. M. Safhi, "Effect of Stabilizers and Process Parameters for Budesonide Loaded PLGA- Nanoparticles," *Int. J. Drug Deliv.*, vol. 3, pp. 371–380, 2011.
- [175] R. C. Rowe, P. J. Sheskey, and M. E. Quinn, *Handbook of Pharmaceutical Excipients*, 6th ed. Pharmaceutical Press, 2009, pp. 675–678.
- [176] L. M. Nolan, L. Tajber, B. F. McDonald, A. S. Barham, O. I. Corrigan, and A. M. Healy, "Excipient-free nanoporous microparticles of budesonide for pulmonary delivery.," *Eur. J. Pharm. Sci.*, vol. 37, no. 5, pp. 593–602, Jul. 2009.
- [177] R. Bienert, F. Emmerling, and A. F. Thünemann, "The size distribution of 'gold standard' nanoparticles.," *Anal. Bioanal. Chem.*, vol. 395, no. 6, pp. 1651–60, Nov. 2009.
- [178] T. Linsinger, G. Roebben, D. Gilliland, L. Calzolari, F. Rossi, N. Gibson, and C. Klein, "Requirements on measurements for the implementation of the European Commission definition of the term 'nanomaterial,'" 2012.
- [179] A. T. Neffe, M. von Ruesten-Lange, S. Braune, K. Lützwow, T. Roch, K. Richau, A. Krüger, T. Becherer, A. F. Thünemann, F. Jung, R. Haag, and A. Lendlein, "Multivalent grafting of hyperbranched oligo- and polyglycerols shielding rough membranes to mediate hemocompatibility," *J. Mater. Chem. B*, vol. 2, no. 23, p. 3626, 2014.
- [180] D. D. Ankola, A. Battisti, R. Solaro, and M. N. V. R. Kumar, "Nanoparticles made of multi-block copolymer of lactic acid and ethylene glycol containing periodic side-chain carboxyl groups for oral delivery of cyclosporine A Nanoparticles made of multi-block copolymer of lactic acid and ethylene glycol containing per," *J. R. Soc. Interface*, 2010.
- [181] R. L. Cleek, K. C. Ting, S. G. Eskin, and A. G. Mikos, "Microparticles of poly (DL -lactic-co-glycolic acid)/poly (ethylene glycol) blends for controlled drug delivery," *J. Control. Release*, vol. 48, pp. 259–268, 1997.
- [182] L. Mu, M.-M. Teo, H.-Z. Ning, C.-S. Tan, and S.-S. Feng, "Novel powder formulations for controlled delivery of poorly soluble anticancer drug: application and investigation of TPGS and PEG in spray-dried particulate system.," *J. Control. Release*, vol. 103, no. 3, pp. 565–75, Apr. 2005.
- [183] L. Cruz, L. U. Soares, T. D. Costa, G. Mezzalira, N. P. da Silveira, S. S. Guterres, and A. R. Pohlmann, "Diffusion and mathematical modeling of release profiles from nanocarriers.," *Int. J. Pharm.*, vol. 313, no. 1–2, pp. 198–205, Apr. 2006.

- [184] N. M. Khalil, T. C. F. do Nascimento, D. M. Casa, L. F. Dalmolin, A. C. de Mattos, I. Hoss, M. A. Romano, and R. M. Mainardes, "Pharmacokinetics of curcumin-loaded PLGA and PLGA-PEG blend nanoparticles after oral administration in rats.," *Colloids Surf. B. Biointerfaces*, vol. 101, pp. 353–60, Jan. 2013.
- [185] S. Guo, R. Al-Sadi, H. M. Said, and T. Y. Ma, "Lipopolysaccharide causes an increase in intestinal tight junction permeability in vitro and in vivo by inducing enterocyte membrane expression and localization of TLR-4 and CD14," *Am. J. Pathol.*, vol. 182, no. 2, pp. 375–87, Feb. 2013.
- [186] P. E. Porporato, V. L. Payen, C. J. De Saedeleer, V. Pr at, J.-P. Thissen, O. Feron, and P. Sonveaux, "Lactate stimulates angiogenesis and accelerates the healing of superficial and ischemic wounds in mice.," *Angiogenesis*, vol. 15, no. 4, pp. 581–92, Dec. 2012.
- [187] K. K. Chereddy, R. Coco, P. B. Memvanga, B. Ucakar, A. des Rieux, G. Vandermeulen, and V. Pr at, "Combined effect of PLGA and curcumin on wound healing activity.," *J. Control. release*, vol. 171, no. 2, pp. 208–15, Oct. 2013.
- [188] N. Bertiaux-Vanda le, S. B. Youmba, L. Belmonte, S. Leclaire, M. Antonietti, G. Gourcerol, A.-M. Leroi, P. D chelotte, J.-F. M nard, P. Ducrott , and M. Co ffier, "The expression and the cellular distribution of the tight junction proteins are altered in irritable bowel syndrome patients with differences according to the disease subtype," *Am. J. Gastroenterol.*, vol. 106, no. 12, pp. 2165–73, Dec. 2011.
- [189] J. Linnankoski and J. Ma, "Paracellular Porosity and Pore Size of the Human Intestinal Epithelium in Tissue and Cell Culture Models," *J. Pharm. Sci.*, vol. 99, no. 4, pp. 2166–2175, 2010.
- [190] C. Medina, M. J. Santos-Martinez, a Radomski, O. I. Corrigan, and M. W. Radomski, "Nanoparticles: pharmacological and toxicological significance.," *Br. J. Pharmacol.*, vol. 150, no. 5, pp. 552–8, Mar. 2007.
- [191] G. Thews, E. Mutschler, and P. Vaupel, *Anatomie, Physiologie, Pathophysiologie des Menschen*, 5th ed. wissenschaftliche Verlagsgesellschaft mbH Stuttgart, 1998, pp. 131–131.
- [192] J. North and K. Whaley, "Complement : Measurement," *Encycl. LIFE Sci.*, pp. 1–7, 2001.
- [193] C. Villiers, H. Freitas, R. Couderc, M.-B. Villiers, and P. Marche, "Analysis of the toxicity of gold nano particles on the immune system: effect on dendritic cell functions.," *J. Nanopart. Res.*, vol. 12, no. 1, pp. 55–60, Jan. 2010.
- [194] M. Faure, C. L. Villiers, and P. N. Marche, "Normal differentiation and functions of mouse dendritic cells derived from RAG-deficient bone marrow progenitors.," *Cell. Immunol.*, vol. 228, no. 1, pp. 8–14, Mar. 2004.
- [195] R. A. Jain, "The manufacturing techniques of various drug loaded biodegradable poly(lactide-co-glycolide) (PLGA) devices.," *Biomaterials*, vol. 21, no. 23, pp. 2475–90, Dec. 2000.
- [196] B. Semete, L. Booyesen, Y. Lemmer, L. Kalombo, L. Katata, J. Verschoor, and H. S. Swai, "In vivo evaluation of the biodistribution and safety of PLGA nanoparticles as drug delivery systems.," *Nanomedicine*, vol. 6, no. 5, pp. 662–71, Oct. 2010.

- [197] J.-C. Olivier, L. Fenart, R. Chauvet, C. Pariat, C. Roméo, and W. Couet, "Indirect Evidence that Drug Brain Targeting Using Polysorbate 80-Coated Polybutylcyanoacrylate Nanoparticles Is Related to Toxicity," *Pharm. Res.*, vol. 16, no. 12, pp. 1836–1842, 1999.
- [198] World Health Organization, "Toxicological evaluation of certain food additives with a review of general principles and of specifications," Geneva, 1974.
- [199] D. Akhilesh, K. B. Bini, and J. V. Kamath, "Review on Span-60 Based Non-Ionic Surfactant vesicles (Niosomes) as Novel Drug Delivery," *Int. Journl Res. Pharm. Biomed. Sci.*, vol. 3, no. 1, 2012.
- [200] Z. Teixeira, C. a. Dreiss, M. Jayne Lawrence, R. K. Heenan, D. Machado, G. Z. Justo, S. S. Guterres, and N. Durán, "Retinyl Palmitate Polymeric Nanocapsules as Carriers of Bioactives," *J. Colloid Interface Sci.*, May 2012.
- [201] C. G. Venturini, E. Jäger, C. P. Oliveira, A. Bernardi, A. M. O. Battastini, S. S. Guterres, and A. R. Pohlmann, "Formulation of lipid core nanocapsules," *Colloids Surfaces A Physicochem. Eng. Asp.*, vol. 375, no. 1–3, pp. 200–208, Feb. 2011.
- [202] L. a Perrin-Cocon, C. L. Villiers, J. Salamero, F. Gabert, and P. N. Marche, "B cell receptors and complement receptors target the antigen to distinct intracellular compartments," *J. Immunol.*, vol. 172, pp. 3564–3572, 2004.
- [203] K. Vandenbroeck, I. Alloza, M. Gadina, and P. Matthys, "Inhibiting cytokines of the interleukin-12 family: recent advances and novel challenges," *J. Pharm. Pharmacol.*, vol. 56, no. 2, pp. 145–60, Feb. 2004.
- [204] K. Tozawa, H. Hanai, K. Sugimoto, S. Baba, H. Sugimura, T. Aoshi, M. Uchijima, T. Nagata, and Y. Koide, "Evidence for the critical role of interleukin-12 but not interferon-gamma in the pathogenesis of experimental colitis in mice," *J. Gastroenterol. Hepatol.*, vol. 18, no. 5, pp. 578–87, May 2003.
- [205] J. N. Temblay, E. Bertelli, J. L. Arques, M. Regoli, and C. Nicoletti, "Production of IL-12 by Peyer patch-dendritic cells is critical for the resistance to food allergy," *J. Allergy Clin. Immunol.*, vol. 120, no. 3, pp. 659–65, Sep. 2007.
- [206] P. Mannon, I. Fuss, L. Mayer, C. Elson, W. Sandborn, and D. Present, "Anti-Interleukin-12 Antibody for Active Crohn's Disease," *N. Engl. J. Med.*, pp. 2069–2079, 2004.
- [207] L. Camoglio, N. P. Juffermans, M. Peppelenbosch, A. a te Velde, F. J. ten Kate, S. J. H. van Deventer, and M. Kopf, "Contrasting roles of IL-12p40 and IL-12p35 in the development of hapten-induced colitis," *Eur. J. Immunol.*, vol. 32, no. 1, pp. 261–9, Jan. 2002.
- [208] M. F. Neurath, I. Fuss, B. L. Kelsall, E. Stüber, and W. Strober, "Antibodies to interleukin 12 abrogate established experimental colitis in mice," *J. Exp. Med.*, vol. 182, no. 5, pp. 1281–90, Nov. 1995.
- [209] J. Gottfries, S. Melgar, and E. Michaëlsson, "Modelling of mouse experimental colitis by global property screens: a holistic approach to assess drug effects in inflammatory bowel disease," *PLoS One*, vol. 7, no. 1, p. e30005, Jan. 2012.
- [210] E. L. McConnell, A. W. Basit, and S. Murdan, "Measurements of rat and mouse gastrointestinal pH, fluid and lymphoid tissue, and implications for in-vivo experiments," *J. Pharm. Pharmacol.*, vol. 60, no. 1, pp. 63–70, Jan. 2008.

-
- [211] I. Andújar, J. L. Ríos, R. M. Giner, J. Miguel Cerdá, and M. D. C. Recio, "Beneficial effect of shikonin on experimental colitis induced by dextran sulfate sodium in BALB/c mice.," *Evid. Based. Complement. Alternat. Med.*, vol. 2012, p. 271606, Jan. 2012.
- [212] M. M. Bradford, "A rapid and sensitive method for the quantitation of microgram quantities of protein utilizing the principle of protein-dye binding.," *Anal. Biochem.*, vol. 72, pp. 248–54, May 1976.
- [213] I. Koboziev, F. Karlsson, S. Zhang, and M. B. Grisham, "Pharmacological intervention studies using mouse models of the inflammatory bowel diseases: translating preclinical data into new drug therapies.," *Inflamm. Bowel Dis.*, vol. 17, no. 5, pp. 1229–45, May 2011.
- [214] S. Melgar, A. Karlsson, and E. Michaëlsson, "Acute colitis induced by dextran sulfate sodium progresses to chronicity in C57BL/6 but not in BALB/c mice: correlation between symptoms and inflammation.," *Am. J. Physiol. Gastrointest. Liver Physiol.*, vol. 288, no. 6, pp. G1328–38, Jun. 2005.
- [215] M. Banić, B. Anić, T. Brkić, N. Ljubicić, S. Plesko, C. Dohoczky, D. Erceg, M. Petrovecki, I. Stipancić, and I. Rotkvić, "Effect of cyclosporine in a murine model of experimental colitis.," *Dig. Dis. Sci.*, vol. 47, no. 6, pp. 1362–8, Jun. 2002.
- [216] P. Wachsmann and A. Lamprecht, *Polymeric nanoparticles for the selective therapy of inflammatory bowel disease.*, 1st ed., vol. 508. Elsevier Inc., 2012, pp. 377–97.
- [217] P. Rafiee, C. P. Johnson, M. S. Li, H. Ogawa, J. Heidemann, P. J. Fisher, T. H. Lamirand, M. F. Otterson, K. T. Wilson, and D. G. Binion, "Cyclosporine A enhances leukocyte binding by human intestinal microvascular endothelial cells through inhibition of p38 MAPK and iNOS. Paradoxical proinflammatory effect on the microvascular endothelium.," *J. Biol. Chem.*, vol. 277, no. 38, pp. 35605–15, Sep. 2002.

12. Scientific output

Publications in international peer-reviewed journals:

Christina Draheim*, Francois de Crécy*, Steffi Hansen, Eva-Maria Collnot, Claus-Michael Lehr, *A Design of Experiment Study of Nanoprecipitation and Nano Spray Drying as Processes to Prepare PLGA Nano- and Microparticles with Defined Sizes and Size Distributions*, Pharmaceutical Research, in press (doi: 10.1007/s11095-015-1647-9)

Alexis Guillot, **Christina Draheim**, Markus Limberger, Steffi Hansen, Claus-Michael Lehr, *A new concept for in vitro drug release testing of micro- and nanoformulations using a fiber optic system and derivative spectrophotometry* (to be submitted)

Christina Draheim*, Julia Susewind*, Alexis Guillot, Brigitta Loretz, Steffi Hansen, Eva-Maria Collnot, Markus Limberger, Claus-Michael Lehr, *PLGA based nano- and microsized particles for inflammatory bowel disease therapy: evaluation of size-dependent accumulation and anti-inflammatory effect in an in vitro triple culture model* (to be submitted)

Ana Melero*, **Christina Draheim***, Elisa Giner, Raquel Talens, Teresa María Garrigues, José Esteban Peris, M^a Carmen Recio, Rosa Giner, Steffi Hansen, Claus-Michael Lehr, *Evaluation of cyclosporine A loaded PLGA based drug delivery systems for inflammatory bowel disease in DSS Balb/C mice model* (to be submitted)

Poster presentations:

2014

C. Draheim*, J. Susewind*, A. Guillot, B. Loretz, C. de Souza Carvalho, E.-M. Collnot, S. Hansen, C.-M. Lehr. *Evaluation of PLGA based drug delivery systems for the therapy of inflammatory bowel disease in a 3 D cell-culture model*. 10th International Conference and Workshop on Biological Barriers, February 16-24, 2014, Saarland University, Saarbruecken, Germany

Alexis Guillot, **Christina Draheim**, Markus Limberger, Steffi Hansen, Claus-Michael Lehr. *Derivative spectrophotometry with a fiber optic system to monitor in situ the drug released from loaded PLGA-nanoparticles*, 10th International Conference and Workshop on Biological Barriers, February 16-24, 2014, Saarland University, Saarbruecken, Germany

* These authors contributed equally to this work.

Ana Melero, Juan Pablo Sanchez-Rivera, **Christina Draheim**, Alexis Guillot, Steffi Hansen, Teresa-Maria Garrigues, Claus-Michael Lehr. *Cyclosporine loaded PLGA-NP for treatment of intestinal inflammatory disease: in situ studies in Wistar rat*, 10th International Conference and Workshop on Biological Barriers, February 16-24, 2014, Saarland University, Saarbruecken, Germany

Ana Melero, Juan Pablo Sanchez-Rivera, **Christina Draheim**, Alexis Guillot, Steffi Hansen, Teresa-Maria Garrigues, Claus-Michael Lehr. *Cyclosporine loaded PLGA-NP for treatment of intestinal inflammatory disease: in situ studies in Wistar rat*, PBP world meeting, March 31-April 03, 2014, Lisbon, Portugal

Susewind J.*, **Draheim C.***, de Souza Carvalho C., Loretz B., Lehr C.-M., *In vitro* triple culture of inflamed human intestine as a model to investigate nanoparticle safety and efficacy, 9th World Congress on alternatives and Animal Use in the Life Science, August 24-28, 2014, Prague, Czech Republic

2013

Guillot, A., **Draheim, C.**, Collnot, E.-M., Limberger, M., Kraemer, J., Lehr, C.-M.: *Measuring drug release from micro- and nanoformulations by derivative spectrophotometry in combination with a fiber optic system*, 3rd HIPS Symposium, July 18, 2013, Saarland University, Saarbruecken, Germany

C. Draheim*, F. de Crécy*, A. Salas, C. Villiers, P. Marché S. Hansen, E.-M. Collnot, C.-M. Lehr, *A Design of Experiment Study Applied to a New Nano Spray Drying Technic and Nanoprecipitation for Producing PLGA Drug Delivery Systems with Defined Sizes and Size Distributions*, 40th Annual Meeting & Exposition of the Controlled Release Society, July 21-24, 2013, Honolulu, HI, USA

Guillot, A., **Draheim, C.**, Collnot, E.-M., Limberger, M., Kraemer, J., Lehr, C.-M.: *Measuring drug release from micro- and nanoformulations by derivative spectrophotometry in combination with a fiber optic system*, 40th Annual Meeting & Exposition of the Controlled Release Society, July 21-24, 2013, Honolulu, HI, USA

* These authors contributed equally to this work.

C. Draheim*, F. de Crécy*, A. Salas, C. Villiers, P. Marché, S. Hansen, E.-M. Collnot, C.-M. Lehr, *A Design of Experiment Study Applied to a New Nano Spray Drying Technique and Nanoprecipitation for Producing PLGA Drug Delivery Systems with Defined Sizes and Size Distributions*, Doktorandentag der NTF III, November 13, 2013, Saarland University, Saarbruecken, Germany

A. Guillot, **C. Draheim**, M. Limberger, J. Kraemer, C-M. Lehr. *Removing light scattering interferences using derivative spectrophotometry*, AAPS 2013 Annual Meeting and Exposition, November 10-14, 2013, San Antonio, TX, USA

2012

Christina Draheim*, Hussain Ali*, Claus-Michael Lehr, Eva-Maria Collnot. *Novel drug delivery systems for the therapy of inflammatory bowel disease*, 9th International Conference and Workshop on Biological Barriers, February 29–March 03, 2012, Saarland University, Saarbruecken, Germany

Guillot, A., **Draheim, C.**, Collnot, E.-M., Limberger M., Lehr, C.-M.. *Characterization of nanoparticulate systems for an innovative therapeutic concept for targeting inflammatory bowel disease*, 9th International Conference and Workshop on Biological Barriers, February 29–March 03, 2012, Saarland University, Saarbruecken, Germany

Nico Alexander Mell, **Christina Draheim**, Hussain Ali, Fransisca Leonard, Claus-Michael Lehr, Eva-Maria Collnot. *Targeting by nanomedicines in inflammatory bowel disease*, 2nd HIPS Symposium, June 28, 2012, Saarland University, Saarbruecken, Germany

2011

Eva-Maria Collnot, Fransisca Leonard, Carsten Schmidt, Hussain Ali, Nico Mell, **Christina Draheim**, Andreas Stallmach, Claus-Michael Lehr. *Nanomedicines for the therapy of inflammatory bowel disease*, 1st HIPS Symposium, June 16, 2011, Saarland University, Saarbruecken, Germany

Christina Draheim, Claus-Michael Lehr, Eva-Maria Collnot. *A nanocapsule drug delivery system for the therapy of inflammatory bowel diseases*, 3rd European Science Foundation Summer School, June 19-24, 2011, Lutherstadt Wittenberg, Germany

* These authors contributed equally to this work.

13. Acknowledgement/Danksagung

Nach einem Moment des Innerhaltens, möchte ich die Gelegenheit nutzen, um vielfältigen Dank auszusprechen. Nach Art und Umfang unterschiedlich, jedoch stets zutiefst ehrlich empfunden und von Herzen kommend.

Zu allererst danke ich meinem Doktorvater Prof. Dr. Claus-Michael Lehr für die Überlassung dieses überaus spannenden und aktuellen Forschungsprojektes, seine vielfältigen Anregungen und sein stets offenes Ohr, auch in stressigen Zeiten.

Prof. Dr. Rolf W. Hartmann danke ich für die Betreuung als mein wissenschaftlicher Begleiter und seine Bereitschaft zur Übernahme des Zweitgutachtens.

Zudem danke ich allen weiteren Mitgliedern der Prüfungskommission.

Des Weiteren bedanke ich mich bei Dr. Eva-Maria Collnot, Dr. Steffi Hansen und Dr. Brigitta Loretz, die in der genannten Reihenfolge die Arbeit betreut und das BIBA-Projekt begleitet haben. Ich danke euch dreien für eure Hilfe, für die aufmunternden Worte, wenn mal wieder wochenlang nichts klappen wollte und für eure immer offene Tür, durch die ich nur allzu oft gegangen bin – in die eine Richtung mit bohrenden Fragen bewaffnet, in die andere mit inspirierenden Antworten ausgestattet.

Ein großer Dank geht an apl. Prof. Dr. Ulrich F. Schäfer, vor allem für seine fachliche Unterstützung, aber auch die zahlreichen persönlichen Worte sowie die wertvollen Anregungen im Rahmen des Projektes.

Großer Dank gilt auch Dr. Ana Melero, Elisa Giner, Prof. Dr. Theresa María Garrigues und Prof. Dr. Rosa Giner sowie dem gesamten Team der *Farmàcia i Tecnologia Farmacèutica* und *Farmacologia* der Universität Valencia, die bei der Durchführung der *in vivo* Studien mitgewirkt haben. Ana, Dir danke ich, neben der fachlichen und persönlichen Unterstützung, auch für die tolle Zeit in Valencia.

Darüber hinaus bedanke ich mich bei den Projektpartnern des BIBA-Projektes: Francois de Crécy, Christian Villiers, Patrice Marché, Anne-Claude Couffin, Fabrice Navarro, Alexis Guillot, Johannes Krämer, Markus Limberger, Azucena Salas, Sebastian Cerdan, Caroline Maake und Doris Hinger, für die tolle fachliche wie auch persönliche Zusammenarbeit. Es hat mir sehr viel Freude bereitet, Teil eines solchen interdisziplinären, europäischen Forschungsteams gewesen zu sein. Ich werde immer gerne daran zurückdenken. Vielen Dank für eure Unterstützung während der gesamten Dauer meiner Promotion.

Ganz besonders möchte ich Dr. Alexis Guillot für unsere nette Zusammenarbeit danken. Alexis, ich wünsche Dir alles Gute für die Zukunft.

Zudem bedanke ich mich bei Prof. Dr. Andreas Thünemann, von der Bundesanstalt für Materialforschung und –prüfung in Berlin, für die SAXS Analyse sowie bei Sebastian Slawik vom Material Engineering Center Saarland (MECS) für die Durchführung der XRD Messungen.

Mein großer Dank gilt auch meinen engsten Mitstreitern und Bürokolleginnen, mit denen ich die dreieinhalb Jahre am Institut gemeinsam bestritten habe. Danke Sandra, Julia und Anne. Ich bin sehr froh euch an meiner Seite gehabt zu haben. Ihr habt Saarbrücken zu meiner Heimat werden lassen. Julia, dir danke ich auch für deinen Einstieg in das BIBA-Projekt und natürlich für die Durchführung der Zellkulturversuche, in die Du so viel Arbeit und Mühe investiert hast. Danke!

Ich bedanke mich auch bei allen anderen Mitarbeitern des Instituts für Biopharmazie und Pharmazeutische Technologie der Universität des Saarlandes und der Abteilung Wirkstoff-Transport des Helmholtz-Institutes für Pharmazeutische Forschung (HIPS). Die enge fachliche Zusammenarbeit, wie auch unsere vielen gemeinsamen persönlichen Erlebnisse haben die Arbeit am Institut und meine Zeit in Saarbrücken zu etwas ganz Besonderem werden lassen. Man sagt, dass jeder Mensch, der einem im Leben begegnet, dieses ein Stück weit mit prägt und so habt auch ihr alle einen Teil zum Entstehen dieser Arbeit beigetragen. Ich wünsche euch allen nur das Beste für die Zukunft. Insbesondere danke ich in diesem Rahmen allen Mitgliedern aus Evas ehemaligem „Darmteam“, den Mitgliedern des „Steffi-Hautteams“ und „Brigittas Team“. Danke Ankit, Nico, Emad, Clemens, Simon, Mardi, Salem und Florian für unsere Gespräche im „Partikellabor“.

Großer Dank gilt auch allen unseren Technikern (Petra, Peter, Chiara, Chris, Heike, Marijas, Jana) und dem gesamten Office-Team (Karin, Sarah, Stephanie und Isabelle) für die immer offen Türen und auch Ohren für das große, aber auch das kleine Leid im Rahmen meiner Institutszeit.

Ein großer und herzlicher Dank geht an meine Braunschweiger Mädels Katha, Frederike und Sonja und an Betti für eure Unterstützung und die aufmunternden Worte.

Thomas, Worte sind einfach zu wenig!

Danke!